UNIVERSITÉ DU QUÉBEC À TROIS-RIVIÈRES

IDENTIFICATION DE LA TRANSITION DE L'ODEUR ANTE-MORTEM À L'ODEUR POST-MORTEM

IDENTIFYING THE TRANSITION FROM ANTE-MORTEM ODOUR TO POST-MORTEM ODOUR

THÈSE PRÉSENTÉE

COMME EXIGENCE PARTIELLE DU

DOCTORAT SUR MESURE (BIOCHIMIE) 1401

PAR

DARSHIL PATEL

NOVEMBRE 2022

Université du Québec à Trois-Rivières
Doctorat sur mesure (Biochimie) (Ph.D.)

Direction de recherche:

Prof. Shari L. Forbes	
Prénom et nom	Directrice de recherche
Prof. Benoit Daoust	
Prénom et nom	Codirecteur de recherche

Jury d'évaluation

Prof. James Harynuk	
Prénom et nom	Evaluateur externe
Prof. Pierre-Hugues Stefanuto	
Prénom et nom	Evaluateur externe
Prof. Cyril Muehlethaler	
Prénom et nom	Président de jury
Prof. Benoit Daoust	
Prénom et nom	Codirecteur de recherche
Prof. Shari Forbes	
Prénom et nom	Directrice de recherche

Thèse soutenue le 9 Juin 2023

Résumé

Les chiens de recherche et de sauvetage et les chiens de détection de restes humains suivent l'odeur des victimes vivantes et décédées pour les localiser à la suite d'une catastrophe de masse. Déployer l'un ou l'autre de ces chiens afin de localiser les victimes de catastrophes de masse est difficile, car on ne sait pas si l'odeur d'une victime récemment décédée ressemble à celle des vivants (odeur ante-mortem) ou des morts (odeur post-mortem) durant le début de la période post-mortem. Cette thèse étudie le profil des composés organiques volatils (COV) libérés par les cadavres au commencement de la période post-mortem (0-10 jours). Une méthode optimisée a été développée pour recueillir les profils de COV des cadavres humains reçus à la morgue de l'UQTR. La méthode optimisée a ensuite été appliquée à l'analyse des profils de COV de cadavres dans un environnement contrôlé de la morgue, ainsi qu'au site de Recherche en Sciences Thanatologiques [Expérimentales et Sociales] (REST[ES]) à différentes saisons (printemps, été, et automne), afin d'identifier la transition des COV de l'odeur ante-mortem à l'odeur de décomposition. Les échantillons ont été analysés à l'aide de la désorption thermique et de la chromatographie gazeuse à deux dimensions, couplées à un spectre de masse à temps de vol (TD-GC × GC-TOFMS). Les profils de COV recueillis à la morgue et au REST[ES] comprenaient des classes de composés incluant des alcools, des composés aliphatiques linéaires, des composés azotés, des composés soufrés et d'autres classes couramment associées à l'odeur de décomposition au début de la période post-mortem. L'étude à la morgue a démontré que bien que l'abondance des COV liés à la décomposition variait, ces COV peuvent être identifiés dès 14 à 40 h post-mortem. Les profils de COV recueillis au REST[ES] ont démontré une variabilité intrajournalière et saisonnière en ce qui concerne l'abondance de COV et de classes parmi tous les donneurs. La journée expérimentale au cours de laquelle la transition visuelle vers le stade de ballonnement a été observée chez les donneurs placés à l'installation REST[ES] pendant les saisons d'été et de printemps a coïncidé avec un changement identifiable de leurs profils de COV. Cette modification du profil de COV a été notée par une abondance accrue de composés azotés qui a persisté jusqu'à la fin de la période d'essai de chaque donneur. Le changement du profil de COV et la transition de la

décomposition au début de la période post-mortem n'ont pas été observés chez les donneurs placés pendant la saison d'automne. La comparaison des profils de COV recueillis à la morgue et au REST[ES] a permis d'identifier les COV ante-mortem comme omniprésents tout au long de la période post-mortem précoce. Il a été déterminé que le passage des profils de COV des COV ante mortem aux COV de décomposition a commencé 48 à 72 h après le dépôt des donneurs au REST [ES] et que le profil de COV ressemblait à l'odeur post mortem après le troisième jour expérimental. Les résultats de cette thèse élargissent notre compréhension des COV libérés par les cadavres au début de la période post-mortem, ce qui pourrait aider à localiser plus rapidement les victimes dans les scénarios de catastrophe de masse et les opérations de recherche et de sauvetage. La connaissance du profil de COV au début de la période post-mortem améliore également la formation des chiens de détection de cadavres pour reconnaître la transition distincte de l'odeur au cours de cette période.

Certificate of authorship and originality

I certify that the work in this thesis has not previously been submitted for a degree nor has it been submitted as part of requirements for a degree except as fully acknowledged within the text.

I also certify that the thesis has been written by me, Darshil Patel. Any help that I have received in my research work and the preparation of the thesis itself has been acknowledged.

In addition, I certify that all information sources and literature used are indicated in the thesis.

Darshil Patel

Author

Dedication

This thesis is dedicated to my late grandparents.

Kashibhai Bakorbhai Patel

Savitaben Kashibhai Patel

Ishwarbhai Dhulabhai Patel

Savitaben Ishwarbhai Patel

and loving parents

Ashwinbhai Kashibhai Patel

Sheelaben Ashwinbhai Patel

Acknowledgements

Firstly, I would like to acknowledge my supervisor, Prof. Shari Forbes, for giving me this excellent opportunity to work on this PhD research project in Canada. Thank you for your continuing support and feedback throughout my PhD project. You have always pushed me towards excellency, and I have only continuously improved working under your supervision. You have always shown me a path to overcome the challenges I face, believed in me, and always taught me to push the boundaries. Without your encouragement and guidance, I would not have reached this stage in my personal or professional life, and I am extremely grateful.

Secondly, I would like to acknowledge my co-supervisor, Prof. Benoit Daoust. You have always addressed my questions and given me a different perspective on my research through your expertise. Thank you for all your invaluable inputs and feedback throughout my PhD.

To Prof. Wesley Burr, you have been an integral part of my success in my PhD. You provided your crucial expertise with statistical analysis and patiently taught me R. Thank you for being available, answering my questions and addressing my silly errors in R.

I would also like to acknowledge the technicians at the UQTR morgue and CIPP. Thank you for supporting me during the sample collection and patiently helping me to manage the instrument lab. You all have always welcomed me and tolerated my terrible French. Your constant encouragement kept me motivated to learn French. Merci Beaucoup!

I want to thank everyone in the team REST[ES] for helping me with my sample collection at the morgue and REST[ES]. Thank you for creating unforgettable memories; without you guys, my time in Trois-Rivieres would have been terrible. I am proud to be part of a great team that welcomed my wife at every event. This city only feels like home because of you guys. A special thanks to Rushali Dargan; I could not have asked for a better friend and a "labmate" on this

journey; it has been a blessing. I appreciate all your help with proofreading and your wizardry with excel. Especially these last few months have been difficult, but I am lucky to have a friend like you who always has my back!

Finally, on a personal note, I would like to thank my wife, Vrutti, for being my pillar; you have always been there with me at every step. You have always shown me the mirror. Thank you for your patience, love, and support! As you already know, I cannot function without you. I would like to thank my family, especially dad, mom, bhai and bhabhi, thanks for supporting my decisions. Coming to Canada for my PhD would not have been possible without your support.

Table of Contents

List of Figures

List of Tables

Abbreviations

^{1}D	First-dimension
1D	One-dimensional
^{2}D	Second-dimension
2D	Two-dimensional
ADD	Accumulated degree days
AFTER	Australian Facility for Taphonomic Experimental Research
ATP	Adenosine triphosphate
d_f	Film thickness
DMDS	Dimethyl disulfide
DMS	Dimethyl sulfide
DMTS	Dimethyl trisulfide
ED	Experimental day
EPA	U.S. Environmental Protection Agency
F_{crit}	Critical F value
GC	Gas chromatography
GC-MS	Gas chromatography–mass spectrometry
GC×GC	Comprehensive two-dimensional gas chromatography
HRD	Human remains detection (dogs)
HS-SPME	Headspace solid phase microextraction
Id	Identification number
ID	Inner diameter
n/a	Not available
NIST	National Institute of Standards and Technology
REST[ES]	*Recherche en Sciences Thanatologiques [Expérimentales et Sociales]*
ROS	Reactive oxygen species
S/N	Signal-to-noise ratio
SAR	Search and Rescue dogs

SPME	Solid phase microextraction
TD	Thermal desorption
TOFMS	Time-of-flight mass spectrometry
UQTR	Université du Québec à Trois-Rivières
USAR	Urban search and rescue
VOC	Volatile organic compound

Abstract

Search and rescue dogs and human remains detection dogs track the odour of living and deceased victims to locate them following a mass disaster. Deploying either of these dogs to locate victims of mass disasters is challenging as it is unknown whether the odour of a recently deceased victim resembles the living (ante-mortem odour) or the dead (post-mortem odour) during the early post-mortem period. This thesis investigates the VOC profile released from cadavers during the early post-mortem period (0-10 days). An optimised method was developed to collect VOC profiles from human cadavers received at the UQTR morgue. The optimised method was then applied to the analysis of the VOC profiles from cadavers in a controlled morgue environment as well as at the facility for *Recherche en Sciences Thanatologiques [Expérimentales et Sociales]* (REST[ES]) across different seasons (spring, summer, and autumn) to identify the VOC transition from ante-mortem odour to decomposition odour. Samples were analysed using thermal desorption coupled with comprehensive two-dimensional gas chromatography time-of-flight mass spectrometry (TD-GC×GC-TOFMS). VOC profiles collected at the morgue and REST[ES] facility comprised of compound classes such as alcohols, linear aliphatic compounds, nitrogen-containing compounds, sulfur-containing compounds, and other classes commonly associated with decomposition odour in the early post-mortem period. The morgue study demonstrated that although the abundance of decomposition VOCs varied, these VOCs can be identified as early as 14-40 h post-mortem. The VOC profiles collected at the REST[ES] facility demonstrated intra-day and seasonal variability in terms of VOC and class abundance across all donors. The experimental day on which the visual transition to the bloat stage was observed in donors placed at the REST[ES] facility during summer and spring seasons, coincided with an identifiable change in their VOC profiles. This change in VOC profile was noted by an increased abundance of nitrogen-containing compounds which persisted until the end of the trial period of each donor. The change in the VOC profile and transition of decomposition in the early post-mortem period was not seen in donors placed during the autumn season. The comparison of the VOC profiles collected at the morgue and REST[ES] facility identified ante-mortem VOCs as pervasive

throughout the early post-mortem period. It was determined that the shift in the VOC profiles from ante-mortem to decomposition VOCs started after 48-72 h post placement at the REST[ES] facility and the VOC profile resembled post-mortem odour after the third experimental day. The findings of this thesis broadens our understanding of the VOCs released from cadavers in the early post-mortem period, which could assist in more rapidly locating victims in mass disaster scenarios and search and rescue operations. Knowledge of the early post-mortem period VOC profile also enhances the training of cadaver-detection dogs to recognise the distinct transition of odour during this timeframe.

Chapter 1: Introduction

Volatile organic compounds (VOCs) released during the process of human decomposition is an important research area within the field of forensic taphonomy[1]. Each individual, when alive, has a unique ante-mortem odour. It is a combination of volatiles released from blood and sweat, and volatiles released through the action of microbes on the skin's surface (1-4). After a person dies, this unique scent transitions from an ante-mortem odour to a post-mortem odour. VOCs make up the "characteristic smell of death," which is released continuously throughout the decomposition process during the post-mortem period. An understanding of these VOCs can assist with locating human remains, training human remains detection (HRD) dogs (5), and developing biosensors (6, 7). Studying decomposition VOCs also has the potential to aid in determining post-mortem interval (PMI); however, their application in this field is limited and needs to be validated (8). Knowledge of the VOC profile produced in the early post-mortem period (0-10 days) can be applied in mass disaster scenarios or search and rescue (SAR) operations to rapidly locate living and deceased victims using SAR and HRD dogs.

This thesis aims to investigate the VOC profile released from cadavers during the early post-mortem period. For this study, 0-10 days was considered a suitable early post-mortem period, at the end of which all the donors had reached the beginning of putrefaction at the facility for Research in Experimental and Social Thanatology / ***Recherche en Sciences Thanatologiques [Expérimentales et Sociales]*** (REST[ES]). Herein, Day 0 was the day when the donor was placed at the REST[ES] facility. VOC profiles were collected from cadavers in a controlled morgue environment as well as in an outdoor environment to identify the VOC transition from ante/peri-mortem odour to decomposition odour. VOC profiles were collected using stainless steel dual sorbent tubes and analysed using thermal desorption coupled with comprehensive two-dimensional gas chromatography time of flight mass spectrometry (TD-GC×GC-TOFMS). Statistical techniques were applied to determine VOCs linked with the early post-mortem period and the transition of odour (ante/peri-mortem odour to post-mortem odour). The

[1] Taphonomy is derived from the Greek words *taphos*, which means burial, and *nomos*, which means law.

combination of sampling from cadavers just after they arrived in the morgue (6-72 h after death) and during the early post-mortem period outside along with statistical techniques enabled an understanding of the VOC profile and its change over time as decomposition progressed. The ante-mortem odour is not under the scope of this thesis and for ethical reasons, this study investigates the pervasiveness of VOCs related to ante-mortem odour soon after death to evaluate the transition. It is believed that the ante-mortem odour associated with the living is still potentially detectable in the early hours following death and that this odour transitions as decomposition is initiated. This chapter introduces forensic taphonomy which is a multidisciplinary field that facilitates the understanding of human decomposition. It provides an overview of the decomposition processes during the early post-mortem period which lead to VOC production, along with the chemical (analytical instrumentation) and biological (Human Remains Detection dogs) detection of VOCs in the field of forensic taphonomy.

1.1 Forensic taphonomy

In 1940, Ivan Efremov first coined the term *taphonomy*, defining it as the study of any *death assemblage*, as taphonomy was concerned with the transition from a living organism to a fossil (9). The field of taphonomy was classified as a subdiscipline of palaeontology. Researchers conducted purely observational studies in the initial era of taphonomy (10). After the 1970s as research in the field grew, the focus shifted to conducting longitudinal experiments in the laboratory and field to study decomposition processes and aspects leading to preservation of the remains (9). As the body of research grew, the principles of taphonomy were applied in several other disciplines such as geology, anthropology, biology, and forensic science. Therefore, the definition of taphonomy is slightly different in different fields (11). Haglund and Sorg defined forensic taphonomy as “the use of taphonomic experiments, analyses, and approaches in relation with forensics to estimate time since death, reconstruct the circumstances before and after decomposition and discriminate the products of human origin

from those created by earth's biological, physical, chemical and geological subsystems" (11). More recently, Schotsmans et al. (12) defined taphonomy as the "interdisciplinary field studying the decomposition process of an organism between death and its recovery". The scope of forensic taphonomy includes evaluating the ante- (before death), peri- (at the time of death) and post-mortem (after death) processes and depositional environment, as well as the impacts of these factors on preservation and degradation of remains, which enables researchers to differentiate between human-induced (e.g., coverings) and natural processes (e.g., freezing) (12). A vital role of forensic taphonomy is to serve the justice system and law enforcement agencies. Forensic taphonomy can be applied to forensic investigations to estimate the post-mortem interval, identify victim remains, investigate events surrounding death including the cause and manner of death, and if applicable, interpret evidence to identify the person who committed the crime.

1.2 Human decomposition

The decomposition process is a natural consequence of death, and every organism goes through the process, unless inhibited by some external factor (12). Decomposition commences immediately after death and is characterized by continuous post-mortem changes. Human remains subjected to natural (e.g., freezing) or artificial (e.g., embalming with chemicals) preservation are resistant to these post-mortem changes for a period of time (13). The progression of the process of decomposition has been classified into distinct stages; namely fresh, bloat, active decay, advanced decay, and dry/skeletonised remains (14). The early post-mortem period encompasses the fresh stage of decomposition. During this period gross post-mortem changes such as rigor mortis (biochemical stiffening of muscle after death), algor mortis (cooling of the body post-mortem), and livor mortis (peripheral pooling of blood) are seen on the body as all the biochemical processes cease in the body. The microscopic changes such as autolysis and putrefaction also commence during the early post-mortem period (15). As the decomposition progresses these changes lead to more distinct decomposition stages (bloat, active decay, advanced decay, skeletonised and dry remains). The onset of each stage in

humans is variable and can occur concomitantly during the decomposition process (13). Numerous environmental factors such as availability of oxygen, presence of clothing (16), temperature (17) (18), moisture (8) , microorganisms (19), the method of burial (20), and the chemistry of the surrounding soil, and/or water (21, 22) affect the decomposition process.

1.3 Microscopic changes during the early post-mortem period

1.3.1 Autolysis

Autolysis is defined as the "self-digestion" of tissues resulting from the breakdown of cell function post-mortem (6, 17). The cell membrane loses integrity with the continuous reduction in cytoplasmic pH and oxygen supply, releasing lysosomes and their digestive enzymes (hydrolases). The rate of autolysis depends upon the hydrolytic enzyme content, the internal body temperature, and the external temperature (23, 24). Organs such as the spleen, pancreas, and lungs show signs of autolysis faster than other organs with lower hydrolytic content. Warm temperatures accelerate the onset of autolysis, whereas the process is slower in colder conditions. Autolysis is also accelerated by pathological conditions such as fever and infection prior to death. Visually, a cloudy appearance of the cornea will be the earliest sign of autolysis. Although the hydrolytic enzymes technically cause autolysis, microbial activity can occur in parallel, and both enzymatic and microbial activity are often seen simultaneously (25).

1.3.2 Putrefaction

The microbial degradation of soft tissue is referred to as putrefaction. After death, the internal microflora changes as the environment in the human body transitions from aerobic to anaerobic. Anaerobic microorganisms spread from the intestines into the blood vessels. Several factors affect the onset, duration, and progression of putrefactive processes, but temperature is one of the most important factors (14). The putrefactive changes are accelerated in warm and hot temperatures, whereas colder temperatures often slow the rate of putrefaction.

Moreover, infection or sepsis in the ante-mortem or peri-mortem period can accelerate the putrefactive changes. Other factors such as open wounds and obesity can also accelerate putrefactive changes during the post-mortem period (23, 25).

The simultaneous action of enzymes on cells along with microbial activity leads to visual changes seen during putrefaction (26). The enzymes autolyse erythrocytes and produce hydrogen sulfide, which combines with haemoglobin forming sulfhaemoglobin. This process gives a characteristic greenish discolouration of the skin commonly known as "venous marbling". Venous marbling is one of the earliest signs of putrefaction. Skin slippage (slipping of the top layer of skin), formation of fluid blisters, purging of fluids from the nose and mouth, a brownish-blackish appearance of the skin, and swelling of the abdomen, penis, and scrotum (seen only in biological males) can also be observed during putrefaction. During the bloat stage, there is a shift from aerobic to anaerobic flora within the decomposing remains, and their increased activity leads to the characteristic bloated appearance. The increase in anaerobic flora results in catabolic metabolism leading to "active decay" (19, 24). During active decay, anaerobic microorganisms migrate into different tissue systems breaking down the naturally occurring macromolecules (e.g., proteins, lipids, and carbohydrates) into by-products including VOCs, thus releasing the characteristic odour of decomposition. Advanced decay happens when the biomass has largely reduced with reduction in fly activity. The final stage of decomposition is dry remains, where the skeleton is exposed directly to the environment, and the outer skin and visceral organs no longer protect it. In this stage, typically just connective tissues and bones are left due to the skeletonisation process (19). During the post-mortem period, a body goes through different decomposition stages, and understanding the VOCs that are released during these stages could provide knowledge about the capability of the dogs to locate remains in distinct stages (27).

1.4 Decomposition chemistry

The human body undergoes the process of autolysis and putrefaction, predominantly in the absence of oxygen. The simultaneous degradation of proteins, lipids, and carbohydrates in the

absence of oxygen produces various volatile and semi-volatile inorganic and organic compounds that comprise the characteristic odour of decomposition (28-30).

1.4.1 Chemical pathway of VOC production from different macromolecules following death

Proteolytic enzymes cause the lysis of proteins; however, this process does not occur uniformly (17, 31). The proteins present in the epidermis, collagen, reticulin, and muscles are more resistant to decomposition than proteins found in the gastrointestinal tract's epithelial lining and neural tissues (28). External factors such as temperature, moisture, and pH play an essential role in the metabolism of proteins. Polypeptides, peptones, proteases, and amino acids are produced due to the breakdown of proteins (Figure 1-1). The metabolism of proteins produces different gases, which depend upon the core elements of the individual protein. For example, sulfur-containing amino acids, such as cysteine, and methionine, undergo desulfhydralation to produce VOCs such as ammonia, sulfur, and hydrogen sulfide (inorganic compounds). The sulfides such as hydrogen sulfide, dimethyl disulfide (DMDS), and dimethyl trisulfide (DMTS) combine with iron and form a black discolouration of the body. The nitrification of ammonia produces nitrates. Skatole and indole are the end products of the continuous metabolism of proteins. Furthermore, thiols or mercaptans are the gases produced during the decomposition of the sulfur-containing amino acids (e.g., cysteine, cystine and methionine)(29). Some aromatic compounds can form thiols, which after the formation can be converted to disulfides. The decarboxylation of amino acids such as ornithine and lysine can produce cadaverine and putrescine (17, 29, 31, 32).

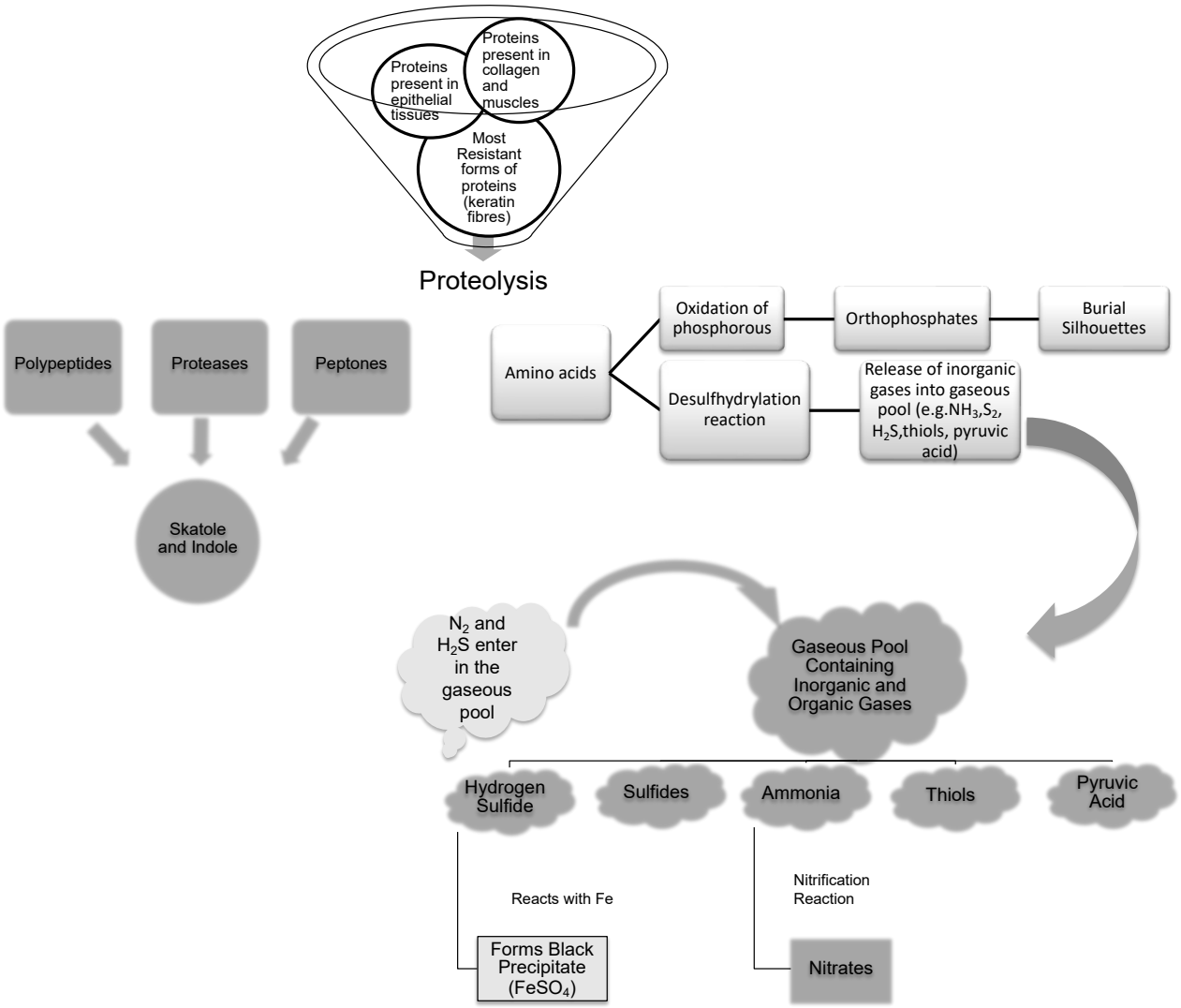

Figure 1-1 *Simultaneous proteolysis of proteases, polypeptides, peptones, and amino acids during the process of decomposition into possible VOCs. Note that multiple pathways of protein degradation reported in the literature are combined in this figure.*

Phosphorous is another important core element present within amino acids that are released as the protein structure is degraded. Phosphorous is mainly present in the cell walls, nucleic acids, and phospholipids of the brain and spinal cord. The disintegration of phosphorous is pH-dependent: phosphates remain in an insoluble state above pH 7 and below pH 5. At a pH between 5 and 7, phosphorous is converted into oxidised forms of orthophosphates. The soil around the body is stained dark due to phosphate deposition, and this phenomenon is known as a burial silhouette (or cadaver decomposition island) (24).

Adipose tissue is one of the significant types of tissue present in the body, which comprises approximately 80% lipids, 5% proteins, and 15% water (Figure 1-2). Lipids at a molecular level are present as triglycerides, fatty acids, phospholipids, steroids, and sphingomyelins (33). The major components of lipids are triglycerides, which comprise more than 60% of the total lipids in the body. Following death, the lipids in adipose tissue undergo hydrolysis due to the presence of intrinsic lipases and are converted into glycerol and a mixture of unsaturated and saturated fatty acids (27).Depending on the temperature, pH, and microbial activity, these saturated and unsaturated fatty acids undergo hydrolysis, hydrogenation and oxidation reactions to form hydroxy- and oxo-fatty acids, as well as forming salts of fatty acids with sodium or calcium in the body or surrounding environment (present during adipocere formation) (29, 34, 35). Fungi, bacteria, atmospheric oxygen, and visible and ultraviolet light facilitate the breakdown of fatty acids via oxidation. Alcohols, ketones, and aldehydes are the primary by-products of fatty acid oxidation (29, 34, 35). VOCs belonging to these compound classes have been reported through different stages of human decomposition and are one of the most reported compound classes in decomposition studies (36-39).

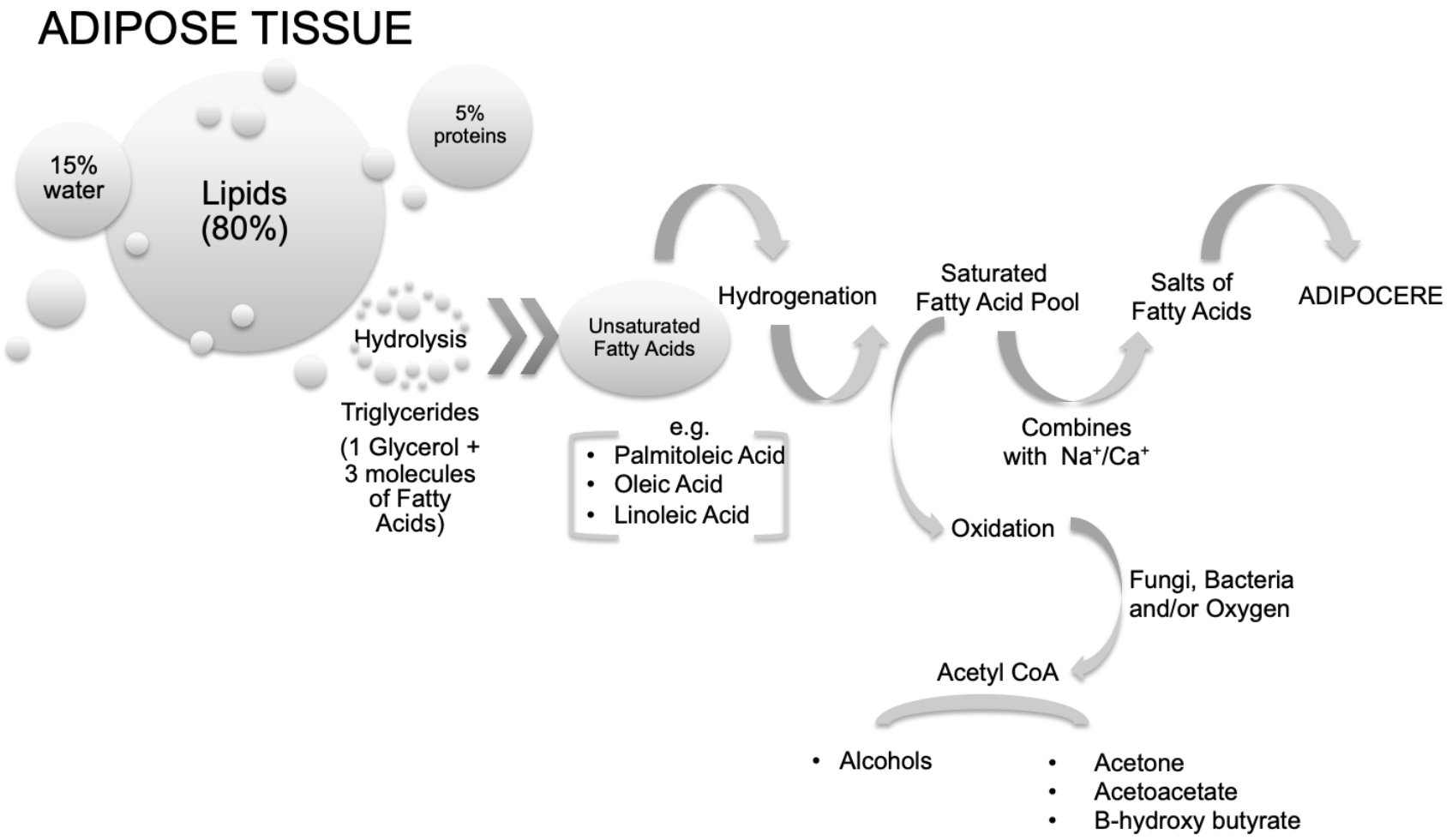

Figure 1-2 *Breakdown of lipids into unsaturated and saturated fatty acids during the process of decomposition into possible VOCs. Note that further breakdown of unsaturated and saturated fatty acids into VOCs depend upon temperature, pH, and microbial activity. Moreover, in this figure multiple pathways of lipid degradation reported in the literature are combined.*

Carbohydrates stored as glycogen are considered one of the primary energy sources in the living body (40). Complex polysaccharides (e.g., glycogen) are broken down into simpler forms of monosaccharides (e.g., glucose monomers) during the early post-mortem period (Figure 1-3). Their breakdown depends upon the extent of microbial conditions. Complete breakdown leads to carbon dioxide, while incomplete breakdown leads to organic acids and alcohols. Fungi and bacteria play an essential role in the metabolism of carbohydrates, but the end products of fungi differ from bacteria. Fungi decompose sugars into glucuronic acid, citric acid, and oxalic acid, while bacterial end products are dependent upon the type of environment. Under anaerobic conditions, acids (e.g., lactic acid, butyric acid, and acetic acid), alcohols (e.g., butyl and ethyl alcohol) and ketones (e.g., acetone) are produced. Under aerobic conditions, glucose monomers are degraded to pyruvic acid, acetaldehyde, and lactic acid. The breakdown of carbohydrates by microbial flora leads to the production of several gases, including methane, hydrogen sulfide, and hydrogen (29, 31, 34).

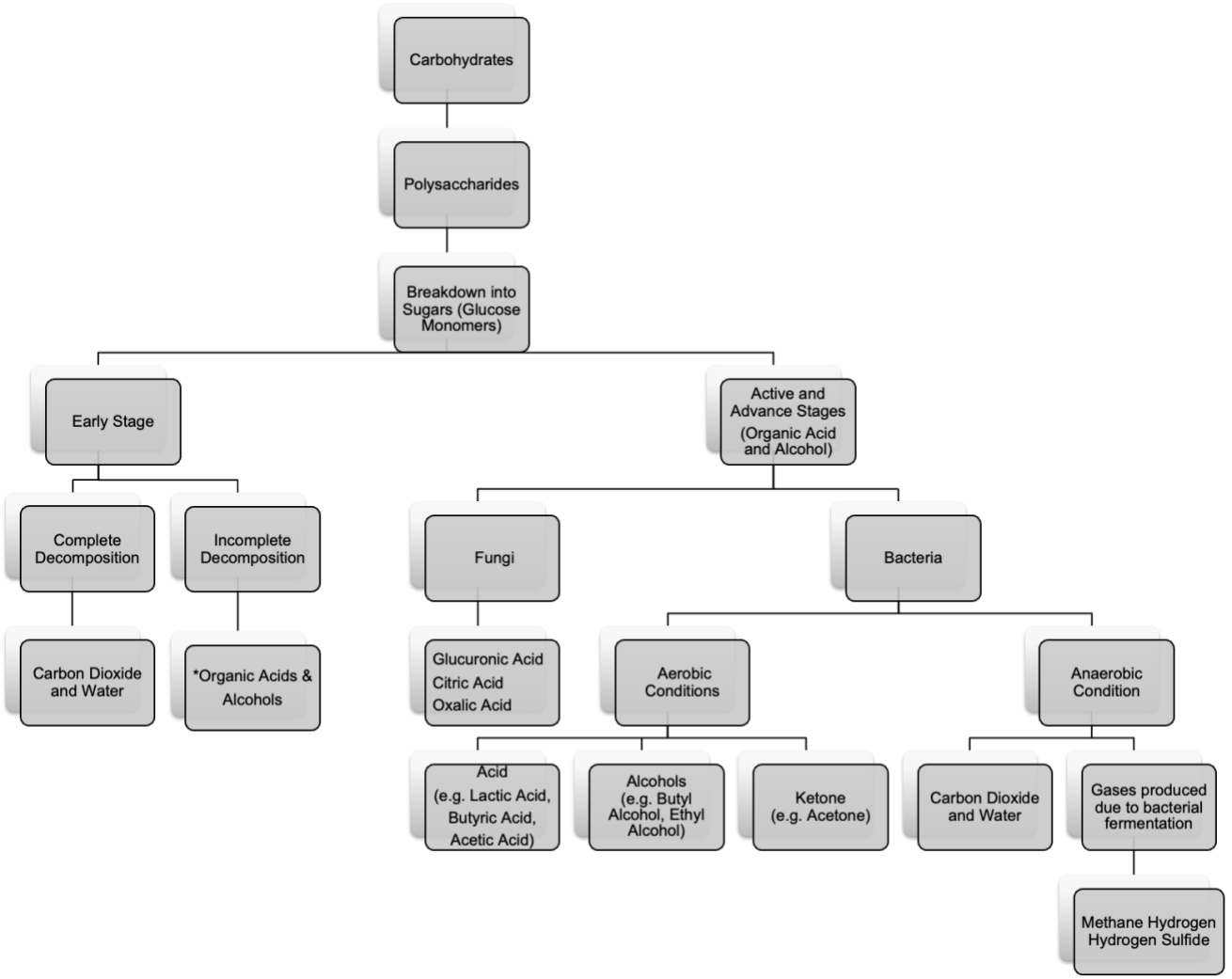

Figure 1-3 *Degradation of carbohydrates during the process of decomposition into possible VOCs. Complex polysaccharides are broken into simpler forms of sugars. Further breakdown of these simpler forms of sugars into VOCs is dependent on the decomposition stage (early, active, and advanced) and microbial activity (bacteria vs fungi). Additionally, in this figure multiple pathways of carbohydrate degradation reported in the literature are combined.*

1.4.2 Factors affecting VOC production

Climatic conditions are the most influential exogenous factors because of their significant influence on the chemical reactions occurring in the body during the various stages of decomposition (41). The rate of chemical reactions (e.g., hydrolysis) is directly proportional to the temperature (42). An increase in temperature accelerates the rate of hydrolysis of tissues, which causes the further breakdown of proteins resulting in an increased production of basic nitrogenous products, namely ammonia and amines. These nitrogenous by-products neutralise the acids produced by carbohydrate metabolism, raising the pH to alkaline levels, and supporting the growth of microbial flora. This process increases the rate of putrefaction and thus increases the production of gases, including VOCs (42).

In contrast, a decrease in temperature reduces the onset of various biological and chemical processes, altering the decomposition rate. Lower temperatures affect the decomposition processes occurring externally as well as internally. The internal processes such as autolysis and putrefaction are significantly affected due to reduced microbial activity, which causes a delay in the onset of the different stages of decomposition and production of VOCs. Moreover, colder weather in the winter season can impact biological activity since the low temperatures reduce invertebrate activity, thus reducing the rate of soft tissue loss during this period (43). A lack of VOC production is also likely to reduce the odour attraction for vertebrates, further reducing the loss of soft tissue due to invertebrate and vertebrate scavenging.

The environmental factors are an area of research interest due to their influence on VOC production and their effects on the progression of human decomposition. Deo et al. (38) conducted a study in 2020 using five clothed human cadavers to collect and analyse VOC profiles across various seasons (Australian autumn, winter, and spring). It was observed in this study that cadavers placed in warmer temperatures demonstrated higher variations in compound classes while the cadavers which experienced colder temperatures showed a reduced number of VOCs detected. The differences in the decomposition processes were not attributed to the presence of clothing which might have impacted the effects of the soil

environment and promoted preservation by trapping moisture (44). Therefore, this study highlighted the effect of climate on the overall decomposition process and the VOCs released.

The effects of temperature on human decomposition processes have been investigated in detail, but the role of moisture on human decomposition has only been briefly discussed (19, 45). It is reported that rainfall combined with soil moisture could potentially reduce the decomposition rate in the immediate short term (27, 42). During rainfall, the internal core temperature is reduced due to evaporative cooling, which interferes with the ongoing chemical reactions occurring in the cadaver, thus slowing the entire process (46). Nevertheless, knowledge about the effect of rainfall on the decomposition rate and VOC production is limited, and no statistical data exists which supports or contradicts the current findings in the literature (27, 42). Microbial functions such as diffusion of nutrients, waste disposal, enzymatic actions, and motility are dependent upon the availability of moisture. Moisture also plays a vital role in the decomposition of buried remains (24). Low moisture content in the soil leads to desiccation of human remains buried in soil, while a high moisture content in the soil promotes reduction reactions, which further slow the decomposition rate (21).

Gilles et al. (45) investigated seasonal variables (temperature, rainfall and humidity) and their effect on decomposition in the early post-mortem period (1 to 7 days) using cadavers (n=26) at the University of Tennessee's Anthropology Research Facility (ARF). The seasonal variables were recorded using weather stations and data loggers. Their study found that unlike temperature, which varied between the seasons (summer and autumn), the humidity was comparable between summer and autumn. These similarities in humidity between these seasons can be a critical factor in driving the visual changes of decomposition during the early post-mortem period (45). Therefore, even though the temperature has been reported as one of the most influential external variables, other variables such as humidity and rainfall should also be considered collectively to understand their impact on decomposition processes in different seasons.

1.5 VOC collection

Decomposition odour research uses air above (e.g., headspace) the decomposing cadaver or human remains to identify the VOCs that contribute to the odour. In order to identify these VOCs a concentration and collection step is necessary to allow their trace detection (47). The two most commonly used methods, sorbent tubes and headspace solid-phase microextraction (HS-SPME), have been used to collect VOCs in different studies investigating decomposition VOCs (48, 49).

HS-SPME is a passive sampling technique that relies on the establishment of equilibrium between the sorbent and sample headspace (50, 51). The SPME fibre is optimised using reference samples before the sample is analysed. The selected fibre is exposed in the headspace of the vial and the vial is heated; this enhances the release of volatiles. The fibre may also be exposed to internal standards before it is exposed to the sample vial (34, 52). The HS-SPME method provides a high throughput but is unsuitable for in situ sample collection in field decomposition studies. Perrault et al.(50) reported that during transport and storage of the SPME fibre, sample components present in the vapour phase can be lost due to difficulties associated with sealing the fibre from external contamination. This can affect the quality of samples collected. Moreover, the SPME fibre is fragile and has limited application in fieldwork compared to sorbent tubes (50). Furthermore, increases in exposure time cause displacement of the lighter volatiles by heavier volatiles. The number of sorbents that can provide a complete range suitable for decomposition VOC collection is thus fewer compared to sorbent tubes (50). VOCs reported in studies using SPME collection methods are often different from those reported from sorbent tubes, resulting from the different sorbents and their sorbing mechanisms (53).

One of the more commonly employed techniques for collecting VOCs involves drawing air through a sorbent tube packed with adsorbent materials with a trapping efficiency for the desired analytes (54). Sorbent tubes can comprise a glass or stainless-steel body with single or multiple sorbents depending upon the target analytes. If the analytes have broad properties,

then a combination of adsorbent is selected to increase strength from weakest to strongest sorbent (55). VOCs are trapped on the selected sorbent when air is drawn through the tubes, either actively or passively. Sorbent tubes and SPME are preferred methods of VOC collection that have been standardised for environmental studies (56, 57). Sorbent tubes are the preferred technique for collection of decomposition odour as the targeted VOCs can be pre-concentrated onto the tubes actively or passively and analysed later in the laboratory (Figure 1-4) (58).

Figure 1-4 *Stainless-steel dual sorbent tube with brass caps.*

1.6 VOC introduction

Several methods have been optimised for sample introduction of decomposition VOCs before subsequent analysis by gas chromatography (GC). These techniques include dynamic headspace, solvent desorption, and thermal desorption. In dynamic headspace, the volatile fraction released from the matrix in the vapour phase is continuously removed by an inert gas flowing through or over the matrix from the headspace of the sealed vessel. This volatile fraction is captured and concentrated in the above flow stream, through cryo-trapping, or by using materials that capture volatiles with different methods (e.g., sorption, adsorption, partition on low-volatility liquid stationary phases coated on a solid support, or selective reactions to isolate specific class(es) of compounds). Further the collected analytes are recovered from the trap by thermal desorption or solvent elution online or offline to a GC or GC-MS system for analysis (59-61).

This technique facilitates direct analysis from vials and replicate analysis. Although dynamic headspace provides enhanced recoveries of analytes over headspace, additional optimisation of parameters such as purge flow rate and volume, sorbent type, trap temperature of sorbent and sample incubation temperature is required. For the analysis of complex matrices involved in decomposition studies (e.g. human tissues, grave soils), it can be challenging to develop a method that optimally recovers the analytes with a wide range of volatilities and polarities. In these scenarios, most volatiles can breakthrough[2] due to excessive volumes of transfer gas, or in some cases of solid samples where less-volatile analytes cannot be adequately recovered due to a low volume of transfer gas or a sampling temperature (59, 60).

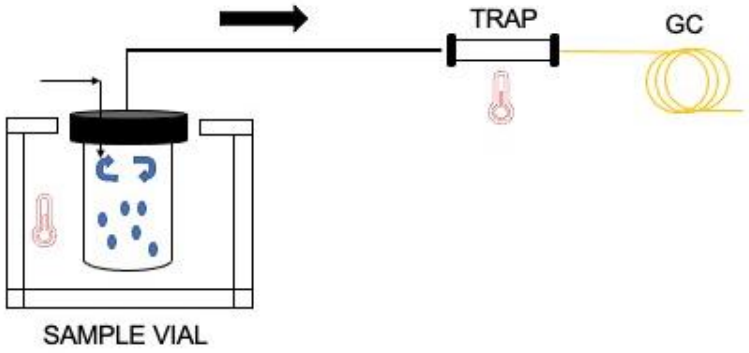

Figure 1-5 *Schematic of dynamic headspace as a method for sample introduction onto the GC column.*

Solvent desorption is used primarily to desorb VOCs from passive sorbent cartridges, followed by direct liquid injection. The sorbent is washed by an organic solvent (e.g. carbon disulfide, ether) thus releasing the analytes into a liquid extract that can be directly injected into the gas chromatograph. Solvent desorption is a simple technique that is compatible with thermally unstable and high molecular mass compounds. However, disadvantages of this technique include (i) after concentration on the sorbent tubes with organic solvent the VOCs present in the sample are diluted, (ii) sampling period can be longer when VOCs are collected passively,

[2] Breakthrough volume: The breakthrough volume of a given compound on a given adsorbent is defined as the maximum air volume that can be sampled using a trap made with a given quantity of the adsorbent, before the compound exits the trap

(iii) poor desorption efficiencies with more polar and reactive compounds (47, 55). The thermal desorption (TD) technique has been widely used for sample introduction in decomposition VOC studies (6, 32, 62-64). This technique can be applied to SPME fibres as well as sorbent tubes. A thermal desorption instrument is used for the desorption of sorbent tubes, whereby the tubes are placed inside a heated oven constantly supplied with an inert carrier gas. The sorbent tubes are subjected to two thermal desorption processes, primary and secondary desorption. In primary desorption, the sorbent tubes are desorbed at high temperatures (e.g., 300 °C). The desorbed VOCs are then focused on a cold trap (-10 °C to -25 °C) where secondary thermal desorption of the cold trap is performed, and the sample is directly injected onto the column of the gas chromatograph (53). Compared to solvent desorption, thermal desorption has advantages such as higher sensitivity due to the focusing step in the cold trap, lower possibility of contamination and loss of analytes, and is, therefore, the preferred injection method for decomposition VOC analysis (54). However, it is challenging to analyse compounds which are thermally unstable or compounds with higher boiling points (>300 °C) due to their risk of degradation. (55, 65)

1.7 VOC analysis

The conventional one-dimensional gas chromatograph (GC) was developed in 1952 by James and Martin (66). Since then, it has been used extensively in various fields, including environmental science, forensic science, chemical engineering, food, flavour, fragrance, security, and medicine (6, 8, 67-70). The sample inlet (e.g. injection port), column, oven, and detector are the essential components of a gas chromatograph. Further, a computer is used to operate the instrument and visualise the data output (71). In GC analysis, a microsyringe is used to introduce the sample for vaporisation in the heated injection port. An inert carrier gas (mobile phase) such as helium, hydrogen or nitrogen carries the vaporised sample onto the column through the inlet, chromatographic column, and detector (Figure 1-6a) (72) . The inert carrier gas consistently flows through the injection port, chromatographic column and detector and its supply is controlled by a flow or pressure regulator. The chromatographic column most

commonly used in GC analysis is a capillary column (usually 10-60 m) (72). The column is placed within an oven that can be heated with a temperature program ramp or isothermally. The interior of the capillary column is coated with a stationary phase. If the stationary phase of the column is a liquid or viscous polymer, the technique is referred to as gas-liquid chromatography (GLC), while a technique is referred to as gas-solid chromatography (GSC) if the stationary phase is solid. In a forensic context, given that the GLC is the only type of GC commonly employed, it will be referred to as GC in this thesis (72). The analytes in the sample are separated into individual components through partitioning between the mobile and stationary phase. This separation is based on the relative vapour pressure and the relative solubility in the liquid phase of the analytes. Analytes then elute from the column and pass to a detector.

In forensic applications, a GC is typically connected to an MS detector which enables identification and, if required, the quantification of unknown substances with a higher degree of certainty. The analytes are eluted from the GC column, a mass spectrometer (MS) identifies and detects compounds by the generation and detection of the ions based on their mass-to-charge (m/z) ratio (76). The ion source, mass analyzer and the detector are the main components of the MS. A typical process in MS analysis is as follows: (i) sample introduction in gas, liquid, or solid phase, (ii) sample ionisation, (iii) separation of ions according to their m/z, (iv) detection of ions present in sample using a mass analyser, used to measure charged particles, (v) display of resulting mass spectrum on a computer, (vi) interpretation of spectrum using fragmentation data and/or intact mass values (72). One-dimensional (1D) GC-MS produces a chromatogram, which displays the retention time on the x-axis and the signal intensity on the y-axis. The peaks acquired in the chromatogram can be tentatively identified using mass spectral libraries such as the National Institute of Standard and Technology (NIST) or Wiley and confirmed through the analysis of standards (73, 74).

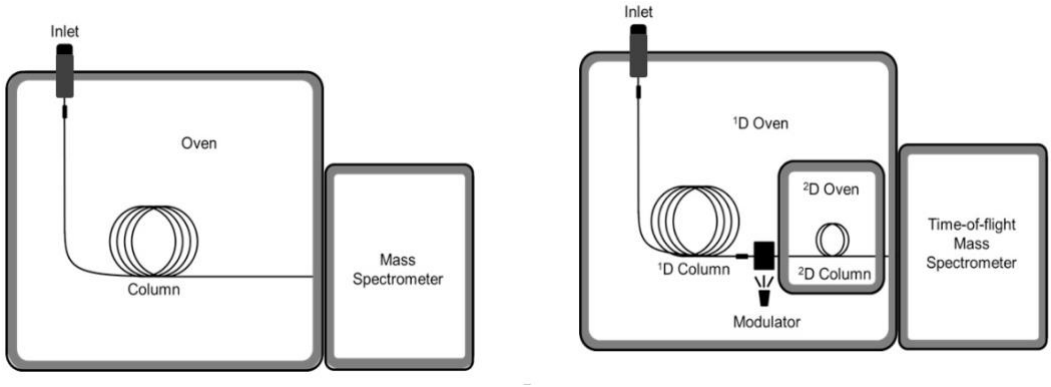

a) GC-MS b) GC×GC-TOFMS

Figure 1-6 *Schematic comparison of a) one-dimensional GC-MS and b) GC×GC-TOFMS.*

Analysing decomposition VOCs using 1D GC-MS can be challenging due to limitations such as insufficient selectivity, limited peak capacity, and inability to manage the dynamic range. Peak capacity is defined as the maximum number of components theoretically separable in a chromatographic system (63, 74). The peak capacity of comprehensive two-dimensional gas chromatography-time-of-flight mass spectrometry (GC×GC-TOFMS) (Figure 1-6b) is higher than conventional 1D GC-MS due to the addition of a second column and a modulator, which provides a higher number of satisfactorily resolved peaks per unit length of the column (63). The addition of a modulator allows analytes eluting from the first-dimension column to be focused onto a second dimension. The secondary column coated with a different stationary phase offers a different mechanism of separation to the first column. This configuration of two columns with a modulator provides a better separation of analytes by enhancing selectivity, sensitivity, and peak capacity (74).

In 1946, a researcher named Stephens proposed a concept of time-of-flight mass spectrometry (TOFMS). The theory of TOFMS is simple: a group of ions of different mass to charge ratios *(m/z)* will achieve *m/z* dependent velocities when accelerated to the same energy and therefore will require different times to travel through a set distance in a flight tube. The time, t, required for the ions to cover the field-free (FF) distance, D, can be calculated as per equation 1.1:

$$t = \left(\frac{m}{zq_eU}\right)^{1/2} D \qquad 1.1$$

where m is the mass and z is an integer number of fundamental charges, qe. Thus, the output of an ion detector is calculated at the exit of the flight region. This represents the complete mass spectrum where the observed flight time taken by an ion is proportional to the square root of *m/z*. In TOFMS, the spectra are quickly generated, and ion flight times are in 10s to 100s of microseconds due to simple accelerating potentials (75, 76). In TOFMS, the spectral measurement of an analyte during its change in concentration is devoid of any spectral skew. These advantages make TOFMS suitable in applications with temporal-varying signal sources, such as rapid ionisation events or ion reaction and chromatographic separation. The combination of acquisition speed, high mass-spectral, and architectural simplicity gives TOFMS the ability to produce a higher number of ions at the ionising source and researchers have regularly employed it with comprehensive two-dimensional gas chromatography (77). Furthermore, in GC×GC analysis, the modulator produces narrow peaks, and the detector must be efficient at sampling those peaks at a higher acquisition rate. For these reasons, GC×GC-TOFMS is often employed to overcome the limitations of GC-MS for the analysis of complex samples containing a broad dynamic range of VOCs including decomposition odour (75, 78)

1.8 Application of VOCs to search and rescue (SAR) and human remains detection (HRD) dogs

Canines have highly developed olfactory systems and for decades have been used for scent-detection in various law enforcement disciplines to detect drugs, explosives, blood, missing persons and human remains. The search for live missing persons and human remains is typically carried out by search and rescue (SAR) and human remains detection (HRD) dogs, respectively. Technological advancements have allowed other search equipment, such as robots, sensors,

UAVs, and fibre optic cables to be used to search for victims living and deceased, particularly following mass disasters (e.g., earthquake, tsunami, wildfires, avalanche etc.). However, SAR and HRD dogs are still considered the gold standard when it comes to searching for victims of mass disasters rapidly (3).

Canines are the preferred resource used for locating victims and victim remains as they are a non-destructive method for searching potential crime scenes, and they are known to have a highly advanced olfactory system. Moreover, they are also considered versatile, highly reliable, and can relatively quickly cover a large search area (79). The SAR dogs are trained to find human scent and are used to search for live victims during missing persons and mass disaster investigations while HRD dogs are trained to locate the decomposition odour of deceased victims. Researchers have profiled healthy individuals; individuals in distressed states; human remains in a morgue; and human remains in an outdoor environment to identify VOCs linked with a specific sample class (alive vs deceased) and to discriminate between sample classes (8, 80, 81). This knowledge of VOC profiles (ante-mortem and post-mortem, respectively) could assist in understanding the transition of odour from ante-mortem odour to post-mortem odour. Furthermore, this knowledge can also be applied in the training of SAR and HRD dogs leading to early detection of victims and victim remains in a mass disaster scenario.

The VOC profile of human scent is a combination of VOCs linked with exhaled breath, blood, sweat, urine and skin (82). Statheropoulos et al. compared the VOC profiles of exhaled air from fasting and healthy individuals (80, 83), urban waste disposal bins (82), and headspace samples of body bags containing decomposing remains (80). Their objective was to determine the combination of VOC profiles that could discriminate between the VOC profile of expired air of living entrapped humans in buildings and the background sources of VOCs in the entrapment zone. The data was acquired with TD-GC-MS and evaluated with chemometric techniques such as discriminate analysis (DA) and cluster analysis (CA) (82). Based on the scores plot of DA, they reported that the headspace of human remains could be clearly distinguished from the other sample groups. This was the first study that compared experimental samples from alive individuals and human remains, with background odour (urban air and waste disposal bins) and

proposed the use of chemical information to indicate the status of entrapped people during a mass disaster.

Recent studies conducted using bodies in an outdoor environment have focused on studying the differences in the VOC profiles of pig and human remains. This is an important topic of research as law enforcement agencies sometimes use human analogues (e.g., pigs) and human remains (e.g., decomposition fluid, soft tissues, and cadaveric blood) to train HRD dogs in the absence of access to cadavers. Knobel et al. (37) compared the VOC profile of human and pig remains over two distinct seasons (summer and winter) at the Australian Facility for Taphonomic and Experimental Research (AFTER) site. The study demonstrated that although common VOCs were detected between human and pig remains, the ratio of VOCs released during the decomposition processes of pig remains were not comparable to human remains. Thus, the study emphasised the need for further research on VOC profiles of cadavers and recommended the use of human remains to train HRD dogs in order to maintain their enhanced scenting capabilities. This further emphasised the need for research on the VOCs released from cadavers.

The majority of studies profiling the VOCs from human remains have focused primarily on the compounds released during the overall process of decomposition and particularly during the active decay stages when VOCs are most prevalent. However, only a few studies have focused on the VOCs released during the early post-mortem period (0-96 h). Statheropoulos et al. (6) analysed VOCs released from a human donor during the early post-mortem period. The donor was placed in a body bag on the 4^{th} day after death, and headspace VOCs released from the human remains were collected onto sorbent tubes at four different time intervals (0, 4, 8, and 24 h) in a morgue. The samples were analysed using TD-GC-MS and the results were classified into different compound classes, namely organic sulfides, ketones, alcohols, aldehyde, aliphatic, and aromatic hydrocarbons. The compounds such as acetone, dimethyl sulfide (DMS), ethanol, toluene, octane, 2-butanone, o-, m-, and p-xylene were found at all sampling intervals. It was concluded that profiling the VOCs over a longer time (days or weeks) could help to understand the human decomposition profile during the early post-mortem period. They also proposed the

application of the early post-mortem VOC profile in developing field detection equipment and training HRD dogs.

DeGreeff et al. (48) performed a study on human cadavers (n=27). One VOC sample was collected per cadaver during the early to mid-stage of decomposition in an indoor morgue scenario (n=21) and crematorium (n=6). The headspace VOCs were collected using a dynamic headspace field-portable scent transfer unit (STU-100) in a non-contact manner. The objective was to trial this portable unit on cadavers in an indoor scenario during the early post-mortem period and minimize the sample background interference. The STU-100 pre-concentrated the headspace VOCs released from cadavers onto a sorbent material. Two types of collection materials were evaluated in this study: polyester material and cotton-blend gauze. The loose woven material, such as cotton gauze, produced significantly fewer total VOCs than other sorbent materials. The samples were also collected from living human subjects, and animal remains, and all the samples, including those collected from cadavers, were analysed using SPME-GC-MS. The statistical analysis performed on the data highlighted the differences in the VOC profiles between cadavers, animals, and living subjects. Thirteen VOCs were attributed to human origin, out of which eight VOCs were reported in previous studies. p-xylene and DMDS, which are commonly reported VOCs, were not detected in this study. The researchers attributed the absence of these VOCs to the sampling technique or the sampling period (early to mid-decomposition) stage (48).

Stefanuto et al. (63) conducted the first study using GC×GC-TOFMS with multivariate statistical techniques (principal component analysis and fisher ratio) to investigate and compare the VOC profile of pigs and humans in the early post-mortem period (0-6 days). The VOC samples were collected using stainless steel dual sorbent tubes (Tenax GR® and Carbopack™). Differences were noted in the decomposition pattern between pigs and humans, where pigs decomposed quicker than humans in the early stage. The study also noted that the VOCs were produced in lower concentrations, which could be attributed to the decomposition process. The application of statistical analysis helped to filter the large amount of data produced by GC×GC-TOFMS. However, the authors emphasized the importance of replicates so that seasonal variation and

inter-species variation can be better reported (63). Although the study highlighted challenges of the early post-mortem VOC profile, it did not focus on the intraday variability and VOC profile transition during the early post-mortem period as this was outside the scope of the study. The study did focus on analytical technique and data handling, which is also a significant research problem for the analysis of decomposition VOCs.

Armstrong et al. (64) conducted the only study to date which has investigated the variation in VOC profile during the early post-mortem period. Pigs were used as analogues for human remains, and samples were collected from three pig carcasses at different time intervals during the first 72 h post-mortem and analysed using comprehensive two-dimensional gas chromatography-time-of-flight mass spectrometry (GC×GC-TOFMS). A total of 105 compounds were identified during the early post-mortem period. The transition from early ante-mortem to post-mortem odour was reported at the 43rd-49th hour post-mortem in the summer months in an Australian climate. Furthermore, a shift in compound classes was detected hourly and daily. This study added new information about the transition of VOCs soon after death that could be helpful during mass disaster responses. The authors suggested that similar studies in the future could guide urban search and rescue teams (USAR) to use both SAR and HRD dogs effectively (64). However, there is still a clear need to determine the VOC profile released during the early post-mortem period for human remains to effectively utilize SAR and HRD dogs in mass disasters.

1.9 Project aims and objectives

There are several methods developed to collect and analyse the VOCs released from human decomposition, but these have not been applied to the early post-mortem period. Therefore, the study of decomposition odour released during the early post-mortem period remains a challenge. The primary aims of my research are outlined as follows:

- Phase 1 - Develop an optimised TD-GC×GC-TOFMS method for analysing VOCs in the early post-mortem period to identify the decomposition VOC profile released from human remains within a 0-10 day post-mortem period.

- Phase 2 - Investigate the early post-mortem VOC profile from human remains donated to the *Department d'Anatomie* at the *Université du Québec à Trois-Rivières* (UQTR) morgue within a 0-10 day post-mortem period.

- Phase 3 - Investigate the early post-mortem VOC profile from human remains donated to the facility for REST[ES] and placed in an outdoor environment in Bécancour (Québec). Samples will be collected for a longer period according to the accumulated degree days (ADD) as seasonal fluctuations will impact the rate of transition to decomposition VOCs.

It is hypothesised that despite decomposition processes beginning in as little as four minutes after death (84), a portion of the early post-mortem VOC profile will more closely resemble an ante-mortem or peri-mortem VOC profile (e.g., the living human scent). It is further hypothesised that during the early post-mortem period, there will be a change in the VOC profile to more closely resemble decomposition odour as time progresses and the decomposition processes commence. It is anticipated that this transition will vary based on seasonal temperature differences and physiology of the donor (e.g., weight, age, body size, stomach contents before death) (84).

The results of this project will add to a growing body of research that aims to better understand the VOC profile that comprises decomposition odour. Ultimately, this will assist in a better understanding of how ante/peri-mortem odour transcends into post-mortem odour. Thus, during a mass disaster scenario the knowledge of human odour can help to allocate the most appropriate search dogs to locate victims, living and deceased.

Chapter 2: Method optimisation and application to profiling VOCs released from cadavers in a morgue during the early post-mortem period.

2.1 Introduction

The simultaneous biochemical activity of enzymes, microorganisms, reactive oxygen species (ROS), and scavengers releases a diverse range of VOCs as end or by-products of decomposition (35, 85). These mixtures of VOCs create the unique VOC profile of decomposition. A complete characterisation of VOCs released during the entire process of cadaver decomposition from the fresh to skeletonisation stage has been the focus of studies conducted on decomposition odour (37, 43, 63, 84). Research on the VOC profile released throughout this timeframe is essential and can be applied in homicide investigations and missing person cases (86). The first 72 h are critical from the USAR perspective since the likelihood of survival of victims declines after the first 48 h following a mass disaster. The human body can survive three weeks on fasting, but survival chances reduce to three to seven days without water and four minutes without oxygen (4, 64). Therefore, there is a need for improved methods that can be applied during the first 72 h to rapidly locate live victims and victim remains in a mass disaster scenario.

Autolytic and putrefactive processes are predominantly related to the production of VOCs. These processes occur in the beginning stages during the early post-mortem period, when the VOCs are less abundant which adds analytical challenges. Only a few taphonomic studies in the literature have used a cadaver to profile the odour released during the early post-mortem period due to ethical challenges relating to the use of human remains (63, 64). Statheropoulos et al. (6) and DeGreeff et al. (48) collected the VOC profile of cadavers during the early post-mortem period in a morgue. Although the concentrations of VOCs were low, their experimental design enabled the collection and identification of VOCs related to decomposition odour during the early post-mortem period. The results of these studies were not comparable and is

attributed to different sorbents used for sample collection (sorbent tubes vs gauze pieces). The authors of these studies analysed their samples using GC-MS. This analytical technique suffers from issues such as co-elution of complex mixtures, an inability to manage the dynamic range of VOCs, complexities of background samples and limitations in sensitivity making it less ideal for VOC samples collected during the early post-mortem period. Further details of these studies can be found in section 1.8.

GC×GC-TOFMS is the preferred technique to study the decomposition VOC profile. The instrument has two different columns with two different stationary phases, providing users with an increased capability of separating the different range of VOCs present in decomposition odour based on different retention mechanisms (37, 63, 86). Its application to the early post-mortem VOC profile of cadavers released in a controlled indoor environment (e.g., morgue) can assist in identifying the less abundant VOCs released in low concentrations during this period. A morgue is a controlled indoor environment where chemical (embalming) and natural (freezing) preserving techniques protect donated bodies from decomposition. Profiling VOCs released from unembalmed cadavers during the early post-mortem period upon their arrival in the morgue (6-72 h) can provide a baseline VOC profile of a person soon after death. This baseline VOC profile can be used to understand the transition of odour from the peri-mortem period to the post-mortem period.

This chapter has been divided into two phases; Phase 1: method development and Phase 2: application of the developed method to profile VOCs released from cadavers in a morgue. This study aims to optimise the method for collecting the VOCs released from cadavers and identify their VOC profile in the early post-mortem period. The objective was to determine the VOCs released from human remains in a controlled environment in the absence of external factors that contribute to the decomposition process. Furthermore, the method was developed in a manner that would enable further comparison between samples collected from the same cadavers in the morgue and after being placed at the outdoor human decomposition facility.

2.2 Ethics statement

The cadavers used in this study were donated through the UQTR Body Donation Program, which includes consent for the remains to be used for the purpose of research at the UQTR morgue. This project was approved by the UQTR Human Research Ethics Committee (CER-19-261-07.11). The cadavers were transported to the UQTR morgue by funeral directors licensed to transport human remains. The date and time of the donor arrival was fixed before the experimental trial, whereby donor availability and delivery dictated the sample collection.

2.3 Quality control procedure

A QC protocol was developed to ensure the optimal working of instruments used to collect and analyse the decomposition VOCs released from cadavers. The steps undertaken at each stage are as follows:

Sample collection:

- Prior to sample collection, a digital flow meter was used to calibrate the flow rate (e.g., 100 mL/min) of the ACTI-VOC low flow pump; the calibration step was performed once a month to ensure a constant pump flow rate (100mL/min).

- Stainless steel sorbent tubes were reconditioned before sample collection and after sample analysis for every sample collected in this study. The sorbent tubes were reconditioned at the manufacturers recommended reconditioning temperature of 330 °C for 30 mins.

- After the reconditioning of the sorbent tube, and prior to its storage, random batch testing was conducted to assess the reconditioning process by analysing the blank reconditioned sorbent tube using the same method employed for sample analysis.

- Following a direct injection of external standards, reconditioning was carried out for 60 mins to ensure the removal of analytes.

- Sorbent tubes stored without use for three months or longer were reconditioned again prior to use.

- Desorption and reconditioning cycle of each sorbent tube was logged.

- After method optimisation, control samples were collected every time the experimental samples were collected in the morgue (background morgue air sample) and at the REST[ES] facility (area without a body).

Sample Analysis:

Thermal desorption:

- Pre-desorption, each sorbent tube was pressurised and subjected to an ambient temperature leak test without carrier gas flow. The failed tubes were not allowed to be desorbed. The tubes were pre-purged with carrier gas for 1 min in the desorption direction to remove excess moisture.

- Cold trap was reconditioned periodically.

GC x GC-TOFMS:

- A tune performance was run daily before sample acquisition regardless of the number of samples present in the sequence. The tune performance performed actions such as leak checking and mass calibration (m/z 69, PFTBA tune compound). A report of the tune performance was generated and saved for review. Further, the performance report had to pass to proceed with sample acquisition every time.

- The tune performance report also provided comparisons with the most recent previous report to monitor the changes in the instrument conditions between the analysis.

- An auto-tune was performed monthly or after a routine maintenance procedure.

- A defrost cycle was added at the end of the sample acquisition sequence to prevent the formation of ice plugs and to evaporate water condensed within the cold jet tubing. This procedure ensured the optimal performance of cold jets during the analysis.

Standards

Internal Standard

Before analysis, 0.2 uL of 10 ppm bromobenzene (HPLC grade, Sigma-Aldrich, St. Louis, MO, USA) in methanol (HPLC Grade, Sigma-Aldrich) was injected using a calibrated eVol® XR handheld automated analytical syringe (SGE Analytical Science, Wetherill Park BC, NSW, Australia). For QC of the internal standard, it was also injected onto a blank sorbent tube and analysed separately after every batch (10 to 15 samples) before the subsequent sample analysis.

Decomposition Standard Mix

The decomposition standard mix comprised of three custom-made standard mixes ordered through Restek. The three mixes contained 25 compounds belonging to different compound classes (e.g., alcohols, esters, aldehydes, etc.) (Appendix A: Table A-1). These compounds were previously identified through cadaveric studies (8, 37). These standards were analysed during the 2020 and 2021 sample collection trials conducted at the morgue and REST[ES] facility. The standards allowed us to calculate relative concentration comparisons between the standard compounds and those present in the experimental samples. Moreover, they allowed to monitor deviations in the retention times.

2.4 Phase 1: Method optimisation

The experimental design and method were adapted from a previous study by the author (87). The previous (pilot) study profiled the VOCs released during the early post-mortem period for human remains placed in an outdoor human decomposition facility in Sydney, Australia. The study highlighted numerous challenges such as a reduced number of VOCs being detected (87). Notably, 15 VOCs were detected during the pilot study, and these did not correlate with the VOCs detected in previous studies (37, 64) during similar months and seasons in the same environment which investigated the entire decomposition process. Therefore, there was a need to adapt and optimise the sample collection and sample analysis method during this phase of the current study, in order to apply it successfully to the early post-mortem period. VOC sample collection involving the use of sorbent tubes with a low-flow pump and subsequent analysis by TD-GC-MS or TD-GC×GC-TOFMS has been previously reported in the literature (6, 8, 48, 63, 64, 84). This method has been applied to cadavers and human remains and involves creating a headspace (e.g., body bag) to concentrate VOCs for a fixed period of time (e.g., 15-20 min)(6, 8, 48). The VOCs are collected onto the sorbent tube containing a sorbent material. These studies have focused on the complete process of decomposition from fresh to skeletonisation and were designed to capture VOCs released at different stages of decomposition.

In order to develop an optimised method for collecting VOCs from human remains during the early post-mortem period, the optimisation was carried out on donors in the UQTR morgue to assess the sample collection technique and the analytical output using a newer and more sensitive Pegasus®BT 4D GC×GC-TOFMS instrument (LECO Corporation, ST Joseph, MI, USA) than Pegasus® 4D GC×GC-TOFMS (used in the pilot study). Following optimisation (Phase 1), the method was then applied to collect VOCs released from a larger cohort of donors in the UQTR morgue (Phase 2), and subsequently from donors placed at the REST[ES] facility for decomposition studies in an outdoor environment enabling comparison of the VOC profiles (morgue vs outdoor) across the entire early post-mortem period (Phase 3) (discussed in Chapter 3).

2.4.1 VOC collection optimisation

2.4.1.1 Experimental Design

The sample collection method was initially tested using human cadavers in the UQTR morgue in the UQTR Department of Anatomy. A total of 11 cadavers were sampled with 4 out of 11 cadavers sampled in August 2019 and the remainder sampled in September and October 2019. The samples were collected as the donors became available. Of these cadavers, 4 were female and 7 were male. All donors were in the fresh stage of decomposition when they arrived in the morgue. The history of preserving the bodies before they were brought to the UQTR morgue was not known as they were received from various hospitals and nursing homes. Table 2-1 shows the details of the donors that were available, including the date and time of death, arrival at the UQTR morgue, age, sex, and if the body was refrigerated.

The donors were sampled in a clean sterile indoor morgue environment with access to authorized personnel only. Control samples (background room air) were not collected in the method optimisation phase. The sample collection method was still being tested and it was unknown if the VOC collection and accumulation time was able to pre-concentrate the VOCs in the headspace of the body bag. The sample collection method was tested on multiple donors to determine the reproducibility of the technique in terms of determining the VOCs in the headspace of donors. The arrival of donors was infrequent and occurred at varying post-mortem periods ranging from 12 to 72 h. To address this variability, the body bag was opened for 5 mins and resealed with the assistance of morgue technicians to minimize the influence of the body bag on VOC accumulation before VOC accumulation at the UQTR morgue after the arrival of the donors. The samples were collected as soon as the donor arrived at the morgue and before the body was processed or treated. The objective was to test the experimental design and to identify the range of VOCs that could be collected using the method.

Table 2-1 *Details of the donors sampled for method optimisation in the UQTR morgue.*

No	UQTR donor id	Age (yrs)	Sex	Date and time of death (dd/mm/yy) and (hr:min)	Date and time of arrival at the UQTR morgue (dd/mm/yy) and (hr:min)	Donor refrigerated
1	2019-33	71	F	05/08/19 and 12h:00	05/08/19 and 18h:00	Yes
2	2019-34	78	M	07/08/19 and 10h:45	07/08/19 and 18h:00	No
3	2019-35	69	M	11/08/19 and 07h:54	11/08/19 and 13h:40	Yes
4	2019-39	89	F	31/08/19 and 04h:05	31/08/19 and n/a	Yes
5	2019-40	67	M	20/09/19 and 20h:00	22/09/19 and n/a	Yes
6	2019-41	88	M	21/09/19 and 19h:40	22/09/19 and n/a	Yes
7	2019-42	72	M	22/09/19 and 05h:10	22/09/19 and n/a	Yes
8	2019-43	77	F	22/09/19 and 09h:50	22/09/19 and n/a	Yes
9	2019-44	68	M	09/10/19 and 14h:06	09/10/19 and 17h:15	No
10	2019-46	67	M	14/10/19 and 01h:20	14/10/19 and n/a	Yes
11	2019-47	68	F	14/10/19 and 15h:35	15/10/19 and n/a	Yes

2.4.1.2 VOC sample collection

The headspace samples were dynamically collected onto the stainless steel Tenax TA/ Carbograph 5TD dual sorbent tubes (Markes International Llantrisant, UK) using an ACTI-VOC low flow pump (Markes International Ltd, Llantrisant, UK) to sample headspace VOCs at a constant flow. The ACTI-VOC low flow pump easily attaches to the sorbent tubes, it is light weight, easy to operate, and has a long-lasting battery. These advantages made it an ideal choice for the field sampling studies. Furthermore, this pump and type of sorbent tube had been previously used in several human and animal decomposition studies (7, 37, 38, 43, 64). The body shroud in which the donor arrived was sealed as soon as the donor was received at the UQTR morgue. The headspace VOCs were accumulated for 10 min. A small opening was created over the upper chest region in the body bag, one end of the sorbent tube was inserted in the headspace of the body bag and the other end was attached to the ACTI-VOC low flow pump (Figure 2-1). The sampling arrow was pointing towards the pump (Figure 2-1). The VOCs were collected at a constant flow rate of 100 mL/min. Initially, the sample volume collected was 500 mL. In accordance with the US EPA method TO-107 (88), the tubes were capped with brass

storage caps, wrapped in aluminium foil, and stored in a glass jar for transportation to the laboratory. These sorbent tubes were stored in an airtight glass jar at 4 °C until analysis. Control samples were not collected during this phase of the study.

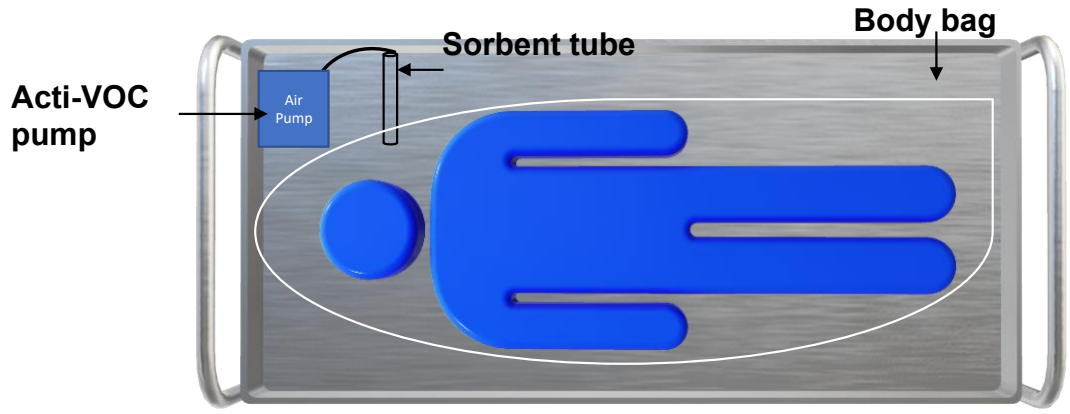

Figure 2-1 *Sample collection method from donors in the UQTR morgue using the ACTI-VOC low flow pump and sorbent tube.*

2.4.2 Method development

To characterise the human odour in the early post-mortem period it was essential to develop a suitable analytical method. The newer Pegasus®BT 4D GC×GC-TOFMS (LECO Corporation, St Joseph, MI, USA) had several key differences to the Pegasus® 4D GC×GC-TOFMS (LECO Corporation, St Joseph, MI, USA) used in the pilot study (87), such as a new BenchToF configuration which has a higher sensitivity. The default ion source temperature had increased to 250 °C, an increase of 50 °C from the previous instrument in the pilot study. This higher ion source temperature could lead to changes in the spectra of heavier *m/z* compounds. The 2D column had a smaller film thickness (µm df) of 0.25 mm compared to 0.50 mm for the pilot study. This change in the film thickness was due to the manufacturer's availability, the column provided had a film thickness of 0.25 µm instead of 0.5 µm and thus, the secondary column had reduced film thickness compared to the column used in the pilot study. Therefore, different parameters were applied to ensure adequate separation with the new instrument. The method

development was conducted in two trials and the results acquired were visually assessed in terms of chromatographic separation.

The analytes collected onto sorbent tubes were thermally desorbed using a TD100-xr autosampler thermal desorption unit (Markes International, Llantrisant, UK) and analysed using the Pegasus®BT 4D GC×GC-TOFMS (LECO Corporation, St Joseph, MI, USA). A 1.2 m uncoated silica fused transfer line connected the TD100-xr to the Pegasus®BT 4D GC×GC-TOFMS system. This transfer line was maintained at 150 °C and the TD100-xr was controlled by Markes Instrument Control (MIC) (version 2.0). ChromaTOF® (version 5.51.6.0; LECO) was used to control the Pegasus®BT 4D GC×GC-TOFMS (LECO Corporation, St Joseph, MI, USA). The sorbent tubes were thermally desorbed at 300 °C for 4 min onto the general-purpose cold trap held at -10 °C followed by trap desorption at 280 °C for 3 min. A 30 m × 0.250 mm (ID), 1.40 µm film thickness (df) Rxi®-624Sil MS column (Restek Corporation, Bellefonte, PA, USA) was used in the first-dimension (1D). A 2 m × 0.250 mm ID, 0.25 µm df Stabilwax® column (Restek Corporation, Bellefonte, PA, USA) was used in the second-dimension (2D). A SilTite µ-Union (Restek Corporation, Bellefonte, PA, USA) was used to connect the 1D and 2D columns. High purity helium (Linde Inc, Trois-Rivières, Québec, Canada) was used as the carrier gas at a constant pressure of 17.8 psi. The modulator temperature was offset +15 °C relative to the 1D oven. The temperature of the MS transfer line was maintained at 250 °C. The parameters mentioned above were not changed during the method optimisation.

2.4.2.1 Method development: First stage

During the first stage of the method development the column flow and temperature ramp were calculated with Restek EZGC® method translator and flow calculator software (Restek Corporation, Bellefonte, PA, USA). The modulation period and acquisition rate were derived from the Simply GC×GC™ tool developed by LECO (LECO Corporation, St Joseph, MI, USA). The free online software assists users in GC×GC method development for a given column configuration. The parameters such as GC ramp temperature (^{o}C/min), trap split, 2D oven offset

to 1D (^{o}C), modulation period (s), and acquisition rate (spectra/s) were changed after review of visual output for each sample (Table-2-2).

Table 2-2 *TD-GC×GC-TOFMS parameters used in the first stage of the method development for each sample.*

Sample Id	**UQTR Donor Id**	**Trap Split**	**GC Parameters ^{1}D (^{o}C/min)**	**^{2}D Oven Offset to ^{1}D (^{o}C) and Modulation Time (s)**	**Acquisition Rate (spectra/s)**
601947	2019-33	Splitless	Initial temperature 40 ^{o}C for 5 min then raised to 230 ^{o}C at 6.60 ^{o}C/min	10 ^{o}C and 3 s	100
601938	2019-34	Splitless	Initial temperature 40 ^{o}C for 5 min then raised to 230^{o}C at 6.60 ^{o}C/min	5 ^{o}C and 1.8 s	230
601920	2019-35	Splitless	Initial temperature 40 ^{o}C for 5 min then raised to 230^{o}C at 6.60 ^{o}C/min	5 ^{o}C and 3 s	230
601914	2019-46	5 mL/min	Initial temperature 40 ^{o}C for 2 min then raised to 230 ^{o}C at 6.60 ^{o}C/min	10 ^{o}C and 3 s	230
601944	2019-44	5 mL/min	Initial temperature 40 ^{o}C for 2 min then raised to 230 ^{o}C at 4 ^{o}C/min	10 ^{o}C and 4 s	250

The visual chromatographic results of the first stage are shown in Figures 2-2 and 2-3. The results of the method development were evaluated in terms of peak resolution. Please note that VOC profiles of cadavers can vary significantly due to internal and external factors (Section 1.4.1), and this fact was considered during the assessment of the chromatograms. The results showed that the sample collection method was able to capture volatiles from the headspace of the body bag. The spitless and 5 mL/min trap split injection caused sample overload and co-elution in the column. The ramp of 6.60 ^{o}C/min reduced ^{1}D separation as the temperature increased. Moreover, the lower modulation period of 3 s and 1.8 s led to second-dimension peak tailing as shown in Figure 2-2 and 2-3 below. The Restek EZGC and LECO method

development tools helped to understand the chromatographic outcomes and areas where parameters could be improved.

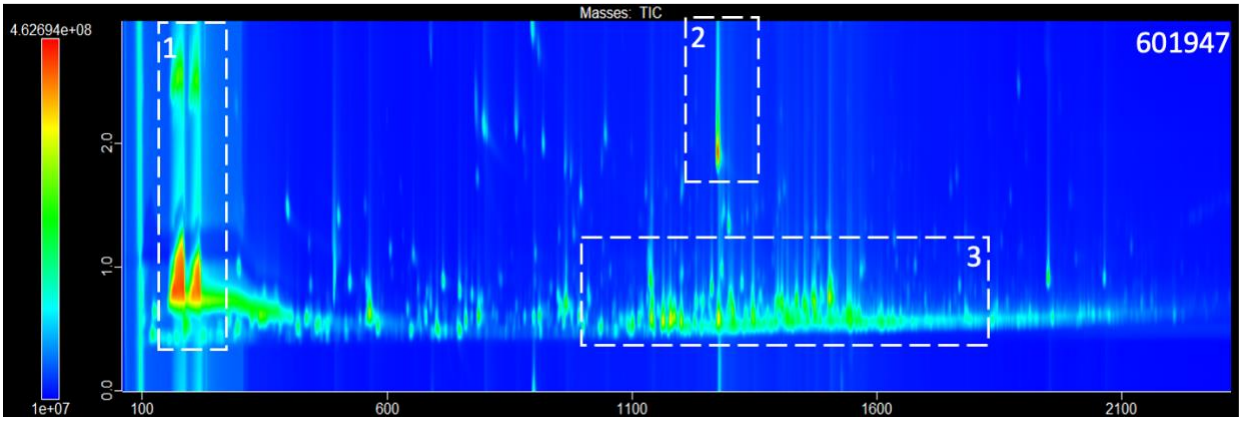

Figure 2-2 *2D chromatogram of the sample 601947 analysed in phase 1 showing 1) wraparound of ethanol peak, 2) second-dimension peak tailing, and 3) poor separation in 1D with a splitless injection, 10 ^{o}C 2D oven offset and 3 s modulation.*

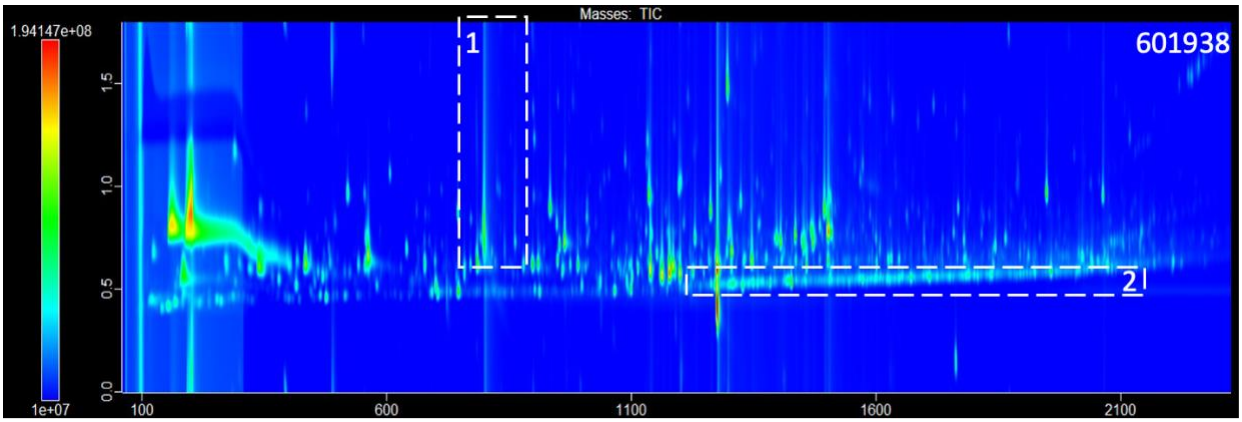

Figure 2-3 *2D chromatogram of the sample 601938 showing 1) second-dimension peak tailing, and 2) poor 1D separation with a splitless injection, 5 ^{o}C 2D oven offset and 1.8 s modulation.*

Following the analyses and review of samples (601947, 601938, 601920, and 601914), several GC parameters were changed since the sample accumulation time and volume planned for future morgue and outdoor studies was going to be double the time (10 mins vs 20 mins) and volume (500 mL vs 1 L) used in the method optimisation. Thus, the degree of second dimension peak tailing was a concern at the first stage of method optimisation. Specifically, the GC ramp

was slowed down to 4 ^{o}C/min, and a 10^{o}C 2D oven offset to ^{1}D was selected to reduce the 2D retention time of the analytes (see Table 2-2). The modulation period was increased to 4 s to prevent second-dimension peak tailing. The acquisition rate was changed to 250 spectra/s to address the narrow peak width produced with this instrument (see Table 2-2). For the 5th sample (601944) the second-dimension peak tailing was significantly reduced (Figure 2-4) following the adjustments listed above. The total trap split was increased and finalised to 20 mL/min (11:1) to counter highly concentrated samples that might be analysed in the future.

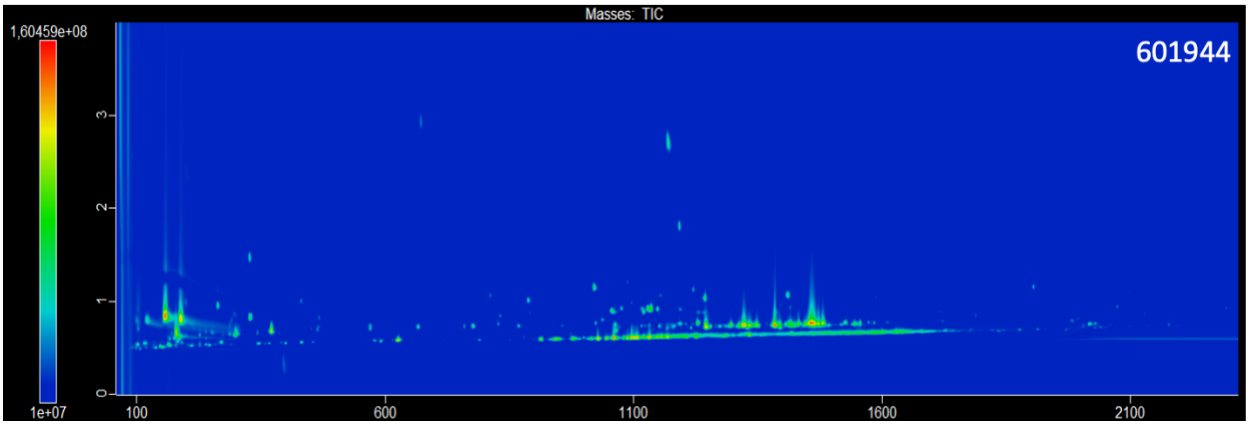

Figure 2-4 *2D chromatographic output of 601944 analysed in the first trial with 4 ^{o}C/min ramp and 4 s modulation period showing a reduction in second-dimension peak tailing of peaks.*

2.4.2.2 Method optimisation: Second stage

In the second stage, another six samples collected from donors in the UQTR morgue were analysed. Prior to sample analysis by the Pegasus®BT 4D GC×GC-TOFMS (LECO Corporation, St Joseph, MI, USA), an internal standard consisting of 0.2 µL of 150 ppm bromobenzene (HPLC grade, Sigma-Aldrich, Oakville, ON, Canada) was prepared in methanol (HPLC Grade, Sigma-Aldrich) and injected onto each sorbent tube using an eVol® XR handheld automated analytical syringe (SGE Analytical Science, Wetherill Park , NSW, Australia) for the purpose of internal standard normalisation of analytes.

The 1D oven temperature was maintained at 40 °C for 2 min and then increased to 230 °C at a rate of 4 °C/min, held at 230 °C for 5 min. The modulator temperature offset was +15 °C and the 2D oven temperature offset was +10 °C. The modulation period was 5 s with a 1.25 s hot pulse. The temperature of the MS transfer line was maintained at 250 °C. Spectra were acquired at a rate of 250 spectra/s with a mass acquisition range of 29-300 amu. The ion source temperature was 250 °C, the electron ionisation energy was 70 eV. After thermal desorption, each sorbent tube was reconditioned for 30 min at 330 °C under a split flow of 50 mL/min. The total run time, including sorbent tube desorption, GC×GC-TOFMS analysis and sorbent tube reconditioning was 1 h and 30 min. The sorbent tubes were wrapped in aluminium foil and stored in a glass jar at room temperature, ready for further sample collection.

The introduction of a higher split ratio (11:1) and 5 s modulation period improved separation and reduced co-elution of peaks in ^{1}D (Figure 2-5). The concentration of the internal standard was reduced to 0.2 µL of 50 ppm for future analysis to prevent the overloading of the internal standard onto the column. This analytical method was finalised for future sample analysis.

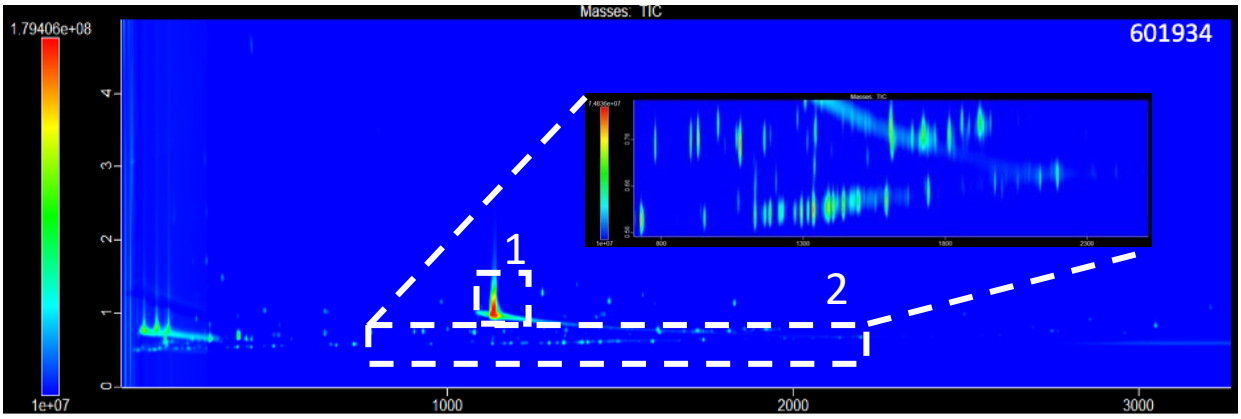

Figure 2-5 *GC×GC-TOFMS total ion current (TIC) contour plots of headspace samples collected from the sample 601934 analysed in the second stage with a 11:1 mL/min split injection, 4 °C/min ramp, and 5 s modulation period with the highlighted sections: 1) the internal standard peak, and 2) magnified aspect showing better peak separation in ^{1}D.*

2.5 Phase 2: Application of the optimised method to identify VOCs from cadavers in a controlled morgue environment during the early post-mortem period

Collection of headspace VOC samples was subject to the availability of the donors. During this study, eight human cadavers were sampled, of which four were female donors, and four were male donors. These donors were also placed for sample collection at the REST[ES] facility as reported in Chapter 3. The objective of this part of the study was to determine the VOCs released from human remains in a controlled environment in the absence of external factors that contribute to the decomposition process. Table 2-3 shows details of the donors sampled in a controlled, clean, and sterile morgue environment.

Table 2-3 *Details of donors sampled in Phase 2 of the study (Note: VOC samples were collected again after the placement of these donors at the REST[ES] facility).*

Donor id	**Age (yrs)**	**Sex**	**Date of death (dd/mm/yy)**	**Receipt date at UQTR morgue (dd/mm/yy)**	**Sample collected at PMI (h)**
H1	55	M	05/08/20	07/08/20	40
H2	71	M	07/08/20	08/08/20	21
H3	69	F	27/09/20	28/09/20	22
H4	79	F	04/10/20	05/10/20	33
H6	77	M	10/05/21	10/05/21	16
H7	91	M	21/06/21	22/06/21	24
H8	93	F	09/07/21	09/07/21	18
H9	72	F	30/07/21	30/07/21	14

2.5.1 VOC collection

In Phase 2, the VOC accumulation and sample collection time were modified from 10 to 20 min and 500 mL to 1 L, respectively. These modifications kept the sample collection method consistent, allowing future VOC profile comparison between donors profiled at the morgue and the REST[ES] facility. Additionally, the samples were collected in triplicates, and morgue blank samples were also collected during the sample accumulation time to account for the background VOC profile of the morgue. However, collecting a control sample released from the body bag with a representative sample volume of the experimental sample (1L) was challenging in this study. The following practical considerations for studying (i) and comparing the VOC profile of the body bag (ii) should be considered. Note that the practical consideration while studying the body bag is discussed first.

I. Practical consideration while studying the VOC profile of the body bag:

- The clean body shrouds that were used at the local hospital to transport the donors were inaccessible.

- The body shroud in which the donor was transported could not be used to collect a control sample as the material collapsed without a body, limiting the chances of creating a headspace and collecting a representative volume (1L) as the experimental sample.

- In cases when sample collection was attempted with the empty body shroud, the fault indicator turned on the Markes ACTI-VOC pump, indicating changes in flow and flow fault due to excessive back pressure.

- Thus, a background sample of the morgue room was collected instead where the body was placed after its arrival.

II. Practical considerations while comparing the body bag materials:

Around the world, morgue and local hospitals have different protocols for transporting and handling human remains. Moreover, materials (e.g., body bags, hospital tags, paperwork) used to transport a donor can vary depending on local supply chain and biohazard protocols of provincial and federal authorities. Thus, the materials used vary making it difficult to compare body bag data across the limited, published studies conducted in a morgue (6, 8). Further, there is a lack of studies conducted on cadavers in a morgue environment during the early post-mortem period and the discussion within these reported studies (1,2) is more focused on the early post-mortem VOC profiles of human remains.

Based on the experience of the author working in the anatomical and surgical departments in India, Australia and Canada, body bags used to transport donors will also change when a donor has been received from a different province or state. Having said that, the author acknowledges the importance of studying VOCs released from body bags. Therefore, in the future work section of the thesis, the development of universally available body bags (such as those recommended for disaster victim recovery) for VOC sample collection in a morgue was proposed for future VOC research.

2.5.2 VOC analysis

Prior to sample analysis by Pegasus®BT 4D GC×GC-TOFMS (LECO, St Joseph, MI, USA), an internal standard consisting of 0.2 µL of 50 ppm bromobenzene (HPLC grade, Sigma-Aldrich, Oakville, ON, Canada) was prepared in methanol (HPLC Grade, Sigma-Aldrich) and injected onto each sorbent tube using an eVol® XR handheld automated analytical syringe (SGE Analytical Science, Wetherill Park BC, NSW, Australia) for the purpose of internal standard normalisation of analytes. The analytical method used for the rest of the study is the same as indicated in the second stage of the method optimisation (section 2.4.2.2).

2.5.3 Data processing

ChromaTOF® (v.5.51; LECO), a new software version provided with the Pegasus®BT 4D GC×GC-TOFMS instrument, was used to process the GC×GC-TOFMS data. Previously, to analyse the VOCs released during the decomposition process, studies using the LECO Pegasus® 4D GC×GC-TOFMS instrument have used ChromaTOF (v.4.5) along with the Statistical Compare package for data processing and peak table alignment. The data processing method in ChromaTOF® (v.5.51; LECO) provided with the BT instrument has several key differences compared to the older version of the software and Pegasus 4D GC×GC-TOFMS, detailed in Table 2-4.

***Table 2-4**: Differences in the data processing options between ChromaTOF v.4.5 and v.5.51.*

Available options within the data processing method	**ChromaTOF (v.4.5)**	**ChromaTOF (v.5.51)**
Baseline integration (note: this feature has different name in ChromaTOF v.5.5.1)	Included	Included
Baseline offset	Included	Not included
Target analyte find feature integration with peak finding	Not included	Included
Sub-peak settings (minimum S/N ratio for sub-peaks)	Included	Not included
Expected Peak widths in 2nd dimensions	Included	Not included
Spectral match required to combine	Included	Included
Statistical Compare integration with the acquired data	Included	Not included
Library search options	Included	Included

An optional ChromaTOF Statistical Compare software (v.4.74) sold separately was available, but due to the considerations listed below, this software was not used for the current study. (Note: the manufacturer provided these considerations).

1. BT data has less noise than HT or 4D data, therefore higher S/N will be calculated at a higher value in ChromaToF (v.4.74) software than would be calculated in the BT 4D (v.5.51) software. A minimum S/N threshold of 500 to 1000 was recommended as appropriate to reduce small noise peaks.

2. The deconvolution algorithm was designed for Pegasus HT/4D and there were concerns that the software may not perform optimally for the imported BT 4D data.

3. Differences in the common mass values were noted between data exported to ChromaToF (version 4.74) and ChromaToF (v.5.51). Differences in the masses prevented the sample export into the statistical compare step in the ChromaTOF (v.4.74).

4. Both the software programs used different file formats (netCDF vs .smp). Therefore, a single file had to be processed and stored in two different file formats due to the differences in the data processing options which led to different data outputs.

Data Processing in ChromTOF (v.5.51;LECO)

Pegasus®BT GC×GC-TOFMS data was acquired and processed with ChromaTOF® (v.5.51; LECO). The data processing steps included: non targeted deconvolution (NTD®) peak finding with integration baseline; GC×GC subpeak combining; and library searching. During the NTD peak finding, the minimum S/N ratio of 1 was used for peak finding and for integration baseline the default option of 'auto-calculated' was selected. The minimum spectral match required to combine GC×GC sub-peaks was set at 650. The minimum similarity for spectral matches was set to 600 and minimum similarity before a hit was set to 800. Lower primary match selection criteria for the S/N ratio were used during the data processing step to increase the library

search results. Further alignment and data filtering steps at the peak table level were performed in RStudio Workbench (2022.02.2, build 485.pro2), as described below.

Data Processing in R

The peak tables of each sample with their respective replicates and controls were exported as xlsx files. The exported peak tables contained information including peak number; name; formula; retention times (RTs); 1st dimension retention times (RT1); 2nd dimension retention time (RT2); similarity; area; height; quant mass; base mass; quant S/N; and peak S/N.

Peak Table Alignment

Decomposition studies published in the literature have commonly used a LECO software produced, integrated peak table alignment solution called Statistical Compare (7, 37, 38, 63, 64). The integrated software solution was not available with the current software package, as discussed above. The absence of an integrated software solution led to the development of a series of peak table alignment scripts in the R programming language [https://zenodo.org/record/7713417#.ZAoXiNLMK-Y], which would allow alignment of peak tables across the samples using the peak table output. These R programming scripts were written in collaboration with Prof. Wesley S. Burr, an Assistant Professor of Statistics at Trent University. The peak table alignment was based on retention times matching criteria and mass values (base mass and quant mass), following a spectral match performed with the NIST library. All the peaks within the peak table had a similarity and reverse spectral match factor > 800 with the NIST spectral library. The retention time match criteria were set to 2 modulation periods: the first-dimension (10s), and second-dimension (0.06s). The values of retention time match criteria for the first and second-dimension were derived from the retention time values of the internal standard and decomposition standard mix. A chromatographic region after 2500 s in the first-dimension was excluded from the alignment process, as the majority of the peaks identified after this period were not compounds of interest (e.g., siloxanes and non-detects).

Before peak alignment, the dataset was classified into controls and experimental classes. The control class comprised samples collected as background samples during the morgue and REST[ES] study. The experimental class consisted of donor samples collected in the morgue and at the REST[ES] facility with their respective replicates. During the peak table alignment process, each peak within a peak table was considered to be unique for its consistent pairwise comparisons across all the samples present in the class. For each peak, pairwise comparison criteria such as name, minimum S/N of 100, retention time matching criteria (10s and 0.06s) and mass values were used to ensure consistent matching of integrated peaks identified in the sample, and across all the samples present in the class. Once this was complete, and all identified peaks were isolated by sample, we proceeded to the second stage of the analysis, starting with a sliding window identification of commonality by compound.

Verification of Peak Table Alignment

A sliding window function was used to verify the alignment of peaks within peak tables, as the alignment procedure resulted in multiple RTs and masses per NIST-detected compound. This function consisted of a rectangular window made up of the first and second retention time windows, as used in the retention time match criteria. For a given compound, the sliding window function found the highest number of incidences of any common mass within the rectangular window. The identified maximum window region was then analysed to determine the centroid retention times, and the common mass of a given identified compound. All other "detections" were then removed from the data set. This ensured that every single compound considered in the following stages had common detection identification, common mass, and retention times within the precision of the variation of the internal standard and decomposition standard mix. This should ensure, as much as is possible, that any compound detections in the following are truly considering the same compound, across samples and controls both.

Normalisation and General Function Cleaning

Following the peak table alignment, the samples were normalised to the peak areas of the internal standard, by sample, so that comparisons could be made of peak area across samples. This function was applied to both the morgue and REST[ES] datasets. After the alignment process the normalised inputs of each individual donor for both control and experimental samples were then passed through the following filter and joining procedures. In the peak filtering process, peaks identified in control samples were extracted and compared against their respective triplicate experimental samples. The aim was to remove background peaks and retain relevant peaks within an experimental sample (e.g., donors) and its replicates. Any peaks uniquely identified in control samples were filtered out. Peak area and S/N ratio were used to determine the abundance of a peak. A peak identified in the control and the experimental sample was only retained in the experimental sample if it was identified at an abundance twofold or greater compared to its control sample. After filtering according to the control, joining of the triplicate samples were considered, and peaks which were present only in all three triplicate samples were retained. The average peak area was computed for each compound and each triplicate, in order to be used in the analysis that follows.

For each donor, after the clean function, the remaining outputs were considered relevant to the experimental sample and were merged based on common presence across the respective replicate samples. The compounds such as siloxanes, oxygen peaks, acetone, etc. were removed from the list. After this process, all individual donor data frames were merged into a single file comprising a list of compounds identified across all the donors. Further details on the scripts are available on GitHub [https://github.com/wesleyburr/GCxGC_Morgue_RESTES].

Principal component analysis (PCA) was performed using the Unscrambler X (version 10.5; CAMO Software, Oslo, Norway). Mean centring, standard deviation scaling and unit vector normalisation were all applied to the datasets prior to PCA. The data contained no outliers by way of Hotelling's T^2 95% confidence limit.

2.6 Results

The VOC profiles of the donors were collected during the fresh stage of decomposition, with the exception of H1. H1 died as a result of suicide, was undiscovered for ~24 h, and showed initial signs of autolysis and putrefaction during sample collection. All other donors only showed gross signs of decomposition such as livor mortis, algor mortis and rigor mortis at the time of arrival at the UQTR morgue. During sample collection, a headspace was created by sealing the body shrouds to create a body bag, and the VOCs that accumulated in the headspace of the body bags were actively collected onto the sorbent tubes. The representative contour plots of two dimensional chromatograms of the VOC samples collected in the morgue from different donors have been added in the Appendix A. These sorbent tubes were analysed using the Pegasus®BT 4D GC×GC-TOFMS.

2.6.1 Overall VOC class and individual donor class detected in the morgue

There were 580 VOCs identified as significant in the morgue dataset (n=8 donors). VOCs were considered significant if they were either uniquely present in one or more donors (including the replicate samples) or detected at an S/N twice that of a control sample. Differences in the VOC class were identified when the individual donor VOC class was compared with the overall VOC class (n=580 VOCs). The total number of VOCs detected per donor ranged from 83 to 159 ranging from 14% to 27% of the total VOCs detected (n=580). This highlights the variation observed in the VOCs between donors in the same environment at different post-mortem intervals (Figure 2-6).

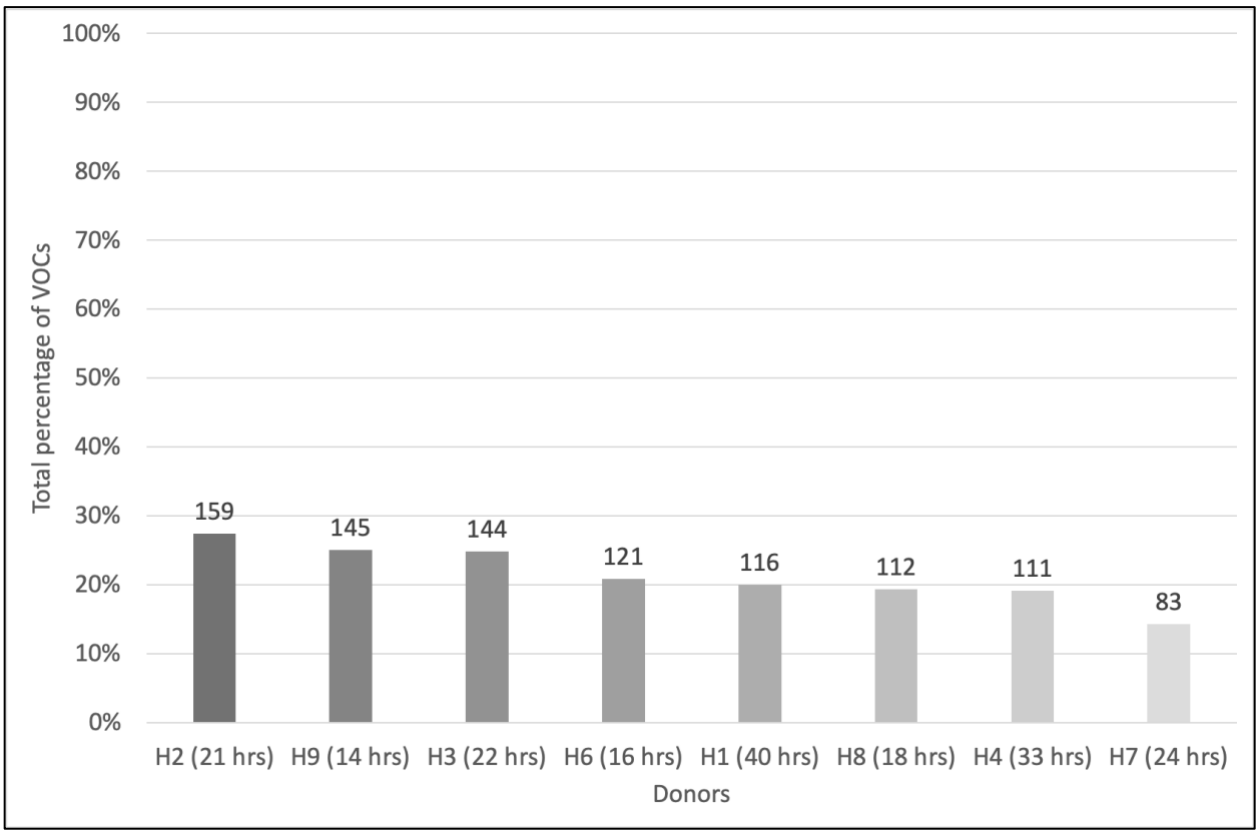

Figure 2-6 *Percentage difference observed at 14 to 40 h PMI between the number of VOCs of an individual donor vs the total VOCs identified in all eight donor samples (Note: PMI intervals are approximate time values and shown in increasing order for the donors).*

The VOCs were classified into their compound classes according to the functional groups: acids, alcohols, aldehydes, aromatics, cyclic aliphatic compounds, esters and analogues, ethers, halogen-containing compounds, ketones, linear aliphatic compounds, nitrogen-containing compounds, and sulfur-containing compounds. The analogues are anhydrides and lactones in the ester and analogue compound class. These VOC classes have been previously reported in human decomposition studies conducted in morgue or outdoor scenarios (37, 48, 81). The linear aliphatic compounds (n=93), esters and analogues (n=83), aromatics (n=79) and alcohols (n=72) were the most abundant chemical classes identified in the early post-mortem VOC profiles of the donors collected in the indoor morgue scenario. Compound classes such as ethers (n=25), aldehydes (n=20), acids (n=11), and sulfur-containing compounds (n=6), were the

least abundant chemical classes. Figure 2-7 shows the number of VOCs identified by compound class in the morgue study.

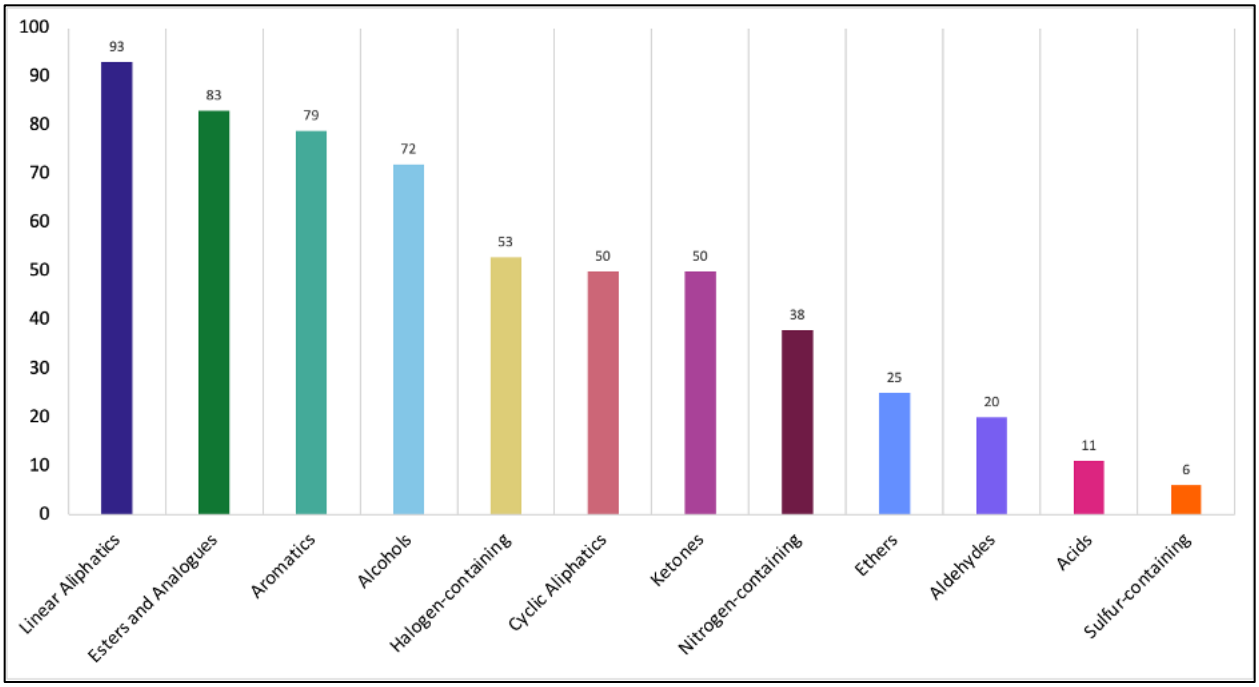

Figure 2-7 *Number of VOCs identified by chemical class (high to low) in the morgue study from all eight donors.*

The compound class with the most abundance varied across the eight donors. The linear aliphatic compound was the most abundant class in donors H6 and H9, while in donors H2 and H4 esters and analogues were the most abundant class. Compound classes that were most abundant in donor H3 and H7 were aromatics and alcohols. The acids and sulfur-containing compounds were the least abundant classes identified in the early post-mortem VOC profiles collected at the morgue (Figure 2-8). These compound classes were not identified in donor H7.

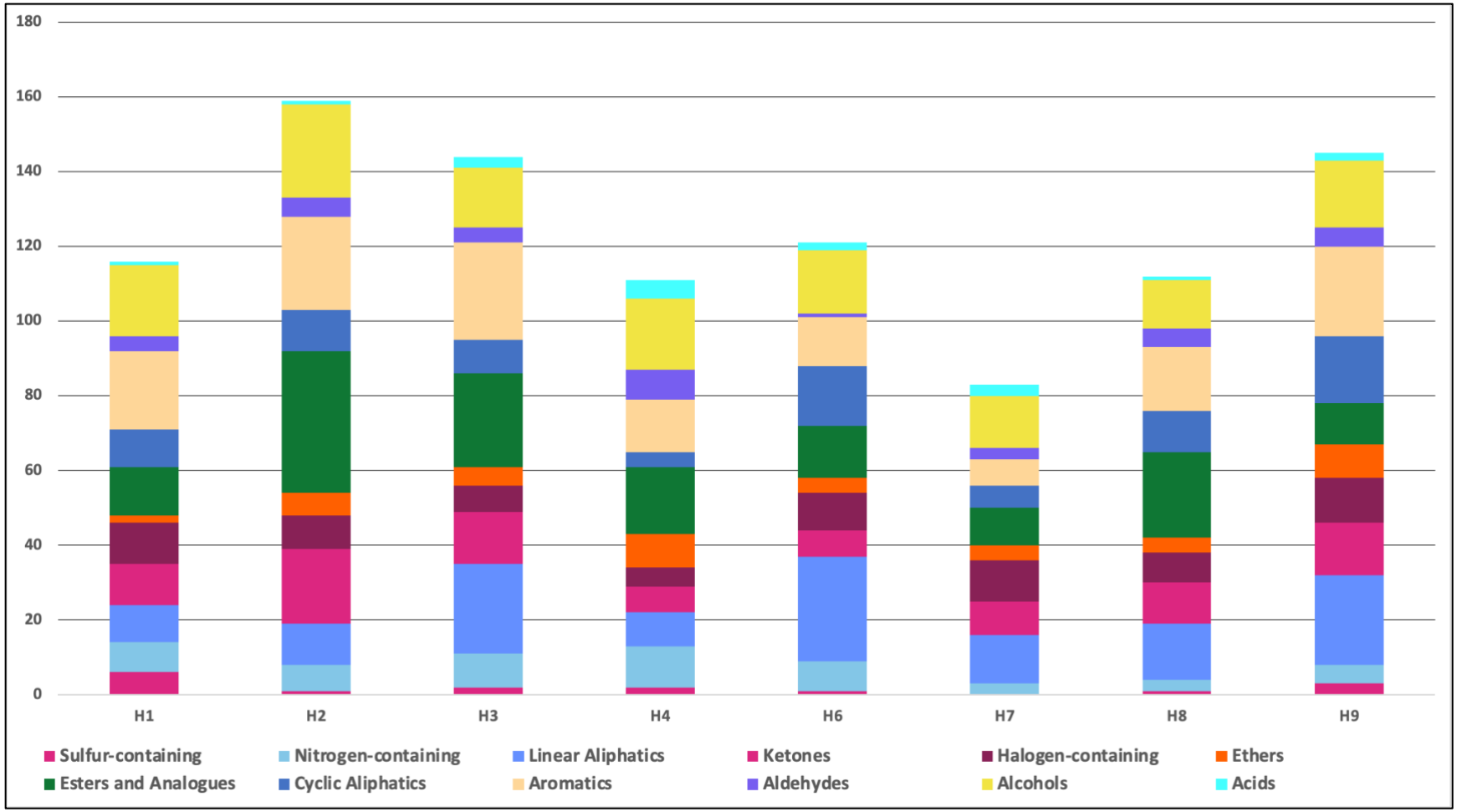

Figure 2-8 *VOC chemical class distribution per donor identified during the early post-mortem period in the morgue study.*

104 VOCs were detected with a minimum detection frequency of 3 which means that these VOCs were detected in a minimum of three donor samples including their replicates from the eight donors analysed in this study (thus, were present in 37.5% of the samples). All the compound classes reported in the overall class abundance were identified within these 104 VOCs (Appendix A).

2.6.2 VOCs related to medication

Two VOCs (propofol and methenamine) related to donor medications were identified in the headspace of donors H3 and H4 (Table 2-5). The compound classes associated with these medications were alcohols and nitrogen-containing compounds. The identification of volatiles related to medication in the headspace of the cadaver during the early post-mortem period is a new and unexpected finding of this study as the information regarding medications administered to these donors were not shared in their death certificate. These medications were identified in donors H3 and H4, but they were not common between the donors.

Table 2-5 *List of VOCs related to medications identified in the headspace of the body bags containing donors in the morgue study.*

VOCs	**Chemical class**	**Donors**	**Uses**	**Reference**
Propofol	Alcohol	H3	Inhalation and intravenous anaesthetic	(89)
Methenamine	Nitrogen-containing compound	H4	Antibacterial urinary tract infection	(90)

2.6.3 Statement of philosophy for data interpretation

To date, decomposition odour research has extensively focused on the VOC profile released from cadavers or human remains during the overall decomposition process. However, it has been reported that the VOC profile during the early post-mortem period is dynamic and can contain remnants of an individual's ante-mortem odour (64). The early post-mortem VOC profile from human remains has rarely been studied in the literature. The current study is a pilot study conducted in Quebec, Canada. Therefore, the significance of the VOCs identified in the early post-mortem VOC profile were based on "coincidences". Coincidences in the context of this study were identification of VOCs during the early post-mortem period across different post-mortem time intervals as a result of the decomposition process. The significance of coincidence in relation to the VOCs presented randomly at different post-mortem intervals in different donors was based on their detection frequency in the experimental samples (e.g., donors) and all its replicates. The detection frequency of the compound across donors was used to determine the significance of the compounds identified in the early post-mortem period. This approach would be unusual in targeted analysis. However, in the context of the current study, this was deliberate as the research being conducted on the early post-mortem VOC profile was exploratory in nature, and there is a lack of prior literature or established understanding of the early post-mortem VOC profile released from cadavers in the field of forensic taphonomy. Thus, this study aims to address this knowledge gap in understanding the early post-mortem VOC profile through VOC collection during the early post-mortem period in a controlled morgue environment and outdoors (REST[ES] facility), and to analyse the data with a newer, more sensitive analytical instrument (Pegasus®BT 4D GC×GC-TOFMS). We also use coincidences to determine significant VOCs relevant to the early post-mortem VOC profile.

2.6.4 Principal component analysis

For principal component analysis (PCA), compounds were chosen based on their frequency of coincidences in multiple donor samples collected at different post-mortem intervals. Before the

PCA analysis, the pre-processing included mean centering, standard deviation scaling, and unit vector normalisation. These processing steps were performed for all the PCAs shown in this chapter. Initially, PCA analysis was conducted on all individual compounds (580 VOCs) having a minimum detection frequency of 1 out of 8 (donors). For example, Propofol has a detection frequency of 1 out 8 donors, which means it has only been detected in one donor (donor H3) across all its replicate samples. Figure 2-9 shows the PCA constructed from VOC samples collected from eight donors and 580 compounds. The principal components (PCs) accounted for 17% (PC-1) and 16% (PC-2) of the explained variance. All the donors except donor H3 were separated along PC-1 and the donor H3 was separated along PC-2, contributing to most of the explained variance among all the donors in the first two PCs (Figure 2-9a). This indicated that donor H3 had a large influence on the overall structure of the scores, which can skew the data. Figure 2-9b shows that the compounds were closely clustered along the origin and these compounds had the loadings values of less than 0.1 indicating weak influence on the donor samples. To further investigate the variance between the other donors, donor H3 was removed from the PCA.

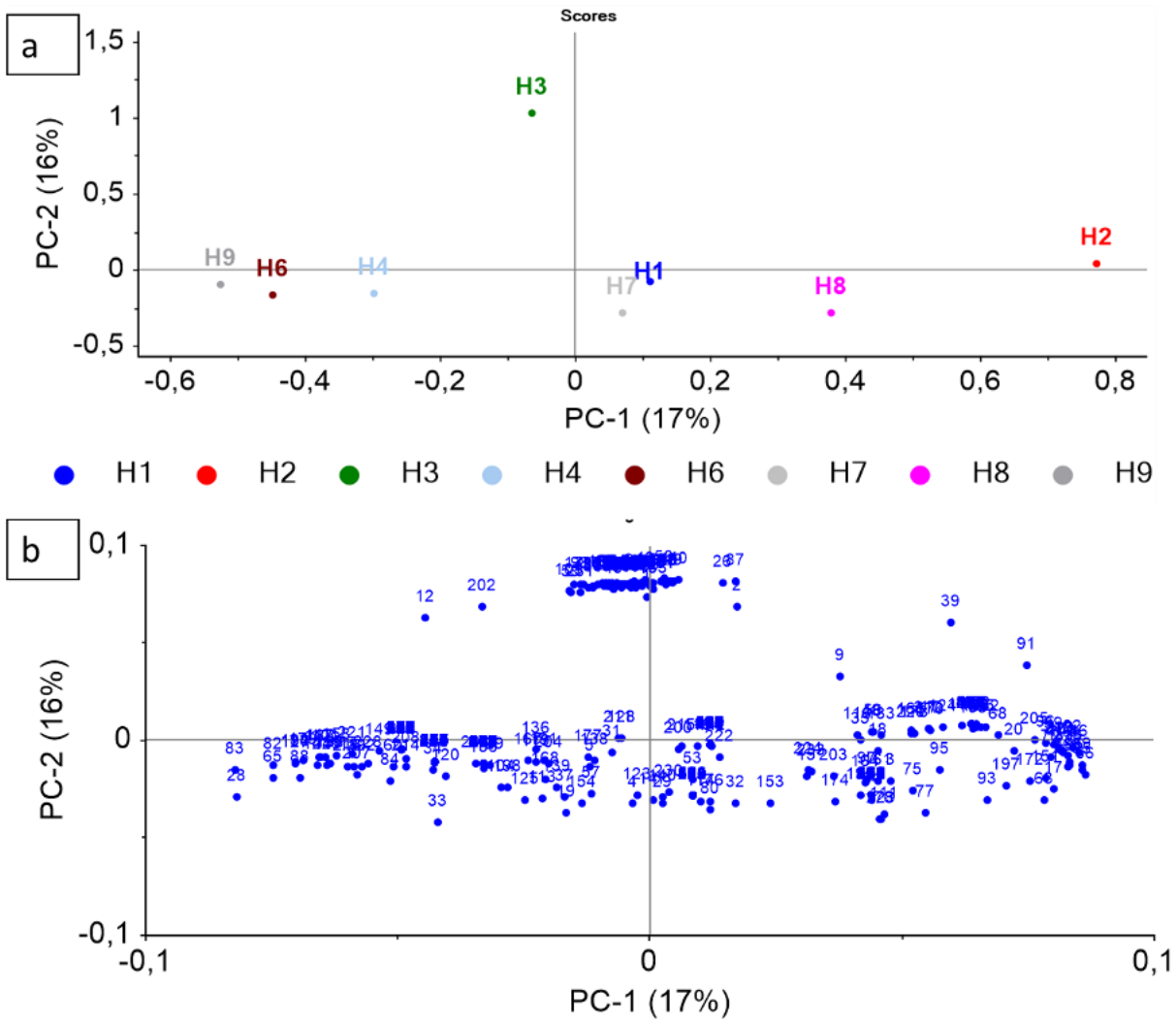

Figure 2-9 *PCA showing a) scores plot and b) loadings plot calculated using pre-processed GC×GC TOFMS data of 580 compounds identified across all eight donors. Donor H3 was separated along PC-2 from all other donors along PC-2. The loadings plot shows the distribution of compounds along PC-1 and PC-2 with compounds having a value less than 0.1 indicating weak association with the donors present in the scores plot.*

Further PCA was conducted on 104 selected VOCs on the basis of coincidences; this step was taken to better visualise the discriminatory information of more prominent analytes identified in the dataset. Figure 2-11 shows the PCA constructed with 104 compounds identified across seven donors. These 104 compounds had a minimum detection frequency of three out of eight (donors). The hotelling T2 95% confidence interval shows that there were no outliers in the data (Figure 2-10). Five PCs explained 88% of the variance in the data. PC-1 and PC-2 captured

42% of the total variation in the data while PC-3, PC-4, and PC-5 captured 17%, 15%, and 14%, respectively of the variation in the data.

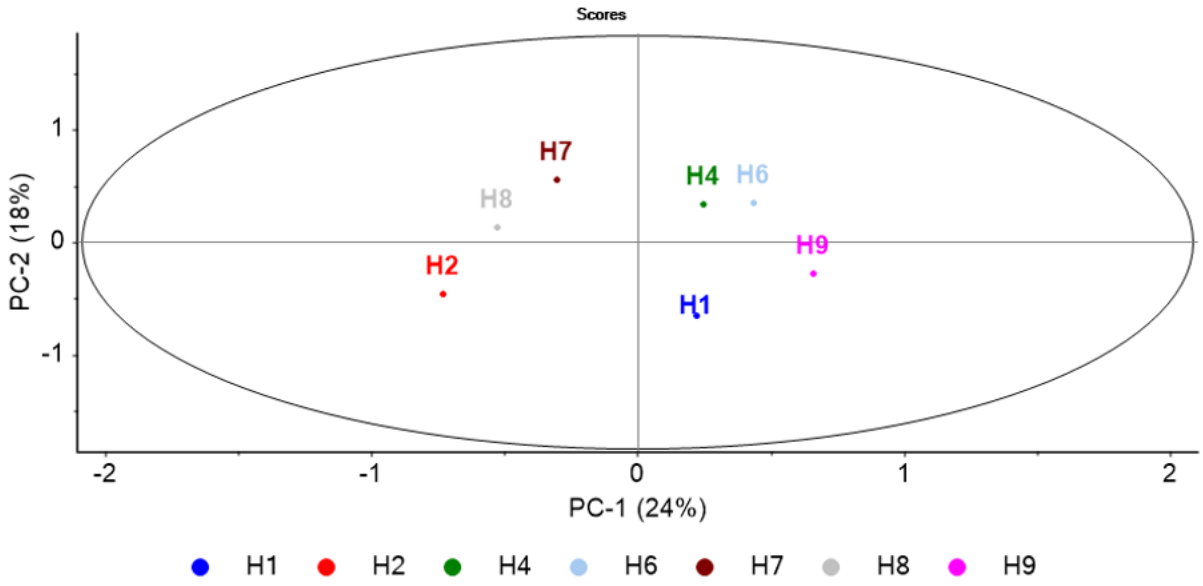

Figure 2-10 *PCA scores plot of first two PCs, PC-1, and PC-2. The scores plot of all the donors except donor H3 with T^2Hotelling ellipse showing no outliers present in the data.*

Notably, PC-1 vs PC-4 showed an interesting clustering pattern that can be related to the post-mortem interval (PMI) of donors (Figure 2-11a). VOC samples from donors H9, H6, and H8 were collected at a lower PMI (14, 16, and 18 hrs, respectively), while VOC samples from donors H1 and H4 were collected at a higher PMI (40 and 33 hrs, respectively). The VOC samples from donors H2 and H7 were collected at a PMI of 21 and 24 hrs. Figure 2-11a shows that the VOC samples collected from donors H9 and H6, at a lower PMI, formed a cluster along PC-1 (highlighted with blue circle), while the VOC samples collected from donors H1 and H4 at a higher PMI, were clustered along PC-4 (highlighted with a grey circle). VOC samples collected from H2 and H7 at a PMI of 21 and 24 hrs made a cluster along PC-1 (highlighted with a green circle), while VOC samples collected from H8 at a PMI interval of 18 hrs is separated from the rest of the donors along PC-4 (Figure 2-11a). The distribution of compounds in the correlation loadings highlighted potential VOCs associated with the corresponding donors (Figure 2-11b). The analytes present inside the region defined by the two ellipses, indicate how much variance

is considered by the PCA model (100% and 50% for the outer and inner ellipses, respectively). The compounds present closest to the outer ring showed strong association to the donor samples and are listed in Appendix A, Table A-3. The correlation loadings plot did not show a strong association of compounds with the corresponding donors H1 and H4. Therefore, the PCA were also performed using compound classes to investigate their influence on VOC profiles.

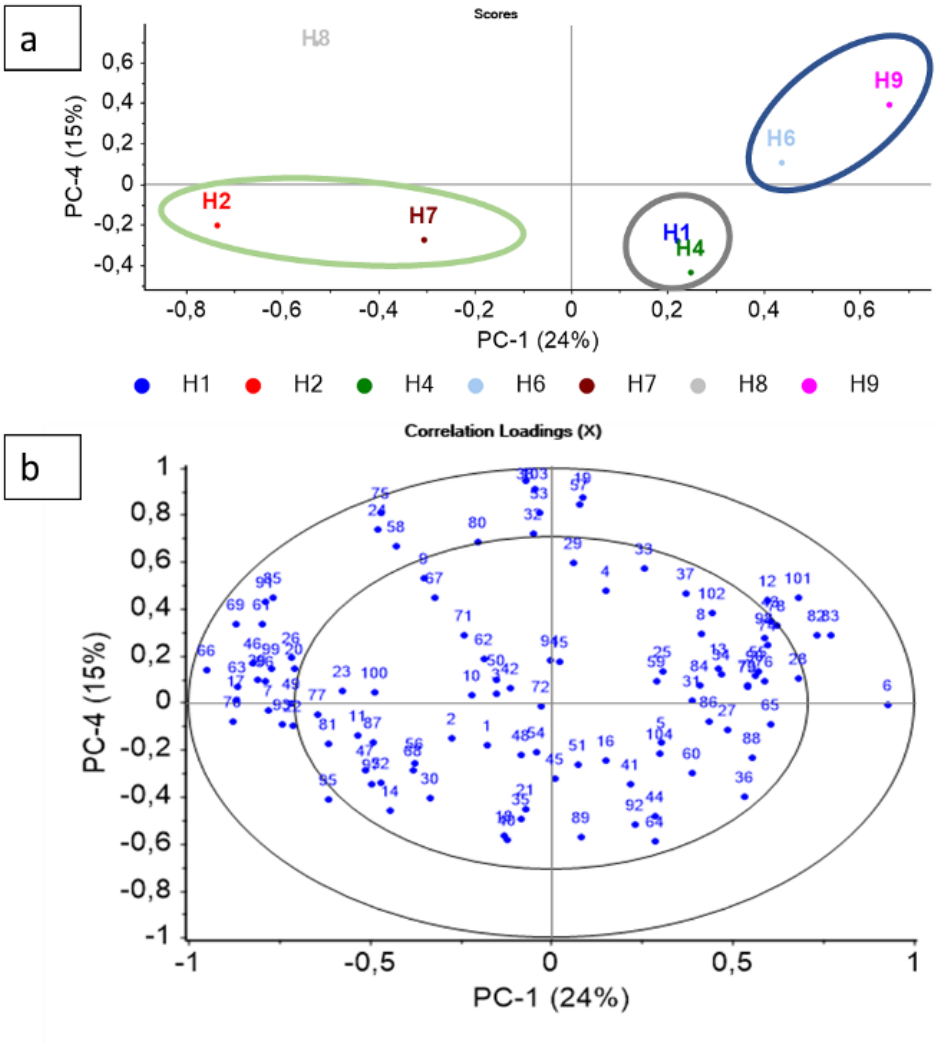

Figure 2-11 *PCA a) scores plot and b) correlation loadings plot for PC-1 vs PC-4. PCA were calculated using pre-processed GC×GC-TOFMS normalised peak areas of 104 compounds identified with a minimum detection frequency of three out eight. The scores plot of PC-1 vs PC-4 shows separation and clustering of donor samples collected at different PMI intervals. Here blue circles represent donor samples (H9 and H6) collected at lower PMI (14 and 16 hrs), grey circles highlight donor samples (H1 and H4) collected at higher PMI (40 and 33 hrs), and green circles highlight donor samples (H2 and H7) collected at PMI of 21 and 24 hrs. The correlation plots highlight VOCs contributing to the variances in the donor VOC profiles.*

Figure 2-12 shows a biplot of the scores and loadings made up of compound classes for the donors. For each compound class in the loadings, normalised peak areas were summed. Overall variability can be observed in the correlation of compound classes with donors (Figure 2-12). Notably, sulfur-containing compounds are positively correlated with the donors (H1 and H4) that had higher PMI (40 and 33 hrs), whereas donor H8 with a PMI of 18 hrs was positively correlated with compound classes such as aldehydes, ketones, and ethers (Figure 2-12).

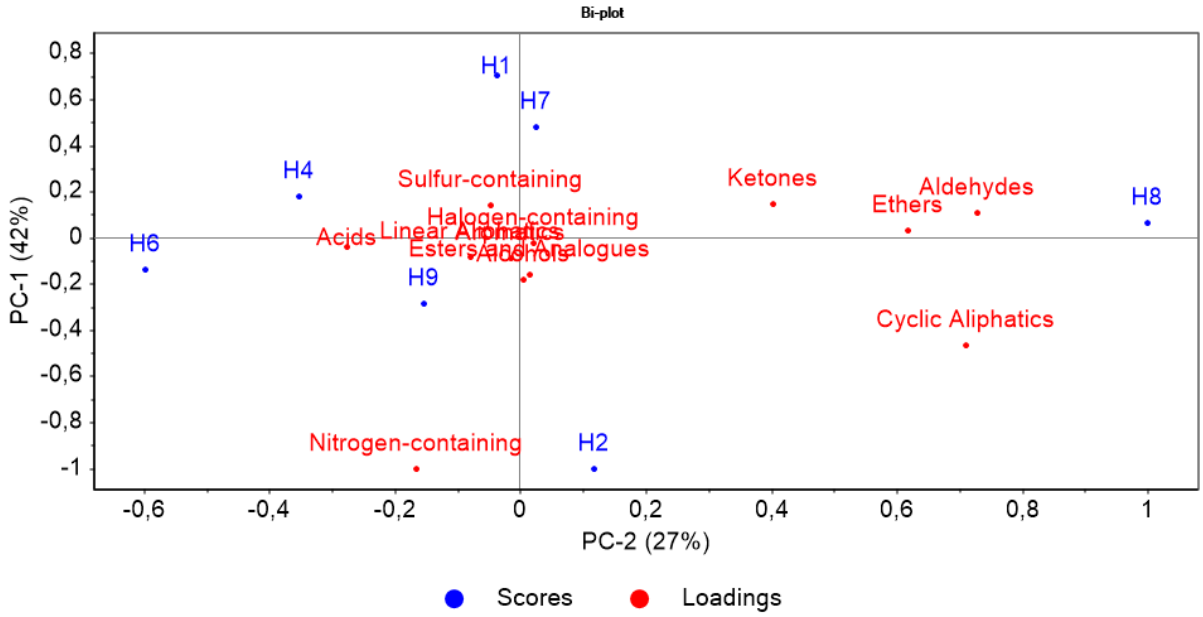

Figure 2-12 *Biplot of donors and compound classes, showing PCA scores and loadings calculated using donor and compound class data. Each compound class represents the sum of all the normalized peak areas of its constituent compounds.*

2.7 Discussion

2.7.1 Overall VOC class and individual donor class abundance detected in the morgue

During the early post-mortem period in the morgue environment, 580 VOCs were identified in the headspace of the body bag containing donors with a PMI between 14 to 40 h. Of the 580, 104 VOCs were detected in three or more donors. In comparison with other studies conducted

in a morgue (6, 8, 48), the number of VOCs detected in this study was on average 5% to 20% higher per donor. The application of two-dimensional chromatography and an optimised VOC collection method provided an analytical advantage in identifying the VOCs when compared to studies reported in the literature that used GC-MS. Previously conducted studies on VOC profiling of cadavers in an outdoor environment has reported an increase in the number of VOCs as the PMI interval increases (37). A correlation was not identified between the number of VOCs detected and the PMI at which the VOC samples were collected, since donor H9 which was sampled at 14 h post-mortem had a higher number of VOCs compared to donor H7, which was sampled at 24 h post-mortem (Figure 2-6). Thus, the trend observed in this study contradicts the previously reported trend of an increase in the number of VOCs as PMI increases in outdoor scenarios. Possible explanations for the variation in the donor VOC profile and the absence of a correlation between the PMI and VOC abundance could be linked to differences in the individual donor's biology, physiology, personal hygiene, and pathophysiology during the ante-mortem period (91). Further studies with a larger sample size and sample collection at different time intervals from the donors in the morgue is necessary to establish this potential relationship. All the donors in this study were refrigerated for a particular duration between their transport from the hospital to the UQTR morgue. A relationship between refrigeration, PMI sampling interval and VOC abundance was not seen during this study. Studying the effects of storage conditions (non-refrigerated vs refrigerated) on the donors was out of the scope of this study but is recommended for future studies.

Inter-donor variability in the number of VOCs and chemical class abundance was observed during the early post-mortem period (Figures 2-7 and 2-8). The variability in the number of VOCs and chemical class abundance suggests that the VOC profiles of the donors during the early post-mortem period are complex. Moreover, different VOC classes linked with complex biochemical processes occurring during life are detected, indicating the persistence of the living scent during the early post-mortem period. The variability among donors in terms of the number of VOCs and individual chemical class abundance per donor was not reported in the studies previously conducted in the morgue (6, 8). The sample size of the study, ethical

challenges, and restrictions for the use of cadavers for studying decomposition could possibly explain the lack of reporting as these studies were conducted on only one or two donors. To date, there has only been one study with a large donor sample set (n=21) conducted in the morgue (48). The authors of this study focused on differentiating between the live, deceased and animal scent and thus class abundance of an individual donor was not the focus of the study. Furthermore, the authors were focused on highlighting the potential application of this novel sample collection technique to identify key compounds related to the decomposition process. In contrast, variation in the number of VOCs among donors has been reported in decomposition studies conducted in an outdoor environment (37, 38). The common aspects in the current study and those studies (37, 38) is the analytical technique which allows separation of complex VOCs present in the decomposition odour allowing for its characterisation.

Different VOC chemical classes such as acids, alcohols, aromatics, aldehydes, linear aliphatic compounds, cyclic aliphatic compounds, esters, ethers, ketones, sulfur-containing compounds, halogen-containing compounds, and nitrogen-containing compounds were detected in this study (Figure 2-7). These compound classes have been previously reported in studies (37, 38, 63) conducted in an outdoor scenario or studies using GC×GC-TOFMS for sample analysis. Furthermore, these VOC classes have been detected in the headspace of skin samples potentially indicating that the VOC profile of an individual donor during the early post-mortem period could comprise VOCs that are by-products of biochemical interactions of microbial species on the skin, as well as due to early decomposition processes such as autolysis. The VOC studies conducted in an outdoor environment have reported these compound classes at later stages of decomposition (>72 h). The presence of decomposition VOCs in our morgue study also supports the theory that the process of decomposition commences as soon as 4 min after death (84). VOCs such as 3-methyl-1-butanol and dimethyl disulfide, previously detected in human decomposition studies, were detected at a PMI interval of 14 h in the current study (92, 93) indicating the initial transition of odour from ante-mortem to post-mortem. This would suggest that a change in the VOC profile from ante-mortem to post-mortem odour can be

detected using this sample collection method. Moreover, this change in odour can be detected as early as 14 h PMI.

Compound classes such as linear aliphatic compounds and esters and analogues were some of the most abundant classes detected in the current study. The production of these classes of VOCs have been linked with the breakdown of carbohydrates and fatty acids during the post-mortem period (29, 34, 94). These compound classes have also been detected in the skin volatilome and are produced due to the interaction of the microbiomes on the surface of the skin and with skin components (sebum, amino acids, sweat) (95, 96). However, the production of VOCs from the surface of the skin is dependent on factors such as physiology and pathology of an individual. Therefore, the VOC profile during the early post-mortem period could comprise VOCs which are linked to both ante-mortem and post-mortem odour making it challenging to characterise.

Sulfur-containing compounds such as DMDS were detected in five donors in this study. This finding supports previous decomposition odour research (6, 8, 37, 38, 97) where DMDS is one of the most commonly reported compounds due to its ability to act as a semiochemical (98). However, sulfur-containing compounds in this study, and in the early post-mortem period were identified with the least abundance. This compound class are end products of protein breakdown. Therefore, their lower abundance might indicate the process of protein degradation is in the beginning stages during the early post-mortem period and has not been sufficiently initiated. Moreover, compound classes such as linear aliphatic compounds and esters and analogues were the most abundant classes which would indicate the breakdown of carbohydrates and fats occurring earlier than proteins.

The most prevalent 104 compounds were chosen based on coincidences and their minimum detection frequency accounting for their presence in 38% of the samples collected. The 104 compounds were chosen as these compounds best represented the dataset and aided in visualisation of the data. Out of these 104 compounds, eight VOCs have been previously

reported in the headspace of skin, urine or in human scent studies. The details of these compounds are provided in Table 2-6.

Table 2-6 *Eight VOCs among the top 104 identified in donors in the morgue, with their frequency of detection, percentage abundance, sources of release, and citation in previous studies.*

VOC	**Frequency (out of 8 donors)**	**Percentage abundance (%)**	**Potential sources**	**Previously reported in the literature**
6-methylhept-5-en-2-one	7	37.5	Human scent study	(49)
Butyl acetate	5	62.5	Skin	(99)
Benzyl alcohol	3	37.5	Skin	(100)
Decanoic acid, ethyl ester	3	37.5	Skin	(95)
Hexanoic acid, methyl ester	4	50	Skin	(101)
1,3-Dioxolane, 2-methyl-	3	37.5	Skin	(1, 48)
2,3-Pentanedione	5	62.5	Skin (axillary skin)/sweat	(102)
1-Octen-3-one	4	50	Urine	(48)

Furthermore, 21 VOCs which have been detected in human decomposition studies conducted on human remains or human cadavers were detected in the headspace of the donors during the early post-mortem period in the morgue study (Table 2-7). This indicates that during the transition from ante-mortem odour to post-mortem odour, VOCs linked with the decomposition process can be detected during the early post-mortem period. Although the

abundance may vary, the headspace analysis of VOCs from the cadavers in an indoor morgue environment can lead to the identification of VOCs linked with the decomposition process and provide a baseline VOC profile of a person soon after death. The morgue study conducted by Statheropoulos et al. (6) and DeGreeff et al. (48) also reported VOCs related to decomposition processes, such as DMDS and DMTS that were detected in the early post-mortem period in a morgue scenario. This study supports the findings from the previous studies conducted by Statheropoulos et al. (6) and DeGreeff et al. (48).

Table 2-7 *Twenty-one VOCs among the most prevalent 104 VOCs identified in donors in the morgue, with their frequency of detection, percentage abundance and citation in previous studies.*

VOC	**Frequency (out of 8 donors)**	**Percentage Abundance (%)**	**Previously reported in the literature**
3-methyl-1-butanol	6	76	(103)
2-Pentanol	4	50	(103)
Octanoic acid, ethyl ester	4	50	(48, 97)
Furan, 2-pentyl-	3	37.5	(104)
3-methylbutanal	4	50	(6)
Pyridine	4	50	(103)
Dimethyldisulfide	5	62.5	(6, 8, 97, 103)
Dimethylsulfone	4	50	(48)

1,2-propanediol	3	37.5	(104)
Butanoic acid, 3-methyl	3	37.5	(103)
2-Octenal	3	37.5	(52)
Heptane,2-4 dimethyl	3	37.5	(6)
Thiocyanic acid, methyl ester	3	37.5	(105)
Butanal, 3-methyl	5	62.5	(6)
Terpineol	3	37.5	(49)
Acetic acid butyl ester	5	62.5	(106)
2-Propenoic acid, butyl ester	3	62.5	(106)
Butanenitrile	3	37.5	(63, 107)
Butanenitrile 3-methyl	3	37.5	(107)
2-pentanol	4	37.5	(106)

2.7.2 VOCs related to medication

In this study, VOCs related to medications were detected in the headspace of the body bag containing donors, along with VOCs related to ante-mortem and decomposition odour. In donor H3, propofol is the only VOC related to donor medication (Table 2-5). Donor H3 suffered from Parkinson's syndrome. Propofol is a type of inhalation and intravenous anaesthetic agent used in adults (89). This donor suffered from serious medical conditions due to old age and could have been hospitalised prior to death due to their respective state of health and pathological conditions. These pathologies are serious, and their treatments may require surgeries where these anaesthetic agents might have been administered to the donors. Donor H3 was received in the morgue at ~22 h PMI and the identification of propofol can suggest that specific volatile classes of medications such as general anaesthetics can be detected within a certain window of the post-mortem period after their potential application during the ante-mortem period.

Methenamine was the VOC potentially related to medications detected in donor H8 (Table 2-5). Methenamine is typically prescribed for urogenital issues (90, 108). The identification of this VOC in donor H4 can be related with the cause of death. The pathway through which these volatiles were detected in the headspace of the donor is unknown. One potential pathway through which these VOCs can be released from the body is through the action of enzymes, reactive oxygen species and microorganisms. Previously a decomposition study on pig remains detected dothiepin, a tricyclic antidepressant medicine detected in the headspace of the pig carcasses. These results can be of interest from a forensic toxicology perspective. The use of TD-GC×GC-TOFMS for screening relevant medications in the headspace can provide an interesting alternative to forensic medicine studies.

2.7.3 Principal component analysis

The initial PCA was conducted with 580 compounds identified in all donors. PC-1 and PC-2 accounted for 33% of the overall variance. The separation of donors along PC-1 and PC-2 highlighted variance in the VOC profiles between these donors. Donor H3 was separated from all other donors along PC-2, which explained 16% variance and this separation of donor H3 indicated that it had a different VOC profile compared to the other donors. Different intrinsic factors such as age, sex, and pathophysiological variation might have led to differences in the VOC profile of donor H3 during the early post-mortem period (91). The loadings value of 580 compounds associated with all the donors were less than 0.1 and for donor H3, most of the compounds in the loadings were congregated towards the origin indicating that overall, these 580 compounds had a weak association with the donors present in the scores plot. Within the 580 compounds, ~60% of the compounds were identified with a detection frequency of one out of eight indicating that these compounds had lower significance and might not strongly associate with all the donors in the scores plot contributing to their variances. Thus, compounds were removed from the PCA as they did not provide any donor specific information. Stefanuto et al. (2) reported a similar finding from PCA based on matrices of data containing 1200 individual compounds identified in the study. However, using all 1200 compounds for PCA provided no valuable information that can highlight the identification of compounds specific to the early post-mortem VOC profile. Thus, further PCAs were constructed with compounds identified at a higher minimum detection frequency of three out of eight donor samples, which reduced the data set to 104 compounds. This cut-off, three of eight, was chosen heuristically on the basis of compound quantity reduction.

The PCA, constructed with all the donors except donor H3, showed an interesting pattern of separation and clustering in the scores plot made up of VOC samples collected from seven donors. This separation and clustering pattern can be correlated to the PMI at which these samples were collected. The separation of VOC samples collected at different PMI intervals highlights the dynamic nature of VOC profiles released during the early post-mortem period.

Moreover, it also highlights the fact that the decomposition process is not a single event but a continuous process (8). The clustering of the VOC samples collected at different PMI intervals indicate a common suite of VOCs appearing at certain PMI, which can be expected across donors. The loadings plot and correlation plots of 104 compounds were used to identify the association of VOCs responsible for causing these patterns in the scores plot. The loadings plot highlighted subtle influences of the VOCs, contributing to the separation and clustering of these donors. For donors with higher PMI (H1 and H4), no VOCs in the correlation loadings showed a strong association. VOCs previously reported in the decomposition literature were identified in the samples of donors H8, H9, H6, H2, and H7 which were collected at lower PMI (Appendix A, Table A-3). These decomposition related VOCs were closest to the outer ring of the correlation loadings indicating strong association with these VOC samples and further contributing to the variances in the VOC sample collected at the lower PMI. Thus, the presence of decomposition related VOCs in these donors indicates the change in the VOC profile as early as 14 hrs PMI. This finding can be useful in the context of search and rescue operations and HRD dog training. Furthermore, the PCAs were able to highlight and support the fact that even in a controlled environment, VOC profiles released during the early post-mortem period can change hourly, and these changes can be driven by VOCs related to the decomposition process. Further studies are required with similar instrumentation and methodology which would allow a direct data comparison and build a dataset of VOCs which are present consistently in the early post-mortem period.

The biplot was constructed with scores plots consisting of VOC samples collected from seven donors and loadings showing 104 compounds classified into their compound class. The normalised areas for each compound within the list of 104 compounds were summed for each class. The biplot highlighted the correlation of different compound classes contributing to the variance in the VOC profiles of the donors in the early post-mortem period. Overall variability can be observed in the compound classes contributing to the variance in the donor profiles. Therefore, no single compound class strongly influences the VOC profiles across all donors during the early post-mortem period. This result supports the findings of an outdoor study

conducted by Deo et al.(38), whereby a similar variability was observed in the donor VOC profiles collected across different donors and seasons.

Notably, sulfur-containing compounds were identified to be positively correlated to the donors H1 and H4, whose samples were collected at a higher PMI. Sulfur-containing compounds are produced due to the breakdown of proteins and are linked with bacterial activity. Thus, the identification of the sulfur-containing compounds can be correlated with the progression of the decomposition for these donors. In the case of donor H1, this positive correlation can be further supported by macroscopic changes such as greenish discolouration and venous marbling associated with the progression of the decomposition process during the early post-mortem period.

2.8 Conclusion

Profiling VOCs from cadavers in indoor and outdoor environments during the early post-mortem period is an analytical challenge due to the low VOC abundance. In the present study, the experimental design and analytical method were optimised on the donors received in the UQTR morgue. This method optimisation aided in collection of the VOCs and investigation of the VOC profile released from the cadavers in the controlled environment (morgue) within a 6-72 h post-mortem period. The early post-mortem VOC profiles of the donors were identified to be complex immediately after death. These VOC profiles comprised of different chemical classes identified at varying abundance. Moreover, several VOCs previously identified in the middle and later stages of the decomposition process were also identified in the VOC profiles of the donors between 14-40 h PMI. Their identification suggests that VOCs related to the decomposition process can be detected as early as 14-40 h PMI.

Non decomposition VOCs related to skin, donor medications and biomarkers related to pathologies were also detected, highlighting the potential of this technique to be applied in forensic pathology and toxicology as a non-destructive approach to sample analysis. These

results indicate that the optimised technique can be substantially applied to study the early post-mortem VOC profile of human remains in an outdoor environment. Furthermore, increasing the number of donors in future studies can aid in identifying the correlations of VOC abundance with PMI interval and effects of refrigeration. A larger sample size will also allow to build a database of VOCs which can consistently be detected during the early post-mortem period and act as biomarkers linked with the early post-mortem VOC profile.

Chapter 3: Application of the optimised method to identify VOC profiles from human remains in an outdoor environment during the early post-mortem period

3.1 Introduction

During the decomposition process, the release of VOCs from a cadaver to the surrounding environment depends on their physiochemical properties. VOCs with physiochemical properties such as high vapour pressure, low molecular weight and low boiling point have higher volatility and can disperse more readily from the body (109). Entomological species (beetles and flies), canines and other scavengers (such as vultures, bears, etc.) track these VOCs present in decomposition odour to locate the target source of the odour (e.g., human remains or carrion) (109, 110). Understanding the VOC profile released from human remains can assist in determining the key compounds that attract these species (64, 109). Law enforcement agencies that use canines for search and detection can apply this knowledge in forensic casework and mass disasters to locate victims and victim remains. As the decomposition process depends on multiple factors and varies in different climates (dry or cold) and geographical contexts (North America or Europe or Pacific), research on VOCs released from a cadaver in the outdoor environment is essential to advance our understanding of the human decomposition process (43, 111).

Until 2020 due to ethical and legal restrictions, researchers had only conducted taphonomic studies using porcine remains in Canada (112-116). The majority of these studies aimed to understand the environmental impact on the decomposition process (117, 118). The one exception is a retrospective study of human decomposition which used actual but historical case data acquired from local law enforcement agencies (119). In 2017, Cockle et al. (119)

highlighted the variability in the process of decomposition and emphasised that two human cadavers can decompose differently in the same environment (119). Therefore, outdoor studies conducted across different seasons with multiple human donors in a local environment is needed to aid in understanding the trajectory of human decomposition in a Canadian climate.

Additionally, outdoor decomposition studies can assist law enforcement agencies in determining the PMI for human remains discovered locally. Estimating PMI has been particularly challenging for law enforcement agencies and forensic scientists in Canada due to the absence of local data on human decomposition (119, 120). Human taphonomic facilities allow researchers to conduct studies on cadavers for applications in forensic science (121), search and recovery, anthropology and archeology with a focus on subjects like forensic anthropology (122), forensic entomology (123), DNA (124), microbial activity related to decomposition processes (125), biomarker discovery, and search and rescue training (7). There are very few human decomposition facilities that have studied human decomposition VOC profiles to date (7, 37, 38, 84, 126). Ueland et al. (7) recently conducted an outdoor study using six cadavers in a simulated mass disaster scenario involving a collapsed building. Disaster victim identification (DVI) personnel recovered the cadavers after one month as a training scenario, and the VOCs released from the disaster site during this duration were profiled using GC×GC-TOFMS. Differential decomposition was observed during the recovery of the cadavers. A change in VOC profiles demonstrating a detectable change in the decomposition process of cadavers was observed 15 days after the simulated disaster. The authors concluded that the VOC profile could aid the training of HRD dogs for mass disaster events (7).

Notably, the seasonal variations in the early post-mortem VOC profile have not been studied before in an outdoor environment. Focusing exclusively on the early post-mortem period and studying the inter-day variation in the VOC profile can assist in determining the transition of the VOC profile from peri-mortem to post-mortem odour of a cadaver. Moreover, studying the VOC profile during this period in different seasons (spring, summer, and autumn) can broaden our understanding of the change and progression in the VOC profile during the early post-mortem period.

This study aims to investigate and characterise the early post-mortem VOC profile from human remains donated to the REST[ES] facility situated in an outdoor environment in Bécancour (Québec). The secondary aim of this project was to study this VOC profile over different seasons, namely spring, summer, and autumn, to provide a comprehensive understanding of the VOC profile in an eastern Canadian environment. The objective was to collect the VOC profile during the early post-mortem period and identify the VOCs using a Pegasus®BT 4D GC×GC-TOFMS.

3.2 Materials and methods

3.2.1 Donor information

VOC samples were collected from the same eight donors sampled in the UQTR morgue (Phase 2), with all donors refrigerated until arrival at the REST[ES] facility. Donor information such as age, sex, height, and date of death have been previously listed in Table 2-3 (section 2.5). The arrival date at REST[ES] and cause of death is detailed in Table 3-1 below. The cadavers were deposited on the surface of the soil soon after their arrival at the REST[ES] facility. Three to four samples were collected throughout a sampling day to capture the inter-day variation in the VOC profile.

Table 3-1 *REST[ES] donor id, date of arrival at REST[ES] and cause of death for eight donors sampled at the UQTR morgue (Phase 2) and subsequently placed at the REST[ES] facility for trials conducted in 2020-2021.*

Donor id	**Date of arrival at REST[ES] (dd/mm/yyyy)**	**Cause of death**
H1	10/08/2020	Asphyxiation due to hanging
H2	10/08/2020	Hepatic cirrhosis, anuric renal insufficiency (e.g. kidney failure due to anuria)
H3	28/09/2020	Parkinson syndrome
H4	05/10/2020	Inferior STEMI [ST Elevation Myocardial Infarction], vascular dementia, multiple strokes, MCAS [Mast Cell Activation Syndrome]
H6	11/05/2020	Stage 4 Metastatic melanoma in lungs, brain, bones, muscles, kidneys, adrenal glands, and liver
H7	23/06/2021	Metastatic cancer in lungs and prostate
H8	10/07/2021	Likely thrombosis in lower limb, dementia
H9	01/08/2021	Malignant arrhythmia

3.2.2 Experimental design

Donors were placed at the REST[ES] facility from August 10, 2020, to August 1, 2021. REST[ES] is the first outdoor human decomposition facility in Canada located in Becancour, Québec, that allows decomposition research to be conducted using human cadavers. The field site for this research is privately owned by the *Société du Parc Industriel et Portuaire de Bécancour* (SPIPB) and has been approved for research and educational purposes. The field site is a mixed temperate forest with maple and spruce trees making up the majority of the woodland. It is surrounded by a high security fence with infrared cameras to monitor access to the site. The soil type at the REST[ES] facility is a sandy loam soil. All donors are placed unclothed on the soil surface under anti-scavenging cages (2 m × 1.2 m × 0.75 m) when not being sampled. The progression of decomposition was observed and photographed twice daily during the summer trials (June, July, and August) and once daily during the spring (May) and autumn (September and October) trials. The samples were not collected during the winter and early spring months due to freezing conditions and the presence of snow on the ground, thus this thesis does not report data for donor H5 placed during these months. The stages of decomposition were characterised and recorded based on the visual appearance of the remains adapted from the stages developed by Payne (1965) (e.g., fresh, bloat, active decay, advanced decay, and dry remains/ skeletonisation).

A Hobo Weather Station equipped with a U30 No Remote Communication data logger (Onset Computer Corporation, Bourne, MA, USA) was used to record hourly measurements of ambient temperature (°C), rainfall (mm), relative humidity (%), wind direction (Ø), wind speed (m/s), and solar radiation (W/m2) (Figure 3-1). The weather station is located within the high security fence and less than 20 m from the placement of all human remains in this study. Hobo MX 2302A bluetooth temperature probes (Onset Computer Corporation, Bourne, MA, USA) were inserted into the oral and rectal cavity of each donor to measure relative internal temperature. Donors were placed on the assigned plots at the REST[ES] facility and were not moved throughout the study. Photos of the plots from all four directions were recorded before placing the donors. The date, time, and day were noted before sampling commenced. Prior to

placement of the donor, a control site was also established 10 m from the experimental site (and still within the high security fence) to monitor natural fluctuations in ambient VOCs.

Figure 3-1 *Hobo Weather Station (Onset Computer Corporation, Bourne, MA, USA) at the REST[ES] facility used to record measurements of ambient temperature (°C), rainfall (mm), relative humidity (%), wind direction (Ø), wind speed (m/s) and solar radiation (W/m2) every 15 min.*

3.3 VOC sample collection

An aluminium sampling hood (190 cm × 120 cm × 70 cm) was placed over the human remains (or control site) to allow the headspace VOCs to accumulate (Figure 3-2). The headspace accumulation period was 20 min for all samples. The 20 min accumulation period was previously optimised to collect VOCs from human donors during the early post-mortem period at AFTER in Sydney (87) A sorbent tube was attached to the sampling port on the aluminium sampling hood. The sorbent tubes used were stainless-steel dual sorbent tubes containing Tenax TA and Carbograph 5TD from Markes International Ltd. An ACTI-VOC low flow pump (Markes international Ltd., Llantrisant, UK) was used to draw air through the sorbent tubes where VOCs were concentrated (Figure 3-3). The sampling rate was 100 mL/min for 10 min. A 1 L sample was collected from the control site and experimental sites. The sampling duration

to collect each sample was 30 min and a control sample was collected every day to monitor any variation in background VOCs. Each sorbent tube was sealed with brass storage caps, wrapped with aluminium foil, and placed in an airtight glass container for transportation to the laboratory. The sample analysis method was the same as previously described in Phase 2 of the study (section 2.4.2.2).

Figure 3-2 *An aluminium hood (190 cm × 120 cm × 70 cm) placed over human remains for VOC accumulation at the REST[ES] facility.*

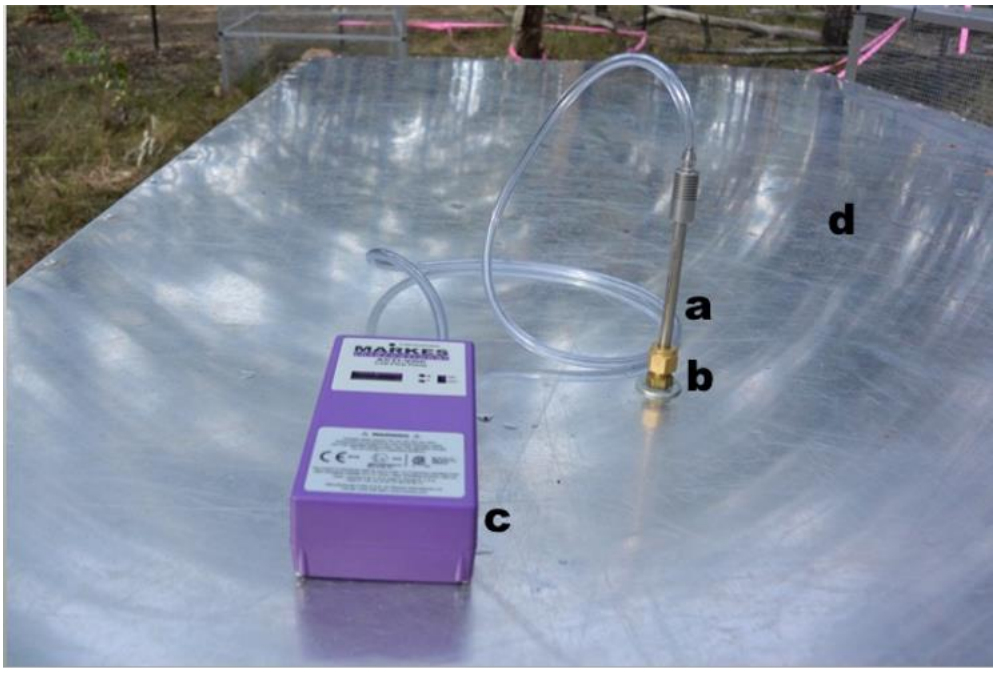

Figure 3-3 *Sampling setup with a) sorbent tube, b) sampling port, c) ACTI-VOC low flow sampling pump and d) aluminium sampling hood.*

3.4 Data processing method

The principal method of data processing and programs listed in section 2.5.3 were applied for the data processing of all REST[ES] samples. These scripts are available on GitHub and can be accessed using the link: https://github.com/wesleyburr/GCxGC_Morgue_RESTES

3.5 Results

3.5.1 Weather conditions

Weather conditions including ambient temperature, relative humidity, and rainfall that were recorded during the sample collection period are listed in Table 3-2.

Table 3-2: *The ambient weather data (temperature, relative humidity, and rainfall) recorded by the* Hobo Weather Station (Onset Computer Corporation, Bourne, MA, USA) *during the sample collection period from 2020-2021 at the REST[ES] facility*

Donor id	**Sample collection period**	**Ambient temperature (°C)**			**Relative humidity (%)**			**Rainfall (mm)**
		Maximum	Minimum	Average	Maximum	Minimum	Average	
H1	10/08/2020	24.1	23.5	24.1	85.0	82.0	84.0	0
H2	10/08/2020 to 14/08/2020	33.3	12.7	22.3	100.0	45.4	79.7	0
H3	28/09/2020 to 01/10/2020	24.9	9.6	15.7	100.0	65.7	92.5	16.0
H4	05/10/2020 to 09/10/2020	17.3	1.9	9.9	99.0	46.8	81.2	5.9
H6	10/05/2021 to 16/05/2021	29.6	6.5	20.1	100.0	31.5	79.0	0
H7	23/06/2021 to 28/06/2021	26.2	1.6	12.7	99.0	24	67.2	0.2
H8	10/07/2021 to 15/07/2021	30.7	9.1	20.6	100.0	45.1	84.1	0
H9	01/08/2021 to 06/08/2021	29.7	11.2	19.7	98.0	46.2	81.0	0.2

In this study, the highest maximum and lowest minimum ambient temperature recorded was during the sample collection of donor H2 (33.3°C, summer) and donor H7 (1.6 °C, autumn), respectively. The lowest relative humidity (24 %) was also recorded during the sample collection of donor H7. The maximum rainfall recorded was 16 mm, and it was experienced during each sample collection for donor H3. Even when the rainfall during a sample collection day was brief, sampling was paused due to moist climatic conditions which can damage the ACTI-VOC pump and sorbent tubes.

3.5.2 Decomposition stages[3]

The cadavers were placed on the surface of the soil during the fresh stage of decomposition, except for donor H1 who had commenced decomposition at their time of arrival at the REST[ES] facility, as the donor died by suicide and remained undiscovered for ~24 h. Accumulated degree days (ADD) in a forensic context is the sum of the average daily temperature on consecutive days under the consideration for a decomposition event and starting from the day of death (127). ADD calculation for this study started after the placement of the donor at the REST[ES] facility and it was used to determine the length of the sampling period since 'the early post-mortem period' could vary by donor based on their time of death and time of arrival at the REST[ES] facility. The ambient ADD was calculated for 72 h after the time of placement of the donor. In the 2020 trials, the sample collection was stopped for a donor when the average ADD of the oral and rectal temperatures equilibrated with the ambient ADD. In this case the ambient ADD was calculated from the weather data collected 72 h prior to the donor placement. The results of the decomposition patterns seen on the donors placed during the 2020 trial are discussed below with ambient ADD values.

During the placement of donor H2 on ED 0 (ADD 20.0) in the summer months, livor mortis was visible in the neck and partially in the torso region. The skin of the forearms had purpura, an

[3] The photos taken during trial 2020 and trial 2021 have been added as supporting information in Appendix B. Please note that the images and or content may be disturbing to some readers, therefore reader discretion is strongly advised.

ante-mortem medical condition related to the presence of blood in the skin, which gave the skin an appearance that looks like bruises. The skin on the neck and lower arms appeared reddish which could potentially be signs of blood clots in the superficial layer of skin. On ED 1 (ADD 44.5), minimal insect activity with no significant change from the previous day in terms of visual decomposition was noted at the time of taking observations. On ED 2 (ADD 53.1), the donor showed skin slippage on the lower part of the left arm and greenish discolouration in the torso. The greenish discolouration is a sign of the commencement of autolysis and putrefaction. Entomological activity was visible and egg masses were seen in the mouth, nose, and ears. On ED 3 (ADD 89.0), the face showed signs of active decay, such as skin blisters which were seen in the face (nose and forehead) and greenish discoloration seen in the torso. On ED 4 (ADD 97.7), the forearms showed signs of active decay with a leathery appearance of the skin and the commencement of bloat in the abdomen.

During the placement of donor H3 on ED 0 (ADD 20.1) in the autumn months, the upper and lower limbs were in rigor mortis. Livor mortis (peripheral pooling of blood) was seen on the side of the neck, back of the head, and inner thighs. The rigor mortis persisted in the upper and lower limbs until ED 3 (ADD 53.4). On ED 3, the livor mortis progressed to the head, shoulder, ears, and torso regions. A greenish discolouration was seen around the torso, genitals, knees, inner thighs, and neck. Egg masses were seen in the groin region. On ED 4 (ADD 78.2), no further significant change was noticed. This could be related to lower ambient temperatures recorded during the autumn season.

During placement of donor H4 on ED 0 (ADD 10.0) in the autumn months, livor mortis was seen in the neck, shoulder, and head regions. The neck and abdomen region showed initial signs of venous marbling. On ED 1 (ADD 23.1) and ED 2 (ADD 34.0), the decomposition process progressed at a slower rate due to the lower ambient temperatures recorded during the autumn season. On ED 3 (ADD 52.0), the fingertips had “washerwoman change”, an early post-mortem sign caused due to waterlogging of the top layer of the skin, giving it a wrinkling appearance.

In the 2021 trials, the sample collection period was slightly modified, whereby samples were collected for 72 h after the average ADD of oral and rectal temperatures reached the ambient ADD. This change was made to encompass (i) the early post-mortem period from the fresh stage of decomposition to the beginning of putrefaction and (ii) the variation in the progression of decomposition during different seasons. The results of the decomposition patterns seen on the donors placed during the 2021 trial are discussed below with ambient ADD values.

During placement of donor H6 on ED 0 (ADD 9.0) in the spring months, livor mortis was seen on the back, while the upper and lower limbs were in rigor mortis which persisted through ED 2 (ADD 32.6). After ED 0, minimal insect activity with no significant change in visual decomposition was observed until ED 2 (ADD 32.6). On ED 3 (ADD 46.1) rigor mortis was passing from the upper and lower limbs. A greenish discolouration began to appear on the lower limbs and abdomen. Initial deposits of egg masses were seen in the nose and palate. On ED 4 (ADD 61.7) the greenish discolouration progressed to regions of the lower limbs such as thighs, calf, and ankle. The number of egg masses increased and were seen in the genitals, face, and arm pits. By ED 5 (ADD 76.8), rigor mortis had completely passed from the upper limbs, but persisted to some degree in the lower limbs.

During placement of donor H7 on ED 0 (ADD 15.5) in the summer months, livor mortis was observed on the back. Rigor mortis was evident in the upper and lower limbs but had passed by ED 2 (ADD 56.3). On ED 1 (ADD 35.7) and ED 2 (ADD 56.3), no significant changes in terms of visual decomposition were seen on donor H7. On ED 3 (ADD 78.0), the soles of the feet showed a wrinkling appearance and high insect activity was recorded along with egg masses in the mouth, eyes, and genitalia. On ED 4 (ADD 103.0), an increase in insect activity with skin slippage was observed in the face and the insect activity continued to increase on ED 5 (ADD 126.0).

During placement of donor H8 on ED 0 (ADD 17.9) in the summer months, a blister was seen on the left leg which could have developed in the ante-mortem period. On ED 1 (ADD 38.0) insect activity was observed on the blister and egg masses were seen in the eyes and nose. On ED 2 (ADD 58.0) an increase in the egg masses in the eyes, nose, and palate were noticed. Skin

slippage was seen around the blister. On ED 3 (ADD 78.0), high insect activity was seen over the head, neck, and genital regions. The insect activity continued to increase until ED 5 (ADD 123.0). Venous marbling was noted over a small region in the upper limbs and lower limbs. On ED 4 (ADD 100.0) the beginning of bloat was seen in the abdomen with spreading of venous marbling occurring in the upper and lower limbs. On ED 5 (ADD 123.0), purging of decomposition fluid was seen from the head and neck region.

During placement of donor H9 on ED 0 (ADD 18.1) in the summer months, livor mortis was noted on the back and patches of pink and red discolouration were seen on the forehead and small regions of the lower limbs. These patches could have developed in the ante-mortem period. On ED 1 (ADD 38.1) and ED 2 (ADD 58.2) a small amount of insect activity was observed in the face. Moreover, no significant changes in terms of visual decomposition were seen on donor 9 until ED 2 (ADD 58.2). On ED 3 (ADD 79.7), slight bloating of the neck region was seen with an increase in the insect activity. On ED 4 (ADD 100.0), greenish discolouration was seen on the chin, upper lip, and eyelids. The pink and red patches seen on ED 0 had become a dark purple colour. On ED 5 (ADD 124.7), there was an increase in bloating across the head and neck regions. The greenish discolouration progressed towards the upper limbs and was seen on the right shoulder and forearm.

Table 3-3 represents ADD data (ambient and internal) and decomposition patterns recorded for the donors during this study. The decomposition process for individual donors varied at the REST[ES] facility. Greenish discolouration was one of the most commonly observed patterns on the donors (Table 3-3) followed by venous marbling. This pattern was seen on the donors between ED 2 and ED 5 on different anatomical landmarks except for donor H4 and H7. The insect activity on the donors generally increased after ED 2 and consistently increased throughout the duration of the trials in summer and spring. On ED 4 and ED 5, the highest amount of decomposition activity was observed visually for donors H2, H6, H7, H8 and H9. A slower progression of decomposition was observed on the donors placed during the autumn season (H3 and H4). Venous marbling was seen after the trial. Note that the internal ADD data for H9 is not available due to mechanical failure of the loggers during the trial.

Table 3-3 *ADD data (ambient and internal) and donor decomposition patterns observed during the 2020-2021 trials conducted at the REST[ES] facility.*

			ADD Data			**Decomposition Patterns Observed**		
Donor id	**Year**	**Season of placement**	**Ambient ADD before the trial**	**Average internal ADD of oral and rectal cavities**	**Days taken to reach ambient ADD**	**Visual signs of autolysis and putrefaction (ambient ADD)**	**Anatomical landmarks showing first signs of autolysis and putrefaction**	**Features related to autolysis and putrefaction observed**
H2	2020	Summer	97.7	97.7	4	53.1	Back of the palms	Greenish discolouration
H3		Autumn	52.7	78.2	3	53.4	Diaphragm region, genitals Knees and inner thighs	Greenish discolouration
H4		Autumn	36.8	52.5	3	92.8	Neck	Venous marbling
H6	2021	Spring	32.0	32.3	3	46.1	Abdomen and lower limbs	Greenish discolouration
H7		Summer	56.0	52.5	3	126.0	Face	Skin slippage
H8		Summer	63.0	68.0	3	68.3	Lower limbs	Venous marbling
H9		Summer	58.3	N/A	N/A	100.0	Face	Greenish discolouration

3.6 VOC class abundance for donors at the REST[ES] facility

The donor VOC profiles were generated using a Pegasus®BT 4D GC×GC-TOFMS. The list of compounds was generated after data processing, peak filtering, and normalisation. To characterise the VOC profiles of donors in an outdoor environment during the early post-mortem period, we studied (i) overall abundance, (ii) individual donor VOC profiles and (iii) seasonal impact on VOC abundance. For this thesis the VOC abundance was calculated as the number of VOCs present in the sample collected during the experimental day. This measurement reflects the overall number of VOCs in the sample. The class abundance, on the other hand, reflects the number of VOCs within a particular chemical class (e.g. alcohols, ketones, aldehydes, etc.). This value was calculated by adding up the number of VOCs identified as belonging to a specific chemical class. For example, if in a sample 10 VOCs were identified in total and 5 of them belonged to the class of alcohols, the VOC abundance would be 10 and the class abundance for alcohols would be 5. This calculation provides a way to compare the relative abundance of different chemical classes within the sample on each experimental day across eight donors.

Overall VOC abundance

A total of 948 compounds were detected in n=36 samples collected during the early post-mortem period in the outdoor REST[ES] environment. For an individual VOC, the minimum detection frequency was in 1/36 samples and the maximum detection frequency was in 24/36 samples. All VOCs were classified in the following compound classes: acids, alcohols, aldehydes, aromatics, cyclic aliphatic compounds, esters and analogues, ethers, halogen-containing compounds, ketones, linear aliphatic compounds, nitrogen-containing compounds, and sulfur-containing compounds. Nitrogen-containing compound classes (n=149) and esters and analogues (n=112) were detected in the highest abundance during the early post-mortem period of decomposition at the REST[ES] facility (Figure 3-4). Acids (21) and ethers (39) were the least abundant compound classes in the VOC profiles collected during the early post-mortem period.

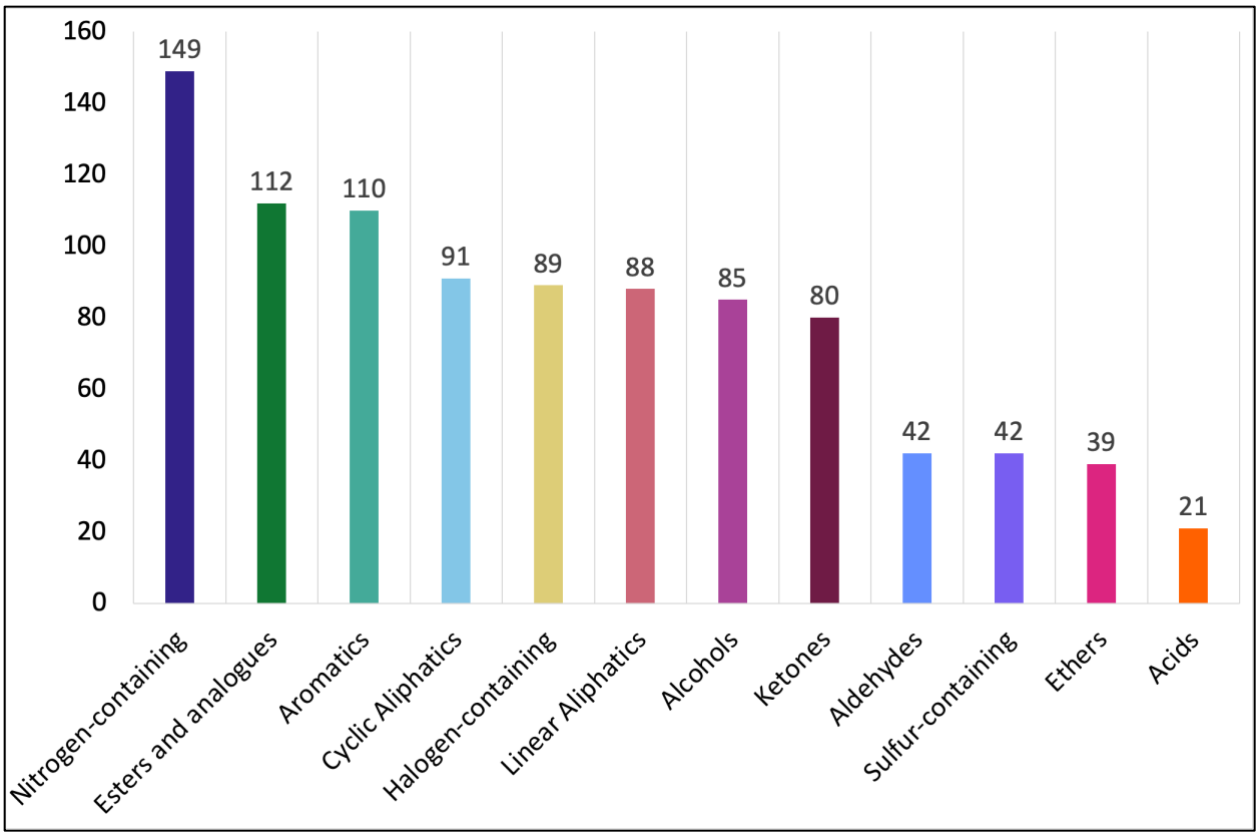

Figure 3-4 *Overall compound class abundance identified in the early post-mortem period VOC profiles of eight donors from 2020-2021 sampled at the REST[ES] facility.*

The number of VOCs and compound class abundance evolved during the early post-mortem period across different experimental days and within inter-day variations in the VOC profiles of the donors. Moreover, the progression of decomposition in each donor varied, as highlighted in (Table 3-3). Therefore, the trends in the VOC profile and compound class abundance for each donor is reported individually below.

3.6.1 Individual VOC abundance identified for donors at the REST[ES] facility

Donor H1

Donor H1 showed signs of autolysis and putrefaction at the time of placement at the REST[ES] facility. As a result, a set of triplicate samples was collected on ED 0 only, as it was determined

that this donor was already passing the early post-mortem period. 114 VOCs were identified in donor H1, these VOCs were either unique to the donor and not identified in the control sample or they were detected at a S/N that was twice that of a control sample. Esters and analogues had the highest class abundance (n=19), while acids had the lowest class abundance (n=2).

Donor H2

A total of 373 VOCs were detected for donor H2 over five experimental days (ED 0, ED 1, ED 2, ED 3, and ED 4) placed in the summer (August 2020) at the REST[ES] facility. Inter-day variation in VOC abundance was observed during the trial. The lowest VOC abundance was recorded on ED 2 (n=45) (Figure 3-5). On ED 4, the beginning of the bloat stage with high insect activity was observed on donor 2; as a result, the highest VOC abundance (n=288) was recorded.

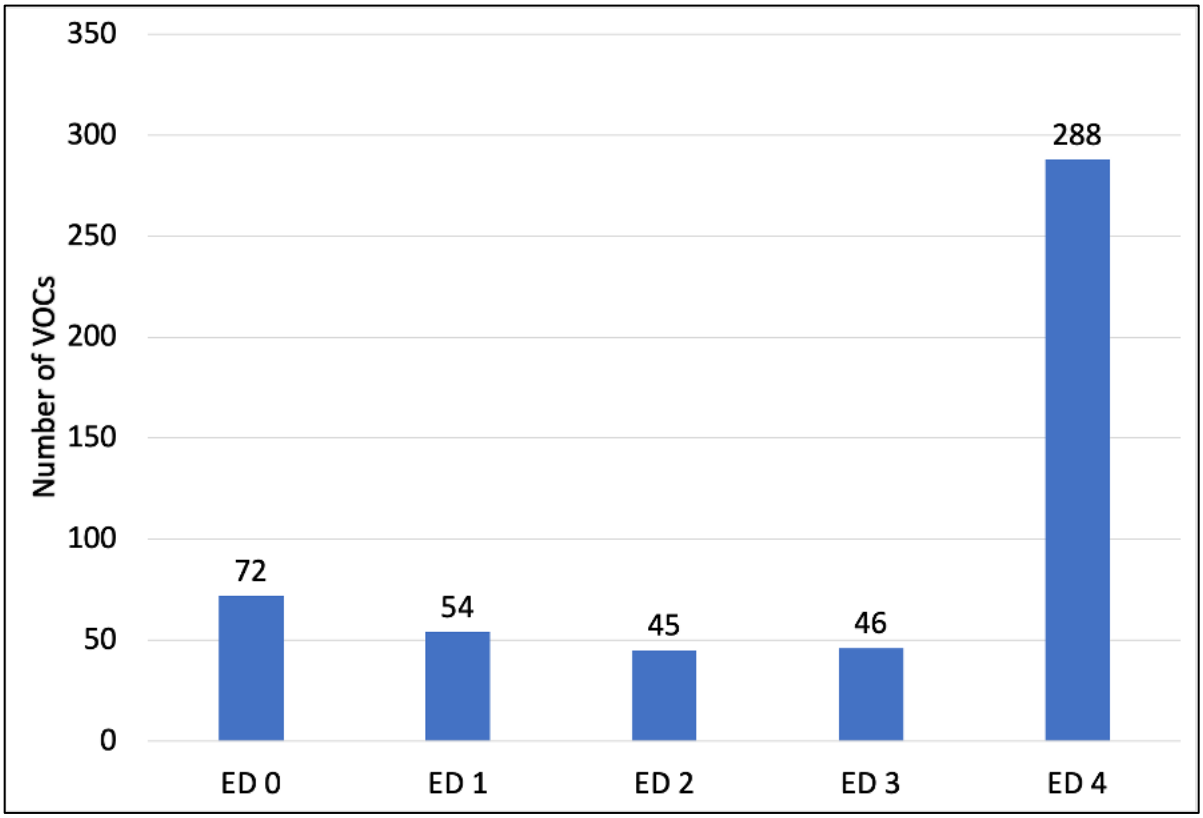

Figure 3-5 *Inter-day variation of VOC abundance in donor H2 observed from ED 0 to ED 4.*

The chemical classes acids, alcohols, aldehydes, aromatics, cyclic aliphatic compounds, esters and analogues, ethers, halogen-containing compounds, ketones, linear aliphatic compounds, nitrogen-containing compounds, and sulfur-containing compounds were detected on all experimental days, except acids which were not detected on ED 0 and ED 2, and ethers which were not detected on ED 1 (Figure 3-6). The class abundance varied across the trial with aromatic compounds being the most abundant class on ED 0 (n=14) as shown in Figure 3-6. On ED 1 and 2, ketones (n=5) and alcohols (n=8) dominated the class abundance (Figure 3-6). Nitrogen-containing compounds (n= 10 and 43) had the highest class abundance on ED 3 and ED 4.

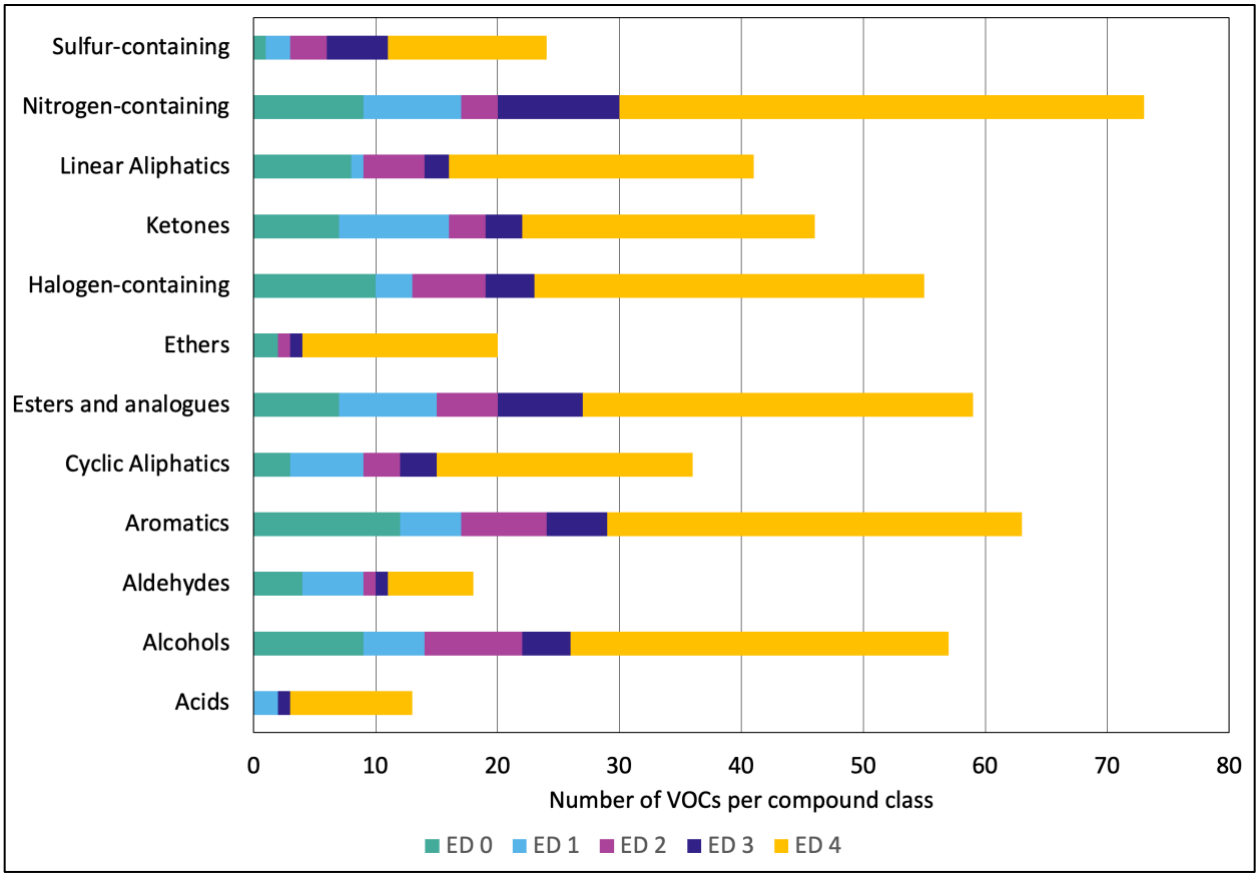

Figure 3-6 C*ompound class abundance identified for donor H2 from ED 0 to ED 4.*

Donor H3

The overall VOC abundance for donor H3 was low with only 98 VOCs detected across the four days of the trial (ED 0, ED 2, ED 3, and ED 4). The donor was placed in the autumn (September 2020) at the REST[ES] facility. Due to heavy rain on ED 1, VOC samples were not collected. Inter-day variation in VOC abundance was observed, with ED 0 having the highest VOC abundance (n=70), followed by a sharp decline (Figure 3-7). On ED 3, the lowest VOC class abundance was observed (n=12).

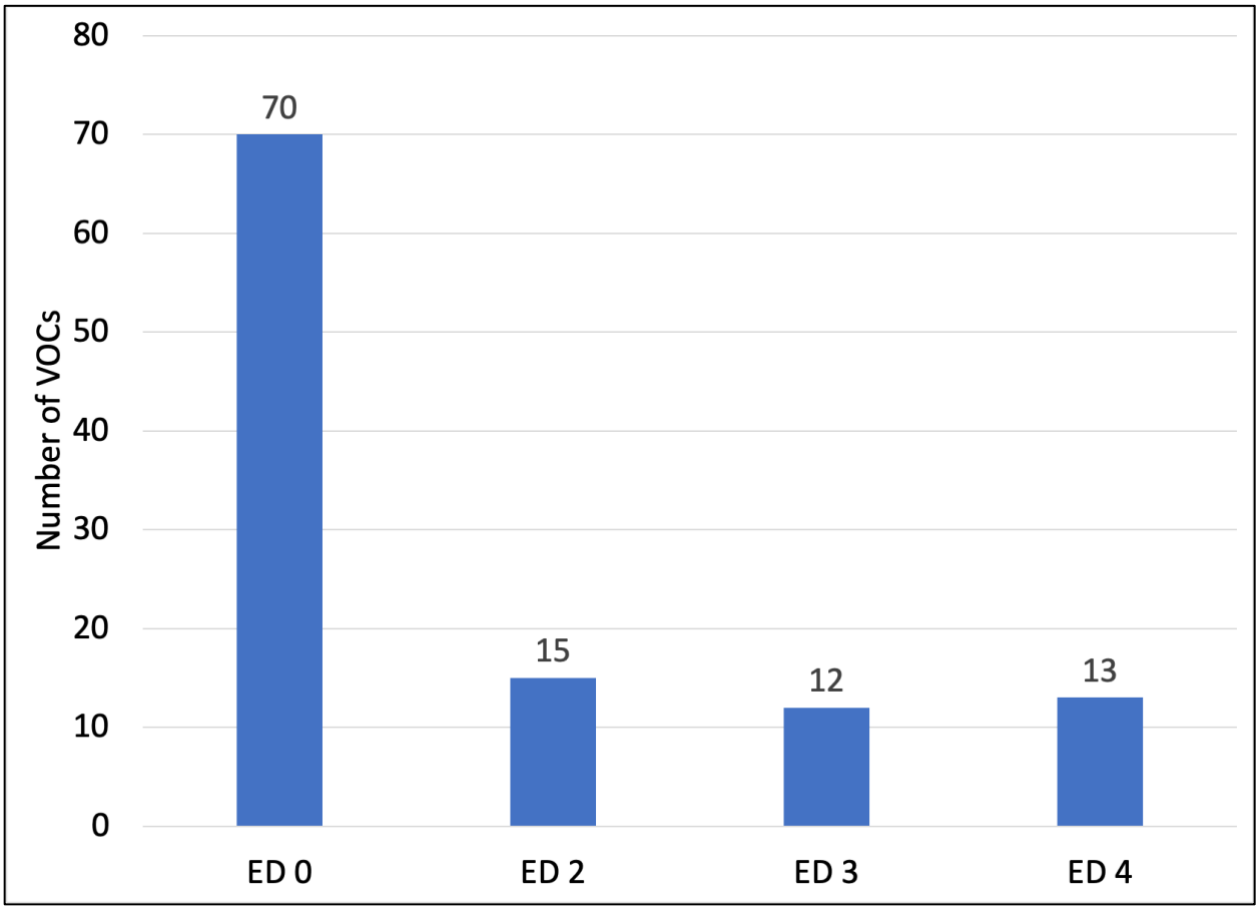

Figure 3-7 *Inter-day variation of VOC abundance in donor H3 observed from ED 0 to ED 4.*

Only on ED 0 were all the chemical classes such as alcohols, aldehydes, aromatics, cyclic aliphatic compounds, esters and analogues, ethers, halogen-containing compounds, ketones,

linear aliphatic compounds, nitrogen-containing compounds, and sulfur-containing compounds detected, except acids which were not detected in donor H3. Compound classes such as alcohols, aromatics, ethers, and sulfur-containing compounds were only detected on ED 0 (Figure 3-8). Cyclic aliphatic compounds had the highest class abundance on ED 0 and ED 2 (n=11 and n=4), esters and analogues and halogen-containing compounds (n=3) had the highest class abundance on ED 3, while nitrogen-containing compounds and halogen-containing compounds (n=4) were the most abundant on ED 4.

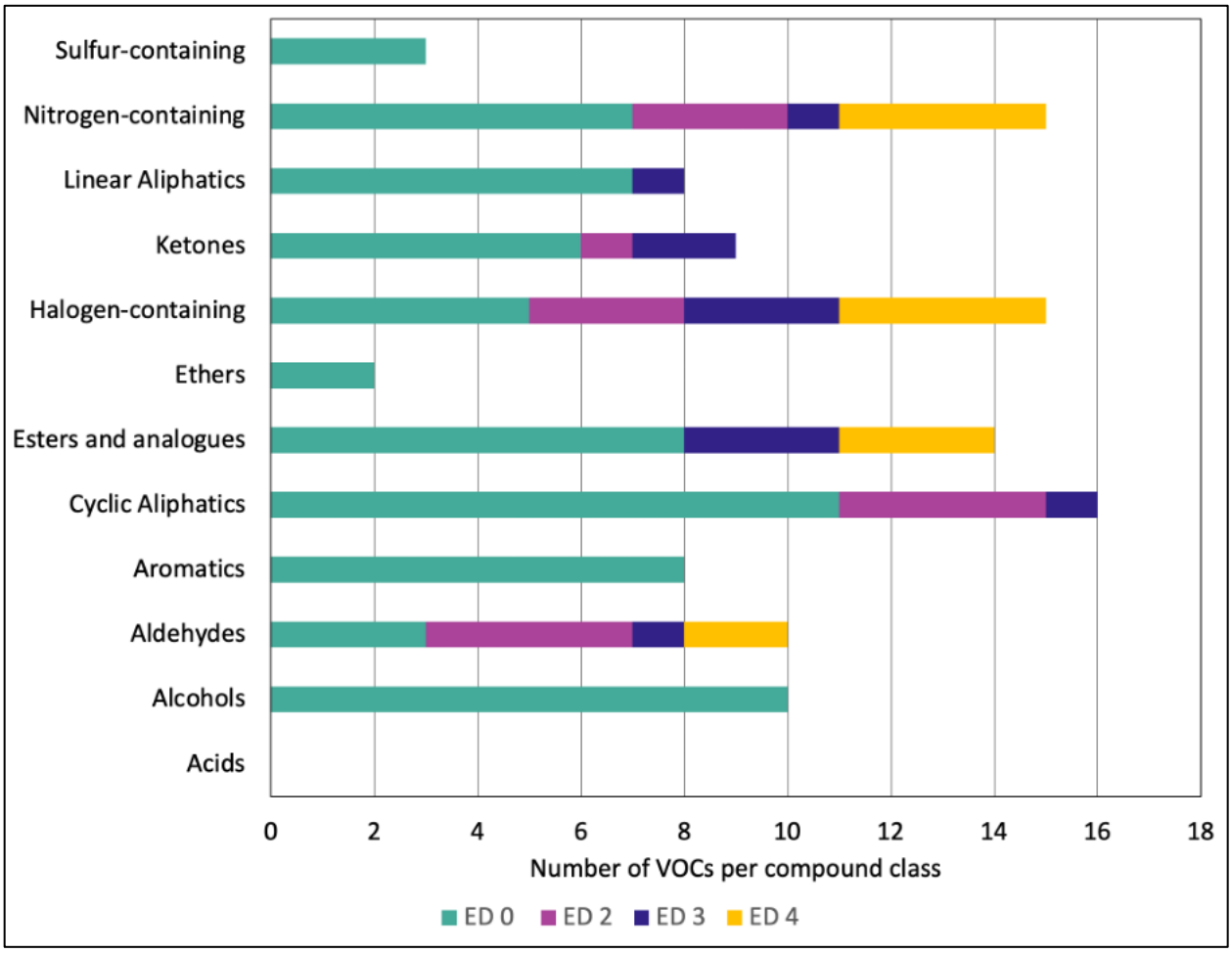

Figure 3-8 *Compound class abundance identified for donor H3 from ED 0 to ED 4.*

Donor H4

A total of 87 VOCs were detected for donor H4 over three experimental days (ED 0, ED 1, and ED 3) in the autumn (October 2020) at the REST[ES] facility. VOC samples were not collected on ED 2 due to rain. The highest VOC abundance was recorded on ED 0 (n=43) and the lowest class abundance was recorded on ED 3 (n=32) (Figure 3-9). This decline in VOC abundance over the early post-mortem period was consistent with that reported for donor H3, also placed during the cooler autumn months.

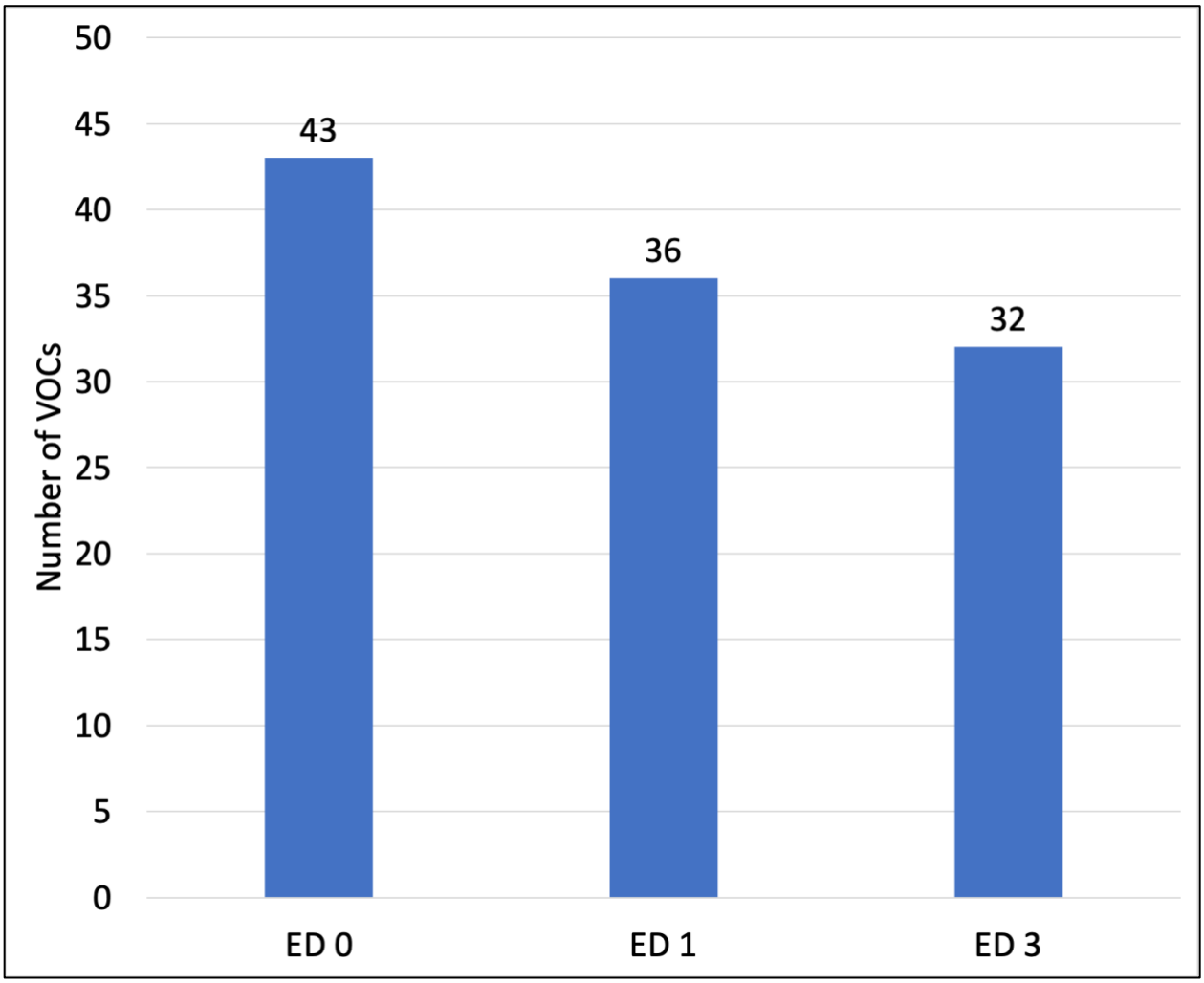

Figure 3-9 *Inter-day variation of VOC abundance in donor H4 observed from ED 0 to ED 3.*

Inter-day VOC abundance varied and the maximum frequency of detection for a VOC was in 3 of 4 samples. The sulfur-containing compounds were not detected in donor H4, and ethers

were only detected on ED 0 (n=1) (Figure 3-10). Esters and analogues (n=8) had the highest class abundance on ED 0, while ketones (n=5) had the highest class abundance on ED 2. On ED 3 aromatics dominated the class abundance (Figure 3-10).

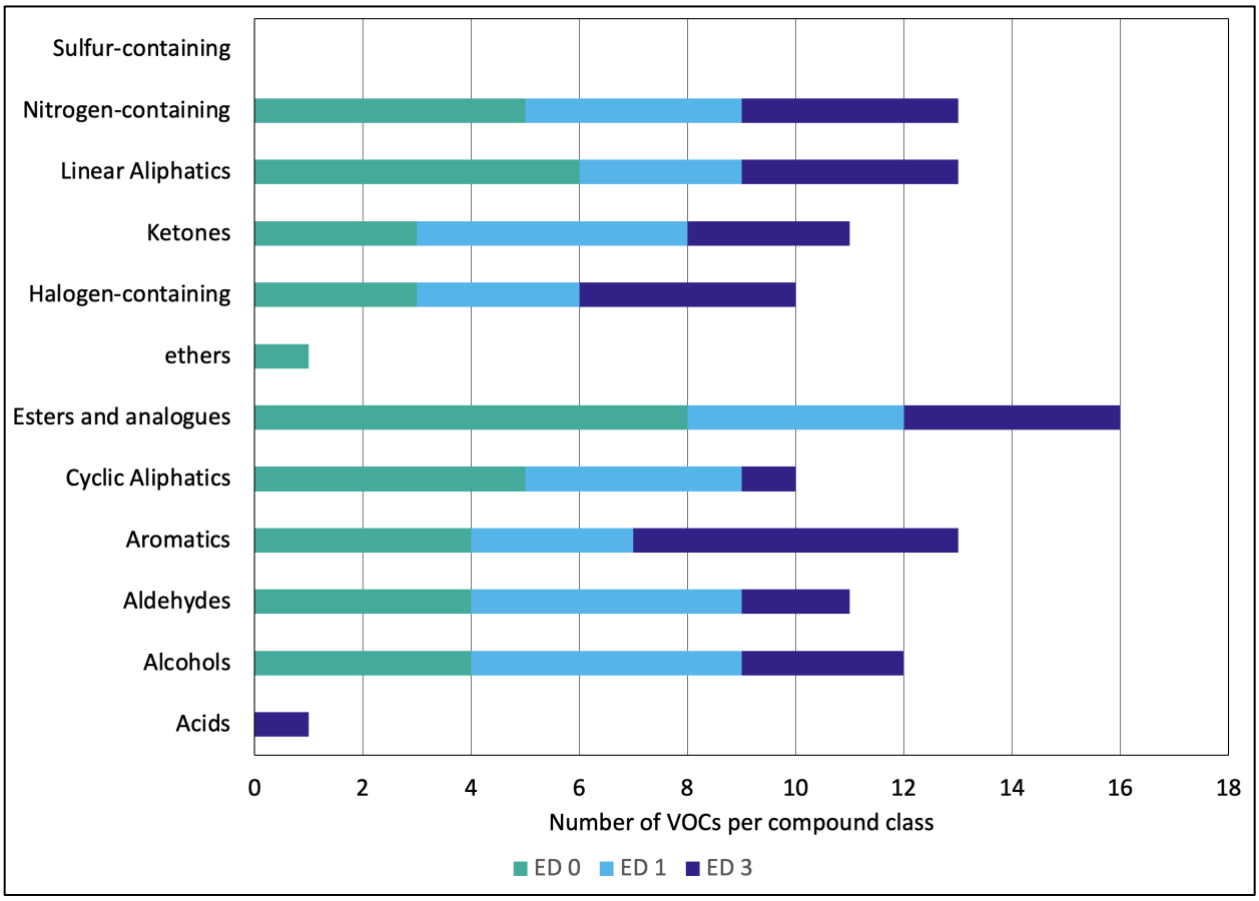

Figure 3-10 *Compound class abundance identified for donor H4 from ED 0 to ED 3.*

Donor H6

A total of 210 VOCs were detected for donor H6 across six experimental days (ED 0, ED 1, ED 2, ED 3, ED 4, and ED 5) in the spring (May 2021) at the REST[ES] facility. ED 4 (n=63) had the highest VOC class abundance while ED 2 and ED 5 had the lowest VOC class abundance (n=40) (Figure 3-11).

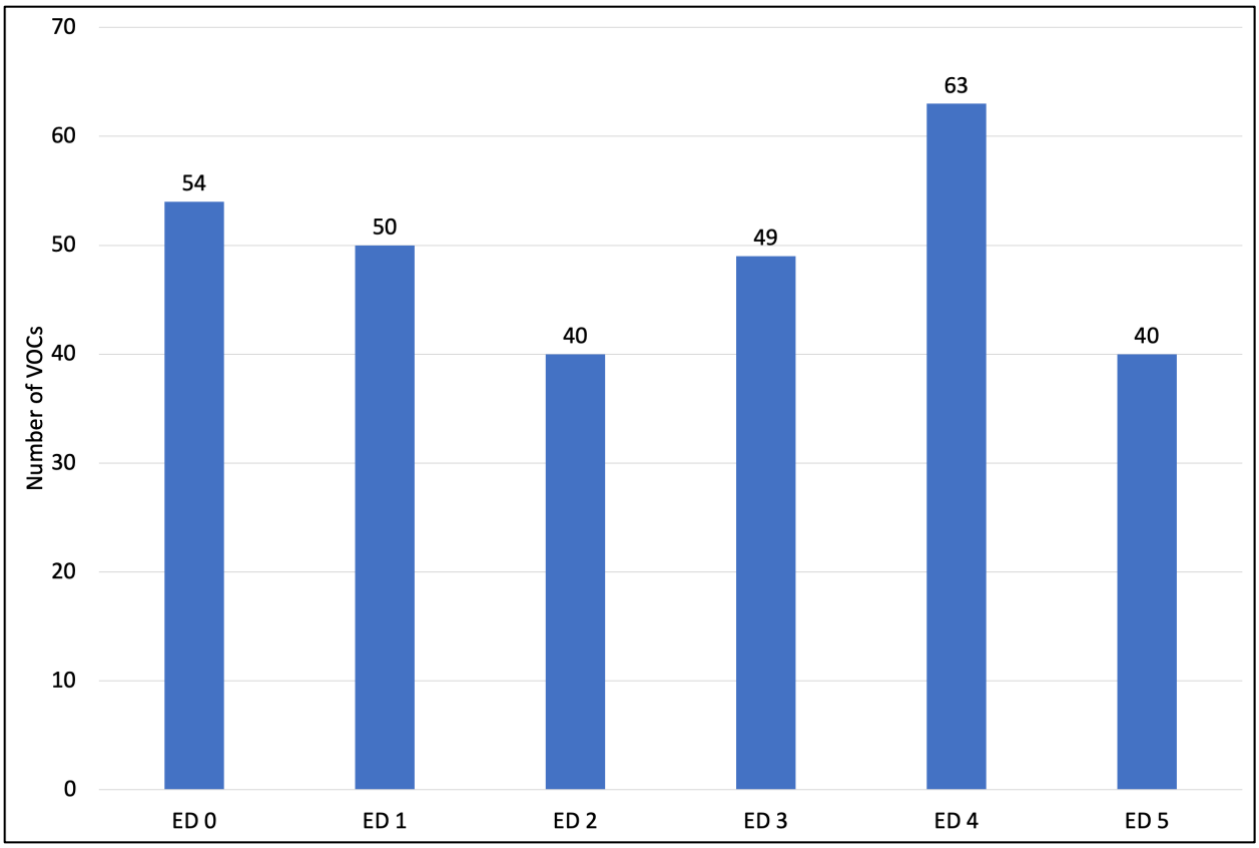

Figure 3-11 *Inter-day variation in VOC abundance observed in donor H6 from ED 0 to ED 5.*

The chemical classes such as acids, alcohols, aldehydes, aromatics, cyclic aliphatic compounds, esters and analogues, ethers, halogen-containing compounds, ketones, linear aliphatic compounds, nitrogen-containing compounds, and sulfur-containing compounds were detected on all experimental days, except acids which were not detected on ED 2. Moreover, alcohols were not detected on ED 2, while sulfur-containing compounds were not detected on ED 3 and acids were not detected after ED 1 (Figure 3-12). The class abundance varied across the trial with nitrogen-containing compounds being the most abundant class on ED 0 (n=11) and ED 4 (n=14) (Figure 3-12). Esters and analogues were the most abundant class on ED 1, while cyclic aliphatic compounds dominated the class abundance on ED 2 (n=7) and ED 3 (n=9) as shown in Figure 3-12. Aromatics were the most abundant class on ED 5 (n=6).

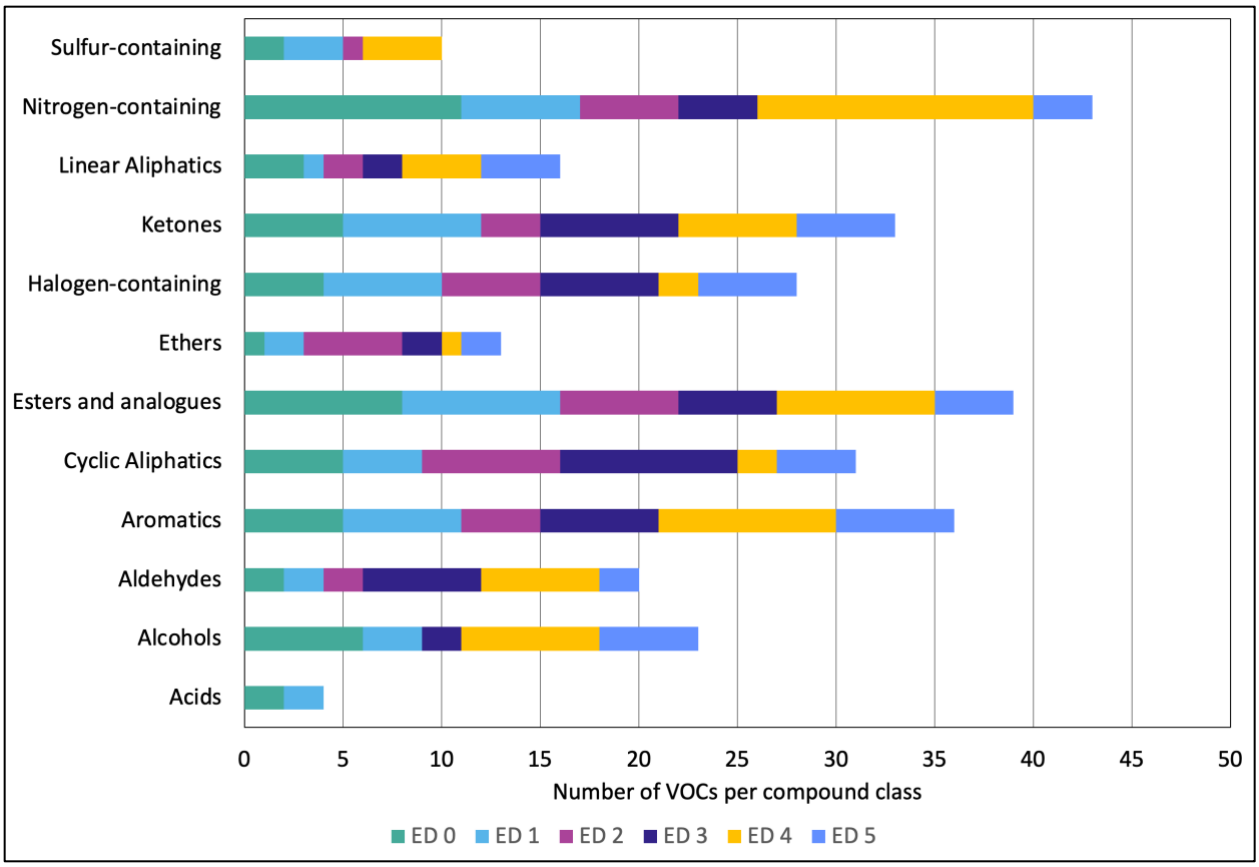

Figure 3-12 *Compound class abundance identified for donor H6 from ED 0 to ED 5.*

Donor H7

A total of 198 VOCs were detected for donor H7 over six experimental days (ED 0, ED 1, ED 2, ED 4, and ED 5) in the summer (June 2021) at the REST[ES] facility. VOC samples were not collected on ED 3 due to rain. Inter-day variation in VOC abundance was observed during the trial. ED 2 demonstrated the highest VOC abundance (n=71), while ED 4 recorded the lowest VOC abundance (n=36) (Figure 3-13).

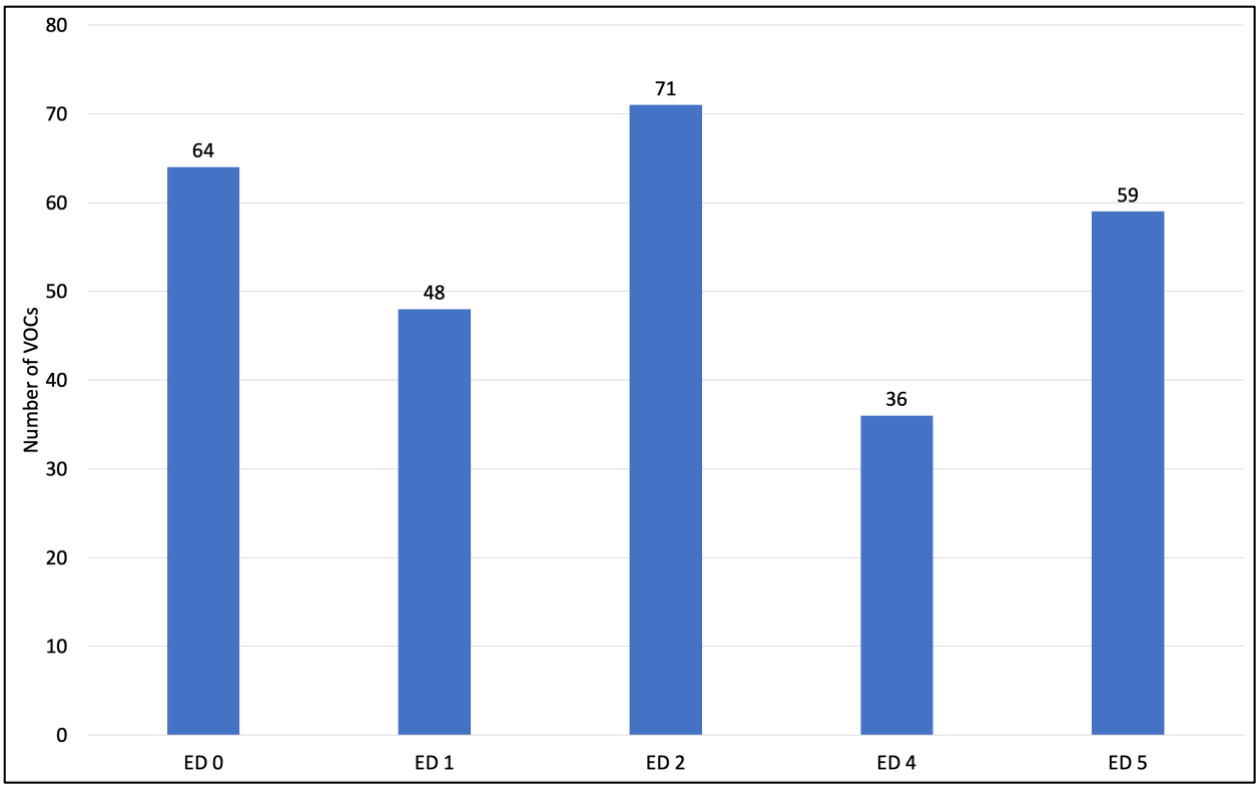

Figure 3-13 *Inter-day variation in VOC abundance observed in donor H7 from ED 0 to ED 5.*

The chemical classes such as alcohols, aldehydes, aromatics, cyclic aliphatic compounds, esters and analogues, ethers, halogen-containing compounds, ketones, linear aliphatic compounds, nitrogen-containing compounds, and sulfur-containing compounds were detected on all experimental days, except sulfur-containing compounds which were not detected on ED 0 and acids which were only detected on ED 2 (Figure 3-14). The class abundance varied across the trial with ketones being the most abundant class on ED 0 (n=10), and nitrogen-containing compounds being the most abundant class on ED 1 (n=12) and ED 5 (n=13) (Figure 3-14). Halogen-containing and nitrogen-containing compounds dominated the class abundance on ED 2 (n=11) and halogen-containing compounds were most abundant class on ED 4 (n=6) as shown in Figure 3-14.

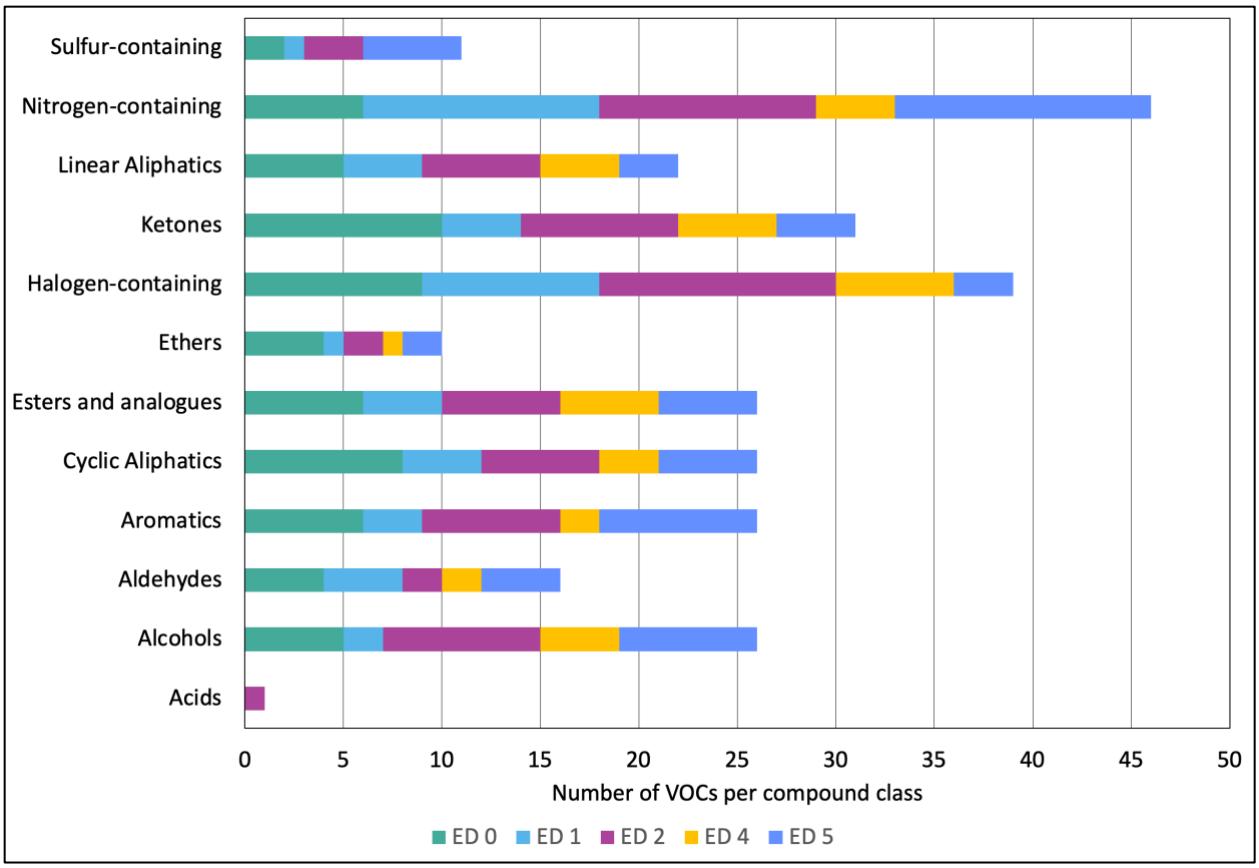

Figure 3-14 C*ompound class abundance identified for donor H7 from ED 0 to ED 5.*

Donor H8

A total of 441 VOCs were detected for donor H9 over six experimental days (ED 0, ED 1, ED 2, ED 3, ED 4, and ED 5) in the summer (July 2021) at the REST[ES] facility. Inter-day variation in VOC abundance was observed with ED 0, ED 1, ED 2, and ED 3 recording low VOC abundance (n < 70), followed by a sharp increase in VOC abundance on ED 4 (Figure 3-15). On ED 4, the abdomen began to bloat and there was high insect activity that led to the highest VOC abundance (n=254) recorded during the trial.

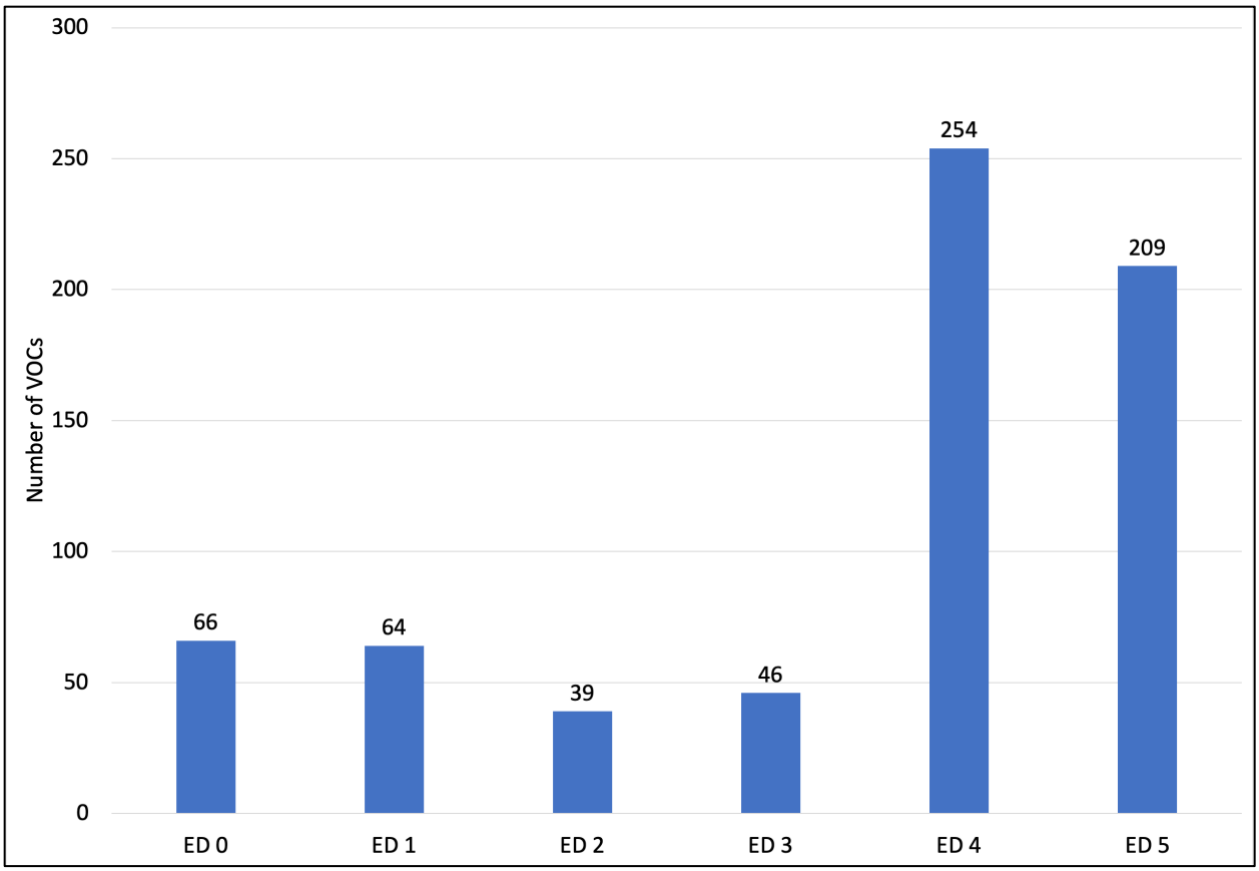

Figure 3-15 *Inter-day variation in VOC abundance observed in donor H8 from ED 0 to ED 5.*

The chemical classes such as acids, alcohols, aldehydes, aromatics, cyclic aliphatic compounds, esters and analogues, ethers, halogen-containing compounds, ketones, linear aliphatic compounds, nitrogen-containing compounds, and sulfur-containing compounds were detected on all experimental days, except aldehydes which were not detected on ED 0 and acids which were not detected on ED 1 and ED 2 (Figure 3-16). The class abundance varied across the trial with esters and analogues being the most abundant class on ED 0 (n=11) and nitrogen-containing compounds being the most abundant class on ED 1 (n=12), ED 4 (n=40) and ED 5 (n=39) as shown in Figure 3-16. Aromatics dominated the class abundance on ED 2 (n=10) and ED 3 (n=9) as shown in Figure 3-16.

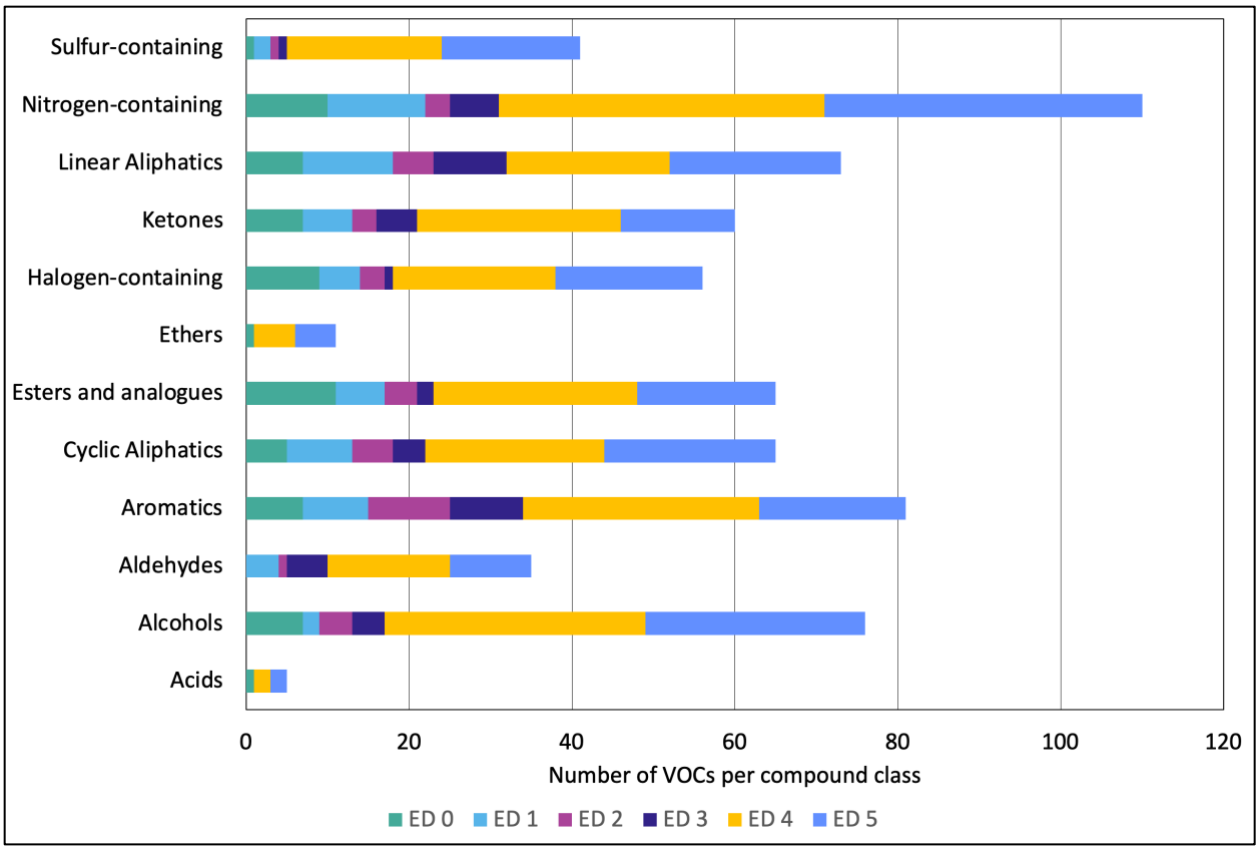

Figure 3-16 C*ompound class abundance identified for donor H8 from ED 0 to ED 5.*

Donor H9

A total of 373 VOCs were detected over six experimental days (ED 0, ED 1, ED 2, ED 3, ED 4, and ED 5) for donor H9 in the summer (August 2021) at the REST[ES] facility. Inter-day variation in VOC abundance was observed during the trial. ED 0 recorded the lowest VOC abundance (n=46), while ED 5 demonstrated the highest VOC abundance (n=206) and on this experimental day the donor showed the beginning of the bloat stage and high insect activity (Figure 3-17).

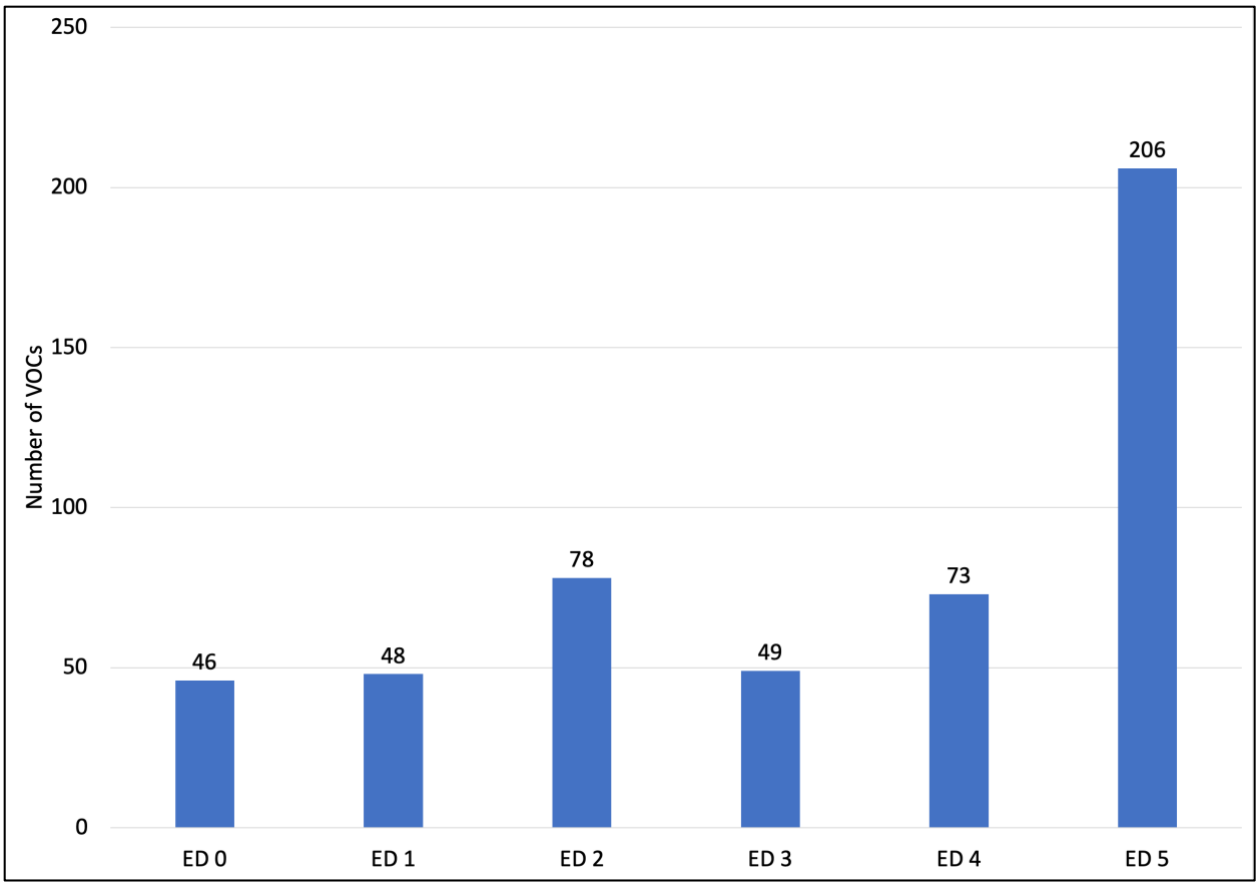

Figure 3-17 *Inter-day variation of VOC abundance in donor H9 observed from ED 0 to ED 5.*

The chemical classes such as acids, alcohols, aldehydes, aromatics, cyclic aliphatic compounds, esters and analogues, ethers, halogen-containing compounds, ketones, linear aliphatic compounds, nitrogen-containing compounds, and sulfur-containing compounds were detected on all experimental days, except aldehydes which were not detected on ED 0, acids which were not detected on ED 0 and ED 1, and ethers which were not detected on ED 1 and ED 2 (Figure 3-18). The class abundance varied across the trial with nitrogen-containing compounds being the most abundant class on ED 0 (n=8), ED 2 (n=14), ED 4 (n=9) and ED 5 (n=37), while aromatic compounds dominated the class abundance on ED 1 (n=7) and ED 3 (n=9) (Figure 3-18).

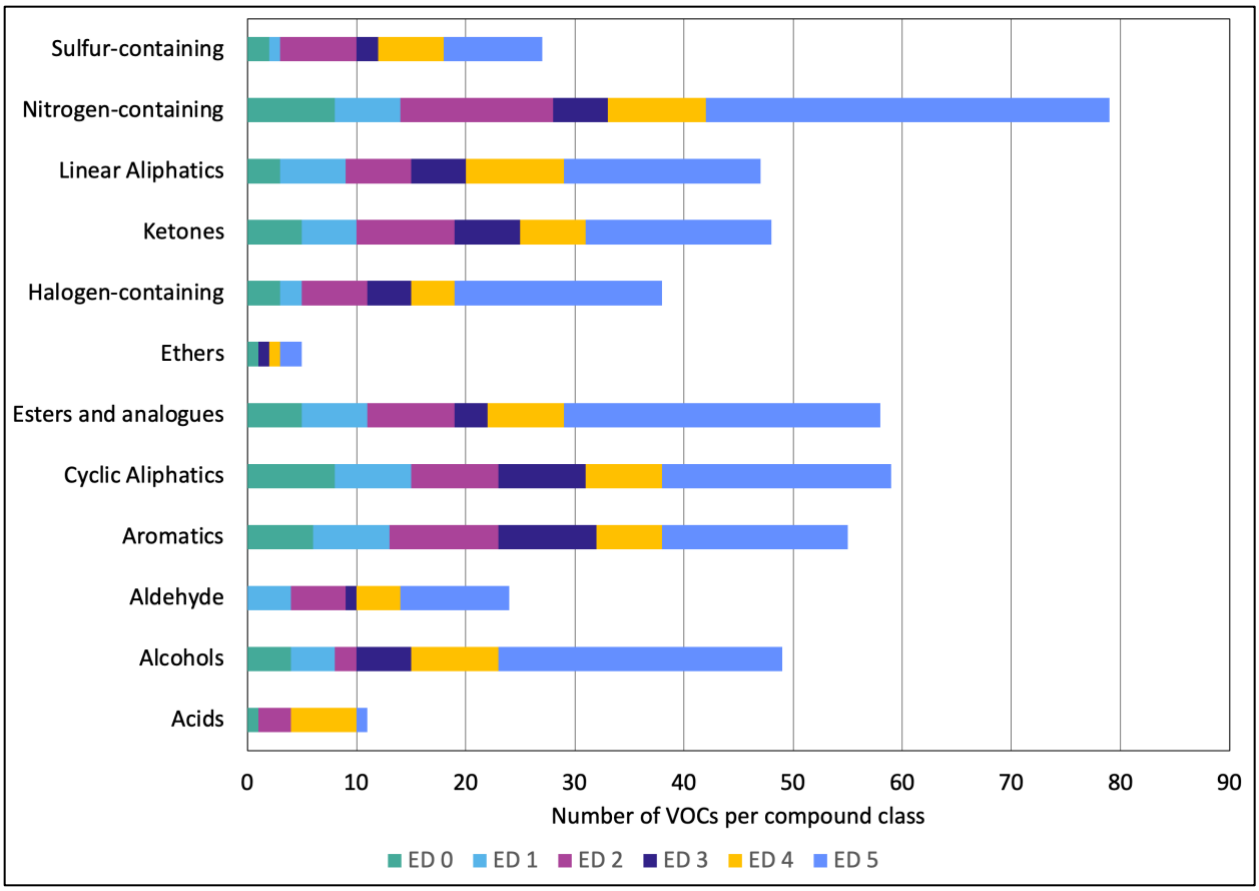

Figure 3-18 *Compound class abundance identified for donor H9 from ED 0 to ED 5.*

3.6.2 Seasonal impact on VOC abundance during the early post-mortem period at the REST[ES] facility

Table 3-4 shows the decomposition patterns and corresponding compound class abundance identified in the donors during the sample collection period across different seasons namely spring, summer, and autumn. The visual features, greenish discolouration and venous marbling which indicate autolysis and putrefaction were the first features noted in all donors except donors H4 and H7 (Table 3-4). Although greenish discolouration was noted on different anatomical landmarks (e.g., diaphragm), this was the first visual feature recorded in multiple donors (H2, H3, H6 and H9) and seasons (summer, autumn, and spring) during the early post-mortem period.

Features indicating the beginning of decomposition, such as autolysis and putrefaction, were recorded in all donors except H4 and H7. These features were noted on ED 2 for donor H2 and on ED 3 for donors H3, H6, H8, and H9. For donor H7, these features were recorded on ED 4. Different compound classes were identified as most abundant when these visual features were recorded for the first time on the donors (Table 3-4). Alcohols (n=8) were identified as the most abundant in donor H2, esters and analogues and halogen-containing compounds (n=3) were the most abundant in donor H3, while cyclic aliphatic compounds (n=9) were the most abundant in donor H6. Halogen-containing compounds had the highest abundance in donor H7 (n=6) while alcohols and aromatics had the highest abundance in donor H8 and H9 (n=9 and n=10) when the first visual features related to autolysis and putrefaction were observed. The transition from the early post-mortem period into the beginning of the bloat stage consistently showed the highest VOC abundance and was identified on the same experimental day (ED 4 and ED 5) for all donors, except donors H3 and H4 which were placed at REST[ES] in the autumn months. Nitrogen-containing compounds had the highest abundance in all donors (H2, H6, H7, H8 and H9) that showed the transition from the early post-mortem period to the bloat stage.

Table 3-4 *Decomposition patterns in relation to VOC abundance and compound class abundance identified on the respective experimental day in donors placed at the REST[ES] facility*

REST[ES] donor id	**Season placed at REST[ES]**	**First visual features indicating autolysis and putrefaction**	**First visual features recorded on (ED)**	**Most abundant compound class when first visual feature was recorded**	**Visual observations related to decomposition process during ED with highest VOC abundance**	**ED with highest VOC abundance**
H2	Summer	Greenish discolouration on palms and torso	2	Alcohols (n=8)	Beginning of bloat stage and high insect activity	4
H3	Autumn	Greenish discolouration on diaphragm	3	Esters and analogues and halogen-containing compounds (n=3)	x	0
H4	Autumn	x	x	x	x	0
H6	Spring	Greenish discolouration on diaphragm, genitals, knee and inner thigh	3	Cyclic aliphatic compounds (n=9)	Spread of greenish discolouration in lower limbs and high insect activity	4
H7	Summer	Entomological activity, no visual changes, egg masses seen	4	Halogen-containing compounds (n=6)	High insect activity on face	2
H8	Summer	Venous marbling on upper and lower limbs	3	Alcohols (n=9)	Beginning of bloat stage, venous marbling and high insect activity	4
H9	Summer	Greenish discolouration on upper limbs	3	Aromatics (n=10)	Bloating of neck and high insect activity	5

** "x" = not recorded*

The seasonal comparison of donor VOC profiles across different seasons was challenging to study as donor availability was variable and donors were not received uniformly across different seasons. To determine average class abundance, the average of each compound class was calculated and then summed. The average class abundance of donors was not solely correlated to the temperature recorded during the sample collection, as shown in Figure 3-19, the class average abundance did not increase with an increase in ADD.

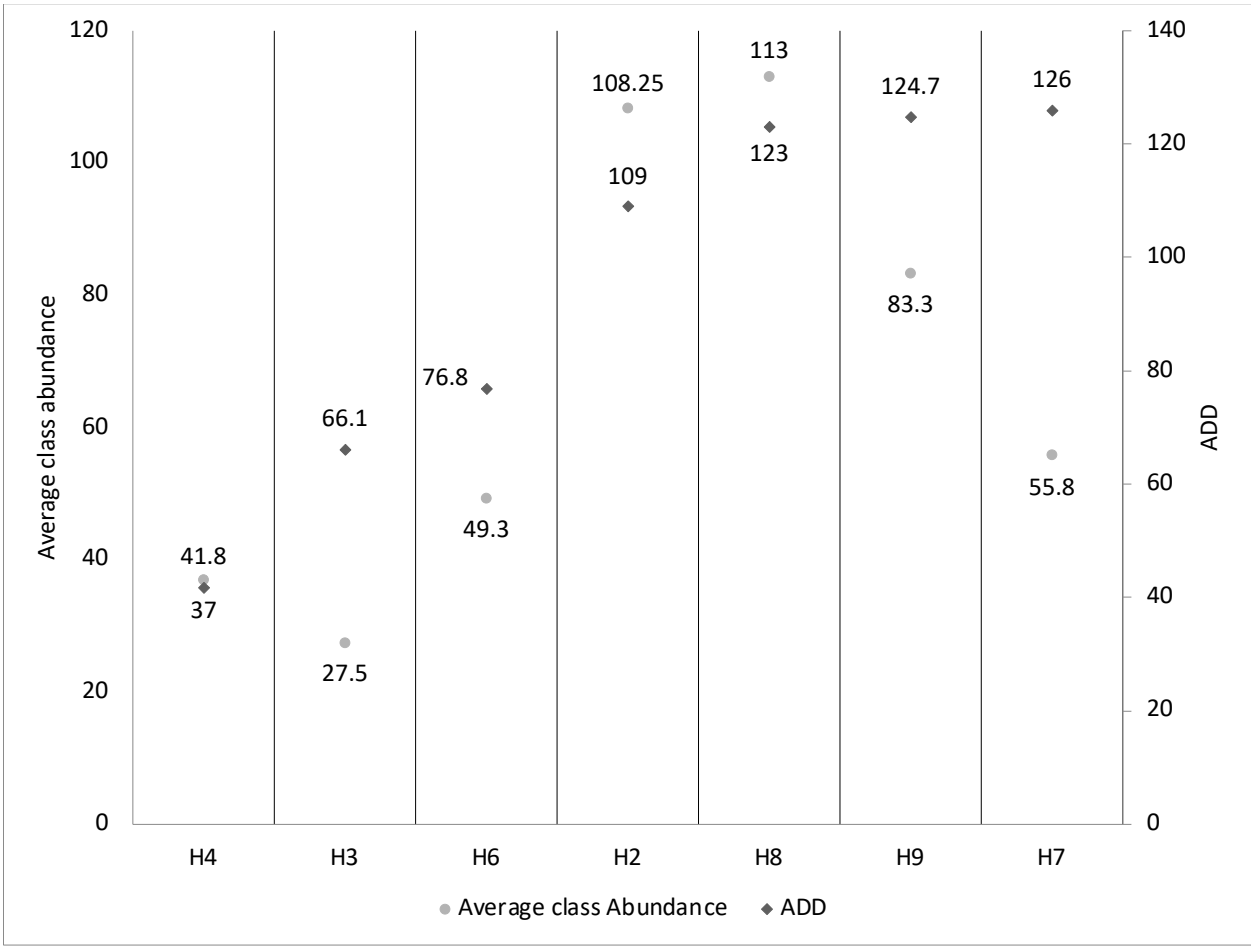

Figure 3-19 *A scatter plot highlighting a non-linear relationship between average class abundance and ADD of donors H2 to H9. Note: the x-axis reports the donors in increasing order of ADD.*

Summer Trials

Five donors were received at the REST[ES] facility during the summer, with two donors placed during the summer of 2020 (H1 and H2) and three donors placed during the summer of 2021

(H7, H8 and H9). Donor H1 is not included in this comparison as only a triplicate sample was collected on ED 0 for this donor. The highest average class abundance was observed during the summer trials for the entire study. Donor H8 (ADD=123) had the highest average class abundance (n=113) among the five donors placed in summer. Donor H7 (ADD=126) had the lowest average class abundance (n=55.8) relative to the average class abundance of donors H8 (n=113) and H9 (n=83.3) as shown in Figure 3-19.

Autumn Trial

Two donors were received in the only autumn trial conducted in 2020. Donor H3 had the lowest average class abundance (n=27.5), even though it had a higher ADD (66.1) than donor H4 (ADD=41.8; class abundance = 37). H3 also had the lowest average class abundance among all the donors.

Spring Trial

At the REST[ES] facility, the VOC sample collection during the spring season is possible after the snow on the ground completely thaws, and the ground absorbs the water accumulated on the surface. H6 was the only donor received during the spring season. For donor H6 (ADD=76.8), the average class abundance observed during the spring trial was n=49.3.

3.6.3 Principal component analysis

PCA analysis was conducted to visualise any inter-day variation in the VOC profiles of the donors, which could be specific to the human decomposition process during the early post-mortem period. The pre-processing treatments, such as internal standard area normalisation and mean centering, were performed prior to the PCA. This approach provided valuable information in terms of identifying decomposition VOCs relevant to the early post-mortem process. There were no outliers flagged in the data through use of Hotelling's T2 statistic at 95% level. The number of VOCs used for constructing the PCA varied due to the variability in the

VOC abundance. For the PCA, the scores plot comprised of VOC samples collected on different experimental days (EDs) and the loadings were calculated from the normalised area of each compound to reflect the contribution of each compound to the overall variance in the donor samples.

Figure 3-20 shows the PCA was constructed using 229 VOCs identified across eight donors with a minimum detection frequency of four out of 36 samples. The first two principal components accounted for 10% (PC-1) and 7% (PC-2) of the explained variance. The scores plot of PC-1 vs PC-2 highlights the intra-donor variability in the VOC profiles. Along PC-1, donors H3 and H4, placed in the autumn season, were separated from the rest of the donors (highlighted with an orange circle), while donor H6, placed during the spring, was separated along PC-1 but on the negative axis (highlighted with a green circle). The separation of donor H6 samples from donors H3 and H4 in the scores plot could highlight the intra donor variation due to the biological processes and/or intra-seasonal variation associated with placement of the donors in different seasons. The donors (H2, H7, H8, and H9) placed during summer were spread across PC-2 (highlighted with a blue circle). The correlation loadings showed that the majority of loadings had a weak influence on the PCs as the compounds are located within the inner ring and close to the axis (Figure 3-20). This could be due to the weak association with the donors present in the scores plot.

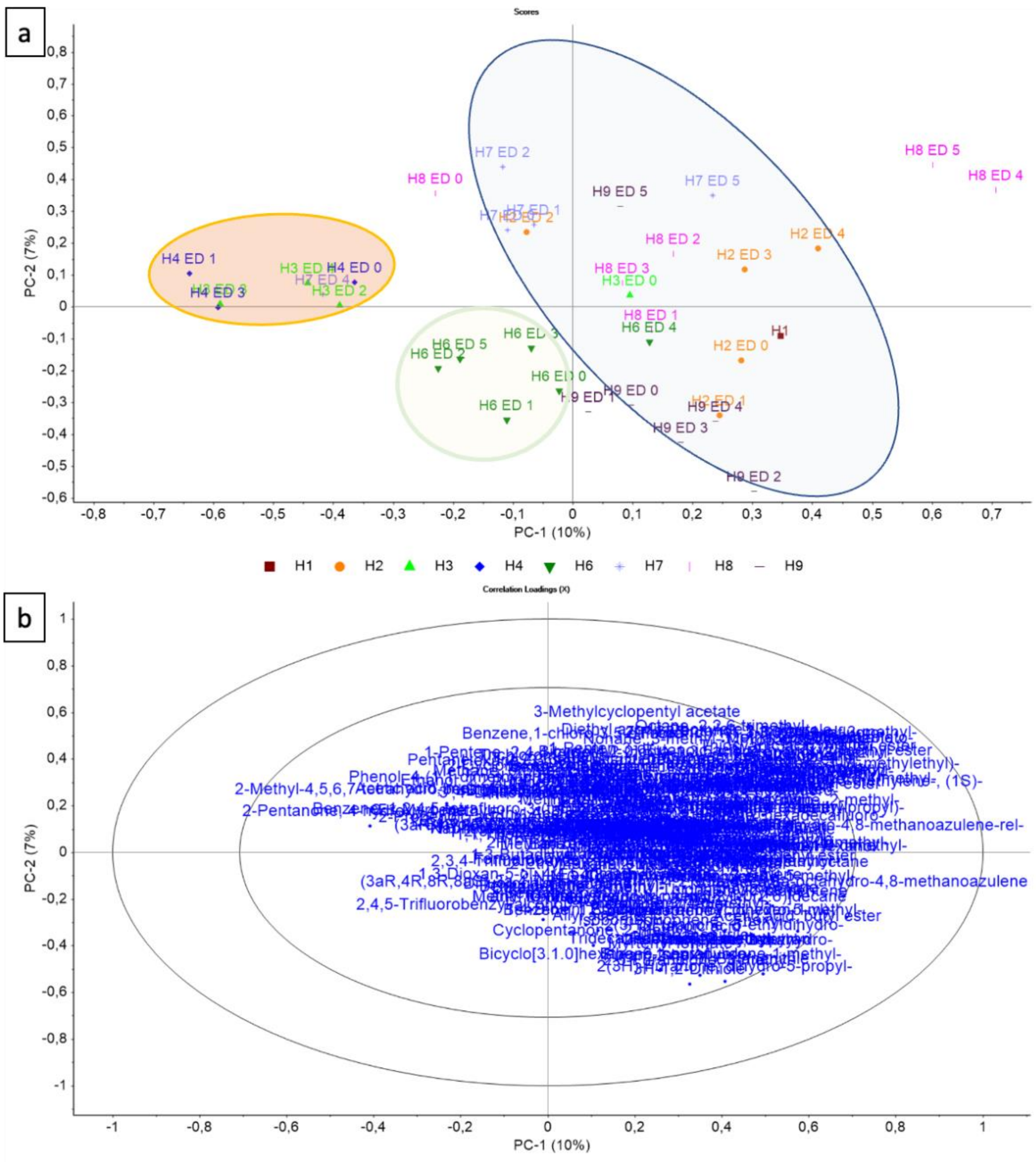

Figure 3-20 PCA a) scores plot and b) correlation loadings plot for PC-1 vs PC-2. PCA were calculated using the pre-processed GC×GC-TOFMS normalised peak areas of 229 compounds identified with a minimum detection frequency of four out of 36 samples. The scores plot of PC-1 vs PC-2 (17% explained variance) shows separation and clustering of donor H3 and H4 samples from all other donor samples. Donor H3 and H4 samples are highlighted by an orange circle, donor H6 samples are highlighted by a green circle, and donor H2, H7, H8 and H9 samples are highlighted by a blue circle. The correlation plots show VOCs close to the intercept and located within the inner ring highlighting weak influences on the VOC samples present in the scores plot.

Donor H2

The PCA was constructed with 82 VOCs identified across five experimental days with a minimum detection frequency of two out of five samples. The first three principal components (PCs) of donor H2 explained 97% of the variance in the data. The scores plot of PC-1 vs PC-2 showed the best representation of inter-day variability in the VOC samples collected at the REST[ES] facility. The sample H2 ED 3 is separated from all the other samples along PC-1 (72% explained variance). Along PC-2, the sample H2 ED 0 collected on the first ED after the donor placement at the REST[ES] facility is separated from sample group H2 ED 1, H2 ED 2, and H2 ED 4. This sample group clustered along the positive axis of the PC-2, while sample H2 ED 0 is located on the negative axis. The location of H2 ED 0 opposite to this sample group indicates differences in the VOCs profiles that can be attributed to decomposition processes such as autolysis and putrefaction after the placement of the donors on ED 0. The loadings show that phenol is causing the separation of the H2 ED 0 sample along PC-1 and methenamine, disulfide dimethyl, and dimethyl trisulfide are responsible for causing separation of H2 ED 3 from all other samples (Figure 3-21b).

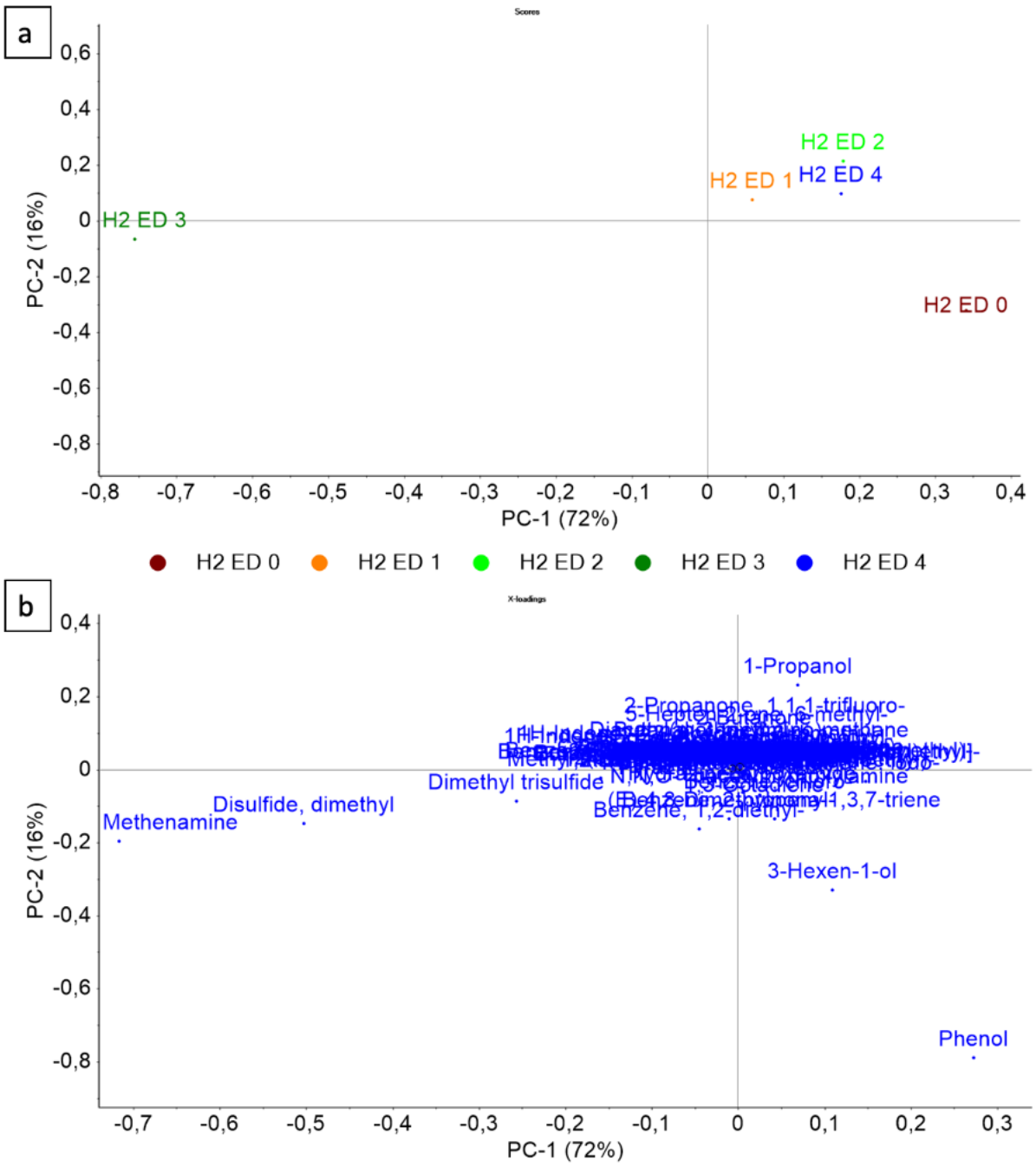

Figure 3-21 *PCA showing a) scores plot and b) loadings plot for PC-1 vs PC-2 of donor H2. PCA were calculated using the pre-processed GC×GC-TOFMS normalised peak areas of 82 compounds identified with a minimum detection frequency of two out of five samples. The sample H2 ED 0 was separated from samples H2 ED 1, H2 ED 2, H2 ED 3, and H2 ED 4 along PC-1. The loadings plot shows the distribution of variables across PC-1 and PC-2, with phenol causing separation of sample H2 ED 0 and methenamine, dimethyl disulfide and dimethyl trisulfide causing separation of sample H2 ED 3 along PC-2.*

Comparison of donors H3 and H4

The individual PCA of donors H3 and H4 did not generate any plots and the PCA model could not predict any variance. The low number of VOCs in these donors caused this error. Thus, the PCA was conducted on the combined VOC data of the donors. Furthermore, the placement of the donors H3 and H4 during the same season allowed for this combined PCA. The PCA for donors H3 and H4 was constructed with 84 VOCs and these VOCs had a minimum detection frequency of one out of seven samples. Five PCs explained 88% of the variance in the data. PC-1 and PC-2 captured 41% of the total variation in the data while PC-3, PC-4, and PC-5 captured 17%, 15% and 15%, respectively, of the variation in the data. The PC-1 vs PC-2 showed the best visual representation of the sample spread collected at the REST[ES] facility and highlighted the intra-donor variation in the VOC profiles between donors H3 and H4. The samples collected after ED0 were clustered and separated along PC-2. The loadings plot is not attached with the scores plot as loadings were clustered along the X and Y intercept demonstrating weak influence on donor H3 and H4 samples.

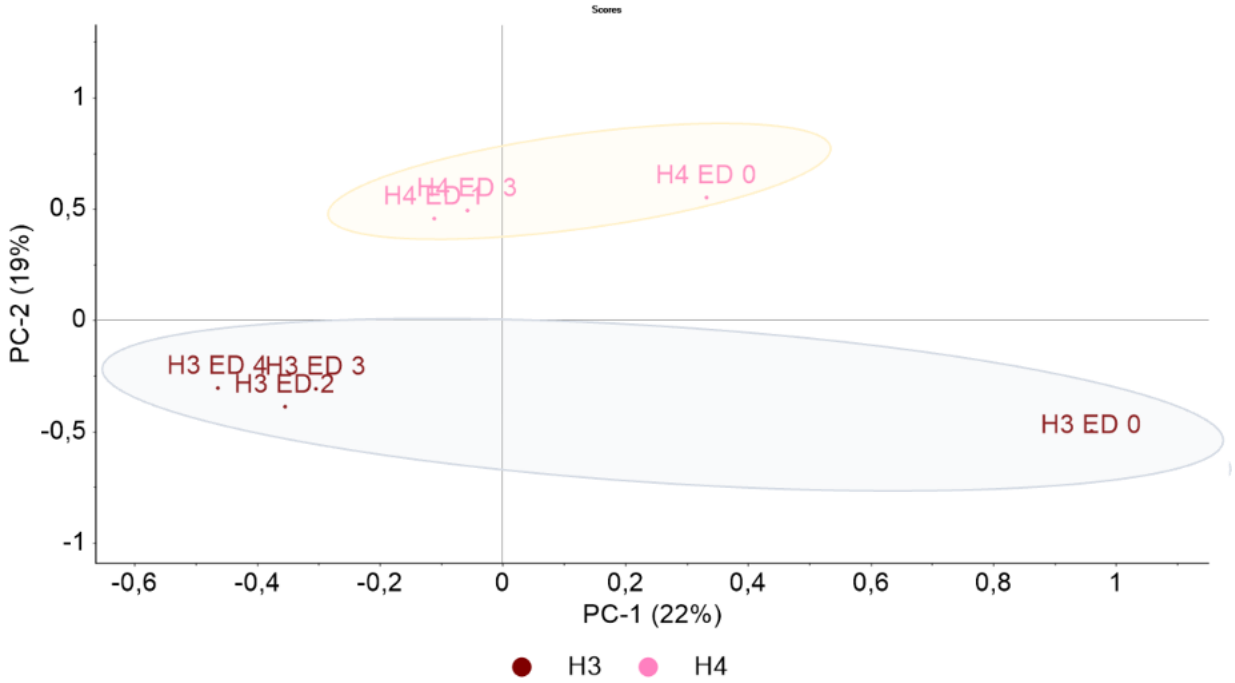

Figure 3-22 *PCA showing scores plot for PC-1 vs PC-2 of donors H3 and H4. PCA were calculated using the pre-processed GC×GC-TOFMS normalised peak areas of 84 compounds identified with a minimum detection frequency of one out of seven samples. The scores plot highlights the intra-donor variation in the VOCs profiles through separation of donors along PC-2. Here the orange circle highlights the donor H4 samples and the blue circle highlights donor H3 samples.*

Donor H6

For donor H6, PC-1 and PC-2 were constructed with 52 VOCs identified across six experimental days with a minimum detection frequency of two out of six samples. The first two PCs explained 76% of the variance in the data. In the scores plot an interesting pattern can be observed along PC-1, whereby samples H6 ED 0, H6 ED 1, and H6 ED 2 are grouped and separated from sample H6 ED 4, while these group of samples are also separated from H6 ED 3 and H6 ED 5 along PC-2. On ED 3, donor H6 showed signs of greenish discoloration and on ED 4, this greenish discoloration progressed to the lower limbs and torso. Moreover, sample H6 ED 4 had the highest VOC abundance and is separated across PC-1 (53% explained variance). For donor H6, the separation of samples H6 ED 3, H6 ED 4 and H6 ED 5 from samples H6 ED 0, H6 ED 1 and H6 ED 2 indicates a change in the VOC profile after ED 2. The loadings plot shows that 2-butanone is responsible for causing the separation of sample H6 ED 4 along PC-1, and

bicyclo[2.2.1]heptane,2,2-dimethyl-3-methylene-(1s) (camphene) and formaldehyde are responsible for causing the separation of samples H6 ED 3 along PC-2 as seen in Figure 3-23b.

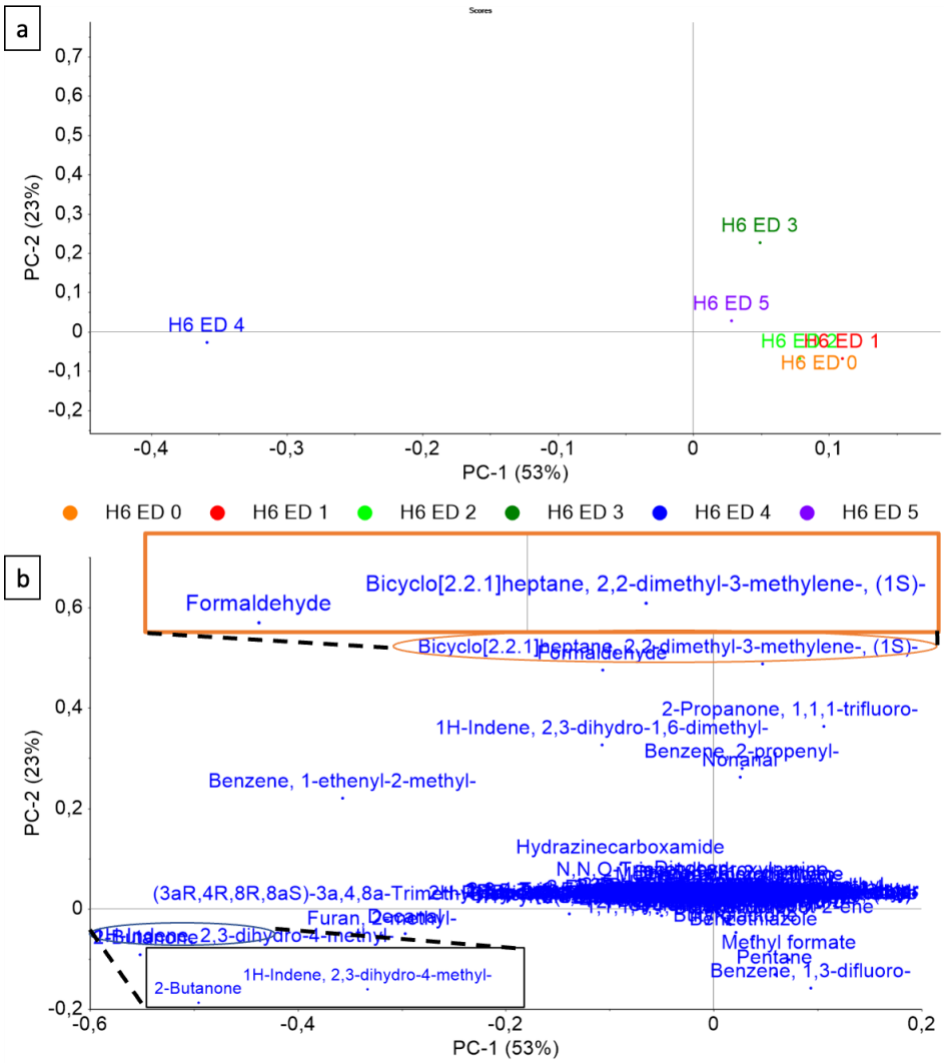

Figure 3-23 *PCA showing a) scores and b) loadings plot for PC-1 vs PC-2 of donor H6. PCA were calculated using the pre-processed GC×GC-TOFMS normalised peak areas of 52 compounds identified with a minimum detection frequency of two out of six samples. The sample H6 ED 4 was separated from the cluster of samples H6 ED 0, H6 ED 1, and H6 ED 2 along PC-1, and samples H6 ED 3 and H6 ED 5 were separated along PC-2. The loadings plot shows the distribution of variables across PC-1 and PC-2, with 2-butanone causing separation of sample H6 ED 4 (highlighted with a black box) and formaldehyde and bicyclo[2.2.1]heptane,2,2-dimethyl-3-methylene-(1s) (camphene) causing separation of sample H6 ED 3 along PC-2 (highlighted with an orange box).*

Donor H7

The PCA on donor H7 was constructed with 53 VOCs identified across five experimental days with the minimum detection frequency of two out of five samples. Three PCs explained 90% of the variance. The PCA scores plot shows the separation of the samples collected on different experimental days (Figure 3-24a). Along PC-2, the samples H7 ED 2, H7 ED 4, and H7 ED 5 samples are positioned on the positive axis, while H7 ED 0 and H7 ED 1 are located on the negative axis (Figure 3-24a). After ED 1, there was an increase in the VOCs abundance and insect activity. Further patterns indicating decomposition processes, such as greenish discoloration, was seen on the body from H7 ED 4 with high insect activity. The distribution of H7 ED 2, H7 ED 4, and H7 ED 5 away from H7 ED 0 and H7 ED 1 samples can be attributed to the differences in the VOC profiles. The loadings demonstrate that styrene caused the separation of the sample H7 ED 0 and H7 ED 1, while 2-butanone was responsible for separation of the H7 ED 1 sample (Figure 3-24b). Isopropyl alcohol caused separation of the sample H7 ED 2 and DMDS, pyrrole, isobutyronitrile, methane isothiocyanato and benzene, 2-propenyl (prop-2-enylbenzene) caused separation of the samples H7 ED 4 and H7 ED 5, as shown in the loadings plot in Figure 3-24b.

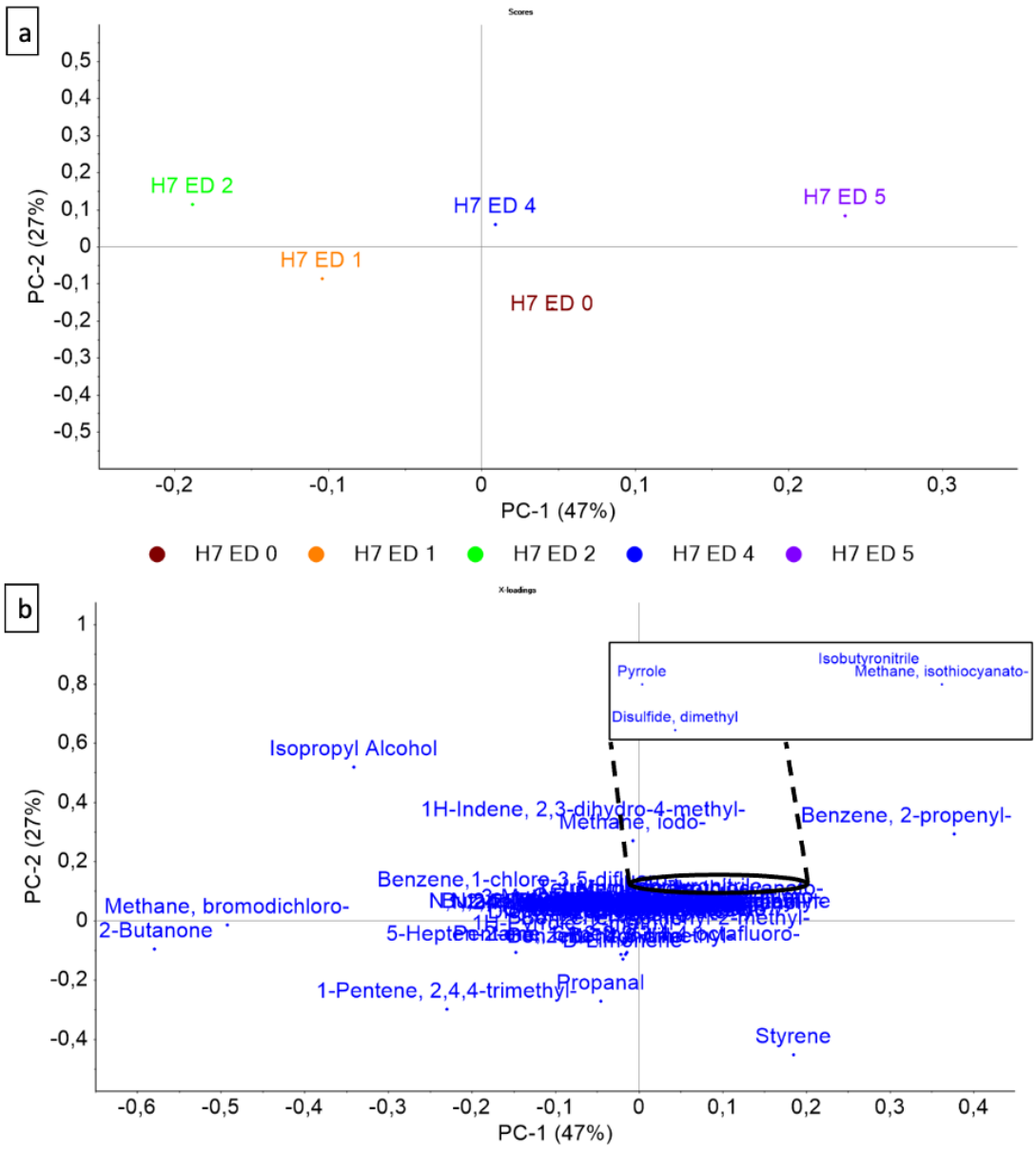

Figure 3-24 *PCA showing a) scores plot and b) loadings plot for PC-1 vs PC-2 of donor H7. PCA were calculated using the pre-processed GC×GC-TOFMS normalised peak areas of 53 compounds identified with a minimum detection frequency of two out of five samples. The scores of PC-1 vs PC-2 shows an interesting pattern of separation for samples H7 ED 4 and H7 ED 5 from samples H7 ED 0 and H7 ED 1. The loadings plot shows the distribution of variables across PC-1 and PC-2, with DMDS, pyrrole, isobutyronitrile, isothiocyanoate (highlighted with a black box) and benzene, 2-propenyl causing separation of the samples H7 ED 4 and H7 ED 5 from H7 ED 0 and H7 ED2 along PC-2.*

Donor H8

The PCA of donor H8 was constructed using 145 VOCs identified with the minimum detection frequency of two out of six samples. The first two PCs explain 94% of the variance in the data (Figure 3-25). The scores plot demonstrates that sample H8 ED 4 is separated from all other samples along PC-1 (84% of explained variance). Along PC-2 an interesting pattern can be observed, the samples H8 ED 0, H8 ED 1 and H8 ED 2 are separated from H8 ED 3 and H8 ED 5 samples. On ED 3, venous marbling indicating decomposition was first seen on the upper and lower body. Thus, the separation pattern of the sample H8 ED 3 from the samples H8 ED 0 to H8 ED 2 indicates a change in the VOC profile that can correlated to the beginning of the decomposition process. The loadings shows that along PC-2, nonanal, isopropyl alcohol, dimethyl disulfide and methylamine, N,N dimethyl were responsible for causing separation of the samples H8 ED 3 and H8 ED 5 from samples H8 ED 0, H8 ED 1 and H8 ED 2. Methenamine and acetamide,2-cyano is responsible for the separation of sample H8 ED 4 from all other samples along PC-1.

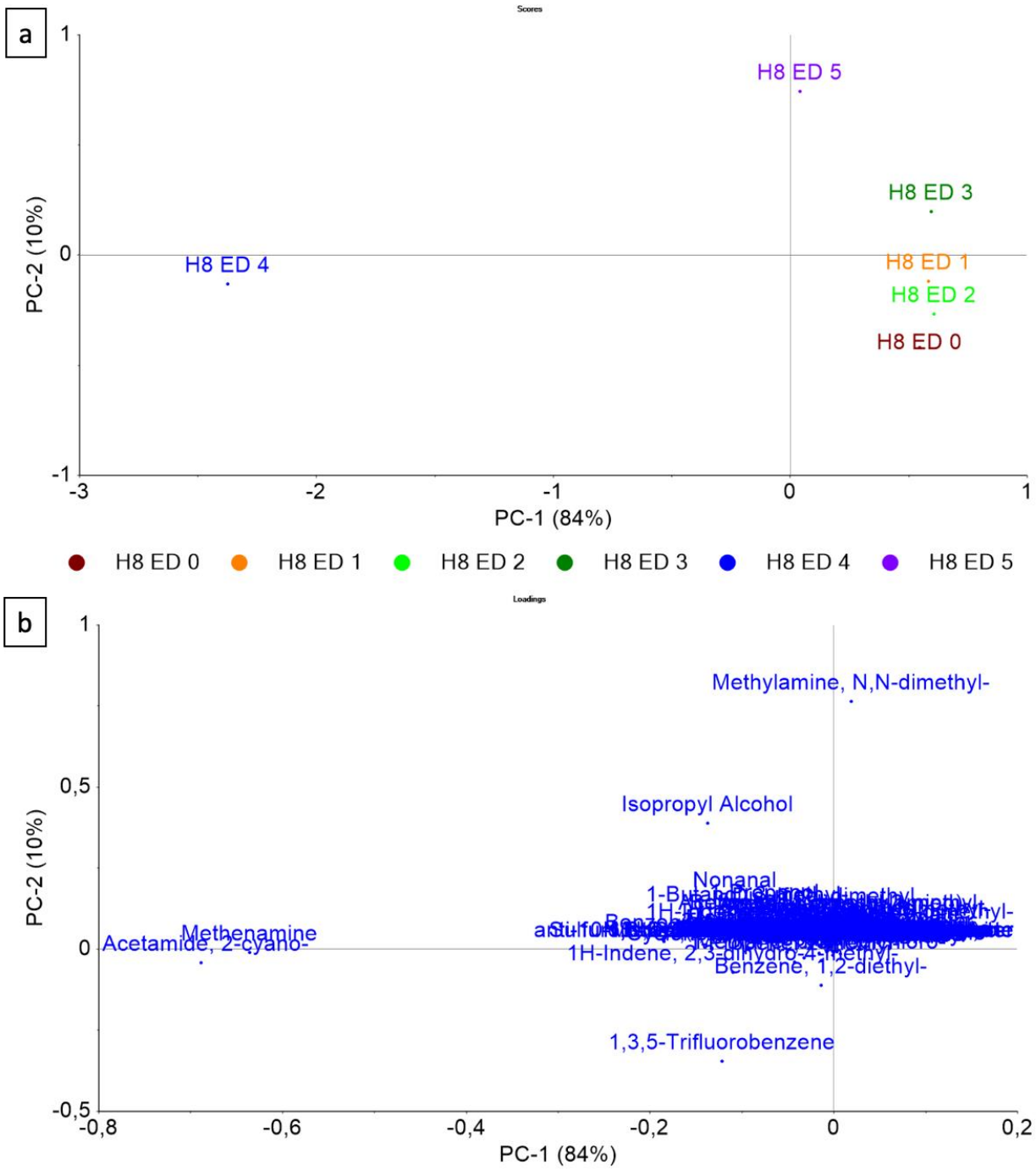

Figure 3-25 *PCA showing a) scores plot and b) loadings plot of donor H8. PCA were calculated using the pre-processed GC×GC-TOFMS normalised peak areas of 145 compounds identified with a minimum detection frequency of two out of five samples. The sample H8 ED 4 was separated along PC-1 from all other samples. The sample H8 ED 3 and H8 ED 5 was separated from the cluster of samples H8 ED 0 to H8 ED 2 along PC-2. The loadings plot shows the distribution of variables along PC-1 and PC-2, with methenamine causing separation of sample H8 ED 4 from all other samples along PC-1 and methylamine, N,N-dimethyl causing separation of samples H8 ED 3 and H8 ED 5 along PC-2.*

Donor H9

The PCA of donor H9 was constructed using 75 VOCs identified with the minimum detection frequency of two out of six samples (Figure 3-26). Four PCs explained 93% of the variance in the data. PC-1 and PC-2 captured 64% of the total variation in the data, while PC-3 and PC-4 captured 18% and 11% of the variation in the data, respectively. Notably, the scores plot PC-3 vs PC-4 showed an interesting pattern of clustering and separation (Figure 3-26a). The samples H9 ED0 and H9 ED1 are separated from H9 ED2 along PC-3. H9 ED 0 represents the sample collected when the donor was placed at the outdoor facility. The H9 ED 4 and H9 ED 5 samples are separated and clustered along the PC-4. The donor showed signs of autolysis and putrefaction during the collection on ED 3 and higher VOC abundance on ED 4 and ED 5. The separation of H9 ED 3, H9 ED 4 and H9 ED 5 from H9 ED 0 indicates a change in the VOC profile to post-mortem odour on H9 ED 3. Benzene,1-ethenyl-2-methyl caused the separation of the samples H9 ED 0 and H9 ED 1 and 2-Propenal benzene caused the separation of the sample H9 ED 2 (Figure 3-26b). Benzonitrile, phenol, and benzaldehyde caused the separation of the H9 ED 3 sample while acetonitrile, 1-Butanol, 3-methyl, butanal, 3-methyl, 1-Propanol, 2 -methyl and disulfide dimethyl caused the separation of samples H9 ED 4 and H9 ED 5 (Figure 3-26b).

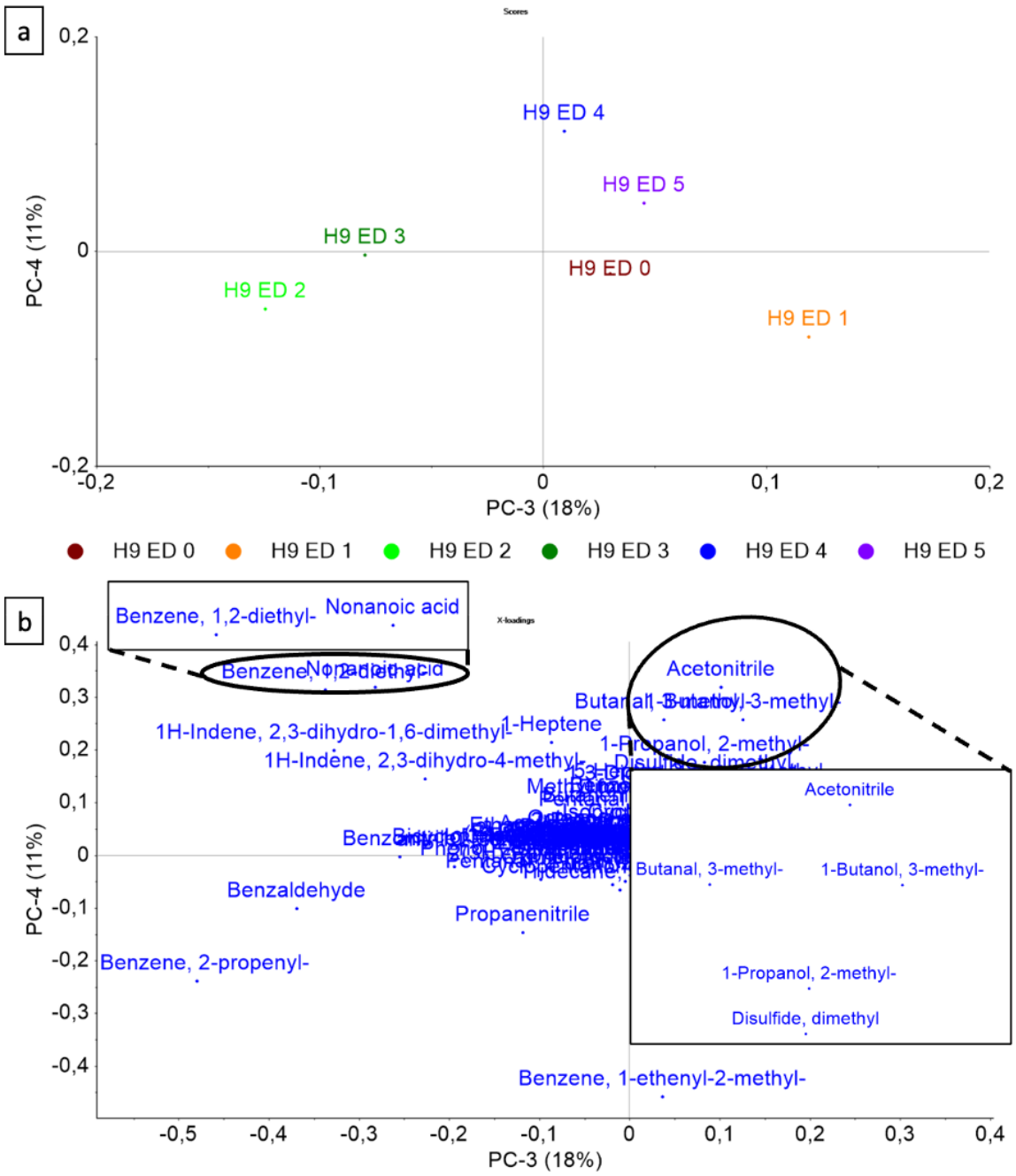

Figure 3-26 *PCA showing a) scores plot and b) loadings plot of donor H9. The scores plot of PC-3 vs PC-4 shows an interesting pattern of separation. Samples H9 ED 0 and H9 ED 1 are separated from H9 ED 2 along PC-3. Samples H9 ED 4 and H9 ED 5 are separated from the cluster of samples H9 ED 0 to H1 ED 2 along PC-4. The loadings plot shows the distribution of variables across PC-3 and PC-4, with DMDS, 1-Propanol, 2 -methyl, 1-Butanol, 3-methyl, butanal, 3-methyl and acetonitrile (highlighted with a black box) causing separation of sample H9 ED0 from all other samples along PC-4.*

Table 3-5 highlights the samples which were clearly separated on the scores plot. In general, the samples collected on ED 0 after the initial placement of the body at the REST[ES] facility were separated from all other samples collected during the relevant trial (e.g., ED 1, ED 2, and others). Samples collected on ED 1 and ED 2 show less relative spread on the scores plot compared to samples collected on ED 4 and ED 5. The samples collected on ED 4 and ED 5 were the last samples collected during each trial. By these experimental days, the early post-mortem period was in the final stages and donors typically showed visual features such as the beginning of bloat and relatively high insect activity compared to ED 0 to ED 2.

The loadings plots demonstrate that the majority of VOCs identified were close to the axis origin showing only a weak influence on the VOC samples present in the scores plot. VOCs such as methenamine and DMDS caused the separation of ED 3 and ED 4 samples in the scores plot of donors H2, H7, H8 and H9.

Table 3-5 *Summary of samples showing highest separation and their corresponding scores and loadings plot.*

Donor Id	**Samples showing highest separation**	**Corresponding scores plot and explained variance**	**Corresponding loadings**
H2	H2 ED 0 and H2 ED 3	PC-1 (72%) and PC-2 (16%)	Dimethyl disulfide, methenamine and dimethyl trisulfide (PC-1) & Phenol (PC-2)
H6	H6 ED 4 & H6 ED 0	PC-1 (53%) and PC-2 (23%)	2-butanone (PC-1) and 1,3-difluro benzene (PC-2)
H7	H7 ED 5 and H7 ED 0	PC-1 (47%) and PC-2 (27%)	Benzene, 2-propenyl (PC-1) and styrene (PC-2)
H8	H8 ED 4 and H8 ED 0	PC-1 (84%) and PC-2 (10%)	Methenamine (PC-1) and no loadings strongly correlated with ED 0

3.7 Discussion

3.7.1 Decomposition patterns and overall VOC class abundance at the REST[ES] facility

In this study, features related to autolysis and putrefaction were noted on all the donors except H4 and H7 during the early post-mortem period. Moreover, the most commonly reported compound classes (e.g., acids, alcohols, aldehydes and others) were identified in the VOC profile of all donors placed in the outdoor environment. These compound classes have been previously reported in decomposition VOC profiles (37, 38, 63). The decomposition features such as greenish discolouration, skin slippage and venous marbling were recorded during the early post-mortem period, and these features are typically observed on a cadaver due to autolysis and putrefaction. The greenish discolouration was one of the first decomposition-related features noted as early as ED 2 on donor H2. This feature was initially seen over the diaphragm region and lower and upper limbs and later was simultaneously seen over other anatomical regions such as the head and neck. The presence of these features on the donors indicate that the decomposition process progressed faster in these regions compared to the rest of the body. It has been reported that organs such as brain, liver, pancreas and intestines are rich in enzymes and microbiota, respectively (128). As enzymes and microbiota in these organs are higher, in the absence of the body's protective mechanism, these organs can autolyse faster. Thus, the faster rate of autolysis and putrefaction in a particular region can be attributed to the high enzymatic and microbial activity (26).

These features were not observed in donors H4 and H7. Donor H4 was placed in the autumn season, where the average temperature was the lowest (9.9 °C) of any of the trials, and a higher volume of rainfall (5.9 mm) was recorded during the trial. This could have reduced the autolytic and microbial activity, thus slowing down the decomposition process. Donor H7 who was placed in the summer season, showed increased insect activity during the trial but visual features indicating autolysis and putrefaction were not recorded. Donor H7 died of metastatic

cancer of the lungs and prostate; this pathology or the treatments prior to death such as radiotherapy and immunotherapy could have altered the tissue characteristics affecting the overall decomposition progression. However, this hypothesis is solely based on visual observation and anecdotal evidence. The treatments received during the ante-mortem period were not disclosed in the death certificate. Nevertheless, visually donor H7 progressed differently than the other donors placed during the summer season of 2021.

Alcohols, ketones, esters and analogues, cyclic aliphatic compounds and aromatics were the most abundant classes on the experimental days when the visual features associated with autolysis and putrefaction were first recorded on donors H2, H3, H6, H7, H8 and H9. Alcohols, ketones, esters and analogues are produced due to carbohydrate and fatty acid breakdown (35, 58, 62). The detection of esters during the early post-mortem period could indicate the reaction of alcohols and fatty acids (produced due to carbohydrate and lipid degradation) in the presence of bacterial esterases (129). Furthermore, production of aromatic compounds are linked with protein degradation (47). The variation in the abundance of compound classes can suggest that macromolecules break down at variable rates and sometimes simultaneously, depending on external (temperature, humidity, etc.) and internal (physiology and pathophysiology) factors. These differences in the rate of macromolecule breakdown during the early post-mortem period may potentially lead to differential decomposition in the later stages of the decomposition process. Differential decomposition refers to different decomposition patterns or stages observed simultaneously on a single cadaver. This phenomenon has been previously reported in outdoor decomposition studies conducted on cadavers (36, 109)

On ED 4 and ED 5, detectable changes such as the highest VOC abundance and beginning of bloat were identified for donors H2, H6, H7, H8, and H9. Visually, these donors showed signs of bloating in the abdomen and neck. The bloat stage of decomposition follows the early post-mortem stage (fresh stage) and is characterised by an increase in autolysis and putrefaction activity causing gas accumulation in the cadavers. During this stage, decomposition odour changes due to high anaerobic activity and putrefactive changes. This causes the transition of

the early post-mortem VOC profile to what is more typically referred to as decomposition odour. The significant increase in the VOC abundance along with visual changes showed that there was a distinct change in decomposition stage. The results suggest a positive correlation of VOC abundance with the transition of odour for donors H2, H6, H7, H8, and H9 during the early post-mortem period.

Nitrogen-containing compounds dominated the compound class abundance during these experimental days (H2 ED 3, H2 ED 4, H4 ED 4, H6 ED 4, H7 ED 5, H8 ED 2, H8 ED 4, H8 ED 5, H9 ED 5). The high abundance of nitrogen-containing compounds is associated with microbial activity and the decarboxylation of amino acids such as lysine, arginine and tryptophan (35, 106). Furthermore, the presence of nitrogen-containing compounds during the early-post-mortem period has been linked to the breakdown of proteins, peptides, peptones and amino acids into nitrogen-containing compounds by enzymes during the autolytic processes (35).The high abundance of nitrogen-containing compounds is contrary to the findings reported in an outdoor decomposition study conducted by Deo et al. (38). The implied absence of nitrogen-containing compounds in their study could be due to the difference in the sample collection and accumulation time. However, the abundance of the nitrogen-containing compounds in the current study varied; they were detected consistently and in relatively high abundance compared to other compound classes during the early post-mortem period, and notably when insect activity was recorded. This result shows that nitrogen-containing VOCs as a compound class can potentially be used as an indicator for the change in the decomposition stage from the early post-mortem (fresh stage) to the beginning of the bloat stage.

Acids and ethers were detected in the lowest abundance across all donors and seasons. Acids have been reported during the active and advanced stages of decomposition and are associated with the breakdown of fat and adipose tissue; this compound class is also associated with the putrefaction of soft tissue (43, 109). The lower abundance of the acid class of compounds in the VOC profiles of donors can suggest that the biochemical processes responsible for the breakdown of adipose tissue was progressing slowly during the early post-mortem period resulting in a lower abundance of acid VOCs relative to other compound classes (43). Ethers are

decomposition by-products of carbohydrates and have been identified at different decomposition stages but with lower abundance also (56). Ethers are most commonly reported in studies using GC×GC-TOFMS (50, 64, 78) for the sample analysis. The identification of ethers can be due to the increased peak capacity of comprehensive GC×GC-TOFMS aiding in the identification of this class of compounds.

Notably, in this study the number of VOCs detected during the early post-mortem period was 50% higher than in other similar studies (37, 38, 87) conducted in an outdoor environment. The higher number of VOCs could be attributed to differences in the experimental design and data processing method. In this study, the accumulation period was increased to 20 min, which is five minutes more than in other studies (37, 38) conducted in outdoor environments. Furthermore, the size of the aluminium hood used in this study was also modified and the overall height was ∼10% smaller compared to the hoods used in the studies previously reported (37, 38). Thus, the longer VOC accumulation time and smaller hood volume likely improved pre-concentration of the volatiles in the headspace above the donors.

The differences in the reported numbers of VOCs could also be attributed to differences in the data processing step. The two-dimensional gas chromatography technique gives users a plethora of options for data processing and further statistical analysis. The minimum S/N ratio in the data processing step was changed from 150 to 1, and a custom R script was used to process the dataset, identify peaks uniquely released from donors and filter out the peaks identified in the control samples. This approach of using the customised data processing method and R script aided in highlighting the inter-day trends in VOC abundance and compound classes observed across each of the eight donors (section 3.6.1). These trends suggested that VOC and overall VOC class abundance on ED 0, ED 1, ED 2, and ED 3 was relatively low compared to ED 4 and ED 5. The VOC abundance typically declined after ED 0 and stayed relatively low until ED 3, (0-72 h post-placement). The internal ADD of the donors equilibrated with ambient ADD after 72 h post-placement (Table 3-3) as the donors were subject to varying ambient temperatures during the trial (e.g., Table 3-2: H2 maximum temperature 33 °C to minimum temperature 12.7 °C). These varying ambient temperatures

slowed the rate at which donors internal ADD equilibrated with the ambient ADD. The lower internal ADD affects the rate of autolysis and microbial activity, which depends on the temperature. Thus, lower internal ADD may have affected the VOC abundance of donors during 24-72 h post-placement as the VOC abundance increased as the internal ADD equilibrated with the ambient ADD (after ED 3). The low VOC and compound class abundance can also be associated with relatively low microbial and insect activity which was recorded during these experimental days. The VOC abundance was low when the donors visually demonstrated localised decomposition patterns and low insect activity between ED 0 to ED 3. A subsequent increase in the VOC abundance was then observed as the bodies showed signs of progression of decomposition (beginning of bloat) and increased insect activity. The lack of studies focusing on early post-mortem VOC profiles in an outdoor environment prevents the comparison of the inter-day variation in VOC and compound class abundance. To date, the inter-day variation in VOC abundance during an early post-mortem period has only been reported in a study which used pig remains (64) and this variation was not observed in a study which used cadavers (63). Moreover, results of the current study support the findings of the study conducted by Deo et al. (38), which highlighted that the VOCs released during the early post-mortem period evolve as the decomposition process progresses. Therefore, the modifications in experimental design and data processing method aided in understanding the early-post-mortem VOC profiles of human remains and capturing a detectable change after ED 3 in the VOC profile during the transition from the early post-mortem stage into the bloat stage in an outdoor environment.

3.7.2 Seasonal impact on VOC abundance during the early post-mortem period in an outdoor environment

The rate of decomposition and VOC abundance fluctuated during the summer, autumn, and spring seasons. The progression of decomposition in autumn was visually slower compared to the spring and summer seasons. The highest average VOC abundance was identified in the summer season and is consistent with high ambient temperatures and biological (microbial,

insect) activity recorded during the summer trials. The total VOC abundance in each compound class was also the highest in the summer season and lowest in the autumn season.

A linear relationship was not observed between the VOC abundance and ADD. Intra-seasonal variation in the VOC abundance was observed, e.g., for donors H3 and H4 which were placed in the autumn season, whereby donor H3 had the lowest average VOC abundance among all the donors. This intra-seasonal variation was also observed in donors placed during the summer of 2021, where the average VOC abundance of donor H7 was approximately 84% less than donor H8 placed during the same season. The intra-seasonal variation in the VOC abundance could be associated with other environmental factors such as rainfall and internal factors such as physiology and pathophysiology of donors during the ante-mortem period, which could influence the decomposition process. One common environmental factor observed was the relatively cooler temperatures recorded during the summer trial of donor H7 and the cold temperature and amount of rain experienced during the trial of donors H3 and H4 in the autumn months. The effect of cooler temperatures has been reported in detail and it is known to reduce the decomposition process and consequently the VOC abundance (38, 42, 43). Nevertheless, the effect of rain on the VOC abundance of cadavers during the early post-mortem period has not been discussed in any studies to date. It is reported in the literature that rain accelerates the process of decomposition during the active stages of decomposition, attracting a new succession of insect activity on mummified tissue and removing the loosely attached tissue on the body (42). A contrasting effect was observed on donors in the early post-mortem period of the current study, where the rain limited the insect activity by displacing the egg masses already oviposited on the cadaver. Furthermore, the VOCs released from the donors could rapidly combine with the high moisture inside the sample hood during wet climatic conditions affecting the pre-concentration of VOCs in the headspace above the body. Thus, rainfall may have affected the overall VOC abundance during the early-post-mortem period for this period of the study.

3.7.3 Principal component analysis

PCA was performed to visualize the inter-day variation in the VOC profiles of the donors and individual compounds during the early post-mortem period. However, the PCA conducted on 229 VOCs identified with a minimum detection frequency of four out of 36 samples did not provide valuable information in terms of capturing the inter-day variation or identifying compounds that contributed to this variation (as shown in Figure 3-20). The PCA did highlight differences between donors placed in autumn, spring, and summer, but the loadings did not show a strong correlation with the donors samples in the scores plot. This lack of explained variance may be due to the variability in the VOCs identified across the eight donors, which reduced the influence of the samples on the score plot and limited the information that could be visualized from the PCA.

The PCA scores plot of the individual donors highlighted the inter-day variation between the samples. The majority of samples collected on ED 1 and ED2 across all donors showed minimal variations and were clustered closely compared to ED 3, ED 4 and ED 5. The VOC abundance recorded on ED 1 and ED 2 was also relatively low compared to ED 3, ED 4, and ED 5, which showed higher VOC abundance. The highest separation in the VOC profiles for an individual donor at the REST[ES] facility was recorded between the sample collected at the time of placement (ED 0) and samples collected from ED 3 onwards. These were the experimental days with the highest VOC abundance and visually increased decomposition and insect activity. This suggests that a detectable change in VOC profiles was observed on ED 3 and thereafter, suggesting a shift in the VOC profiles and a transition from ante-/peri-mortem odour to post-mortem odour in donors H2, H6, H7, H8 and H9.

The PCA scores plot of donors H3 and H4 (autumn trials) showed that the overall explained variance in the model was low, and the first two PCs accounted for the majority of the explained variance (41%). The separation of the samples was along PC-1, which accounted for 22% of the explained variance, indicating samples collected for donors H3 and H4 showed intra-donor variation VOC profiles. For donors H3 and H4, the samples collected after ED 0 formed a

cluster along PC-2. The low ambient temperature and rainfall recorded during the trial affected the progression of decomposition. Visually, these donors progressed through decomposition slowly during the trial with low overall VOC abundance. This is further highlighted by the PCA through the smaller spread of the samples across PC-1 and PC-2. Although the scores plot highlights the intra-donor variation in VOC profiles during the same season, a detectable change in VOC profile was not recorded between donors H3 and H4. This highlights the influence of environmental factors on the progression of decomposition and subsequently VOC abundance.

The PCA loadings plot assisted in identifying VOCs that contributed to the separation of samples (ED 0 vs. ED 3, ED 0 vs. ED 4 and ED 0 vs. ED 5) in the scores plot. Loadings of DMDS, DMTS, 2-butanone and others caused the separation of ED 0 vs. ED 3, ED 0 vs. ED 4 and ED 0 vs. ED 5 in all donors except H3 and H4 (Table 3-5). However, loadings between samples ED 1 and ED 2 were closely grouped along the origin of X and Y axis, and compound names were not clearly separated. The closed grouping may be because several compounds were associated with the variation in the samples collected between ED 1 and ED 2, or that minimal variation occurred in the VOC profiles during this transition.

Sulfur-containing compounds such as DMDS and DMTS are decomposition-related VOCs and have been most commonly reported in the decomposition studies conducted on human remains (7, 37, 38, 97) DMDS was one of the loadings in donors H2, H7, H8, and H9 that caused the separation of VOC samples collected on ED 3 from samples ED 0, ED 1, and ED 2. The identification of DMDS along with other combinations of VOCs can be linked with the change in the peri-mortem VOC profiles of donors H2, H7, H8, and H9 to post-mortem VOC profiles. The significance of this finding lies in the fact entomological species use sulfur-containing compounds like DMDS and DMTS as semiochemicals. This was further supported by the observation of high insect activity and visual signs of decomposition during sample collection from these donors on ED 3 and ED 4. It is important to note that these compounds were identified in donors placed during summer and further research is needed to identify decomposition-related VOCs more consistently in different seasons such as spring, autumn, and

winter. Additionally, more research is needed to understand the full range of decomposition-related VOCs that can be identified consistently across different donors and seasons during the early post-mortem period.

2-butanone is a decomposition-related VOC belonging to the ketone compound class. 2-butanone caused the separation of samples H6 ED 4 and H7 ED 2. Ketones have been linked with the breakdown of fatty acids (6, 130). The identification of 2-butanone suggests that the breakdown of fatty acids in donors H6 and H7 may be linked to the presence of 2-butanone in the post-mortem VOC profile. Further it also suggests that 2-butanone can be one of the compounds that can be linked to the transition in the peri-mortem VOC profile to a post-mortem VOC profile for donors H6 and H7. 2-butanone has been one of the compounds previously reported in decomposition studies conducted by Statheropoulos et al. (6, 8) on human remains during the early post-mortem period. In the study conducted by Statheropoulos et al. (6) 2-butanone was also one of the common core compounds identified in all the sampling cycles during the early post-mortem period. Further research is needed to validate the findings and understand the exact role of ketone compounds like 2-butanone, in the early post-mortem decomposition process and its role in identifying the transition from the peri-mortem to the post-mortem period should be explored.

1,3-diflurobenzene is a halogen-containing compound that has not been previously reported in decomposition studies. The exact pathway which leads to the release of halogen-containing compounds during the early post-mortem period is unknown. One potential pathway that has been reported in the literature is through ingestion of water that contains fluorine and chlorine, which then builds up in bone and soft tissue and is released during decay (6, 97, 131). Studies have also reported similar fluorinated and chlorinated VOCs evolving from human cadavers (7, 97).

2-propenyl benzene and styrene were identified in donor H7 and caused separation of samples H7 ED 5 and H7 ED 0, respectively. 2-propenyl benzene has not been reported in the literature as a decomposition VOC while styrene has been reported as a decomposition-related VOC. The

identification of benzene and benzene derivatives have been linked to oxygen free radicals and these radicals may be responsible for the development of these compounds. Furthermore, microbial modification of various base compounds is believed to create substituted benzene compounds, cyclohexanes and long-chain hydrocarbon compounds (8, 97, 131). The separation of the H7 ED 0 sample due to styrene indicates that the VOC profile collected on H7 ED 0 was predominantly driven by microbial activity. Future studies should be conducted to incorporate microbial sampling in the experimental design during the early post-mortem period. This will further aid in understanding the change in microbiome and identify dominant species present in and on the cadaver during the early post-mortem period. Moreover, collecting two different sample matrixes (microbes and VOCs), will aid in correlating the identification of volatiles such isopropyl alcohol with microbial activity.

Formaldehyde is not a decomposition-related VOC and is a carcinogen detected in humans due to its exposure during the ante-mortem period. Formaldehyde was recently reported in a study that simulated a mass disaster scenario in Australia using cadavers (7). This compound was linked with samples collected before day 15 in the study. One aspect common between the current study and the study conducted in Australia is the use of sorbent tubes for collecting VOCs and the use of statistical methods such as PCA which may have enabled the identification of formaldehyde. This result suggests that there might be a common suite of biomarkers such as formaldehyde which can be consistently detected from human remains in different geographical contexts by using similar analytical and statistical approaches.

Nitrogen-containing compounds are emitted during the break down of proteins and nucleic acids (58). Nitrogen-containing compounds such as methenamine, methylamine, N,N-dimethyl, acetonitrile are decomposition related VOC and these caused separation of the H2 ED 3, H8 ED 4, H8 ED 5, H9 ED 4 and H9 ED 5 samples. The detection of these compounds can be linked to the breakdown of proteins and nucleic acids in these donors. Furthermore, along with sulfur-containing compounds such as DMDS, these compounds also caused the separation of ED 3, ED 4 and ED 5 from ED 0 samples indicating that a combination of sulfur and nitrogen-containing

compounds can be key in determining the transition in the peri-mortem VOC profile to the post-mortem VOC profile during the early post-mortem period.

The PCA results showed that VOCs belonging to compound classes such as alcohols, ketones, sulfur-containing, halogen-containing, and nitrogen-containing compounds caused variance in the donor VOC profiles. These compound classes can potentially be responsible for the characteristic odour released in an outdoor environment during the early post-mortem period. Canines, scavengers, and insects can track volatiles present in compound classes to locate the target scent (e.g., human remains or carrion). Thus, the knowledge of their presence during the early post-mortem period can be used to improve the training of HRD dogs, leading to the faster location of human remains during a mass disaster scenario. Furthermore, information about the abundance of these compound classes can be applied in developing biosensors that identify these compound classes during a mass disaster scenario and act as a complementary tool to facilitate search and rescue operations. Further studies need to be conducted on cadavers during the early post-mortem period to understand the transition of the odour and identify compound classes that are prevalent during the early post-mortem period.

3.8 Conclusion

This study aimed to characterise and investigate the early post-mortem VOC profiles of human remains using the optimised method at the REST[ES] facility. Moreover, these VOC profiles were studied during different seasons (spring, summer, and autumn). The progression of decomposition through the early post-mortem period was studied using eight cadavers and their VOC profiles were collected in different seasons. The VOC data collected were analysed using Pegasus®BT 4D GC×GC-TOFMS and the R package. The optimised VOC collection and data processing methods identified 948 VOCs and these VOCs were classified into the compound classes; acids, alcohols, aldehydes, aromatics, cyclic aliphatic compounds, esters and analogues, ethers, halogen-containing compounds, ketones, linear aliphatic compounds, nitrogen-containing compounds, and sulfur-containing compounds. Variation was observed in terms of the decomposition process and class abundance. These variations observed during the early

post-mortem period led to differences in the progression of the decomposition process and complex VOC profiles. The VOC profiles demonstrated inter-day variation as the VOC and compound class abundance changed daily. This variation was distinctly observed in donors placed during the summer and spring seasons. In contrast, in the autumn season, lower temperature and rainfall recorded during the trial slowed the progression of decomposition and reduced VOC abundance in the donors. Thus, this study showed that the transition from ante-mortem odour to post-mortem odour in an outdoor environment happens on both ED 3 and afterwards (ED 4 and ED 5) in our local environment. Therefore, the optimised method was able to successfully identify a detectable change in the early post-mortem VOC profile. This study provides new information about the early post-mortem VOCs released from human remains in an outdoor environment. The knowledge from this study can be applied in developing methods that will lead to the early detection of human remains during a mass disaster scenario. Further studies must be conducted to replicate these results and compare the VOC profiles collected in the morgue and at REST[ES] during the early post-mortem period.

Chapter 4: Identifying the transition from ante-mortem odour to post-mortem odour

4.1 Introduction

Ante-mortem odour is defined as the scent of an individual during life (ante-mortem period), and contains VOCs released from the skin (83), sweat (4) and breath (2) (Figure 4-1). The ante-mortem odour is unique as a result of an individual's genetics, diet, personal hygiene, and physiological state (82). In ante-mortem odour, skin is a significant source of VOC emanations. The VOCs released from healthy individuals' skin have been proposed to be used as markers of the presence of ante-mortem odour in mass-disaster scenarios (95, 132). It can be theorised that during the peri and early post-mortem period, in the absence of VOCs released from breath and sweat, VOCs can emanate from the skin through the reaction of microbiomes on the skin with the surrounding environment. The unknown aspects of ante-mortem odour are its pervasiveness after death and its period of transition from ante-mortem odour to post-mortem odour (64). Researchers have hypothesised that the ante-mortem odour transitions to post-mortem odour after death during the early post-mortem period (64). However, during the post-mortem period, the odour resulting from human decomposition can vary as decomposition progresses through different stages (Figure 4-1).

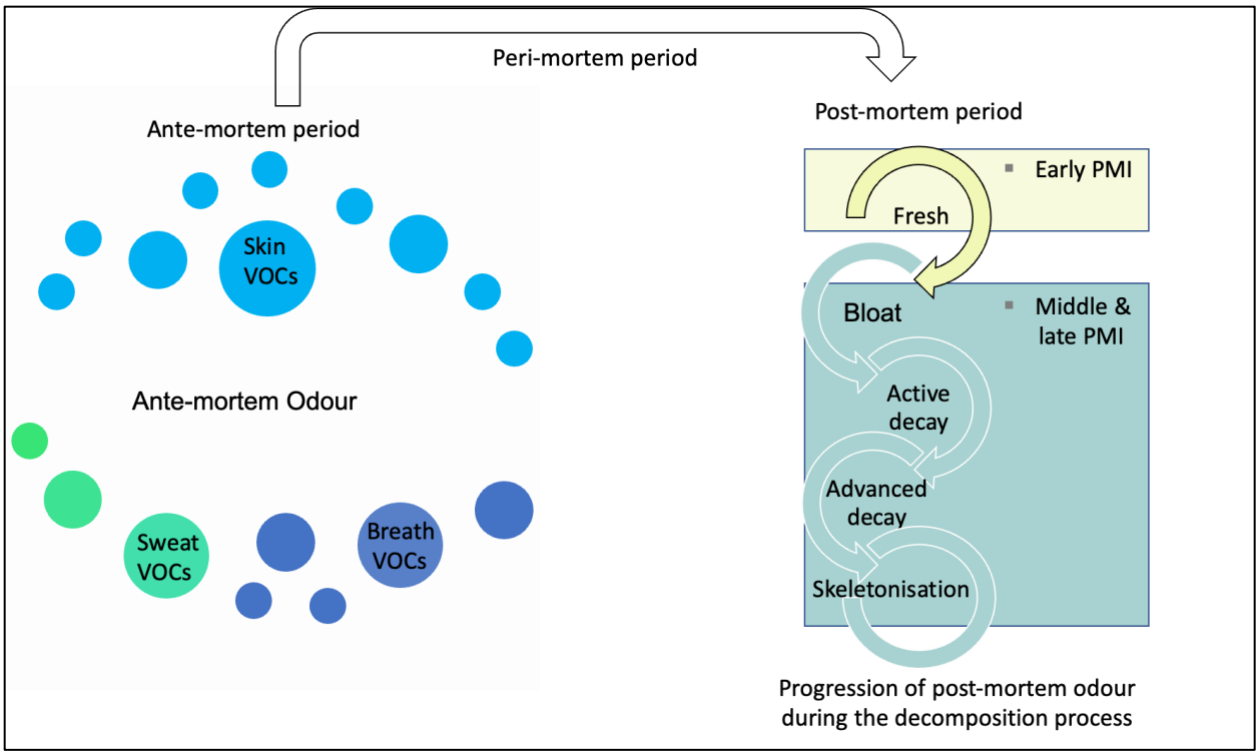

Figure 4-1 *Transition of ante-mortem odour to post-mortem odour during the early post-mortem period and the progression of post-mortem odour during decomposition stages after death. Note that during the ante-mortem period, skin, sweat, and breath are some of the potential sources of odour, but when a person dies, the odour from these sources ceases and post-mortem odour replaces the ante-mortem odour over time. As the decomposition process progresses and the body goes through various stages, the post-mortem odour also goes through various changes.*

In a forensic context, the knowledge of odour transition can be helpful in training HRD dogs and in developing artificial sensors that could be used to locate victims of mass disasters (6, 79). Therefore, collecting, and analysing odour released from cadavers during the early post-mortem period can provide knowledge about the persistence of ante-mortem VOCs associated with the ante-mortem odour and the transition of the odour after death. This study aims to compare VOCs collected at the morgue and REST[ES] facility during the early post-mortem period to identify the transition of the odour. The secondary aim is to track the evolution of the donor VOC profiles from the morgue to the REST[ES] facility. The objective of this chapter is to discuss previously collected data in two different scenarios (morgue vs REST[ES]) during the early post-mortem period.

Note: the materials and methods used in this study are those reported in Chapters 2 & 3. Please refer to section 2.4.3 and 3.4.

4.2 Results

The results of the morgue study (section 2.6.1) determined that some ante-mortem VOCs were identified in the headspace of the body bag, indicating their persistence during the early post-mortem period. These VOCs have been predominantly reported in skin (95, 96). Monitoring the change in the total normalised area of ante-mortem VOCs and decomposition VOCs identified in the profile of donors collected at the morgue and REST[ES] facility can be the key to understanding the pervasiveness of ante-mortem odour through the peri-mortem and early post-mortem period (Figure 4-2). This approach can assist in determining the transition of the odour from ante-mortem odour to post-mortem odour.

A VOC dataset was created using the R package. This dataset was made by compiling the compounds (n=1178) identified in the VOC profiles collected at the morgue and REST[ES] facility (Figure 4-2). A list of 64 VOCs reported previously in the literature (95) as part of ante-mortem VOC profiles (skin-related VOCs) was compared with the entire list of 1178 VOCs detected in the current study. Of these 64 VOCs, 27 VOCs were found in the study across 44 donor samples collected at the morgue and REST[ES] facility. Furthermore, a list of 247 decomposition VOCs previously reported in studies conducted on cadavers or human remains was compared with the entire list of 1178 VOCs detected in the current study. A total of 54 VOCs were identified, which were found in common with the dataset. The resulting list of 27 ante-mortem VOCs and 54 decomposition VOCs were compared with individual donor VOC profiles. This resulting list can be found in Appendix C for both 27 ante-mortem VOCs (Table C-1) and 54 decomposition VOCs (Table C-2). To understand the persistence of ante-mortem odour and to identify the transition of the odour, we calculated total normalised areas using the normalised area for VOCs related to ante-mortem odour and post-mortem odour identified in the samples collected at the morgue and REST[ES] facility. It is important to note that the values obtained were not quantified as it was not within the scope of the current project.

Figure 4-2 *Visualisation of the approach taken to study the evolution of ante-mortem and post-mortem VOCs during the early post-mortem period.*

Apart from comparing 27 ante-mortem VOCs and 54 decomposition VOCs reported in the literature with the current VOC dataset, the relative class concentration for VOCs detected in individual donors was calculated. For this, the VOCs were classified into the following compound classes; acids, alcohols, aldehydes, aromatics, cyclic aliphatic compounds, esters and analogues, ethers, halogen-containing compounds, ketones, linear aliphatic compounds, nitrogen-containing compounds, and sulfur-containing compounds. All 1178 VOCs detected in the 44 donor samples that belonged to either a morgue sample or experimental day at the REST[ES] facility were classified into these compound classes. The total normalised areas of each compound class, identified in an individual donor, were calculated to determine their relative class concentration. This relative class concentration was then tracked from the first sample collected when the donors arrived in the morgue during the early post-mortem period (fresh stage) to the last sample collected at the REST[ES] facility (typically beginning of the bloat

stage). This allowed for the visualisation of any changes in the relative class concentration that occurred during the progression of decomposition.

For donor H1, Figure 4-3 represents the total normalised area of ante-mortem and decomposition VOCs for each of the samples that were common with those reported in the literature. Across all donor H1 samples, a total of nine ante-mortem VOCs and ten decomposition VOCs were found common with the previously cited literature. In the morgue sample (H1_M), three ante-mortem VOCs had a slightly higher total normalised area compared to five decomposition VOCs. In the H1 ED 0 sample, the total normalised area of five decomposition VOCs was higher than that of seven ante-mortem VOCs. Donor H1 showed signs of autolysis and putrefaction at the time of placement at the REST[ES] facility. As a result, a set of triplicate samples was collected on ED 0 only, as it was determined that this donor was already passing the early post-mortem period. It must be noted that each sample had different ante-mortem and decomposition VOCs, which were found common with the literature, and these have been detailed in Appendix C (Table C-3). There was no obvious trend in terms of the transition of ante-mortem to decomposition VOCs, and in fact the reverse was true, even though this donor was already undergoing decomposition at the time of arrival in the morgue and placement at REST[ES].

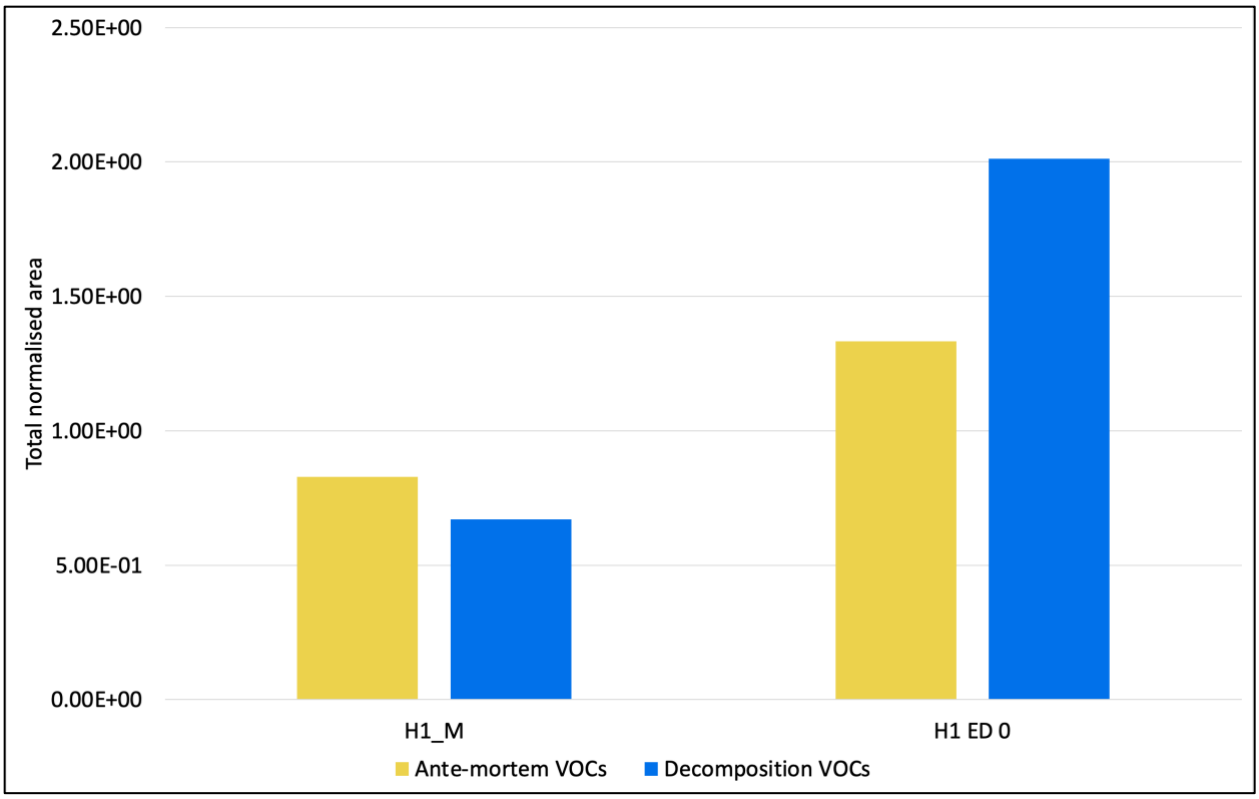

Figure 4-3 *Demonstrating the total normalised area of the literature reported ante-mortem vs decomposition VOCs detected in donor H1's samples collected at the morgue (H1_M) and REST[ES] facility (H1 ED 0).*

Other than those VOCs discussed above, several other VOCs were detected in donor H1 samples. However, since the origin (ante-mortem vs decomposition) of these VOCs cannot be confirmed, these were only classified into compound classes and have been reported here in an attempt to identify trends in the odour transition (Figure 4-4). For the morgue sample H1_M sample, the alcohols had the highest relative class concentration identified at ~40 h PMI, followed by linear aliphatic compounds and halogen-containing compounds, while acids had the lowest relative class concentration, followed by nitrogen-containing compounds and ethers (Figure 4-4). In the H1 ED 0 sample, collected after the placement of the body at the REST[ES] facility, the relative class concentration of alcohols was the highest, followed by esters and analogues and linear aliphatic compounds, while the aldehydes had the lowest relative class concentration, followed by acids and sulfur-containing compounds (Figure 4-4). Overall, for the samples collected at the morgue and REST[ES], the alcohols had the highest average relative class concentration.

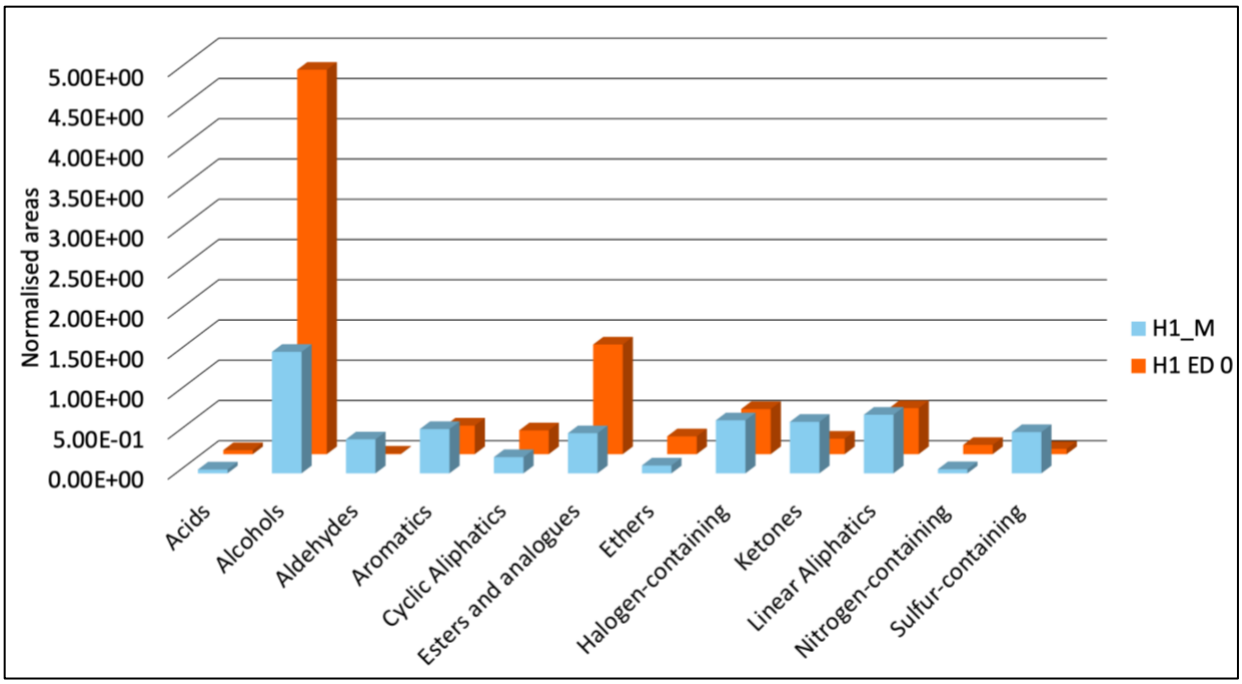

Figure 4-4 *Change in relative class concentration (normalised areas) identified in the VOC samples collected from donor H1 at the morgue (H1_M) and REST[ES] facility.*

For donor H2, Figure 4-5 represents the total normalised area of ante-mortem and decomposition VOCs for each of the samples that were common with those reported in the literature. Across all donor H2 samples, a total of 12 ante-mortem VOCs and 33 decomposition VOCs were found common with previously cited literature. For donor H2 samples, the total normalised area of decomposition VOCs common with the literature was higher than that of ante-mortem VOCs. In the morgue sample (H2_M), 12 decomposition VOCs had a higher total normalised area compared to six ante-mortem VOCs. Likewise, in the H2 ED 0 sample, three decomposition VOCs had a total normalised area higher than that of two ante-mortem VOC. Likewise, in H2 ED 1 sample, the total normalised area of seven decomposition VOCs was higher than that of five ante-mortem VOCs. For sample H2 ED 2, three decomposition VOCs had a total normalised area higher than two ante-mortem VOCs (Figure 4-5). In the H2 ED 3 sample, five decomposition VOCs had a higher total normalised area compared to one ante-mortem VOC. Likewise, in H2 ED 4 sample, the total normalised area of 20 decomposition VOCs was higher than that of five ante-mortem VOCs. It must be noted that other than some common VOCs

across samples, a majority of the literature reported VOCs detected in donor H2 samples were different, and these have been detailed in Appendix C (Table C-4).

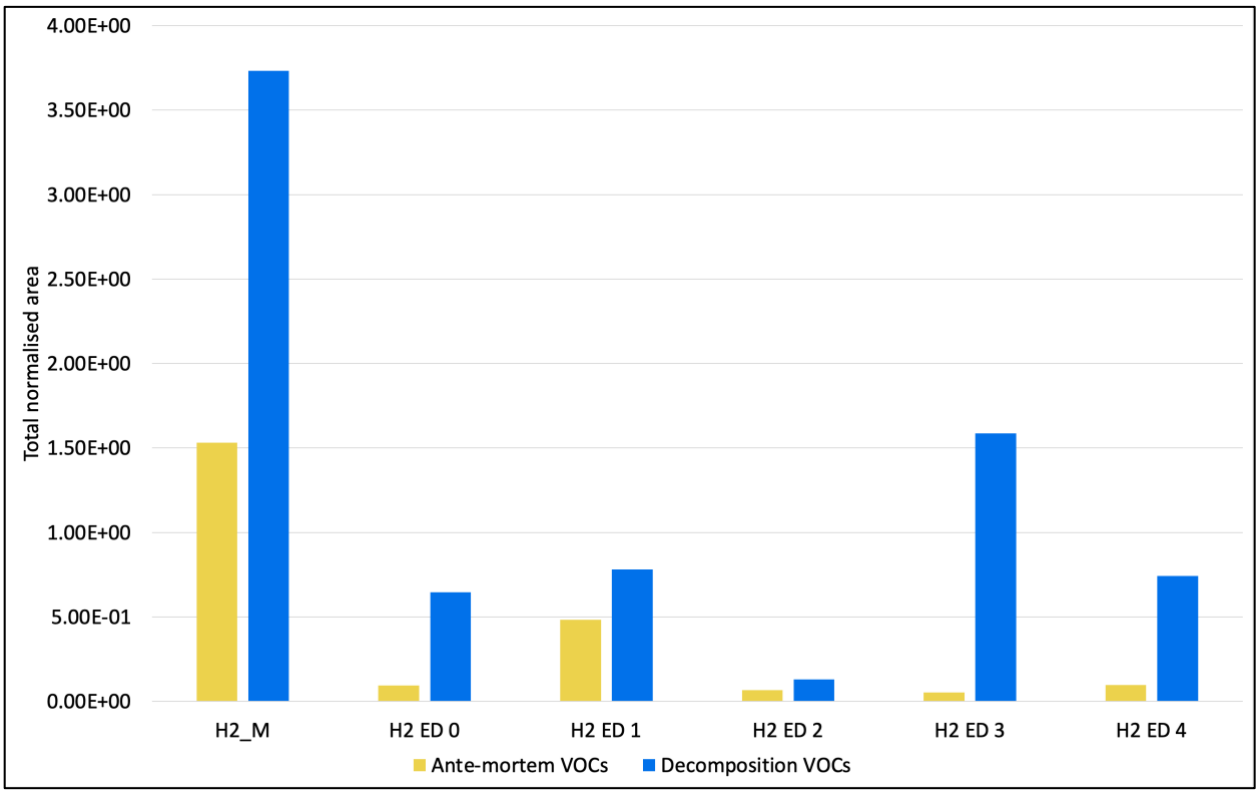

Figure 4-5 *Demonstrating the total normalised area of the literature reported ante-mortem vs decomposition VOCs detected in donor H2's samples collected at the morgue (H2_M) and REST[ES] facility (H2 ED 0 to H2 ED 4).*

Other than those VOCs discussed above, several other VOCs were detected in donor H2 and as their origin cannot be confirmed, these were only classified into compound classes and have been reported here in an attempt to identify trends in the odour transition (Figure 4-6). The esters and analogues class had the highest relative class concentration identified at ~21 h PMI (H2_M), followed by alcohols and aromatics, while acids had the lowest relative class concentration, followed by sulfur-containing compounds and ketones (Figure 4-6). In the sample H2 ED 0 collected after the placement of the body at the REST[ES] facility, the relative class concentration of alcohols was the highest, followed by linear aliphatic compounds, and halogen-containing compounds, while the sulfur-containing compounds had the lowest relative class concentration, followed by aldehydes and ketones. In the sample H2 ED 1, aldehydes had

the highest relative class concentration, followed by ketones and nitrogen-containing compounds, while sulfur-containing compounds had the lowest relative class concentration followed by halogen-containing compounds and ethers were not detected. In the H2 ED 2 sample, the alcohols demonstrated the highest relative class concentration, followed by halogen-containing compounds and linear aliphatic compounds, while ethers had the lowest relative class concentration followed by sulfur-containing compounds and acids were not detected in H2 ED 2 sample. In the H2 ED 3 sample, sulfur-containing compounds had the highest relative class concentration followed by nitrogen-containing compounds and aromatics, while ethers had the lowest relative class concentration followed by acids and halogen-containing compounds. In the H2 ED 4 sample, acids had the highest relative class concentration, followed by nitrogen-containing compounds and sulfur-containing compounds, while aldehydes had the lowest relative class concentration, followed by ketones and aromatics. Overall, for donor H2 samples, the esters and analogues had the highest average relative class concentration at the morgue, while alcohols had the highest average relative class concentration at the REST[ES] facility. Furthermore, acids had the lowest average relative class concentration at the morgue, while ethers had the lowest average relative class concentration at the REST[ES] facility.

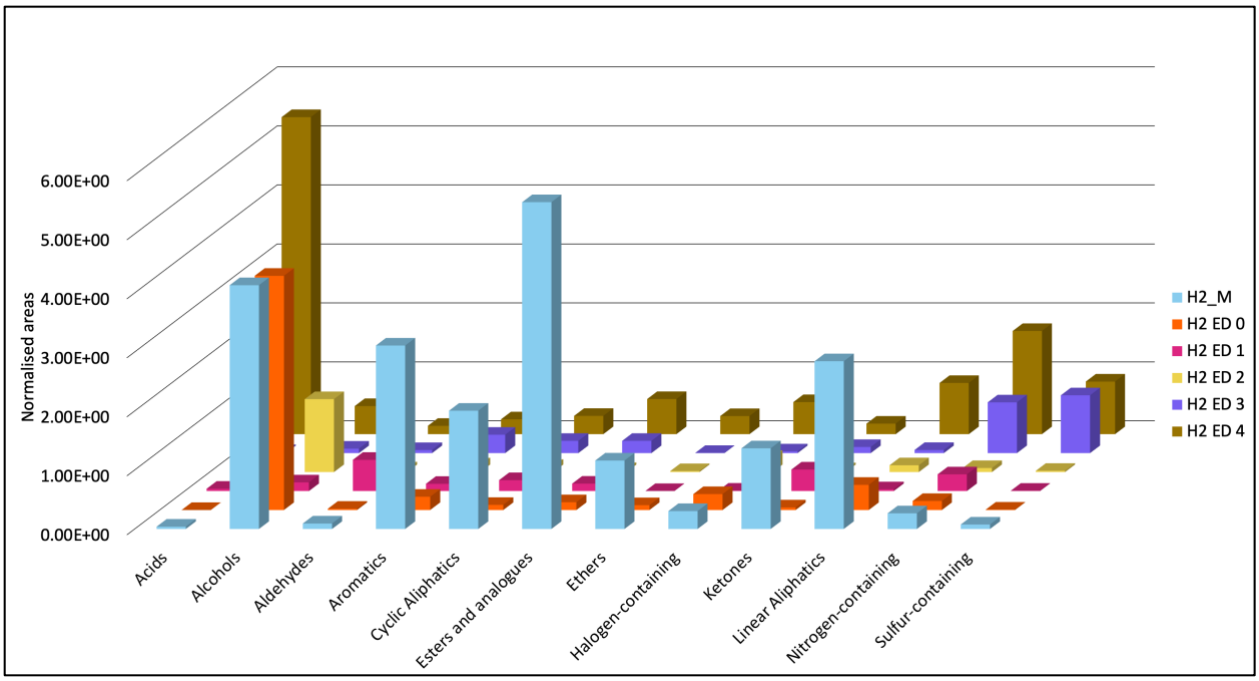

Figure 4-6 *Change in relative class concentration (normalised areas) identified in the VOC samples collected from donor H2 at the morgue (H2_M) and REST[ES] facility.*

For donor H3, Figure 4-7 represents the total normalised area of ante-mortem and decomposition VOCs for each of the samples that were common with those reported in the literature. Across all donor H3 samples, a total of nine ante-mortem VOCs and 14 decomposition VOCs were found common with the previously cited literature. In the morgue sample (H3_M), five ante-mortem VOCs had a higher total normalised area compared to five decomposition VOCs. In the H3 ED 0 sample, five decomposition VOCs had a total normalised area higher than that of three ante-mortem VOCs. Likewise, in the H3 ED 2 sample, the total normalised area of four decomposition VOCs was higher than that of two ante-mortem VOCs. In the sample H3 ED 3, two decomposition VOCs had a higher total normalised area compared to two ante-mortem VOCs. For sample H3 ED 4, two decomposition VOCs had a higher total normalised area than that of one ante-mortem VOC. VOC samples were not collected on ED 1 due to rain. It must be noted that other than some common VOCs across samples, a majority of the literature reported VOCs detected in donor H3 samples were different, and these have been detailed in Appendix C (Table C-5).

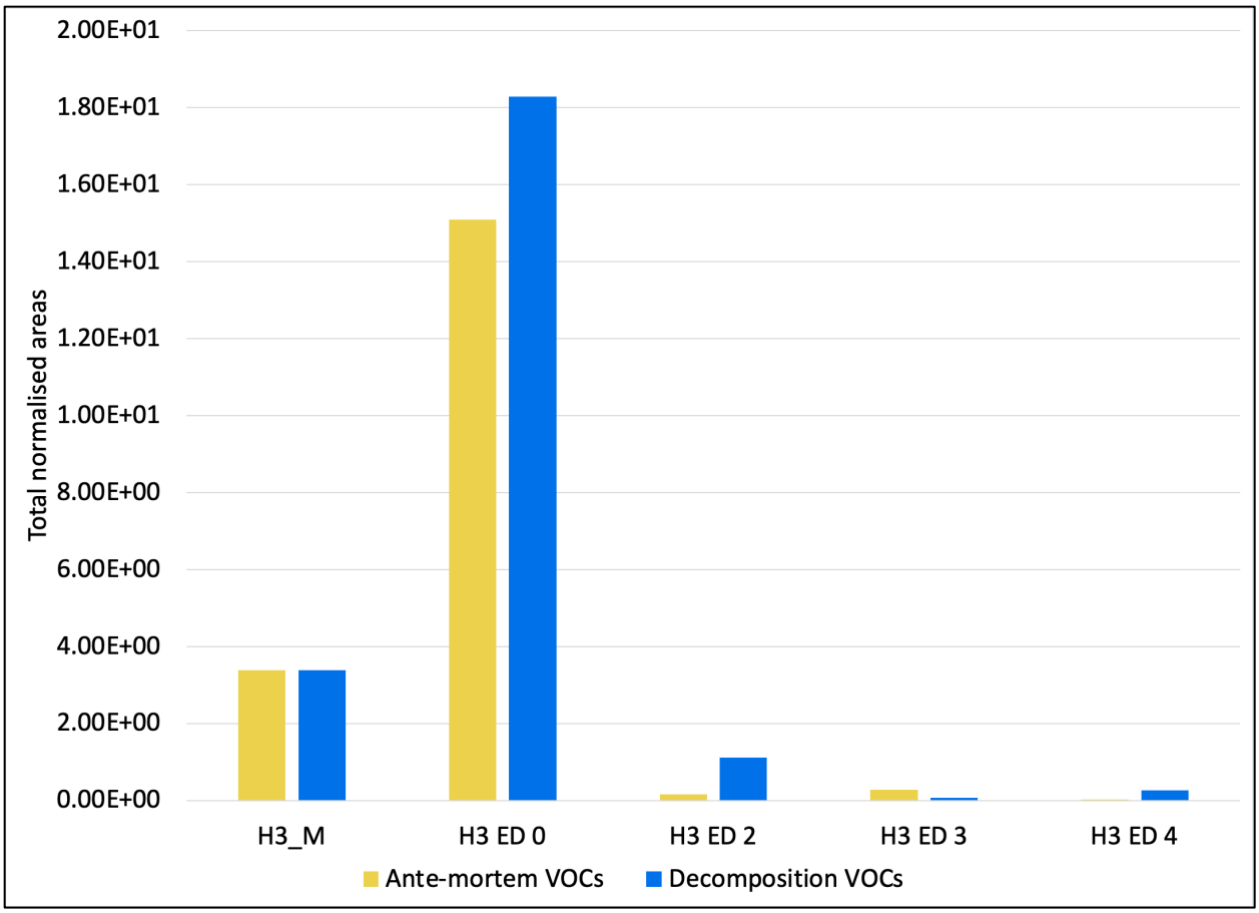

Figure 4-7 *Demonstrating the total normalised area of the literature reported ante-mortem vs decomposition VOCs detected in donor H3's samples collected at the morgue (H3_M) and REST[ES] facility (H3 ED 0 to H3 ED 4).*

In addition to the literature reported VOCs discussed above, several other VOCs detected in donor H3 have been classified into compound classes and reported in this section (Figure 4-8). The linear aliphatic compounds had the highest relative class concentration identified at ~22 h PMI (H3_M), followed by alcohols and aromatics, while aldehydes had the lowest relative class concentration, followed by acids and sulfur-containing compounds (Figure 4-8). In the H3 ED 0 sample collected after the placement of the body at the REST[ES] facility, the relative class concentration of nitrogen-containing compounds was the highest, followed by aldehydes and alcohols, while ethers had the lowest relative class concentration and acids were not detected. In the H3 ED 2 sample, the nitrogen-containing compounds demonstrated the highest relative class concentration, followed by the aldehydes and halogen-containing compounds, while

ketones had the lowest relative class concentration. In the H3 ED 3 sample, esters and analogues had the highest relative class concentration followed by nitrogen-containing compounds and ketones, while the linear aliphatic compounds had the lowest relative class concentration. In the H3 ED 4 sample, esters and analogues also had the highest relative class concentration, followed by nitrogen-containing compounds and halogen-containing compounds, while aldehydes had the lowest relative class concentration. At the REST[ES] facility, the nitrogen-containing compounds had the highest average class concentration and ethers had the lowest average class concentration. In donor H3, nitrogen-containing compounds and aldehydes were detected consistently in all samples collected at the REST[ES] facility. In the H3 ED 0 sample, compound classes such as acids and ethers were not detected, while acids, ethers, sulfur-containing compounds, alcohols, and aromatics were not detected in H3 ED 2, H3 ED 3, and H3 ED 4 samples. The absence of these classes in donor H3 sample collected at the REST[ES] facility, can be due to low temperatures and high rainfall recorded during the trial. Overall, for the samples collected at the morgue linear aliphatic compounds had the highest average relative class concentration and at the REST[ES] facility the nitrogen-containing compounds had the highest average relative class concentration at the REST[ES] facility. Furthermore, aldehydes had the lowest average relative class concentration at the morgue and ethers had the lowest average relative class concentration at the REST[ES] facility.

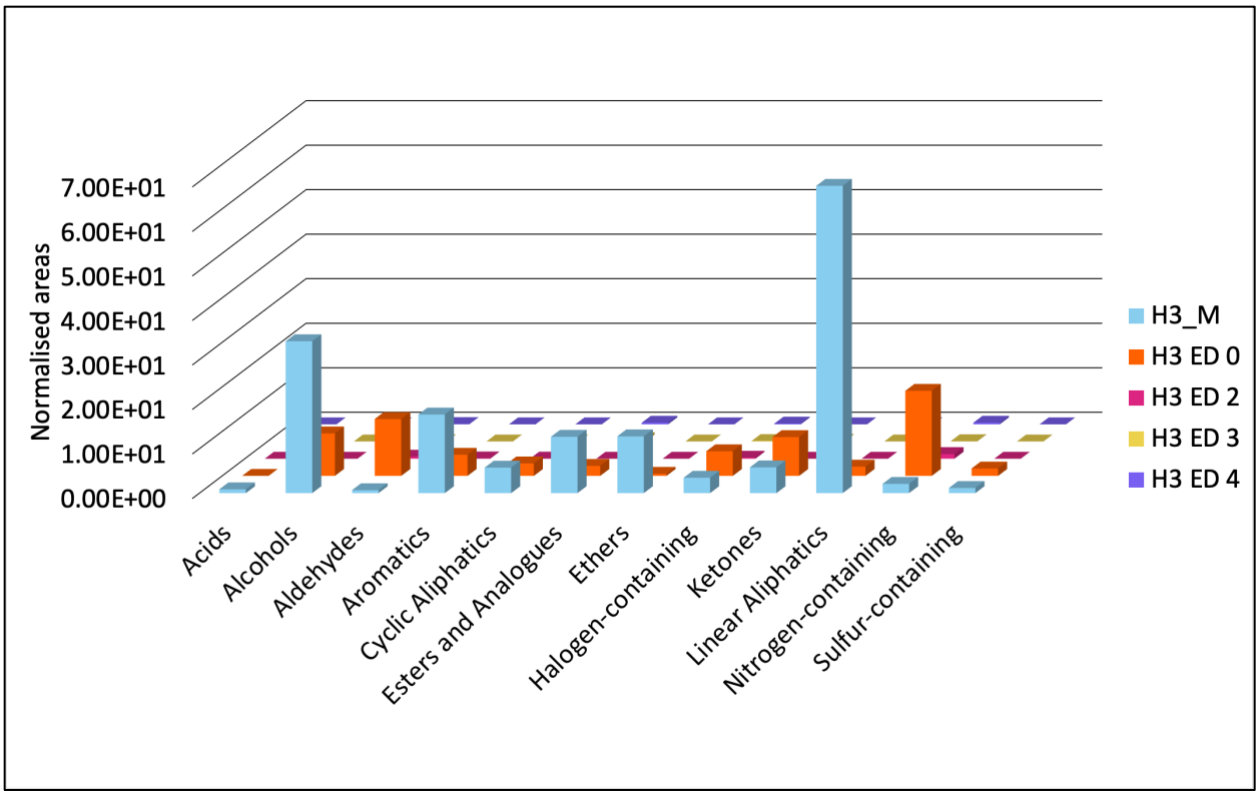

Figure 4-8 *Change in relative class concentration (normalised areas) identified in the VOC samples collected from donor H3 at the morgue (H3_M) and REST[ES] facility.*

For donor H4, Figure 4-9 represents the total normalised area of ante-mortem and decomposition VOCs for each of the samples that were common with those reported in the literature. Across all donor H4 samples, a total of nine ante-mortem VOCs and 15 decomposition VOCs were found common with previously cited literature. In the morgue sample (H4_M), eleven decomposition VOCs had a higher total normalised area compared to three ante-mortem VOCs. In the H4 ED 0 sample, four ante-mortem VOCs had a total normalised area higher than that of two decomposition VOCs. Likewise, in the H4 ED 1 sample, the total normalised area of three ante-mortem VOCs was higher than that of two decomposition VOCs. For H4 ED 3 sample, all the literature reported VOCs identified were decomposition related. This sample could have contained ante-mortem VOCs however, none of the other VOCs detected in the sample have been previously reported in ante-mortem odour. VOC samples were not collected on ED 2 due to rain. It must be noted that each sample had

different ante-mortem and decomposition VOCs which were found common with the literature, and these have been detailed in Appendix C (Table C-6).

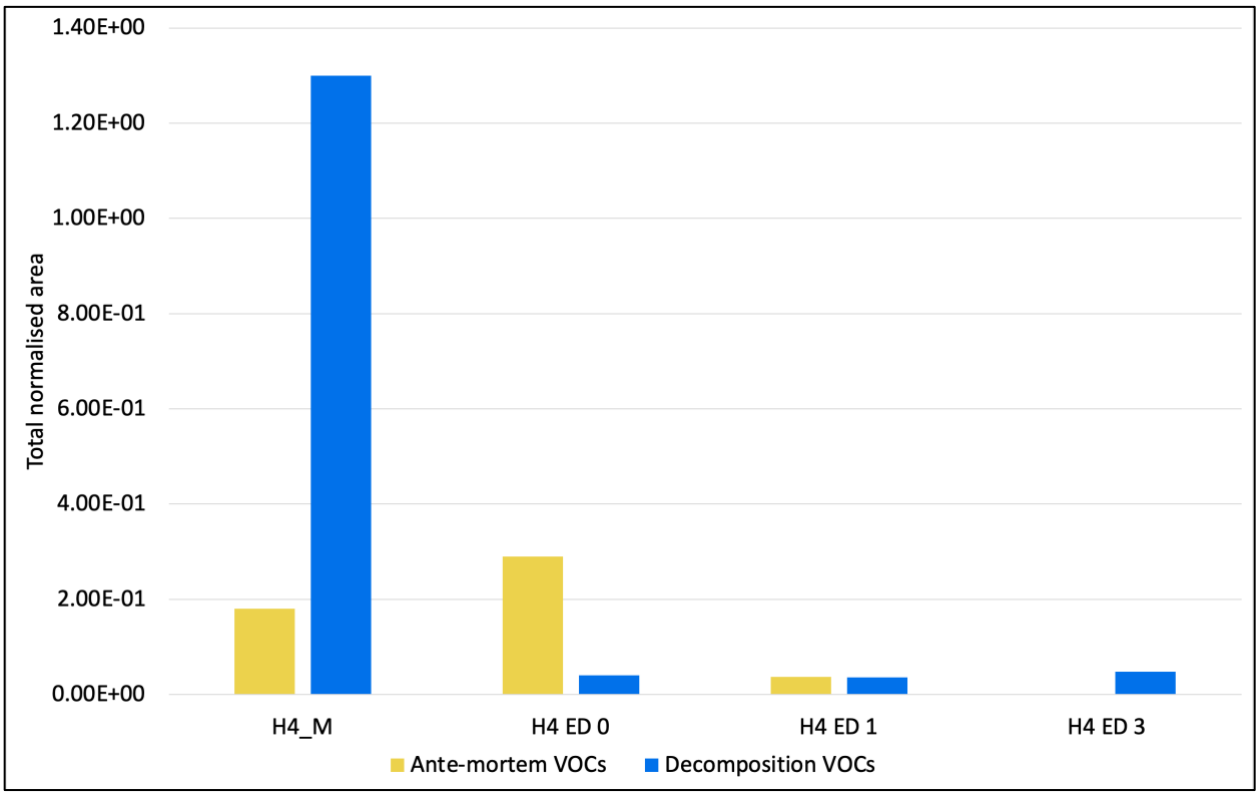

Figure 4-9 *Demonstrating the total normalised area of the literature reported ante-mortem vs decomposition VOCs detected in donor H4's samples collected at the morgue (H4_M) and REST[ES] facility (H4 ED 0 to H4 ED 3).*

In addition to the literature reported VOCs discussed above, several other VOCs detected in donor H4 have been classified into compound classes and reported in this section (Figure 4-10). For the morgue sample (H4_M), the linear aliphatic compounds had the highest relative class concentration identified at ~33 h PMI followed by alcohols and esters and analogues, while sulfur-containing compounds had the lowest relative class concentration, followed by acids and aldehydes. In sample H4 ED 0 collected after the placement of the body at the REST[ES] facility, the relative class concentration of esters and analogues was the highest, followed by linear aliphatic compounds and nitrogen-containing compounds, while ethers had the lowest relative class concentration followed by cyclic aliphatic compounds. Sulfur-containing compounds and acids were not identified. In the H4 ED 1 sample, the esters and analogues demonstrated the

highest relative class concentration, followed by alcohols and halogen-containing compounds, while cyclic aliphatic compounds had the lowest relative class concentration followed by nitrogen-containing compounds. In the H4 ED 3 sample, esters and analogues again had the highest relative class concentration followed by aromatics and nitrogen-containing compounds, while ketones had the lowest relative class concentration followed by aldehydes. Cyclic aliphatic compounds, sulfur-containing compounds, and ethers were not detected in the sample H4 ED 3. Overall, for the samples collected at the morgue the linear aliphatic compounds had the highest average relative class concentration while esters and analogues had the highest average relative concentration at the REST[ES] facility. Moreover, cyclic aliphatic compounds had the lowest average relative class concentration at the morgue and sulfur-containing compounds had the lowest average relative class concentration at the REST[ES] facility.

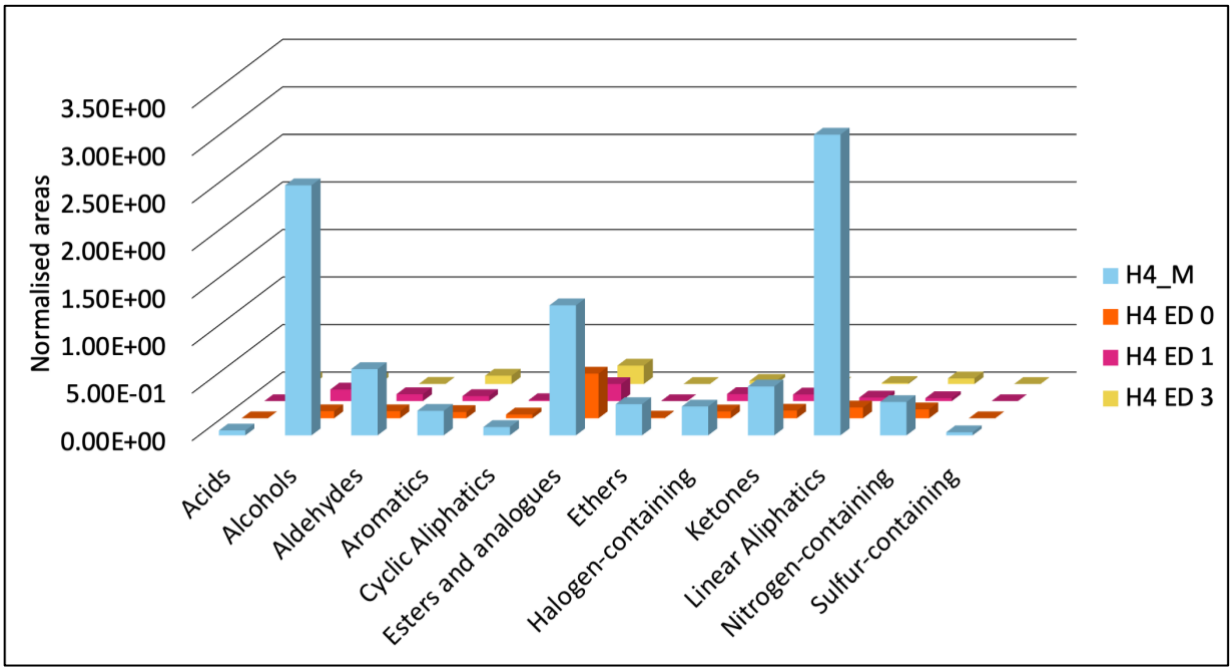

Figure 4-10 *Change in relative class concentration (normalised areas) identified in the VOC samples collected from donor H4 at the morgue (H4_M) and REST[ES] facility.*

For donor H6, Figure 4-11 represents the total normalised area of ante-mortem and decomposition VOCs for each of the samples that were common with those reported in the

literature. Across all donor H6 samples, a total of 11 ante-mortem VOCs and 16 decomposition VOCs were found common with previously cited literature. In the morgue sample (H6_M), five decomposition VOCs had a higher total normalised area compared to three ante-mortem VOCs. In the H6 ED 0 sample, two decomposition VOCs had a total normalised area higher than that of one ante-mortem VOCs. In the H6 ED 1 sample, the total normalised area of three ante-mortem VOCs was higher than that of two decomposition VOCs. For the sample H6 ED 2 and H6 ED 3, all the literature reported VOCs identified were decomposition related. This sample could have contained ante-mortem VOCs, however, none of the other VOCs detected in the sample have been previously reported in ante-mortem odour. In the H6 ED 4 sample, the total normalised area of six ante-mortem VOCs was higher than that of four decomposition VOCs. Finally, for the H6 ED 5 sample, all the literature reported VOCs were ante-mortem odour related. This sample could have contained decomposition VOCs, however, none of the other VOCs detected in the sample have been previously reported in decomposition odour. It must be noted that each sample had different ante-mortem and decomposition VOCs which were found common with the literature, and these have been detailed in Appendix C (Table C-7).

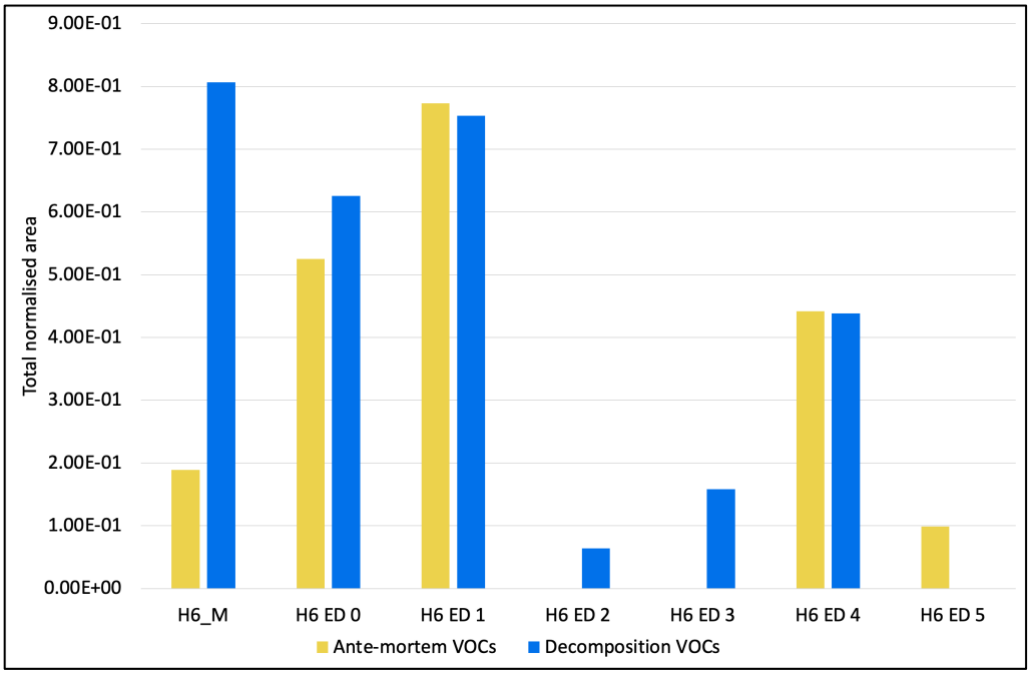

Figure 4-11 *Demonstrating the total normalised area of the literature reported ante-mortem vs decomposition VOCs detected in donor H6's samples collected at the morgue (H6_M) and REST[ES] facility (H6 ED 0 to H6 ED 5).*

In addition to the literature reported VOCs discussed above, several other VOCs detected in donor H6 have been classified into compound classes and reported in this section (Figure 4-12). For the morgue sample (H6_M), the linear aliphatic compounds had the highest relative class concentration identified at ~16 h PMI followed by alcohols and cyclic aliphatic compounds, while aldehydes had the lowest relative class concentration, followed by ethers and acids (Figure 4-12). In the H6 ED 0 sample collected after the placement of the body at the REST[ES] facility, alcohols had the highest relative class concentration, followed by nitrogen-containing and esters and analogues while sulfur-containing compounds had the lowest relative class concentration followed by aldehydes and acids. In the H6 ED 1 sample, the halogen-containing compounds demonstrated the highest relative class concentration, followed by alcohols and sulfur-containing compounds, while linear aliphatic compounds had the lowest relative class concentration followed by acids and ethers. In the H6 ED 2 sample, sulfur-containing compounds had the highest relative class concentration followed by the nitrogen-containing compounds and halogen-containing compounds, while acids had the lowest relative class concentration followed by linear aliphatic compounds. In the H6 ED 3 sample, the cyclic aliphatic compounds had the highest relative class concentration followed by aromatics and aldehydes, while linear aliphatic compounds had the lowest relative class concentration and sulfur-containing compounds and acids were not detected. In the H6 ED 4 sample, aromatics had the highest relative compound class concentration followed by nitrogen-containing compounds and sulfur-containing compounds, while alcohols had the lowest relative class concentration followed by halogen-containing compounds and acids were not detected. In the H6 ED 5 sample, aromatics had the highest relative class concentration followed by aldehydes and halogen-containing compounds, while alcohols had the lowest relative class concentration followed by cyclic-aliphatic compounds. Overall, for donor H6 samples, the linear aliphatic compounds had the highest average relative class concentration at the morgue, while alcohols had the highest average relative class concentration at the REST[ES] facility. Moreover, acids had the lowest average relative class concentration at the morgue and REST[ES] facility.

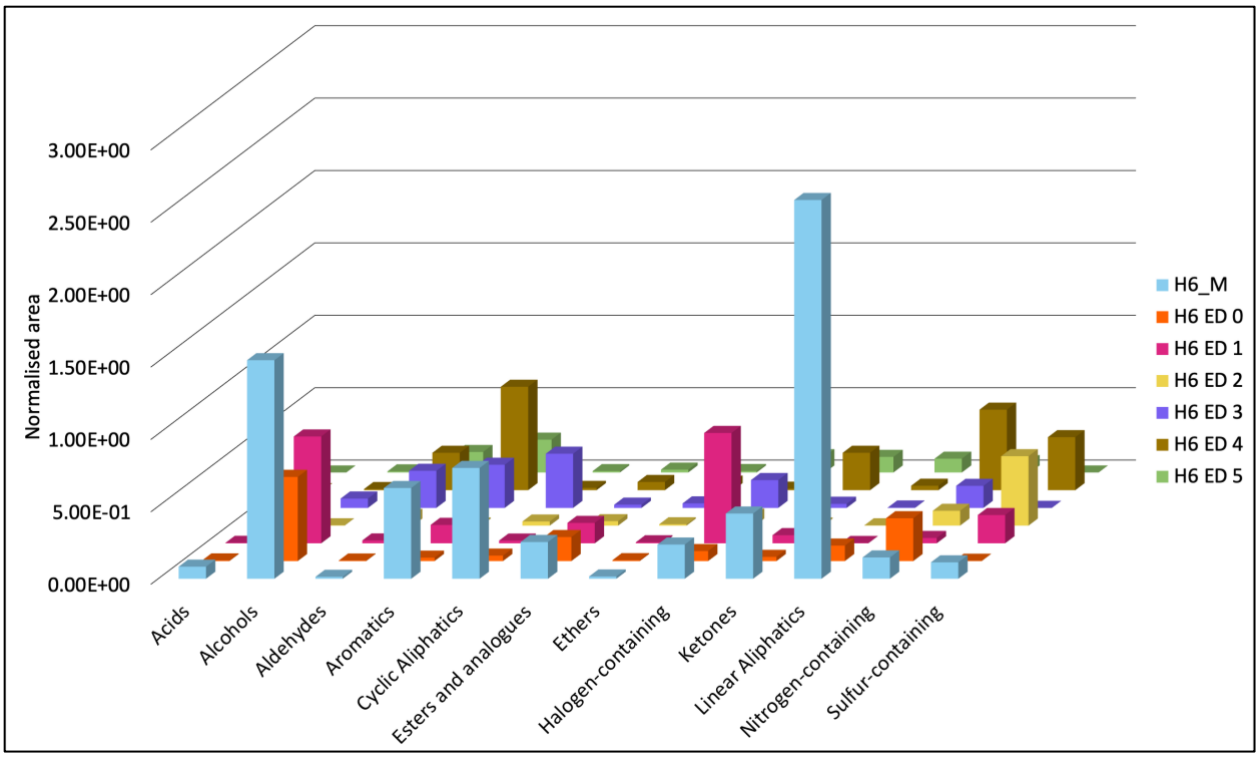

Figure 4-12 *Change in relative class concentration (normalised areas) identified in the VOC samples collected from donor H6 at the morgue (H6_M) and REST[ES] facility.*

For donor H7, Figure 4-13 represents the total normalised area of ante-mortem and decomposition VOCs for each of the samples that were common with those reported in the literature. Across all donor H7 samples, a total of nine ante-mortem VOCs and 22 decomposition VOCs were found common with the previously cited literature. In the morgue sample (H7_M), three decomposition VOCs had a higher total normalised area compared to three ante-mortem VOCs. Likewise, in the H7 ED 0 sample, seven decomposition VOCs had a total normalised area higher than that of three ante-mortem VOCs. In the H7 ED 1 sample, the total normalised area of four decomposition-VOCs was higher than that of three ante-mortem VOCs. In the H7 ED 2 sample three ante-mortem VOCs had a total normalised area higher than that of six decomposition VOCs. In the H7 ED 4 sample, three ante-mortem VOCs had a total normalised area higher than that of three decomposition VOCs. Finally, in the H7 ED 5 sample, eight decomposition VOCs had a higher total normalised area compared to four ante-mortem VOCs. VOC samples were not collected on ED 3 due to rain. It must be noted that other than

some common VOCs across samples, a majority of the literature reported VOCs detected in donor H7 samples were different, and these have been detailed in Appendix C (Table C-8).

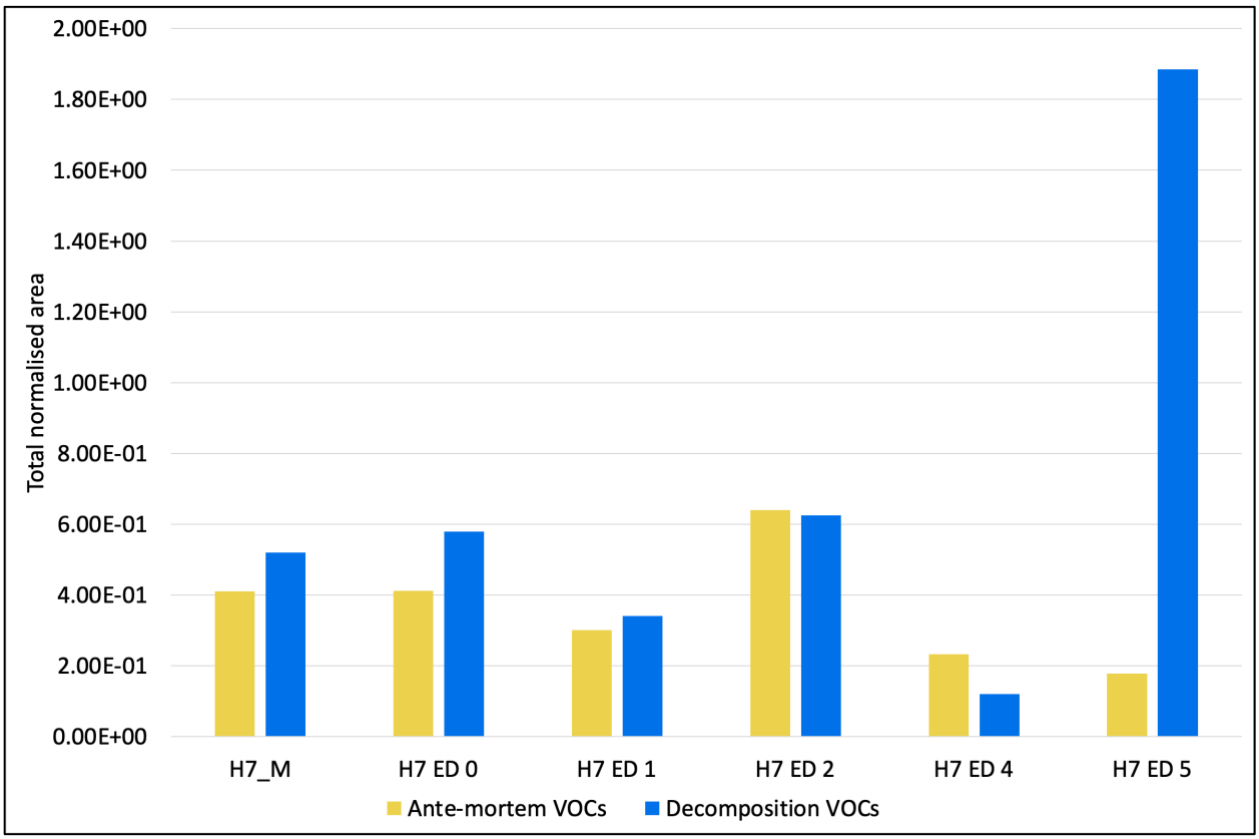

Figure 4-13 *Demonstrating the total normalised area of the literature reported ante-mortem vs decomposition VOCs detected in donor H7's samples collected at the morgue (H7_M) and REST[ES] facility (H7 ED 0 to H7 ED 5).*

In addition to the literature reported VOCs discussed above, several other VOCs detected in donor H7 have been classified into compound classes and reported in this section (Figure 4-14). For the morgue sample (H7_M), the alcohols had the highest relative class concentration identified at ~24 h PMI followed by cyclic aliphatic compounds and esters and analogues, while sulfur-containing compounds had the lowest relative class concentration followed by acids and nitrogen-containing compounds (Figure 4-14). In the H7 ED 0 sample, collected after the placement of the body at the REST[ES] facility, ketones had the highest relative class concentration followed by aromatics and aldehydes, while sulfur-containing compounds had the lowest relative class concentration followed by esters and analogues. In the H7 ED 1

sample, the halogen-containing compounds demonstrated the highest relative class concentration, followed by ketones and cyclic aliphatic compounds, while sulfur-containing had the lowest relative class concentration followed by ethers. In the H7 ED 2 sample, nitrogen-containing compounds had the highest relative class concentration followed by ketones and alcohols, while ethers had the lowest relative class concentration followed by acids and esters and analogues. In the H7 ED 4 sample, ketones had the highest relative compound class concentration followed by halogen-containing compounds and alcohols, while aldehydes had the lowest relative class concentration followed by ethers. In the H7 ED 5 sample, nitrogen-containing compounds had the highest relative class concentration followed by aromatics and ketones, while esters and analogues had the lowest relative class concentration followed by alcohols. Acids were only detected in sample H7 ED 2. Overall, for donor H7 samples, the alcohols had the highest average relative class concentration at the morgue, while nitrogen-containing compounds had the highest average relative class concentration at the REST[ES] facility. Furthermore, sulfur-containing compounds had the lowest average relative class concentration at the morgue, while acids had the lowest average relative class concentration at the REST[ES] facility.

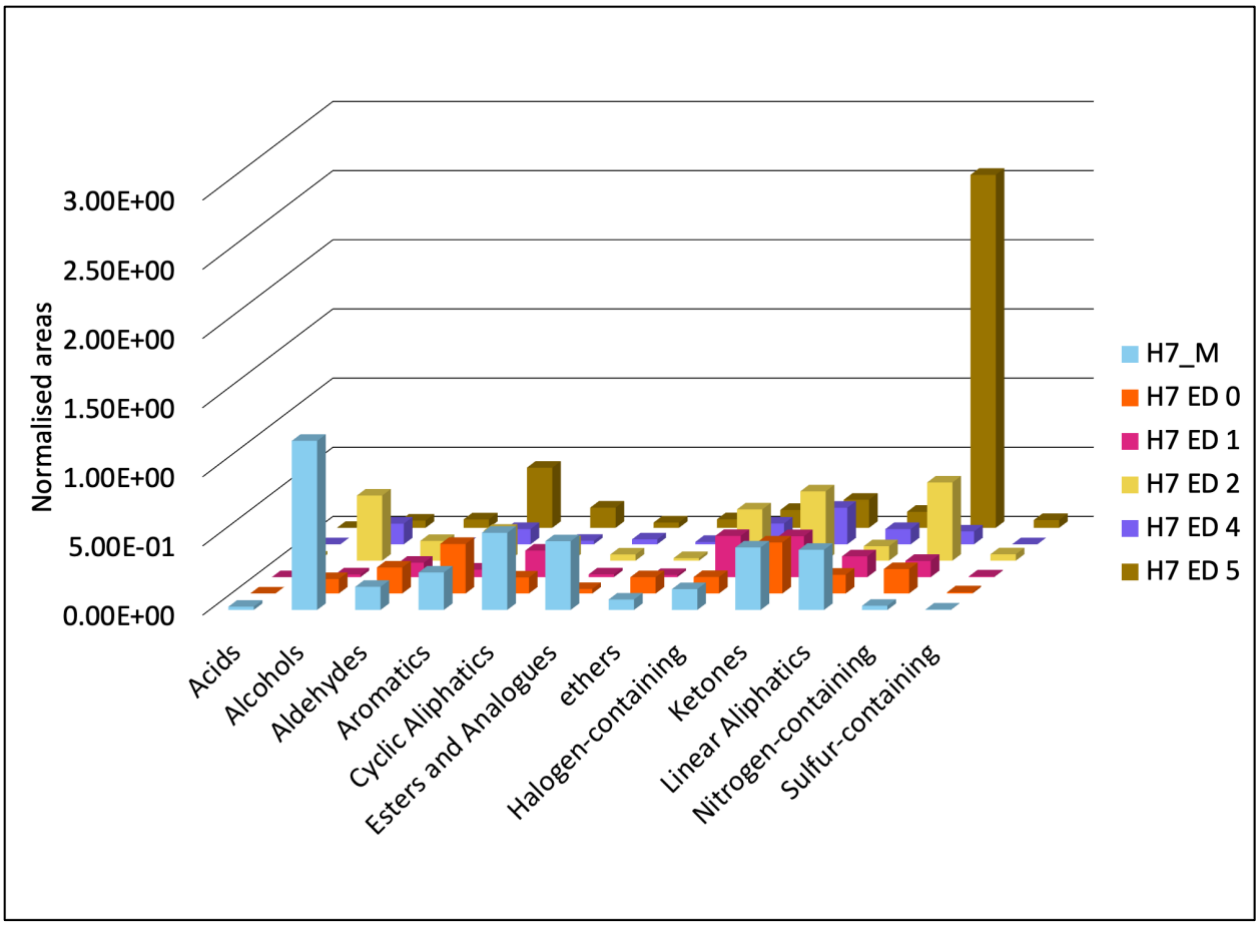

Figure 4-14 *Change in relative class concentration (normalised areas) identified in the VOC samples collected from donor H7 at the morgue (H7_M) and REST[ES] facility.*

For donor H8, Figure 4-15 represents the total normalised area of ante-mortem and decomposition VOCs for each of the samples that were common with those reported in the literature. Across all donor H8 samples, a total of 22 ante-mortem VOCs and 32 decomposition VOCs were found common with previously cited literature. In the morgue sample (H8_M), seven ante-mortem VOCs had a higher total normalised area compared to three decomposition VOCs. Likewise, in the H8 ED 0 sample, the total normalised area of two ante-mortem VOCs was higher than that of one decomposition VOC. In the H8 ED 1 sample, the total normalised area of nine decomposition VOCs was higher than that of five ante-mortem VOCs. In the H8 ED 2 sample, the total normalised area of five ante-mortem VOCs was higher than that of three decomposition VOCs. In the H8 ED 3 sample, five decomposition VOCs had a higher total normalised area compared to five ante-mortem VOCs. In the H8 ED 4 sample, 21 decomposition

VOCs had a higher total normalised area compared to 10 ante-mortem VOCs. Finally, in the H8 ED 5 sample, 15 decomposition VOCs had a higher total normalised area compared to 13 ante-mortem VOCs. It must be noted that other than some common VOCs across samples, a majority of the literature reported VOCs detected in donor H8 samples were different, and these have been detailed in Appendix C (Table C-9).

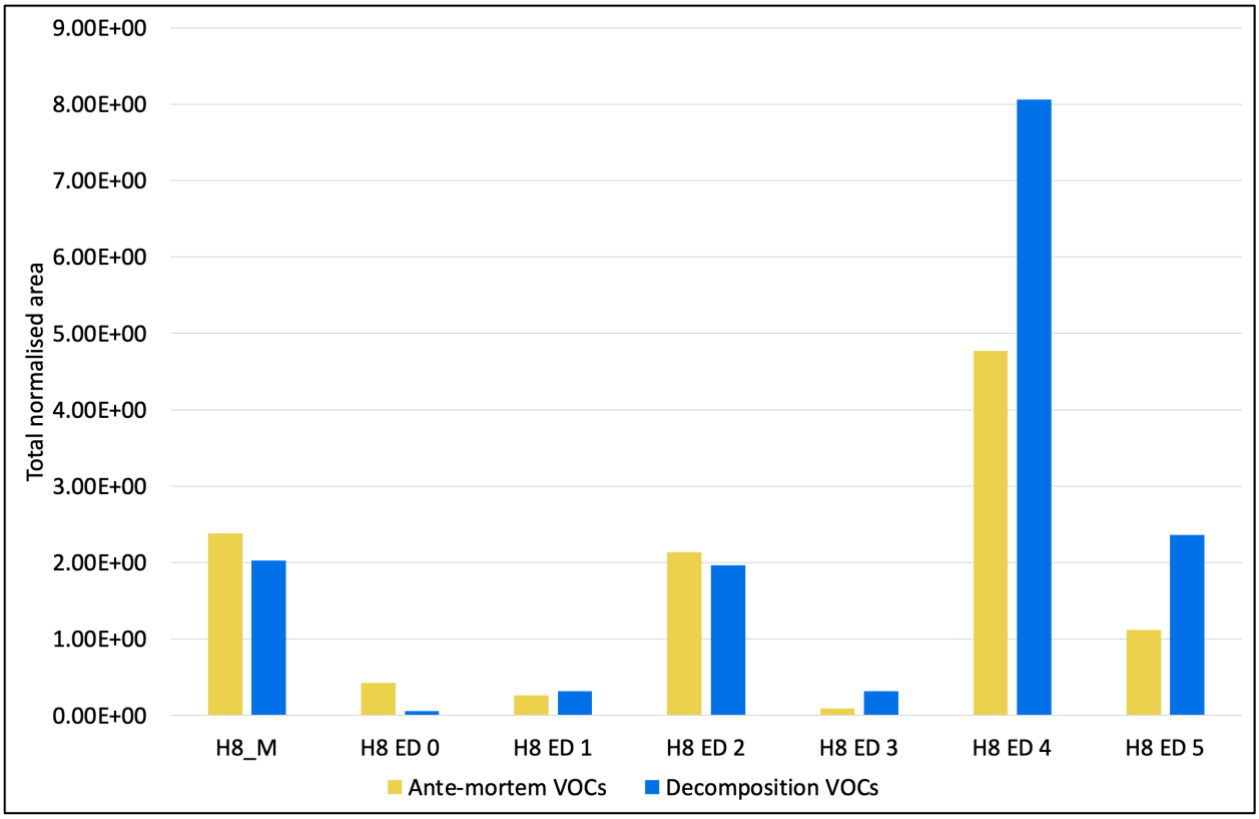

Figure 4-15 *Demonstrating the total normalised areas of the literature reported ante-mortem vs decomposition VOCs detected in donor H8's samples collected at the morgue (H8_M) and REST[ES] facility (H8 ED 0 to H8 ED 5).*

In addition to the literature reported VOCs discussed above, several other VOCs detected in donor H8 have been classified into compound classes and reported in this section (Figure 4-16). For the morgue sample (H8_M), esters and analogues had the highest relative class concentration identified at ~18 h PMI followed by alcohols and linear aliphatic compounds, while acids had the lowest relative class concentration followed by sulfur-containing compounds and nitrogen-containing compounds (Figure 4-16). In the H8 ED 0 sample collected after the placement of the body at the REST[ES] facility, nitrogen-containing compounds had

the highest relative class concentration, followed by halogen-containing compounds and esters and analogues, while ethers had the lowest relative class concentration followed by sulfur-containing compounds and alcohols. In the H8 ED 1 sample, the nitrogen-containing compounds demonstrated the highest relative class concentration followed by cyclic aliphatic and linear aliphatic compounds, while sulfur containing compounds had the lowest relative class concentration and ethers and acids were not detected. In the H8 ED 2 sample, alcohols had the highest relative class concentration followed by aromatics and cyclic aliphatic compounds, while sulfur-containing compounds had the lowest relative class concentration followed by aldehydes. In the H8 ED 3 sample, nitrogen-containing compounds had the highest relative class concentration followed by aromatics and aldehydes, while sulfur-containing compounds had the lowest relative class abundance followed by alcohols. Acids and ethers were not detected in the H8 ED 3 sample. In the H8 ED 4 sample, nitrogen-containing compounds had the highest relative compound class concentration followed by alcohol and acids, while ethers had the lowest relative class concentration followed by esters and analogues and sulfur-containing compounds. In the H8 ED 5 sample, nitrogen-containing compounds also had the highest relative class concentration followed by alcohols and aldehydes, while acids had the lowest relative class concentration followed by aromatics and cyclic aliphatic compounds. Overall, for donor H8 samples, alcohols had the highest average relative class concentration at the morgue, while nitrogen-containing compounds had the highest average relative class concentration at the REST[ES] facility. Furthermore, cyclic-aliphatic compounds had the lowest average relative class concentration at the morgue, while sulfur-containing compounds had the lowest average relative class concentration at the REST[ES] facility.

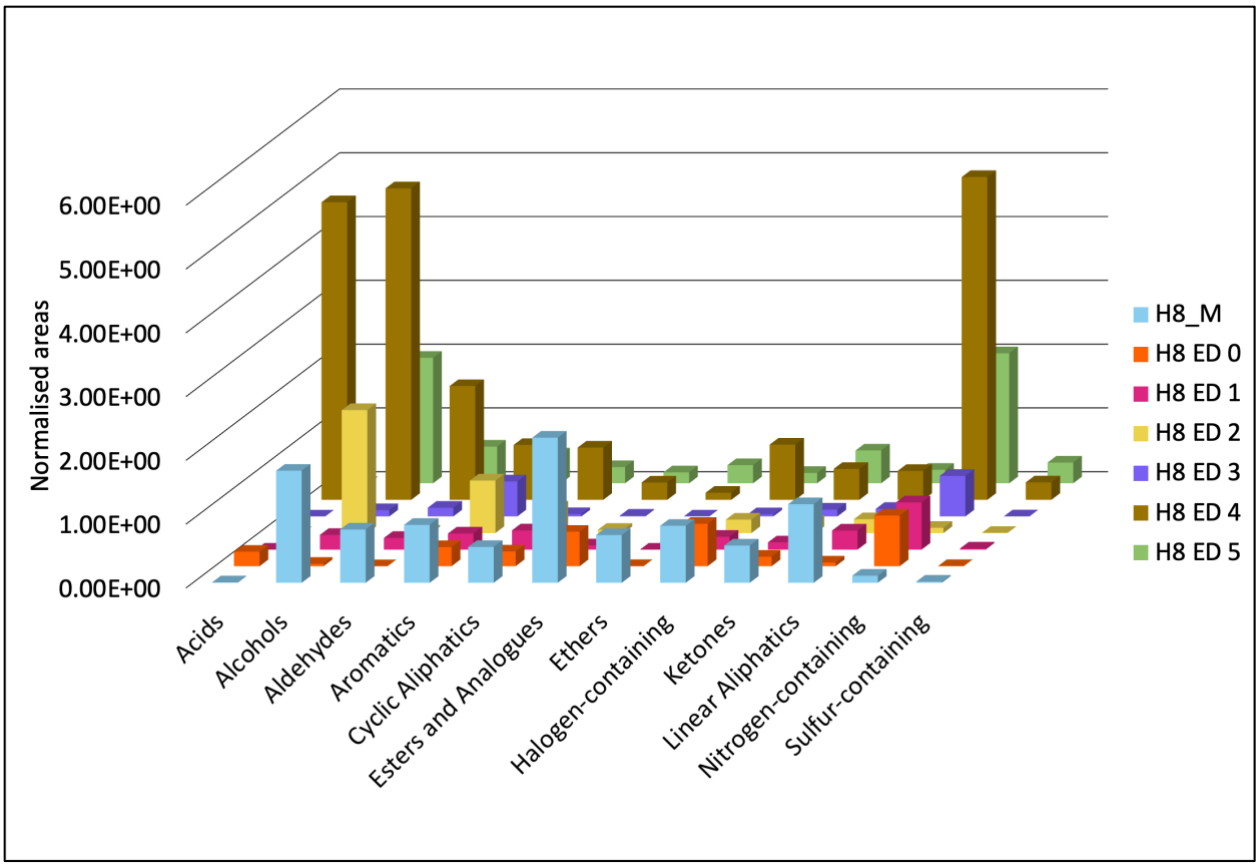

Figure 4-16 *Change in relative class concentration (normalised areas) identified in the VOC samples collected from donor H8 at the morgue (H8_M) and REST[ES] facility.*

For donor H9, Figure 4-17 represents the total normalised area of ante-mortem and decomposition VOCs for each of the samples that were common with those reported in the literature. Across all donor H9 samples, a total of 22 ante-mortem VOCs and 29 decomposition VOCs were found common with previously cited literature. In the morgue sample (H9_M), ten decomposition VOCs had a higher total normalised area compared to ten ante-mortem VOCs. For the H9 ED 0 sample, one ante-mortem VOC had a higher total normalised area compared to two decomposition related VOC. In the H9 ED 1 sample, two decomposition VOCs had a total normalised area higher than that of four ante-mortem VOCs. Likewise, in the H9 ED 2 sample, the total normalised area of five decomposition VOCs was higher than that of four ante-mortem VOCs. In the H9 ED 3 sample, the total normalised area of five decomposition VOCs was also higher than that of one ante-mortem VOC. In the H9 ED 4 sample, eight ante-mortem VOCs had a higher total normalised area compared to five decomposition VOC. Finally, in the

H9 ED 5 sample, 14 decomposition VOCs had a higher total normalised area compared to ten ante-mortem VOCs. It must be noted that other than some common VOCs across samples, a majority of the literature reported VOCs detected in donor H9 samples were different, and these have been detailed in Appendix C (Table C-10).

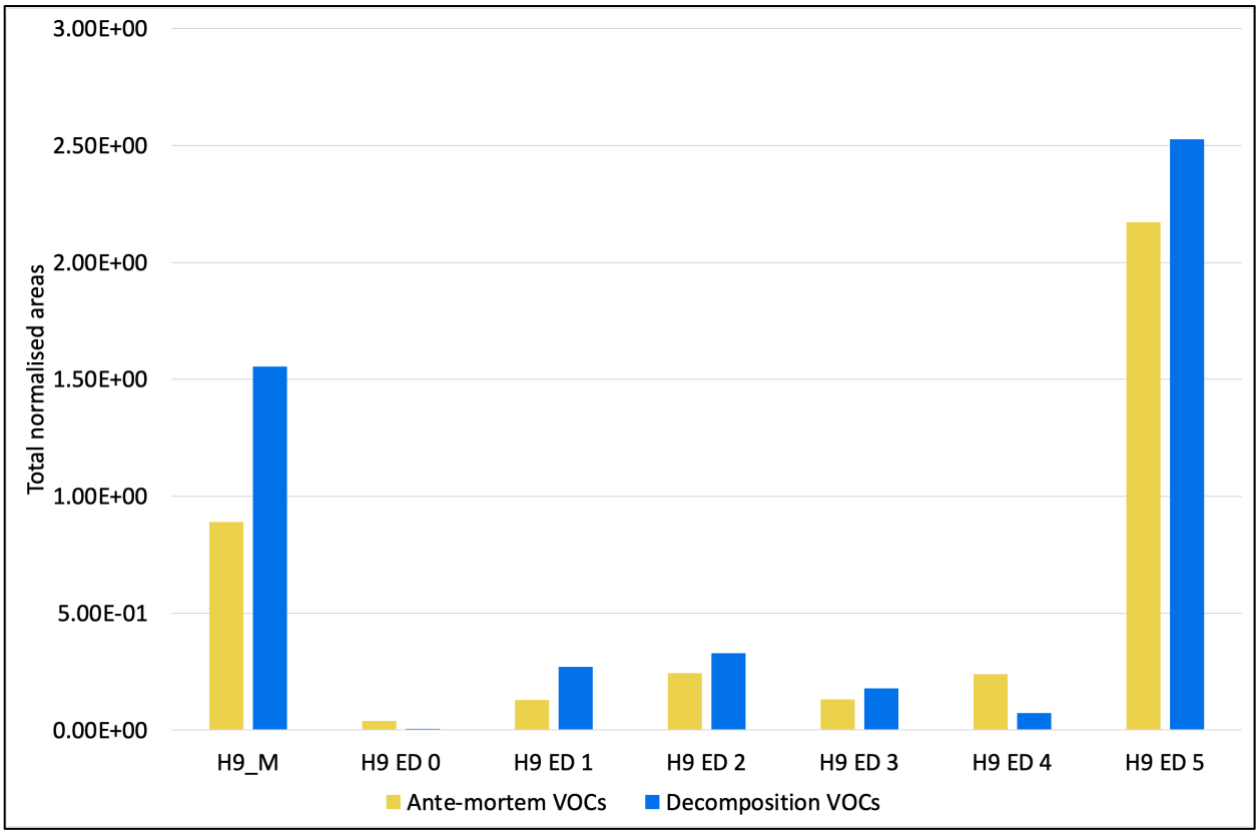

Figure 4-17 *Demonstrating the total normalised area of the literature reported ante-mortem vs decomposition VOCs detected in donor H9's samples collected at the morgue (H9_M) and REST[ES] facility (H9 ED 0 to H9 ED 5).*

In addition to the literature reported VOCs discussed above, several other VOCs detected in donor H9 have been classified into compound classes and reported in this section (Figure 4-18). The alcohols had the highest relative class concentration identified at ~14 h PMI (H9_M), followed by linear aliphatic compounds and aromatics, while sulfur-containing compounds had the lowest relative class concentration, followed by acids and nitrogen-containing compounds (Figure 4-18). In the H9 ED 0 sample, collected after the placement of the body at the REST[ES] facility, the relative class concentration of nitrogen-containing compounds was the highest

followed by aromatics and ketones, while acids had the lowest relative class concentration followed by linear aliphatic compounds. In the H9 ED 1 sample, the aldehydes demonstrated the highest relative class concentration followed by aromatics and ketones, while sulfur-containing had the lowest relative class concentration followed by cyclic aliphatic compounds. Acids and ethers were not detected in H9 ED 1 sample. In the H9 ED 2 sample, halogen-containing compounds had the highest relative class concentration followed by aromatics and aldehydes, while ethers had the lowest relative class concentration followed by cyclic aliphatics and linear aliphatic compounds. In the H9 ED 3 sample, aromatics had the highest relative class concentration followed by linear aliphatic compounds and nitrogen-containing, while ether had the lowest relative class abundance followed by alcohols and sulfur-containing compounds. In the H9 ED 4 sample, sulfur-containing compounds had the highest relative compound class concentration followed by nitrogen-containing compounds and aromatics, while alcohols had the lowest relative class concentration followed by ethers and alcohols. In the H9 ED 5 sample, alcohols had the highest relative class concentration followed by nitrogen-containing compounds and aldehydes, while acids had the lowest relative class concentration followed by esters and analogues and ethers. Overall, for donor H9 samples, the linear aliphatic compounds had the highest average relative class concentration at the morgue, while nitrogen-containing compounds had the highest average relative class concentration at the REST[ES] facility. Furthermore, sulfur-containing compounds had the lowest average relative class concentration at the morgue, while cyclic aliphatic compounds had the lowest average relative class concentration at the REST[ES] facility.

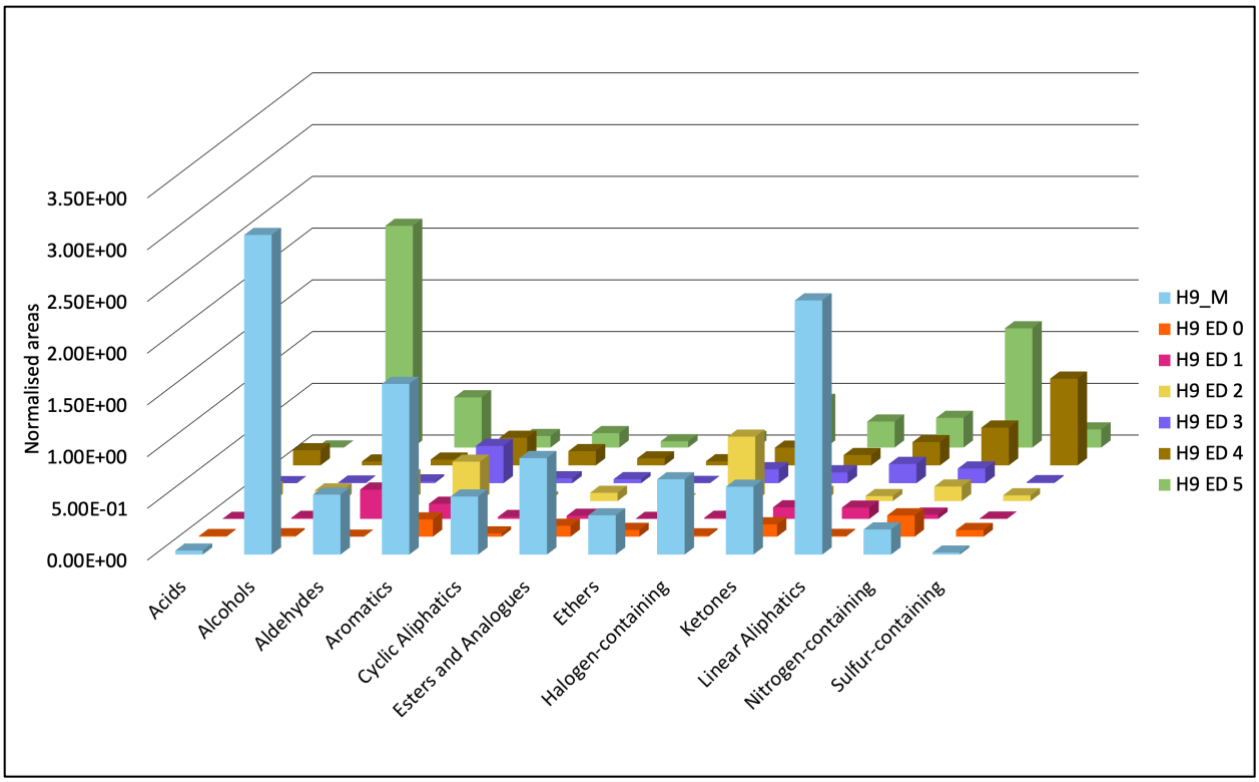

Figure 4-18 *shows the change in relative class concentration (normalised areas) identified in the VOC samples collected from donor H9 at the morgue (H9_M) and REST[ES] facility.*

4.3 Principal component analysis of individual donor VOC profiles (morgue vs REST[ES] facility)

The PCA assisted in further visualisation of the differences between the VOC profiles collected from individual donors at the morgue and REST[ES] facility. The pre-processing treatments such as internal standard area normalisation and mean center, were performed prior to PCA. This approach provided valuable information in terms of identifying decomposition VOCs relevant to the early post-mortem process. There were no outliers flagged in the data through use of Hotelling's T2 statistic at 95% level. The number of VOCs used for constructing the PCA varied due to the variability in the VOC abundance. For the PCA, the scores plot comprised of VOC samples collected at the morgue and on different experimental days at the REST[ES] facility, and loadings were calculated from the normalised area of each compound to reflect the contribution of each compound to the overall variance in the donor samples. Only two samples

were collected for donor H1 (H1_M and H1 ED 0) due to their advanced decomposition upon arrival at the REST[ES] facility. Therefore, a PCA showing the comparison between the morgue and REST[ES] facility was not possible, because in Unscrambler software it is essential to have at least three samples for generating a PCA.

For donor H2, the PCA was constructed using 116 VOCs identified with a minimum detection frequency of two out of six samples that were collected at the morgue and REST[ES] facility. The three principal components (PCs) explained 97% of the variance in the data. The scores plot of PC-1 vs PC-2 showed the best representation of the separation and the clustering of the donor H2 samples (Figure 4-19a). The morgue sample (H2_M) is separated from samples collected at the REST[ES] facility along PC-1 (76% explained variance). Along PC-2, the samples H2 ED 0 and H2 ED 3 collected at the REST[ES] facility have the highest amount of separation. The sample H2 ED 0 was collected on day 0 after the placement of the body at the REST[ES] facility and on ED 3, the donor showed signs of active decay on the face as well as the beginning of bloat. The separation of sample H2 ED 3 from sample H2 ED 0 indicates a change in the VOC profile. Further, the VOC abundance was also higher in samples H2 ED 3 compared to samples H2_M, H2 ED 0, H2 ED 1 and H2 ED 2. The loadings plot (Figure 4-19b) shows that benzyl alcohol (a decomposition VOC) caused the separation of the H2_M sample while phenol (a decomposition VOC) caused the separation of the H2 ED 0 sample. Methenamine, DMDS and DMTS caused separation of the H2 ED 3 sample and these VOCs have been reported as decomposition VOCs in the literature (6, 7, 37, 106).

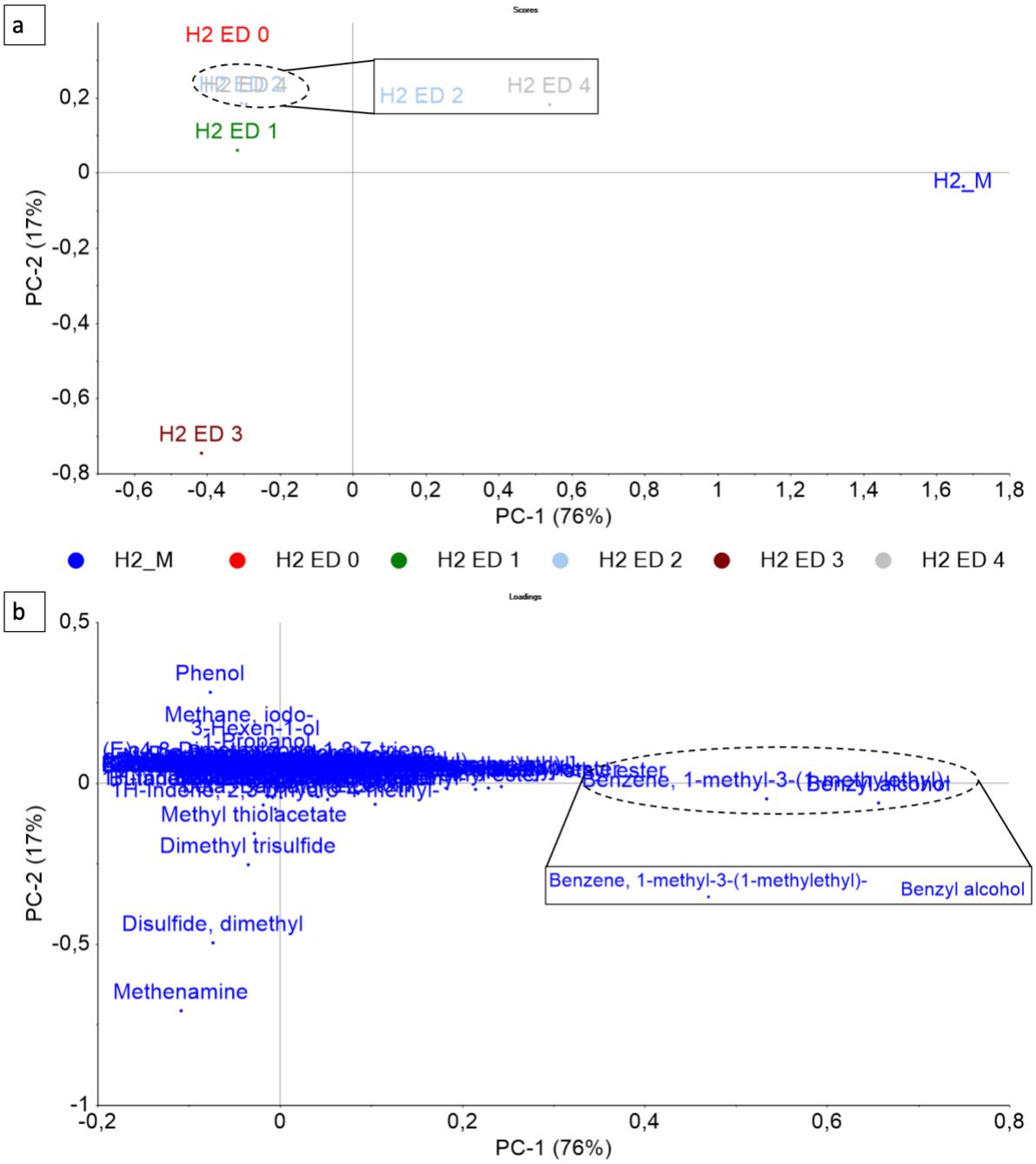

Figure 4-19 *PCA showing a) scores plot and b) loadings plot for PC-1 vs PC-2 of donor H2. The PCA was calculated using the pre-processed GC×GC-TOFMS normalised peak areas of 116 compounds identified with a minimum detection frequency of two out of six samples. The sample H2_M was separated from samples collected at the REST[ES] facility (H2 ED 0, H2 ED 1, H2 ED 2, H2 ED 3, and H2 ED 4) along PC-1. The sample H2 ED 3 is separated from all other samples collected at the REST[ES] facility along PC-2. The loadings plot shows the distribution of variables across PC-1 and PC-2, with benzyl alcohol causing separation of H2_M sample (PC-1) and phenol causing separation of sample H2 ED 0 (PC-2). Methenamine, dimethyl disulfide and dimethyl trisulfide caused separation of sample H2 ED 3 along PC-2*

For donor H3, a PCA was constructed using 28 VOCs identified with a minimum detection frequency of two out of five samples that were collected at the morgue and REST[ES] facility. The two PCs explained 99% of the variance in the data. The scores plot of PC-1 vs PC-2 (79% and 20% explained variance) showed the best representation of the separation and the clustering of the samples (Figure 4-20a). The sample H3 ED 0 (first sample collected at REST[ES] facility) was separated from the H3_M (morgue) sample and all other samples collected at the REST[ES] facility (Figure 4-20a). The sample H3_M is separated from the samples collected at the REST[ES] facility along PC-2. An interesting observation was the clustering of samples H3 ED 2, H3 ED 3, and H3 ED 4 samples. The clustering of these samples can be associated with lower variability in the VOC profiles due to cold temperatures and relatively higher rainfall experienced during the donor H3 sample collection. The loadings plot show that along PC-1, acetaldehyde (an ante-mortem VOC) caused the separation of the H3 ED 0 sample while 1-propoxy-2-propanol caused the separation of the H3_M sample (Figure 4-20b).

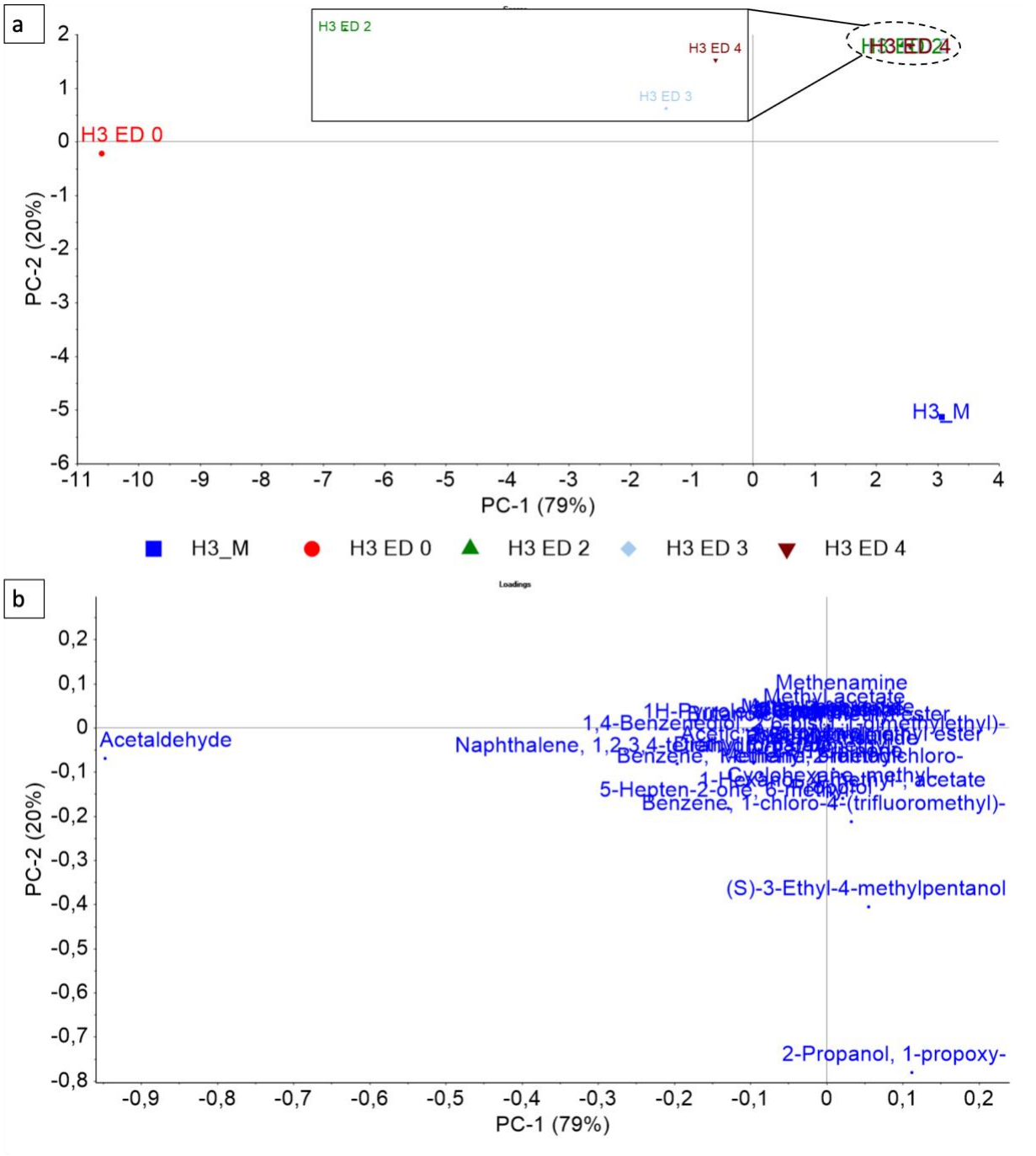

Figure 4-20 *PCA showing a) scores plot and b) loadings plot for PC-1 vs PC-2 of donor H3. The PCA was calculated using the pre-processed GC×GC-TOFMS normalised peak areas of 28 compounds identified with a minimum detection frequency of two out of five samples. The sample H3_M was separated from samples H3 ED 2, H3 ED 3, H3 ED 4 (highlighted with black square) collected at the REST[ES] facility along PC-2. The sample H3 ED 0 is separated from all other samples collected at the REST[ES] facility along PC-1. The loadings plot shows the distribution of variables across PC-1 and PC-2, with 1-propoxy, 2-propanal causing separation of the H3_M sample (PC-2) and acetaldehyde causing separation of the H3 ED 0 sample (PC-1).*

For donor H4, the PCA was constructed with 10 VOCs identified with a minimum detection frequency of three out of four samples that were collected at the morgue and REST[ES] facility. The scores plot showed the separation of the samples collected at the morgue and REST[ES] facility. The first two principal components, PC-1 (91%) and PC-2 (8%), explains 99% of the explained variance in the data (Figure 4-21a). The H4_M sample was responsible for the most variance among all the samples and separated along PC-1 from all other samples collected at the REST[ES] facility. The H4 ED 0 sample was collected at the REST[ES] facility after the placement of the body and it was separated from the samples H4 ED 1 and H4 ED 3 along PC-2. The loadings plot (Figure 4-21b) shows that bromodichloromethane (a decomposition VOC) was causing the separation of the H4_M sample along PC-1 and methyl acetate (acetic acid, methyl ester) (a decomposition VOC) caused the separation of the H3 ED 0 sample. Diethyl fumarate caused the separation of the H4 ED 1 and H4 ED 3 samples. Diethyl fumarate has not been previously reported in the literature as an ante-mortem or decomposition VOC.

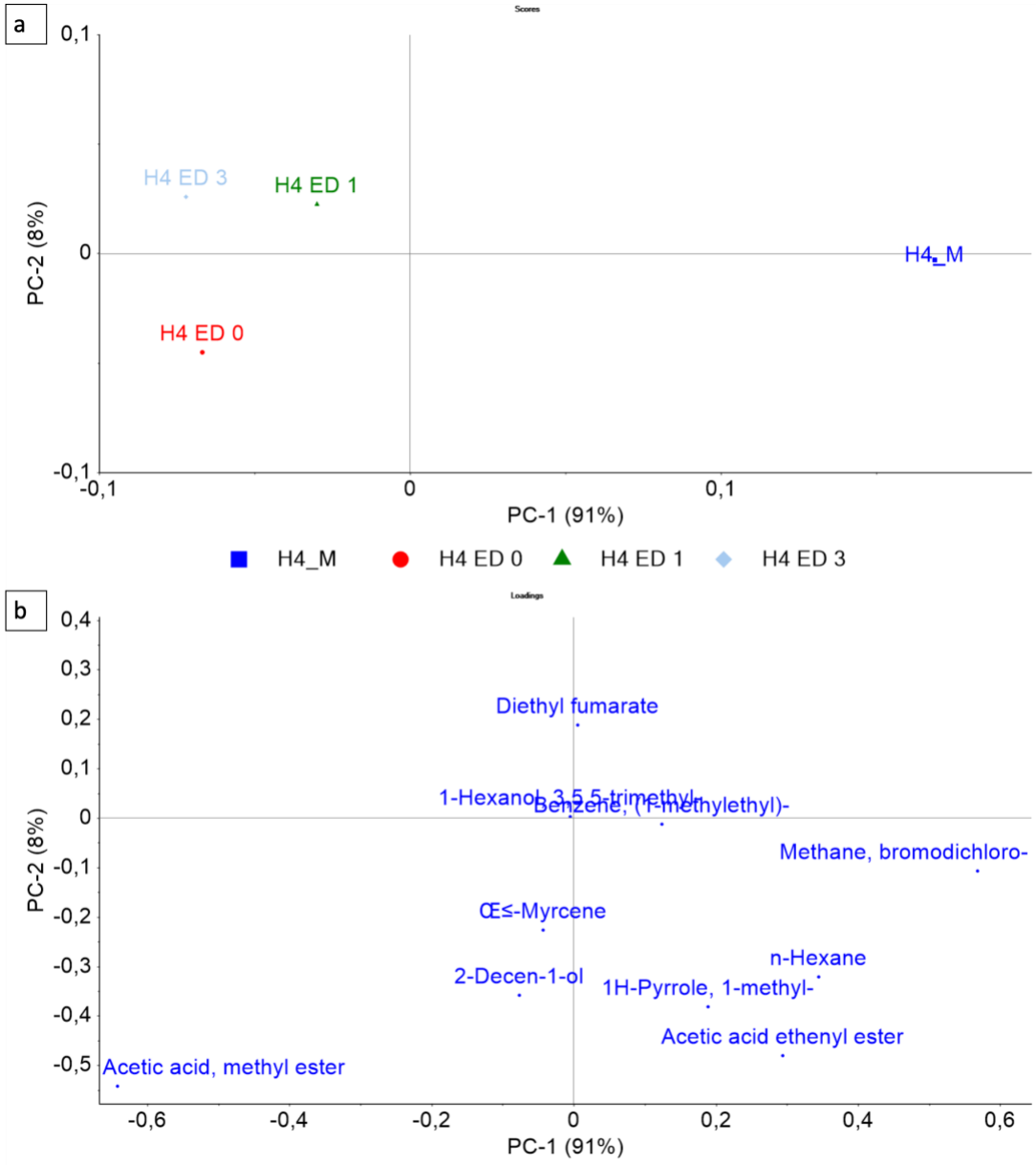

Figure 4-21 *PCA showing a) scores plot and b) loadings plot for PC-1 vs PC-2 of donor H4. The PCA was calculated using the pre-processed GC×GC-TOFMS normalised peak areas of 10 compounds identified with a minimum detection frequency of two out of four samples. The sample H4_M was separated from samples collected at the REST[ES] facility (H4 ED 0, H4 ED 1, and H4 ED 3) along PC-1. The H4 ED 1 and H4 ED 3 samples are separated from the H4 ED 0 sample along PC-2. The loadings plot shows the distribution of variables across PC-1 and PC-2, with dibromochloromethane (methane, bromodichloro) causing separation of the H4_M sample (PC-1) and methyl acetate (acetic acid, methyl ester) causing separation of the H4 ED 0 sample (PC-2). Dimethyl fumarate caused the separation of samples H4 ED 1 and H4 ED 3 along PC-2*

For donor H6, the PCA was constructed with 29 VOCs identified with a minimum detection frequency of three out of seven samples that were collected at the morgue and REST[ES] facility. The five PCs explained 99% of the variance in the data. The scores plot of PC-1 vs PC-2 showed the best representation of the separation between the samples collected at the morgue and REST[ES] facility. Figure 4-22a shows that along PC-2, the morgue sample (H6_M) is separated from the cluster of samples H6 ED 0, H6 ED 1, and H6 ED 2. The sample H6 ED 0 was the first sample collected at the REST[ES] facility after the placement of the donor at the REST[ES] facility. The samples H6 ED 3, H6 ED 4 and H6 ED 5 are closely grouped and separated from the cluster of samples along PC-1. On ED 3, the first visual features indication autolysis and putrefaction (greenish discolouration) were seen on the torso and abdomen. The presence of this feature indicates a change in the VOC profile after ED 3. The loadings plot show that 2-pentyl furan (furan,2-pentyl) (a decomposition VOC) caused the separation of the H6_M sample while there was no VOC strongly associated with the cluster of samples (H6 ED 0, H6 ED 1, and H6 ED 2) (Figure 4-22b). 2,3-dihydro-1,6-dimethyl-1H-Indene, formaldehyde, and 1-ethenyl-2-methylbenzene caused the separation of samples H6 ED 3, H6 ED 5, and H6 ED 4. 2,3-dihydro-1,6-dimethyl-1H-Indene and 1-ethenyl-2-methylbenzene has not been previously reported as and ante-mortem or decomposition VOC.

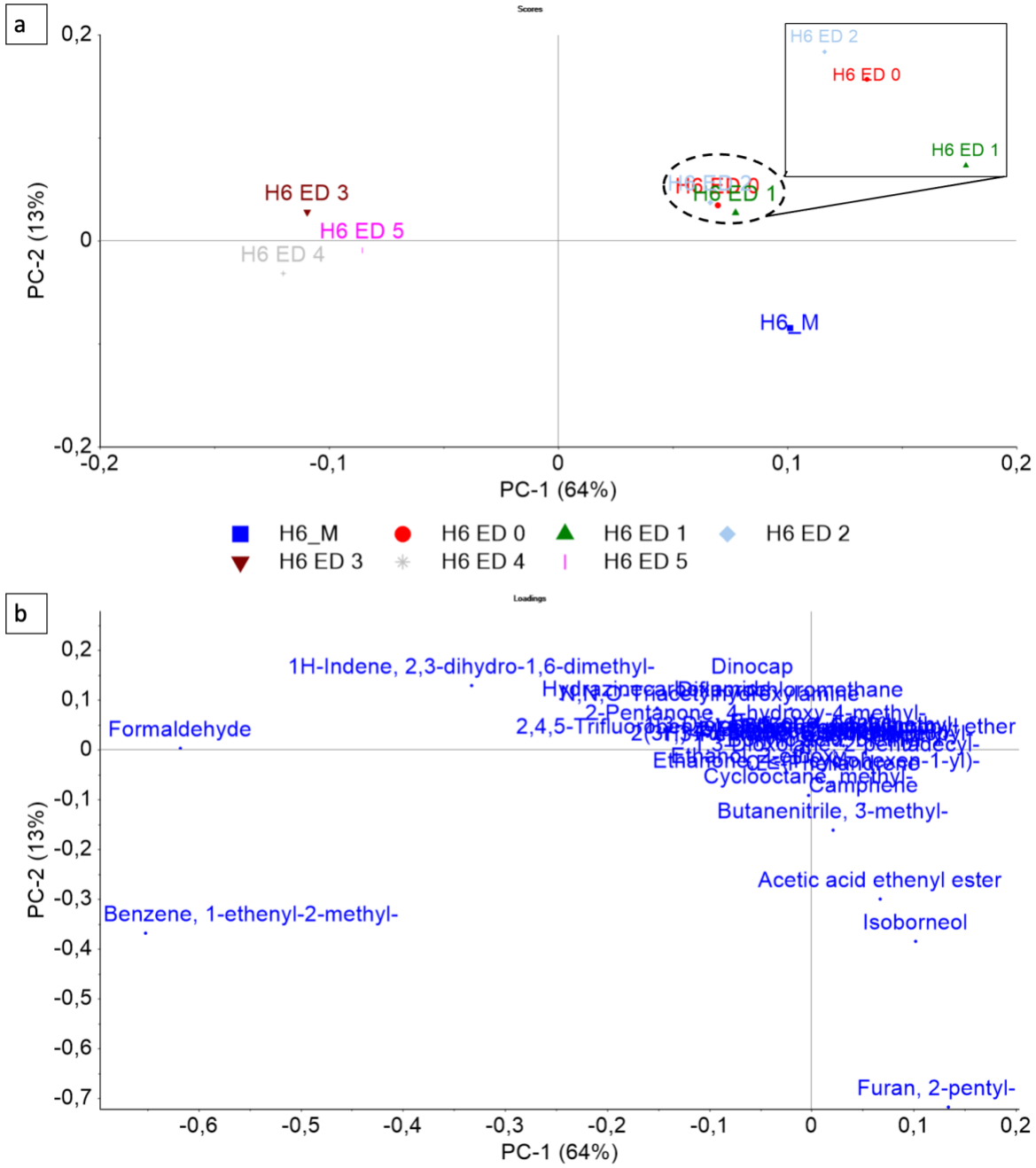

Figure 4-22 *PCA showing a) scores plot and b) loadings plot for PC-1 vs PC-2 of donor H6. The PCA was calculated using the pre-processed GC×GC-TOFMS normalised peak areas of 29 compounds identified with a minimum detection frequency of three out of seven samples. The H6_M sample was separated along PC-2 from the cluster (H6 ED 0, H6 ED 1, and H6 ED 2) collected at the REST[ES] facility. The samples H6 ED 3, H6 ED 4 and H6 ED 5 are separated from samples H6 ED 0, H6 ED 1, and H6 ED 2 along PC-1. The loadings plot shows the distribution of variables across PC-1 and PC-2, with 2-pentylfuran (Furan,2-pentyl) causing separation of the H6_M sample (PC-2), formaldehyde and 1-ethenyl-2-methylbenzene (benzene, 1-ethenyl-2-methyl) causing separation of samples H6 ED 3, H6 ED 4, and H6 ED 5 (PC-1).*

For donor H7, a PCA was constructed with 69 VOCs identified with a minimum detection frequency of three out of six samples that were collected at the morgue and REST[ES] facility. The four PCs explained 94% of the variance in the data. The scores plot of PC-1 vs PC-2 showed the best representation of the separation and clustering of the donor H7 samples (Figure 4-23a). The morgue sample (H7_M) is separated from all other samples collected at the REST[ES] facility. Samples H7 ED 0 and H7 ED 4 are clustered around the intercept indicating weak influence on the PCs. Along PC-1 (42% explained variance), samples H7 ED 1 and H7 ED 2 are separated from samples H7 ED 0 and H7 ED 4. Sample H7 ED 5 is separated from all other samples collected at the REST[ES] facility along PC-2 (22% explained variance). The loadings plot shows that 6-methyl-5-Hepten-2-one (5-Hepten-2-one, 6-methyl) (an ante-mortem VOCs) caused the separation of the H7_M sample while the separation of samples H7 ED 1 and H7 ED 2 was caused by 2-butanone, bromodichloromethane (methane, bromodichloro) and propan-2-ol (isopropyl alcohol) (Figure 4-23b). These VOCs have been previously reported in the literature as decomposition VOCs. 2-propenylbenzene (Benzene, 2-propenyl) caused the separation of H7 ED 5.

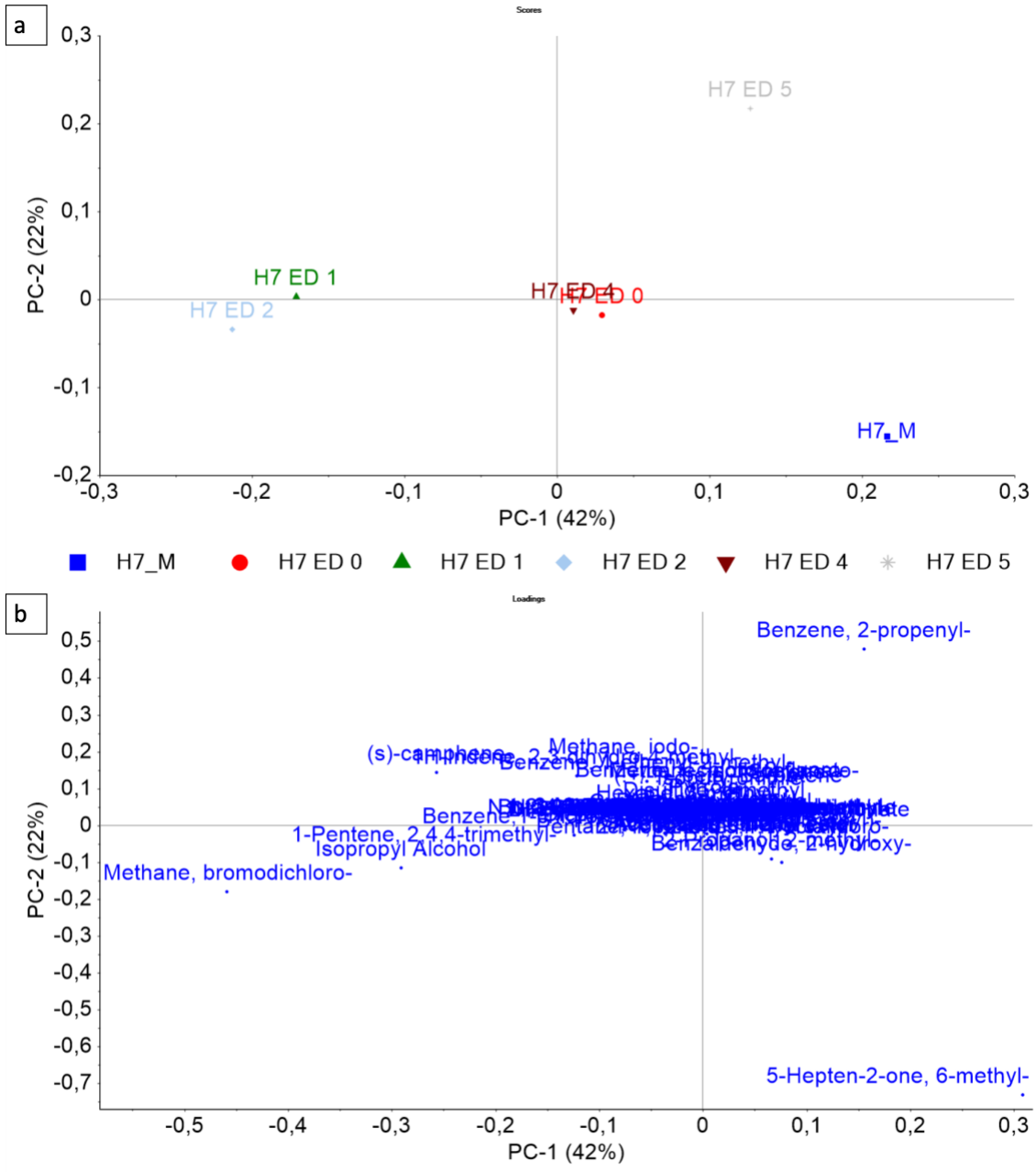

Figure 4-23 *PCA showing a) scores plot and b) loadings plot for PC-1 vs PC-2 of donor H7. The PCA was calculated using the pre-processed GC×GC-TOFMS normalised peak areas of 69 compounds identified with a minimum detection frequency of three out of six samples. In the scores plot PC-1 vs PC-2, the sample H7_M was separated from samples collected at the REST[ES] facility. The sample H7 ED 0 and H7 ED 4 are close to the X and Y intercept indicating week influence on the PCs. Samples H7 ED 1 and H7 ED 2 are separated from sample H7 ED 5 along PC-2. The loadings plot shows the distribution of variables across PC-1 and PC-2, with 6-methyl-5-hepten-2-one (5-hepten-2-one, 6-methyl) causing separation of H7_M (PC-2) and bromodichloromethane (methane, bromodichloro), and propan-2-ol (isopropyl alcohol) causing separation of sample H7 ED 1 and H7 ED 2 (PC-1). 2-propenylbenzene (Benzene, 2-propenyl) caused separation of sample H7 ED 5 along PC-2.*

For donor H8, the PCA was constructed using 69 VOCs identified with a minimum detection frequency of three out seven samples that were collected at the morgue and REST[ES] facility. Figure 4-24a shows that PC-1 and PC-2 explains 93% of the variance in the data. The scores plot of PC-1 vs PC-2 showed the best representation of the separation and clustering of the donor H8 samples. The morgue sample (H8_M) was separated from samples collected at the REST[ES] facility along PC-2. Donor H8 REST[ES] samples show an interesting pattern of separation in the scores plot. H8 ED 0, H8 ED 1 and H8 ED 2 were separated on the negative axis while H8 ED 3, H8 ED 4, and H8 ED 5 were separated on the positive axis (Figure 4-24a). On ED 3, the first visual features indicating autolysis and putrefaction were seen on the upper and lower limbs indicating a change in the VOC profile. The sample H8 ED 4 was responsible for the most variance along PC-1 (Figure 4-24a). 2,2,2-trifluroethanol (Ethanol, 2,2,2-trifluro-) and 1-Penten-3-ol caused the separation of H8_M sample while 6-methyl-5-Hepten-2-one (5-Hepten-2-one, 6-methyl) (an ante-mortem VOCs) caused the separation of the H8 ED 0 and H8 ED 1 samples (Figure 4-24b). 1-propanol, benzonitrile, nonanal (an ante-mortem VOC), propan-2-ol (isopropyl alcohol) and methylamine, N,N-dimethyl caused the separation of the H8 ED 3 and H8 ED 5 samples. Apart from nonanal, VOCs that caused separation of the H8 ED 3 and H8 ED 5 samples were previously reported in the literature as decomposition VOCs. Ethanol (a decomposition VOC) caused the separation of the sample H8 ED 4.

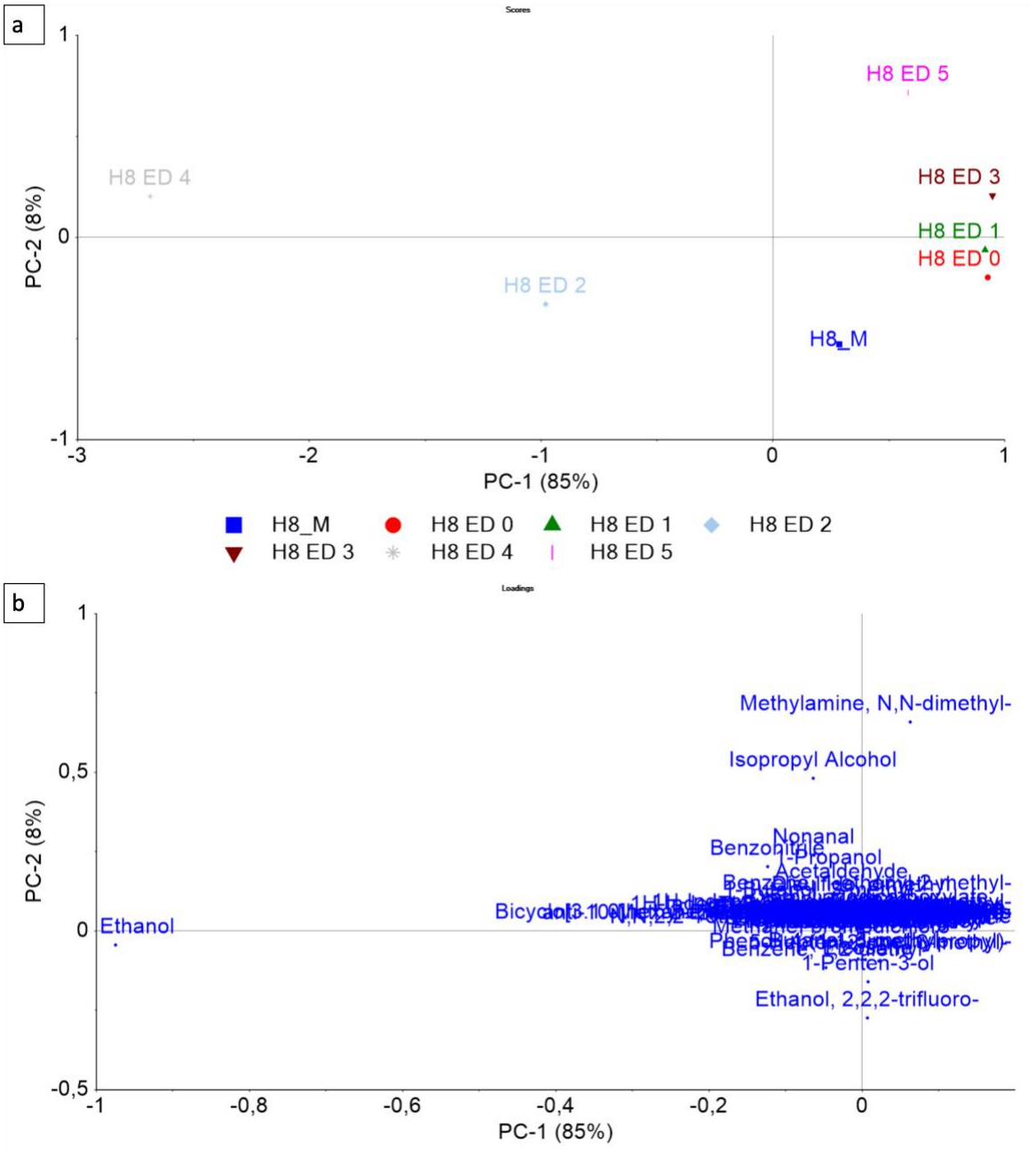

Figure 4-24 *PCA showing a) scores plot and b) loadings plot for PC-1 vs PC-2 of donor H8. The PCA was calculated using the pre-processed GC×GC-TOFMS normalised peak areas of 69 compounds identified with a minimum detection frequency of three out of seven samples. The sample H8_M was separated from samples collected at the REST[ES] facility (H8 ED 0, H8 ED 1, H8 ED 3, and H8 ED 5) along PC-2. The sample H8 ED 4 is separated from all other samples collected at the REST[ES] facility along PC-1. The loadings plot shows the distribution of variables across PC-1 and PC-2, with 2,2,2-trifluoroethanol (ethanol, 2,2,2-trifluoro) causing separation of the H8_M sample (PC-1) and ethanol causing separation of the H8 ED 4 sample (PC-1). Methylamine, N,N-dimethyl and propan-2-ol (isopropyl alcohol) caused separation of sample H8 ED 5 along PC-2.*

For donor H9, the PCA was constructed using 47 VOCs identified with a minimum detection frequency of three out seven samples that were collected at the morgue and REST[ES] facility. Five PCs explained 98% of the variance in the data. The PC-1 and PC-2 captured 74% of the total variation in the data while PC-3, PC-4, and PC-5 captured 12%, 7%, and 4%, respectively of the variation in the data. The scores plot of PC-1 vs PC-3 shows that morgue sample (H9_M) is separated from all other samples along PC-1. The highest separation can be observed between H9 ED 0 and H9_M samples. The sample H9 ED 0 was the first sample collected from donor H9 after the placement of the donor at the REST[ES] facility. Along PC-3, sample H9 ED 3 was separated from samples H9 ED 1 and H9 ED 2 collected at the RES[ES] facility. On ED 3, visual features indicating autolysis and putrefaction were observed on the donor indicating a change in the VOC profile. 3-methylbutanal (Butanal, 3-methyl) (an ante-mortem VOC) caused the separation of the H9_M sample while 1,2-diethylbenzene (benzene 1,2, diethyl) and allylbenzene (benzene 2-propenyl) caused separation of the H9 ED 3 sample. DMDS (a decomposition VOC), 3-methyl-1-butanol (1-butanol, 3-methyl) (a decomposition VOC) and 1-ethenyl-2-methylbenzene (benzene, 1-ethenyl-2-methyl) caused the separation of the H9 ED 5 sample. 1-ethenyl-2-methylbenzene (Benzene, 1-ethenyl-2-methyl) has not been previously reported in the literature as an ante-mortem or decomposition VOC.

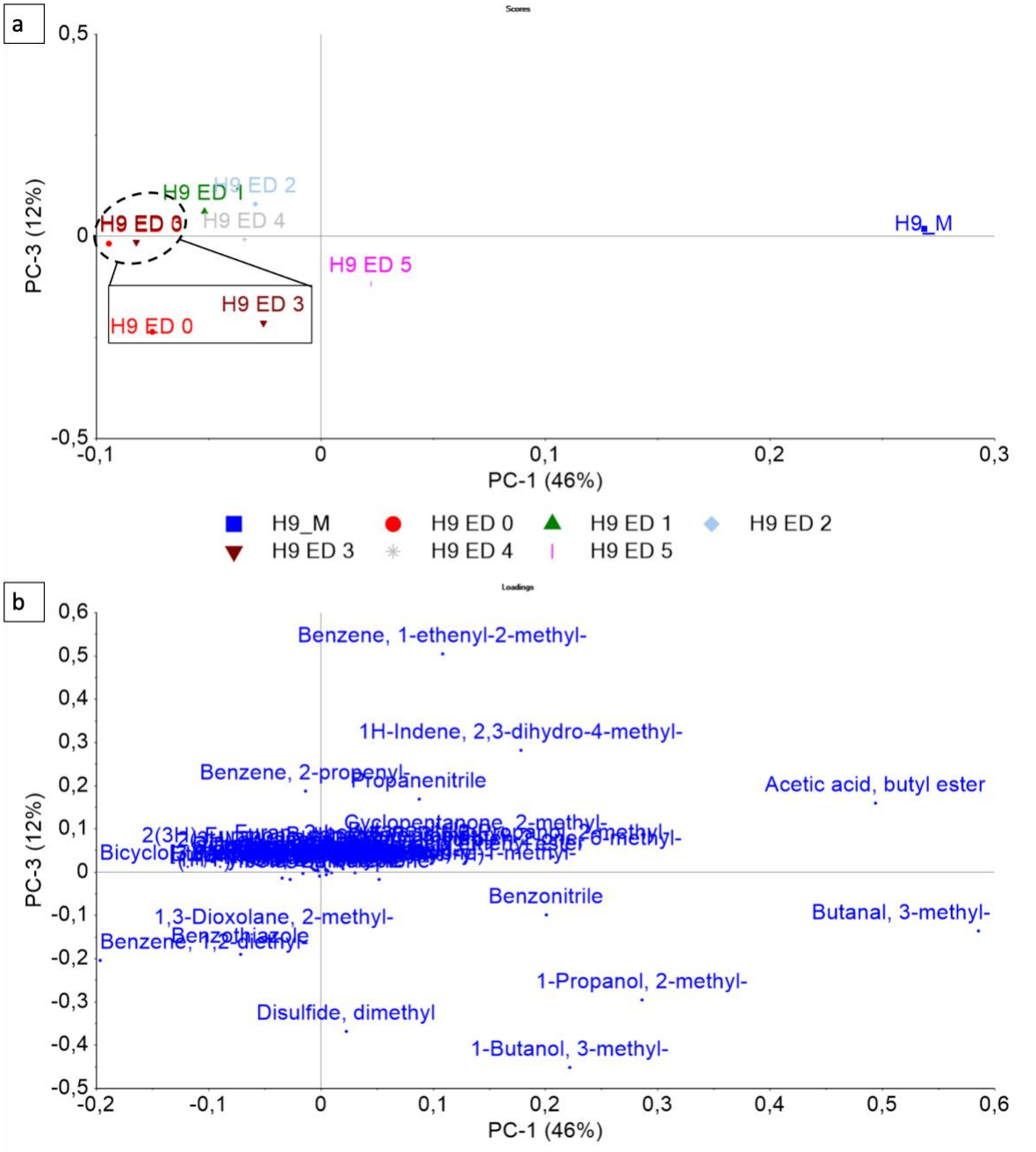

Figure 4-25 *PCA showing a) scores plot and b) loadings plot for PC-1 vs PC-3 of donor H9. The PCA was calculated using the pre-processed GC×GC-TOFMS normalised peak areas of 47 compounds identified with a minimum detection frequency of three out of seven samples. The sample H9_M was separated from samples collected at the REST[ES] facility (H9 ED 0, H9 ED 1, H9 ED 2, H9 ED 3, H9 ED 4, and H9 ED 5) along PC-1. The sample H9 ED 5 is separated from all other samples collected at the REST[ES] facility along PC-3. The loadings plot shows the distribution of variables across PC-1 and PC-3, with butyl acetate (acetic acid, butyl ester) causing separation of the H9_M sample (PC-1) and dimethyl disulfide and 3-methyl-1-butanol (1-butanol, 3-methyl) causing separation of sample H9 ED 5 along PC-3.*

Table 4-1 shows the samples which were clearly separated on the scores plot. In general, the samples collected in the morgue and ED 0 samples collected after the initial placement of the bodies at the REST[ES] facility were separated from all other samples collected during the relevant trials. Apart from samples mentioned above, ED 3, ED 4, and ED 5 samples were frequently separated and contributed to the variance in the scores plot. In the loadings plots, methane, bromodichloro was identified to be causing separation in two donor samples (H4_M, and H7 ED 2) collected at the morgue and REST[ES] facility. DMDS was identified to be causing separation in two donor samples (H2 ED 3 and H9 ED 5). All other compounds that caused separation in the loadings plots were only identified in one sample.

Table 4-1 *Summary of samples showing highest separation and their corresponding scores and loadings plot.*

Donor id	**Samples showing separation**	**Corresponding scores plot and explained variance**	**Corresponding loadings in the loadings plot**
H2	H2 ED 0 and H2_M	PC-1 (76%) and PC-2 (17%)	Benzyl alcohol (PC-1) and phenol (PC-2)
H3	H3 ED 0 and H3 ED 2, H3 ED 3, and H3 ED 4	PC-1 (79%) and PC-2 (20%)	Acetaldehyde (PC-1) and Methenamine (PC-2)
H4	H4_M and H4 ED 0	PC-1 (91%) and PC-2 (8%)	Bromodichloromethane (methane, bromodichloro) (PC-1) and methyl acetate (acetic acid, methyl ester) (PC-2)
H6	H6 ED 4 and H6_M	PC-1 (64%) and PC-2 (13%)	Formaldehyde (PC-1) and 2-pentylfuran (Furan, 2-pentyl) (PC-2)
H7	H7 ED 2, H7_M and H7 ED 5	PC-1 (42%) and PC-2 (22%)	Bromodichloromethane (methane, bromodichloro) (PC-

			1) and allylbenzene (benzene, 2-propenyl) (PC-2) and 6-methyl-5-Hepten-2-one (5-Hepten-2-one, 6-methyl) (PC-2)
H8	H8 ED 4 and H8_M	PC-1 (85%) and PC-2 (8%)	Ethanol (PC-1) and 2,2,2-trifluroethanol (ethanol, 2,2,2-trifluro) (PC-2)
H9	H9 ED 0 and H9_M	PC-1 (46%) and PC-3 (12%)	3-methylbutanal (butanal, 3-methyl) (PC-1) and DMDS and 3-methyl-1-butanol (1-butanol, 3-methyl) (PC-3)

4.4 Discussion

The results of this study show the first-ever comparison of the total normalised area of ante-mortem and post-mortem VOCs identified in the VOC profiles of cadavers during the early post-mortem period (discussed in section 4.4.1). These results help to visualise the differences in the total normalised area of ante-mortem and decomposition VOCs. Furthermore, the changes in the relative class concentration between the samples collected at the morgue and the REST[ES] facility have been discussed in section 4.4.2. Finally, the difference in the VOC profiles collected at the morgue and REST[ES] facility have been visualised via PCA (discussed in section 4.4.3).

4.4.1 Total normalised area of the literature reported (ante-mortem vs decomposition VOCs)

Ante-mortem VOCs were identified in 95.4% (42 of 44) samples collected at the morgue and REST[ES] facility. This shows their pervasiveness during the early post-mortem period (Figures 4-3, 4-5, 4-7, 4-9, 4-11, 4-13, 4-15, 4-17), which is consistent with the previously reported

literature (64). Presence of ante-mortem VOCs is predominantly related to VOCs resulting from action of the microbiome present on the skin's surface (64). Microbiome interaction on the surface of the skin could have continued during the early post-mortem period in the morgue. Moreover, during the early post-mortem period, in an outdoor environment such as the REST[ES] facility, factors such as ozone, UV and solar radiation can induce oxidative stress on the skin's surface, thus, resulting in the presence of ante-mortem VOCs during the early post-mortem period (95, 132).

Overall, the total normalised area of ante-mortem VOCs was higher than the decomposition VOCs in 31.8% (14 of 44) samples. Surprisingly, in samples such as H6 ED 5, and H7 ED 4 and H9 ED 4 the total normalised area of ante-mortem VOCs was higher than decomposition VOCs. These samples were collected during the latter part of the trial when the early post-mortem period was passing (ED 4 and ED 5). The presence of ante-mortem VOCs during the latter part of the early post-mortem period may suggest that their persistence can be dependent on other environmental factors such as solar radiation and atmospheric pressure. The presence of ante-mortem VOCs and their higher total normalised area on ED 4 and ED 5 is contrary to what has been previously reported in the literature. A study conducted on pigs by Armstrong et al. (64) reported that early post-mortem odour closely resembles ante-mortem up to two days PMI (64). Unlike in the current study, Armstrong et al. (64) did not track the persistence of ante-mortem VOCs based on the change in the total normalised area. Their conclusion of the fact that the change occurred after two days was solely based on PCAs, where samples collected after two days clustered separately from the samples collected within the first two days of their study. Thus, from the current and previous studies, ante-mortem VOCs have been predominantly detected up to ED 2 and ED 3 after death. This emphasises that considerations must be made when deploying SAR versus HRD dogs during the early post-mortem period in a search and rescue operation conducted in an outdoor environment. The persistence of ante-mortem VOCs can alter the overall VOC profile of human remains, making it challenging for the HRD dog to associate it with decomposition odour during the early post-mortem period. Thus, it is recommended that SAR and HRD dogs are both deployed at least two to three days following death. However, it is important to note that these results are representative of

Quebec's climate; therefore, further studies are required in different geographical contexts to accurately estimate odour transition in diverse environments. The challenges in comparing the effect of environment and impact of local climate are further discussed in section 4.5.

The decomposition VOCs were identified in both sample sets collected at the morgue and REST[ES] facility and their total normalised area was higher in 68.1% (30 of 44) samples. When comparing intra-donor morgue samples, 3 of 8 donors (H1, H3 and H8) had a higher total normalised area of ante-mortem VOCs, while the remaining donors (H2, H4, H6, H7, and H9) had a higher total normalised area of decomposition VOCs. Note that donors H2, H4, H6, H7 and H9 died of hepatic cirrhosis, myocardial infarction and mast cell activation syndrome, metastatic cancer, and malignant arrhythmia, respectively (Table 3-1). In all these pathological conditions, the liver, heart, and lung tissues become oedematous (swollen), and bacteria can spread faster in these oedematous tissues, leading to faster autolysis and putrefaction compared to other pathological conditions recorded in this study (42). This may be the reason for increased decomposition VOCs in these donors, but this hypothesis needs to be tested further.

Generally, on ED 0 and ED 1 at the REST[ES] facility, the total normalised area of the decomposition VOCs was higher than their morgue samples except for donors H1, H2, and H4. It is an interesting observation for donors H1, H2 and H4 because their morgue samples were collected between 14-40 h PMI and had a higher total normalised area of decomposition VOCs than their respective ED 0 and ED 1 samples collected between ~18 to 57 h PMI. This difference may be attributed to (i) the differences in the sample collection headspace (body bag vs aluminium hood) and (ii) their period of refrigeration at the morgue and external environmental factors such as temperature. The morgue samples were collected using a body bag which creates a smaller headspace than an aluminium hood allowing better pre-concentration of VOCs. For donor H1, these decomposition VOCs were likely already prevalent in the morgue sample due to the extended PMI of the donor. For donors H2 and H4, these VOCs were potentially better concentrated in the body bags during cooler temperatures, than in the aluminium hood. Perrault et al. (50) tested the suitability of sample collection methods

(sorbent tubes vs SPME) for decomposition VOCs. They reported that sorbent tubes have a better ability to collect a wide range of VOCs, which can provide discriminatory differences in VOC detection compared to the use of SPME. However, the headspace comparison (body bag vs aluminium hood) and its effect on sample pre-concentration has not been studied, highlighting the need for further studies.

The inter-day comparison of samples collected for each donor at the REST[ES] facility showed that samples collected on ED 2 onwards had a higher total normalised area of decomposition VOCs compared to all other experimental days. Towards the end of the trial (ED3, ED 4 and ED 5), visually the overall 'fresh' appearance was passing in the donors, except in the case of donors H3 and H4, who still appeared 'fresh' until the end of the trial (ED 4 and ED 5). The donors H3 and H4 were placed during the autumn season; low temperatures and increased rainfall post-placement caused the decomposition process to progress slower compared to all other donors. In this study, the transition of the odour at the REST[ES] facility was detected after ED 3 (~82 to 100 h) in all donors except H1, H3 and H4, noting that donor H1 was placed when the early post-mortem period was already passing. These results suggest that in an outdoor environment, transition of odour is related to the progression of the decomposition observed through visual changes in the donor.

4.4.2 Relative class concentration (normalised areas) identified in the VOC samples

In this study, the relative class concentration of the donors was tracked to show the evolution of classes in samples collected at the morgue and REST[ES] facility. Tracking their relative class concentration highlights the changes in the early post-mortem odour profile. The relative class concentration changed for each donor from the first sample collected in the morgue to each experimental day sample at the REST[ES] facility after the placement of the donor. Moreover, the class with the highest relative concentration also changed from the first sample collected at the morgue to the ED 0 sample collected at the REST[ES] facility. It is essential to note that two consecutive samples collected at the morgue and REST[ES] facility can have different highest

relative class concentrations. This could be due to differences in the sample collection headspace (body bags vs aluminum hoods). These changes in the relative class concentration show the dynamic nature of the early post-mortem odour profile. It also highlights the fact that the decomposition is not a single event, it is a process which evolves with time and can change hourly and daily. This concords with previously reported studies conducted in morgue and outdoor scenarios, which highlighted this dynamic change in the early post-mortem VOC profile (8, 63, 64).

The linear aliphatic compounds had the highest relative class concentration in six of eight donors (H1, H2, H3, H4, H6 and H9) collected in the morgue. As previously mentioned in chapter 2 (Figure 2-8), the linear aliphatic class also had the highest overall abundance (highest number of VOCs) in morgue samples. Linear aliphatic compounds are one of the by products produced through action of reactive oxygen species (ROS) on macromolecules present in the body (2, 35, 48, 130). This action of ROS in the body is accelerated due to the autolysis of the tissues. Moreover, the donors received in this study suffered from different pathological conditions (133). During any pathological condition, there is an increase in ROS species that causes the oxidative stress on different cellular constituents such as lipids, proteins, and DNA (133). This increase in ROS species during the ante-mortem period can cause the breakdown of lipids leading to higher relative concentrations of classes such as linear aliphatic compounds during the early post-mortem period. Thus, the results explained above indicate that the linear aliphatic compounds can have a strong presence in the early post-mortem odour profile between 14 to 40 h PMI. Prior studies have classified linear aliphatic compounds, aromatics, and cyclic aliphatic compounds all under one class e.g., ‘hydrocarbons’. Hydrocarbons have been reported as one of the most prevalent class of compounds in human decomposition studies (37, 97). Due to the differences in classification across studies, trends in the relative class concentration of the identified linear aliphatic compounds cannot be compared with prior decomposition odour studies conducted on cadavers or human remains. It is recommended that future decomposition studies should adapt and follow one standard classification system that will allow more comprehensive comparison of VOCs and their classes identified in post-mortem odour.

Esters and analogues and alcohols were the other two classes with the highest relative class concentration and higher abundance in morgue donor samples. The identification of esters and analogues has been linked with the breakdown of carbohydrates and with the microbial transformation of acids and alcohols into esterases in the body (34, 35). Moreover, the production of alcohols during the post-mortem period has been linked with (i) the action of ROS species on lipids and carbohydrates, (ii) the fermentation of amino acids such as valine, leucine and isoleucine by the Ehrlich pathway, and (iii) with by-products of anabolic biosynthesis (34). Previously, alcohols have been reported in higher abundance in an outdoor decomposition odour study conducted on cadavers (37). Therefore, the relative class concentration of the linear aliphatic compounds, alcohols, and esters and analogues, and the overall abundance of these classes in the morgue samples suggest these were the key classes identified in the early decomposition period (fresh stage) in the morgue environment.

At the REST[ES] facility, the relative class concentration of the compounds was highly variable for all donors, and was typically reduced on ED 0, ED 1 and ED 2 compared to ED 3, ED 4, and ED 5. As previously mentioned in section 3.6.1, VOC class abundance was also relatively low on ED 0, ED 1 and ED 2. From ED 3 onwards, the relative class concentration and VOC abundance increased, and ED 3 also coincided with the day when the internal ADD of the donors reached the ambient ADD. The lower internal temperature of cadavers as demonstrated by their internal ADD could have affected the enzymatic activity and ultimately the relative class concentration on ED 0, ED 1 and ED 2. The lower relative class concentration can therefore be related to the decomposition progression, which was observed to be slower on ED 0, ED 1 and ED 2 relative to ED 4 and ED 5.

The progression of decomposition was slower in donors H3 and H4 relative to all other donors. Additionally, the relative class concentration showed less variability compared to the rest of the donors (Figures 4-8 and 4-10). In donor H3, classes such as acids and ethers were not identified in the samples collected at the REST[ES] facility. Moreover, sulfur-containing compounds, alcohols and aromatics were not identified after ED 0. In donor H4, overall, the relative class concentrations was reduced at the REST[ES] facility. In these two donors, the progression of

decomposition was slower after their placement at the REST[ES] facility, and the transition from the fresh to the bloat stage was not seen within the duration of the trial for these donors. This confirms that environmental factors such as low temperature and high rainfall observed during their trial could have affected the decomposition process in donors H3 and H4. The relative class concentration also showed less variation across samples from different experimental days in the early post-mortem VOC profile. The effect of colder temperatures on class abundance has been previously reported in the study conducted by Deo et al. (38), where fewer classes of compounds were detected in the donor who experienced colder climates post-placement. Moreover, Deo et al. (38) also reported that the relative class concentration of esters and analogues were identified to be higher compared to other compound classes. These results indicate that in colder climates, esters and analogues might be a significant class of compound during the early post-mortem period. This coincides with our previous finding of their prevalence as a class in the morgue samples. It is evident that cooler temperatures (either in the morgue or outdoors) slows the progression of decomposition and therefore the detection of esters and analogues during the early post-mortem (fresh) stage. Further studies should be conducted on cadavers during colder climates to understand the effects of the temperature on the relative class concentrations identified in the early post-mortem VOC profile.

By ED 4 and ED 5, the donors had advanced in their decomposition stages and could not be considered ‘fresh’ any longer. Generally, nitrogen-containing compounds had the highest relative class concentration on ED 3, ED 4, and ED 5. Nitrogen is one of the most abundant compounds in the body, and it forms the cellular basis of components like amino acids, proteins, and DNA (134). The breakdown of these components through the activity of enzymes and bacterial species during the early post-mortem period can lead to the production of several nitrogen-containing compounds identified in this study. Furthermore, bacteria breakdown the nitrogen-containing compounds to generate energy, and during this process additional nitrogen-containing compounds are generated (134). This implies that during the early post-mortem period when there is a shift in the body’s microbiome from aerobic to anaerobic species, nitrogen-containing compounds can be produced through (i) enzymatic breakdown of

proteins and (ii) bacterial metabolism. These could be the reasons for their higher relative class concentration and abundance during the early post-mortem period.

Acids had the lowest average relative class concentration at the morgue and REST[ES] facility. Acids are typically a prominent class of compounds in the active and advanced stages of decomposition (21). Since the donors in this study were only sampled until the end of the early post-mortem period when the donors were transitioning into the bloat stage, it is therefore not surprising that acids were only found in low abundance.

The analysis of the relative class concentrations showed changes in the early post-mortem VOC profile of the donors from the morgue to the REST[ES] facility. The linear aliphatic compounds, alcohols and esters and analogues were key classes identified when the donor was in the fresh stage of decomposition in the morgue. After the placement of the donor at the REST[ES] facility, the relative class concentration evolved with the progression of the decomposition process. The relative class concentration in VOC profiles shifted, and nitrogen-containing compounds had the highest relative class concentration when the transition from the ante-mortem odour to post-mortem odour was recorded. This suggests that compound classes such as nitrogen-containing compounds can be associated with the change in the decomposition stage (early post-mortem to the beginning of the bloat stage).

4.4.3 Principal Component Analysis

The PCA results show the comparisons of the samples collected at the morgue and REST[ES] facility for the individual donors. In this analysis, samples which showed the most variance were separated; thus, enabling us to identify key VOCs that contributed towards the variance and separation of the samples collected at the morgue and REST[ES] facility.

The PCA scores plot constructed for individual donors (Figures 4-19 to 4-25) showed that the morgue samples were variable from the REST[ES] samples either along PC-1 or PC-2 (the first two principal components explaining the highest variance). Generally, the samples collected on

ED 3, ED 4, and ED 5 at the REST[ES] facility showed variance and were separated along PCs, while samples collected on ED 1 and ED 2 were grouped closely and did not contribute significantly to the overall explained variance. Thus, the morgue samples, ED 3, ED 4, and ED 5 samples, were the most variable in PCAs constructed for individual donors. On ED 0, donors were in the fresh stage of decomposition, which explains the reason for its separation from all other samples collected at the REST[ES] facility. The separation of ED 3, ED 4 and ED 5 samples highlights the continuous nature of the decomposition process which starts immediately after death. It is interesting to note that even though the morgue and ED 0 samples were collected only a few hours apart (less than 6 hours for most donors), they still showed major variability in PCAs. This variability in the morgue and ED 0 samples originating from the same donor was also evident in the variable relative class concentration. This variability between morgue and ED 0 samples can be attributed to the difference in the sample collection headspace (body bag vs aluminum hood).

In the PCA loadings plot for individual donors, benzyl alcohol, 1-propoxy-2-propanol (2-propanol, 1-propoxy), 2-pentylfuran (furan, 2-pentyl), 6-methyl-5-hepten-2-one (5-Hepten-2-one, 6-methyl) and 2,2,2-trifluroethanol (ethanol, 2,2,2-trifluro) and butyl acetate (acetic acid, butyl ester) were responsible for causing separation of the morgue samples H2_M, H3_M, H4_M, H6_M, H7_M, H8_M and H9_M, respectively (Table 4-1). Benzyl alcohol has been previously detected in blood samples and the presence of benzyl alcohol in the human body has also been linked with the metabolism of toluene via hydroxylation by cytochrome PC450 (2). 6-methyl-5-hepten-2-one (5-Hepten-2-one, 6-methyl) is an ante-mortem VOC and has been reported in (95). 2,2,2-trifluroethanol (ethanol, 2,2,2-trifluro) and 1-propoxy-2-propanol (2-propanol,1-propoxy) has not been previously reported in the literature as a decomposition VOC. The identification of VOCs that have not been previously reported in the headspace of cadavers, highlights the need for a database of VOCs identified from human remains, which can assist future studies in comparing the results.

For samples collected at the REST[ES] facility, the spread of samples varied in the scores plot highlighting the inter-day variation seen in the early post-mortem VOC profiles; thus, the PCA of the individual donors have been discussed separately below.

For donor H2, the ED 0 and ED 3 showed the highest separation amongst the samples collected at the REST[ES] facility along PC-2 (17% explained variance) (Figure 4-19a). The separation of the ED 0 sample from the sample H2 ED 3 suggests that the VOC profile of donor H2 started changing after their placement at the REST[ES] facility on ED 0 (~48 h PMI). Phenol caused the separation of ED 0 from all other samples (Figure 4-19b). Alcohols had the highest relative class concentration in the ED 0 sample which likely included phenol. Phenol is a decomposition-related VOC produced due to microbial activity (34). The VOC profile on ED 3 changed causing it to separate from all other samples collected at the REST[ES] facility. Additionally, on ED 3, donor H2 progressed to the beginning of the bloat stage and his forearms showed signs of active decay, thus confirming the variation in the VOC profile on this day. DMDS and DMTS are two of the most reported decomposition VOCs during the bloat and active decay stage (6, 8, 37, 43, 97), and caused the separation of the ED 3 sample. The PCA results of donor H2 suggest that the change in the VOC profile began after ED 0 due to dominance of decomposition-related VOCs such as phenol. Moreover, the transition of ante-mortem odour to post-mortem odour occurred after ED 3 due to dominance of decomposition-related VOCs such as DMDS. This was further confirmed through visual observations of the beginning of the bloat stage.

For donor H3, the ED 0 sample was separated along PC-1 (79% explained variance) (Figure 4-20a). Acetaldehyde, an aldehyde class of compound caused the separation of the ED 0 sample from all other samples collected at the REST[ES] facility (Figure 4-20b). The formation of acetaldehyde has been linked with ethanol metabolism and lipid peroxidation during the ante-mortem period (6). Thus, for donor H3, the presence of acetaldehyde, a known ante-mortem VOC, during the post-mortem period highlights the pervasive nature of ante-mortem VOCs and can be associated with the change in the VOC profile on ED 0. No other decomposition VOC contributed to variability of any of the samples in this PCA. This was evident from the fact that the majority of the remaining samples, including the morgue sample, ED 3 and ED 4 samples

were clustered together around the origin of the X and Y axis. Visually, the progression of decomposition was slow and distinct decomposition-related changes such as greenish discolouration were only observed on the last day (ED 4) of the trial. This slow progression can be attributed to the low temperature and high rainfall conditions observed during the trial. The PCA results suggest that the VOC profile of donor H3 changed after ED 0 but no distinct transition to post-mortem odour was observed on ED 4, unlike the summer donor (donor H2) previously discussed.

For donor H4, the PCA showed that the ED 0 sample separated along PC-2 (8% explained variance) from the remaining two samples collected at the REST[ES] facility on ED 1 and ED 3 (Figure 4-21a). The dominance of methyl acetate (acetic acid, methyl ester) in the ED 0 sample caused the variance in this sample (Figure 4-22b). The presence of methyl acetate (acetic acid, methyl ester) in the post-mortem odour profile is linked with the breakdown of carbohydrates and fats (9). For ED 1 and ED 3 samples, diethyl fumarate, an ester compound class, has not been previously reported as an ante-mortem or post-mortem VOC. Esters such as diethyl fumarate could be released due to the breakdown of carbohydrates. Overall, in donor H4, the VOC abundance on ED1 and ED 3 was low. Further, the VOCs associated with their corresponding loadings plot were closely clustered around the origin of the X and Y axis, suggesting that the VOC profiles on these experimental days showed minimal variation after the placement of the donor H4 (Figure 4-21b). Moreover, the absence of decomposition patterns, such as greenish discolouration, suggested that the progression of decomposition was slow at the REST[ES] facility due to low temperatures and increased rainfall. Therefore, the PCA results of donor H4 suggest that, like donor H3, the VOC profile of donor H4 changed after ED 0, but unlike the summer donor (donor H2), no distinct transition to post-mortem odour was observed on ED 4.

For donor H6, the PCA showed that the ED 3 and ED 4 samples were the most variable from all other samples collected at the REST[ES] facility along PC-1 (64% explained variance) (Figure 4-22a). Formaldehyde was responsible for causing the separation of the ED3, ED 4 and ED 5 samples (Figure 4-22b). Formaldehyde was recently reported in a study that simulated a mass

disaster scenario in Australia using cadavers (3). This compound has been associated with the VOC profile of cadavers. Furthermore, on ED 4 the greenish discolouration progressed to other regions of the body such as the thighs, calf, and ankle indicating an increase in putrefaction and progression towards the bloat stage. Thus, the PCA results for donor H6 suggest that the transition to post-mortem odour occurred due to a dominance of decomposition-related VOCs such as formaldehyde after ED 3. This was further confirmed through visual observations of green discolouration on donor H6.

For donor H7, PCA showed that samples ED 0 and ED 4 formed a cluster around the origin of the X and Y axis (Figure 4-23a). The samples H7_M and ED 5 were separated along PC-2 (22% explained variance) and ED 1 and ED 2 samples were separated from this cluster along PC-1 (42% explained variance). The separation of the ED 0 sample can be attributed to the 'fresh' appearance of donor H7. From ED 1 onwards, an increase in the insect activity was observed, implying the presence of decomposition VOCs in the odour profile of the donor H7. This observation suggests the VOC profile changed after ED 0 and supports the theory that during the post-mortem period, insects (carrion flies) can trace decomposition VOCs to the source (donor H7). VOCs such as bromodichloromethane (methane, bromodichloro) and propan-2-ol (isopropyl alcohol) have been linked with microbial activity during the post-mortem period (135). Further, the association of these VOCs with the ED 1 and ED 2 samples supports the fact that the decomposition process is driven microbial and entomological activity. In the ED 5 sample, allylbenzene (benzene, 2-propenyl) has not previously been reported as a decomposition VOC. The identification of benzene derivatives have been linked to oxygen free radicals and these radicals may be responsible for the development of these compounds. Furthermore, microbial modification of various base compounds is believed to create substituted benzene compounds (8, 97, 131). Apart from the changed VOC profile on ED 5, visually high decomposition activity was recorded on the donor with skin slippage on the face. Thus, the PCA results for donor H7 suggest that the change in the VOC profile began after ED 0 due to an increase in insect activity and the transition of the ante-mortem to post-mortem odour occurred after ED 4 due to a dominance of decomposition VOCs such as allylbenzene

(benzene 2 propenyl). This was further confirmed through visual observations such as skin slippage and high insect activity.

For donor H8, the PCA showed that the morgue sample along with ED 0, ED 1, ED 3 and ED 5 samples were separated along PC-2 (Figure 4-24a). The ED 4 sample contributed to the majority of the variance along PC-1 (85% explained variance), while the ED 5 sample was separated along PC-2 (8% explained variance). These samples (ED 4 and ED 5) showed the most variability compared to all other samples due to the dominance of ethanol on ED 4 day and methylamine, N,N-dimethyl on ED 5 (Figure 4-24b). As previously discussed in this section, methylamine N,N-dimethyl is linked with breakdown of proteins and amino acids and ethanol is associated with the breakdown of carbohydrates by bacteria (34, 136). Ethanol identification in the H8 ED 4 sample could be associated with the decomposition process as opposed to its commercial use on donor H8, as any surface application of ethanol before placement of the body at the REST[ES] facility would have dissipated from the body due to the highly volatile nature of ethanol. Additionally, visual observations showed that on ED 4 and ED 5, the donor progressed to the bloat stage and decomposition patterns such as venous marbling were spreading to the upper limbs. Thus, the PCA results for donor H8 suggest that the change in the odour profile and transition of the ante-mortem to post-mortem odour in donor H8 began after ED 3 due to the dominance of decomposition-related VOCs such as ethanol and methylamine, N,N-dimethyl. This transition was further confirmed through visual observation of the beginning of the bloat stage.

For donor H9, the PCA showed that the H9_M sample collected at the REST[ES] facility contributed to the majority of the variance as it was separated along PC 1 (46% explained variance) (Figure 4-25a). 3-methylbutanal (butanal, 3-methyl) an ante-mortem VOC, caused separation of the H9_M sample. The H9_M morgue sample was collected at PMI 16hrs, and the presence of an ante-mortem VOC such as 3-methylbutanal (butanal,3-methyl) highlights the pervasive nature of ante-mortem VOCs during the early post-mortem period (Figure 4-25b). The H9 ED 3 and H9 ED 4 samples were slightly separated from the H9 ED 1 and H9 ED 2 samples indicating some degree of variability in these samples. The first signs of autolysis and

putrefaction were seen on ED 3 indicating a change in the VOC profile began after ED 3. The sample H9 ED 5 was separated from all other samples collected at the REST[ES] facility. 1,2-diethylbenzene (benzene 1,2 diethyl) is a decomposition related VOC. As previously discussed in this section, benzene derivatives such as 1,2-diethylbenzene (benzene 1,2 diethyl) is associated with microbial modification of various base compounds. Decomposition VOCs such as DMDS, 2-methyl-1-butanol (1-butanol,2-methyl) caused the separation of the H9 ED 5 sample. Additionally, on ED 5, the donor H9 showed signs of bloating on the neck and the greenish discolouration progressed to the upper limbs. The PCA results of donor H9 suggest that after ED 3, a change in the VOC profile began, which can be linked with microbial activity due to the identification of 1,2-diethyl-benzene (benzene 1,2-diethyl) (a decomposition VOC) and observations of visual features indicating autolysis and decomposition. Moreover, the transition of ante-mortem odour to post-mortem odour occurred on ED 5 due to the presence of decomposition-related VOCs such as DMDS and 2-methyl-1-butanol (1-butanol, 2-methyl). This transition in odour was further confirmed through visual observation of the increase in the bloat around the neck and progression of greenish discolouration.

In summary, the PCA scores plot of individual donors highlighted the changes in the VOC profiles collected at the morgue and REST[ES] facility. The separation of morgue samples from the ones collected at the REST[ES] facility can be attributed to the differences in the headspace of the samples (body bag vs aluminium hood). The separation of ED 1, ED 2, and ED 3 samples from the morgue and ED 0 samples indicated the change in the VOC profiles after the placement of the donors at the REST[ES] facility. The ED 4 and ED 5 samples represented the last experimental day of the trial for donors. The separation of ED 4 and ED 5 samples in donors (H2, H6, H7, H8 and H9) was associated with decomposition-related VOCs and visual observation (beginning of the bloat stage). PCA also highlighted minimal changes in the VOC profiles of H3 and H4, which did not show a transition to post-mortem odour due to the colder temperature and high rainfall recorded during the trials. Therefore, PCA of individual donors demonstrated the change in the odour profile after ED 0 (~18 to 57 h post-placement of the body at the REST[ES] facility) and the transition of the ante-mortem to post-mortem odour in donors H2, H6, H7, H8 and H9 identified after ED 3 (~82 to 100 h).

4.5 Limitations

The effect of sample collection headspace on the VOC profiles collected in two different environments (morgue and REST[ES] facility) could not be studied due to the experimental design of this study. The environment in which the remains have been deposited affects the progression of decomposition. An indoor environment such as a morgue is a controlled environment whereby the external factors such as temperature and humidity are maintained at a certain setpoint. Moreover, other factors such as entomology were absent in a controlled environment such as the morgue. The decomposition process in these environments is mostly driven by microbial processes. These factors can influence the VOC profiles released from the donors. The donors were only sampled once at the morgue and multiple times at the REST[ES] facility. This limited the comparison of the VOC and class abundance for an individual donor in two different environments as the decomposition progressed.

The transition of odour was not identified in donors placed in the autumn season. The donors placed during this season progressed slowly and the transition of the ante-mortem to post-mortem odour was not seen during the 2020 trial. The experimental design was modified to encompass the seasonal variation, but the application of this modified experimental design was limited to the spring and summer seasons of 2021 due to the availability of donors. Thus, future studies should be conducted in colder temperatures with the modified experimental design to determine the transition of the early post-mortem VOC profiles during the autumn season.

4.6 Conclusion

The presence of the ante-mortem odour and its transition to post-mortem odour was investigated by comparing VOCs collected in two different environments (morgue and REST[ES] facility) during the early post-mortem period. Twenty seven ante-mortem VOCs and 54 decomposition VOCs previously reported in the literature were common VOCs detected in the current study. The relative class concentration of the VOCs was calculated to monitor the

changes in the VOC profiles at the morgue and REST[ES] facility for the entire trial duration. Although the relative concentration of ante-mortem VOCs varied; generally, their concentration was lower in individual donor samples collected at the morgue and REST[ES] facility. The presence of previously reported decomposition VOCs in the samples collected at the morgue highlighted that decomposition-related VOCs can be identified as early as 14-40 h after death. Tracking the relative class concentration of the donors from the morgue to the REST[ES] facility highlighted the dynamic nature of the early post-mortem VOC profile. The linear aliphatic compounds, esters and analogues and alcohols were identified as key compound classes in the samples collected at the morgue, while the nitrogen-containing classes were identified as the key classes at the REST[ES] facility. PCA analysis separated the morgue samples and samples collected at the REST[ES] facility and suggested the transition of the ante-mortem to post-mortem odour after ED 3 post-placement of the body at the REST[ES] facility. Comparisons between the morgue and REST[ES] facility samples were limited due to their differences in the headspace sample collection technique.

Chapter 5: Conclusion and Future Work

5.1 Conclusion

VOCs released from the decomposition of human remains evolve as the body progresses through the various stages of decomposition. To date, decomposition odour research has extensively focused on the VOC profile released from cadavers or human remains during the overall decomposition process. However, it has been reported that the VOC profile during the early post-mortem period is dynamic and can contain remnants of an individual's ante-mortem odour (63). The early post-mortem VOC profile from human remains has rarely been studied in the literature. This thesis aimed to study the early post-mortem VOC profile and identify the transition of odour from ante-mortem odour to post-mortem odour. This was achieved by developing an optimised method for the VOC sample collection and analysis. The analytical methods developed led to the characterisation of the early post-mortem VOC profile and identification of VOCs released during this period.

In chapter 2, VOC sample collection and TD-GC×GC-TOFMS methods were optimised using VOC samples collected from donors received at the UQTR morgue. The parameters which reduced chromatographic coelution were selected for the final optimised method. The final optimised sampling and analytical method were applied to eight donors sampled in the morgue. The data processing workflow and optimised method identified VOCs previously reported in post-mortem odour collected in indoor and outdoor environments. The VOC and class abundance varied for each donor sampled at different PMI intervals. A total of 104 compounds were detected to be the most prevalent in all VOC profiles. Within these 104 compounds, VOCs related to ante-mortem (n=8) and decomposition odour (n=21) were detected, highlighting the challenge of characterising the early post-mortem VOC profile. The presence of decomposition-related VOCs indicated that although their abundance was low, the optimised method identified the VOCs related to post-mortem odour. Thus, these results suggested that the decomposition process starts immediately after death and VOCs related to post-mortem odour

can be identified between 14-40 h PMI with the optimised method. Identifying VOCs related to medication and biomarkers related to donor pathologies, highlighted the potential of TD-GC×GC-TOFMS as a non-destructive technique for screening of drugs and toxins relevant to forensic toxicology. The separation of donors in the scores plot assisted in visualising the differences in their VOC profiles collected in the same environment. The identification of decomposition-related VOCs through headspace sampling of body bags containing cadavers led to the further application of this method to identify the VOCs released from cadavers in an outdoor environment.

In chapter 3, the optimised method was applied to investigate the VOC profiles from cadavers in an outdoor environment during the early post-mortem period. Moreover, the VOC profiles were studied over different seasons, namely spring, summer, and autumn. The intra-day variation was studied to identify the transition of the odour from the peri-mortem to post-mortem odour of a cadaver in an outdoor environment. Monitoring and documenting the decomposition progression of individual donors helped to broaden our understanding of the decomposition process during the early post-mortem period in an outdoor environment. The decomposition patterns indicating autolysis and putrefaction (greenish discolouration and venous marbling) were observed in most donors except donors H4 (autumn season) and H7 (summer season). The absence of these patterns highlighted the impact of external (temperature, rainfall) and internal factors (donor physiology) on the decomposition process during the early post-mortem period. The variation in VOC and class abundance highlighted the inter-day variability in early post-mortem odour profiles of individual donors. In the ED 1 to ED 3 samples, the VOC and class abundance were relatively low. On ED 4 and ED 5 of the summer and spring trials, decomposition activity with the beginning of the bloat stage was observed on all donors. The nitrogen-containing compounds were detected in higher abundance than other compound classes at this time. This showed a detectable change in VOC profile after ED 3 in the donors when the early post-mortem period was passing. The detectable change in VOC and class abundance was not detected in the donors placed during the autumn season. During this season, the relatively low temperature and higher rainfall affected the VOC and class abundance, highlighting the need for further studies during the autumn season. Inter-seasonal

variability was also identified as donors placed during the same season showed differences in the VOC and class abundance. The relatively higher rainfall during the 2020 trial influenced the VOC profile. Therefore, further studies are needed to replicate these trends and study the effect of a colder environment and rainfall on the early post-mortem VOC profile. The PCA of donors H2, H6, H7, H8 and H9 aided in visualising the intra-day variation through the spread of ED 0, ED 1, ED 2, and ED 3 samples away from ED 4 and ED 5 samples in the scores plot. The separation of samples in the scores plot indicated the shift in VOC profiles after ED 3. The corresponding loadings highlighted that VOCs belonging to compound classes such as alcohols, ketones, esters and analogues, and nitrogen-containing compounds caused the separation of ED 4 and ED 5 samples. The association of these classes with the separation of ED 4 and ED 5 samples suggests that these are relevant compound classes during the early post-mortem period. The collection of VOCs at the morgue and outdoor environment for the same donors enabled the comparison of the VOC profiles.

Chapter 4 of the thesis aimed to compare the VOCs collected at the morgue and REST[ES] facility to identify the transition of the odour and track the evolution of the VOC profiles during the early post-mortem period. A dataset was built from the VOCs identified in the VOC profiles collected at the morgue and REST[ES] facility. The VOCs previously reported in the literature as being of ante-mortem and decomposition origin were identified in the dataset, and their total normalised area was tracked across all the samples collected at the morgue and REST[ES] facility. Additionally, VOCs in the dataset were classified into their compound classes, and their relative class abundance was tracked across samples collected at the morgue and REST[ES] facility for all donors. Generally, for samples collected at the morgue, the relative concentration of decomposition VOCs was higher that ante-mortem VOCs, while at the REST[ES] facility a higher relative concentration of decomposition VOCs was identified after ED 3 This suggested that in an outdoor environment, the VOC profile resembled the post-mortem odour after 72 h post-placement of the donor. The relative class concentration of the odour profiles highlighted that the linear aliphatic compounds and alcohols were the key compound classes at the morgue. In contrast, the nitrogen-containing compounds and esters and analogues were the most prevalent classes at the REST[ES] facility. Nitrogen-containing compounds were also the

most abundant when the early post-mortem (fresh) stage was transitioning into the bloat stage, indicating that nitrogen-containing compounds can be associated with the change in the decomposition stage. However, these trends in the early post-mortem period represent the summer and spring seasons of Quebec, and further studies need to be conducted in an outdoor environment to study the trends in the early post-mortem VOC profile in other seasons and geographic climates.

In conclusion, the studies performed in this thesis have characterised the early post-mortem VOC profile, a critical part of decomposition odour research. The experimental and analytical methods presented in this thesis shed light on the dynamic nature of the early post-mortem VOC and highlight its transitions to post-mortem odour. The presented research undoubtedly lays a foundation for future studies that could address the lack of research on cadavers during the early post-mortem period. However, early post-mortem odour research is still a new area within decomposition VOC research, and future studies should build upon our understanding of the early post-mortem odour in indoor and outdoor environments, as detailed further below.

5.2 Future Work

The headspace analysis of human remains in a controlled morgue environment provided baseline information of the early post-mortem VOC profiles. VOCs related to the decomposition process and medications taken by the donor were identified through this sample collection technique in the morgue. Moreover, VOCs related to the post-mortem odour were detected in the VOC profiles of two or more donors, highlighting the potential for identifying biomarkers that might be consistently present in the headspace of the human remains. Increasing the number of donors and collecting VOC samples at different PMI intervals in future studies will assist in further characterisation of the VOC profiles released from cadavers immediately after death. Refrigeration of the cadavers after death can be part of the hospital or morgue protocol for storing cadavers before transferring them to the respective facility. It was suggested in the morgue study that refrigeration can have an impact on VOC abundance. The duration of refrigeration and its effects on the VOC abundance of the cadavers should be further

investigated to understand the influence of storage conditions on the early post-mortem VOC profile.

Furthermore, identifying VOCs related to medications highlighted the potential of the headspace sample collection technique coupled with TD-GC×GC-TOFMS. The forensic pathologist can use this sample collection technique as an auxiliary non-destructive approach and potentially expand its application in determining drug metabolites and toxicology substances. Developing body bags with specialised attachments for sorbent tubes will facilitate sample collection from human remains. The design for the sorbent tube attachment can be similar to the one used in Tedlar bags. The Tedlar bags are currently applied to collect breath samples. The modified designs of body bags would allow further adoption of this technique in an inexperienced user base.

In this study, the sampling trial was modified in 2021 to encompass the entire duration of the early post-mortem period and identify the transition of ante-mortem odour to post-mortem odour in an outdoor environment. The modified sample collection period was not tested in autumn 2021 due to the unavailability of donors. Application or further modification of the 2021 sample collection method could assist in determining the transition of odour during colder seasons. Furthermore, future studies should modify the sample collection apparatus such as the aluminium hood to improve the pre-concentration of VOCs above the headspace of cadavers in colder environments. The aluminium hood is a commonly used apparatus in outdoor studies to create headspace and accumulate the VOCs released from the cadavers. In this study, the height of the aluminium hood was slightly modified to suit the VOC sample collection during the early post-mortem period. This modification in the aluminium hood assisted with the pre-concentration of VOCs released from cadavers during the summer and spring seasons. Future studies should compare VOC profiles collected through different sizes of aluminium hoods. Testing different sizes of aluminium hoods will help to determine the size that creates a concentrated headspace for studying VOCs during colder temperatures.

TD-GC×GC-TOFMS has become one of the most commonly used techniques to analyse complex decomposition odour. This technique has aided in the identification of several compound classes such as alcohols, ketones, aldehydes, and others at various decomposition stages (e.g., fresh, bloat, etc.). With the advancement in data analysing techniques and new software, it becomes critical that future studies adopt a specific standard for the classification of compound classes identified in the cadavers. Adopting a specific compound class classification system would allow for better comparisons of trends between studies that are profiling post-mortem odour.

Overall, the current study has provided a foundation for understanding the VOC profile of human remains during the early post-mortem period. With future advancements in experimental design, method standardisation and data interpretation, it is possible that the transition from ante-mortem to post-mortem odour can be more clearly elucidated for specific climates and seasons. Such research will contribute to determining the optimal use of SAR and HRD dogs when searching for recently deceased persons in outdoor environments.

References

1. Curran AM, Rabin SI, Prada PA, Furton KG. Comparison of the volatile organic compounds present in human odour using SPME-GC/MS. Journal of Chemical Ecology. 2005 2005/07/01;31(7):1607-19.

2. Drabińska N, Flynn C, Ratcliffe N, Belluomo I, Myridakis A, Gould O, et al. A literature survey of all volatiles from healthy human breath and bodily fluids: the human volatilome. Journal of Breath Research. 2021 2021/04/21;15(3):034001.

3. Mochalski P, Unterkofler K, Teschl G, Amann A. Potential of volatile organic compounds as markers of entrapped humans for use in urban search-and-rescue operations. TrAC Trends in Analytical Chemistry. 2015 2015/05/01/;68:88-106.

4. Agapiou A, Amann A, Mochalski P, Statheropoulos M, Thomas CLP. Trace detection of endogenous human volatile organic compounds for search, rescue and emergency applications. TrAC Trends in Analytical Chemistry. 2015 2015/03/01/;66:158-75.

5. DeGreeff LE, Weakley-Jones B, Furton KG. Creation of training aids for human remains detection canines utilizing a non-contact, dynamic airflow volatile concentration technique. Forensic Science International. 2012 2012/04/10/;217(1):32-8.

6. Statheropoulos M, Agapiou A, Spiliopoulou C, Pallis GC, Sianos E. Environmental aspects of VOCs evolved in the early stages of human decomposition. Science of The Total Environment. 2007 2007/10/15/;385(1):221-7.

7. Ueland M, Harris S, Forbes SL. Detecting volatile organic compounds to locate human remains in a simulated collapsed building. Forensic Science International. 2021 2021/06/01/;323:110781.

8. Statheropoulos M, Spiliopoulou C, Agapiou A. A study of volatile organic compounds evolved from the decaying human body. Forensic Science International. 2005 2005/10/29/;153(2):147-55.

9. Allison PA, Bottjer DJ. Taphonomy: Bias and Process Through Time. Taphonomy: Process and bias through time. Dordrecht: Springer Netherlands; 2011;1-17.

10. Sorg M, Haglund W. Advancing forensic taphonomy: purpose, theory, and process. Advances in forensic taphonomy: Method, theory, and archaeological perspectives. 2002:4-29.

11. Haglund WD, Sorg MH. Advances in forensic taphonomy: Method, theory, and archaeological perspectives: CRC Press, 2001.

12. Schotsmans EMJ, Márquez-Grant N, Forbes SL. Introduction. Taphonomy of human remains: forensic analysis of the dead and the depositional environment; 2017;1-8.

13. Collis S, Johnson CP. The decomposed cadaver. Diagnostic Histopathology. 2019 2019/11/01/;25(11):431-5.

14. Lee Goff M. Early post-mortem changes and stages of decomposition in exposed cadavers. Experimental and Applied Acarology. 2009 2009/10/01;49(1):21-36.

15. Forbes SL, Perrault KA, Comstock JL. Microscopic post-mortem changes: The chemistry of decomposition. Taphonomy of human remains:Forensic analysis of the dead and the depositional environment; 2017;26-38.

16. Nizio KD, Ueland M, Stuart BH, Forbes SL. The analysis of textiles associated with decomposing remains as a natural training aid for cadaver-detection dogs. Forensic Chemistry. 2017 2017/09/01/;5:33-45.

17. Vass AA. Beyond the grave-understanding human decomposition. Microbiology today. 2001;28:190-3.

18. Campobasso CP, Di Vella G, Introna F. Factors affecting decomposition and diptera colonization. Forensic Science International. 2001 2001/08/15/;120(1):18-27.

19. Damann FE, Carter DO. Human decomposition ecology and postmortem microbiology. Manual of forensic taphonomy. 2013:37-49.

20. Forbes SL, Stuart BH, Dent BB. The identification of adipocere in grave soils. Forensic Science International. 2002 2002/07/17/;127(3):225-30.

21. Meyer J, Anderson B, Carter DO. Seasonal variation of carcass decomposition and gravesoil chemistry in a cold (Dfa) climate. Journal of Forensic Sciences. 2013;58(5):1175-82.

22. Blau S, Forbes S. Anthropology:Taphonomy in the forensic context. In: Payne-James J, Byard RW, editors. Encyclopedia of Forensic and Legal Medicine (Second Edition). Oxford: Elsevier; 2016;227-35.

23. Tsokos M. Forensic Pathology Reviews Vol 4: Springer, 2007.

24. Carter DO, Yellowlees D, Tibbett M. Cadaver decomposition in terrestrial ecosystems. Naturwissenschaften. 2007;94(1):12-24.

25. Janaway RC, Percival SL, Wilson AS. Decomposition of human remains. Microbiology and aging: Springer; 2009;313-34.

26. Forbes SL, Perrault KA, Comstock JL. Microscopic Post-Mortem Changes: the Chemistry of Decomposition. Taphonomy of Human Remains: Forensic Analysis of the Dead and the Depositional Environment; 2017;26-38.

27. Stuart B. Decomposition chemistry: overview, analysis, and interpretation. Encyclopedia of Forensic Sciences: Academic Press; 2013;11-5.

28. Knight B. Forensic pathology: Oxford University Press, USA, 1991.

29. Dent BB, Forbes SL, Stuart BH. Review of human decomposition processes in soil. Environmental Geology. 2004;45(4):576-85.

30. Clark MA, Worrell MB, Pless JE. Postmortem changes in soft tissues. Forensic taphonomy: the postmortem fate of human remains. 1997:151-64.

31. Gill-King H. Chemical and ultrastructural aspects of decomposition. In: Haglund WD, Sorg MH, editors. Forensic taphonomy: the postmortem fate of human remains: CRC Press: Boca Raton; 1997;93-108.

32. Dekeirsschieter J, Verheggen FJ, Gohy M, Hubrecht F, Bourguignon L, Lognay G, et al. Cadaveric volatile organic compounds released by decaying pig carcasses (Sus domesticus L.) in different biotopes. Forensic Science International. 2009 2009/08/10/;189(1):46-53.

33. Bray GA. Handbook of Obesity--Volume 1: Epidemiology, Etiology, and Physiopathology: CRC Press, 2014.

34. Boumba VA, Ziavrou KS, Vougiouklakis T. Biochemical pathways generating post-mortem volatile compounds co-detected during forensic ethanol analyses. Forensic Science International. 2008 2008/01/30/;174(2):133-51.

35. Paczkowski S, Schütz S. Post-mortem volatiles of vertebrate tissuea. Applied Microbiology and Biotechnology. 2011;91(4):917-35.

36. Dubois L, Perrault K, Stefanuto P-H, Focant J-F. Enhanced chemical profiling of human decomposition in a case study. Forensic Science International. 2017;277:15.

37. Knobel Z, Ueland M, Nizio KD, Patel D, Forbes SL. A comparison of human and pig decomposition rates and odour profiles in an Australian environment. Australian Journal of Forensic Sciences. 2019 2019/09/03;51(5):557-72.

38. Deo A, Forbes SL, Stuart BH, Ueland M. Profiling the seasonal variability of decomposition odour from human remains in a temperate Australian environment. Australian Journal of Forensic Sciences. 2020 2020/11/01;52(6):654-64.

39. Vass AA. Death is in the air: Confirmation of decomposition without a corpse. Forensic Science International. 2019 2019/08/01/;301:149-59.

40. Baynes JW, Dominiczak MH. Medical Biochemistry E-Book: Elsevier Health Sciences, 2014.

41. Archer MS. Rainfall and temperature effects on the decomposition rate of exposed neonatal remains. Science & Justice: Journal of the Forensic Science Society. 2004 2004 Jan-Mar;44(1):35-41.

42. Zhou C, Byard RW. Factors and processes causing accelerated decomposition in human cadavers–an overview. Journal of forensic and legal medicine. 2011;18(1):6-9.

43. Forbes SL, Perrault KA, Stefanuto P-H, Nizio KD, Focant J-F. Comparison of the decomposition VOC profile during winter and summer in a moist, mid-latitude (Cfb) climate. PLOS ONE. 2014;9(11):e113681.

44. Blau S, Forbes S. Anthropology: Taphonomy in the Forensic Context. In: Payne-James J, Byard RW, editors. Encyclopedia of Forensic and Legal Medicine (Second Edition). Oxford: Elsevier; 2016;227-35.

45. Giles SB, Harrison K, Errickson D, Márquez-Grant N. The effect of seasonality on the application of accumulated degree-days to estimate the early post-mortem interval. Forensic Science International. 2020;315.

46. Archer MS. Rainfall and temperature effects on the decomposition rate of exposed neonatal remains. Science & justice : journal of the Forensic Science Society. 2004 2004 Jan-Mar;44(1):35-41.

47. Stefanuto PH, Rosier E, Tytgat J, Focant JF, Cuypers E. Profiling volatile organic compounds of decomposition. Taphonomy of human remains:Forensic analysis of the dead and the depositional environment:Forensic analysis of the dead and the depositional environment. 2017:39-52.

48. DeGreeff LE, Furton KG. Collection and identification of human remains volatiles by non-contact, dynamic airflow sampling and SPME-GC/MS using various sorbent materials. Analytical and Bioanalytical Chemistry. 2011 2011/09/01;401(4):1295-307.

49. Rust L, Nizio KD, Forbes SL. The influence of ageing and surface type on the odour profile of blood-detection dog training aids. Analytical and Bioanalytical Chemistry. 2016 2016/09/01;408(23):6349-60.

50. Perrault KA, Stuart BH, Forbes SL. A longitudinal study of decomposition odour in soil using sorbent tubes and solid phase microextraction. Chromatography. 2014;1(3):120-40.

51. Jinno K, De Pauw E, Porschmann J, Vaes W, Deng Z, Paschke A, et al. Applications of Solid Phase Microextraction. Cambridge, UNITED KINGDOM: Royal Society of Chemistry, 1999.

52. Hoffman EM, Curran AM, Dulgerian N, Stockham RA, Eckenrode BA. Characterization of the volatile organic compounds present in the headspace of decomposing human remains. Forensic Science International. 2009;186(1-3):6-13.

53. Dewulf J, Van Langenhove H, Wittmann G. Analysis of volatile organic compounds using gas chromatography. TrAC Trends in Analytical Chemistry. 2002 2002/09/10/;21(9):637-46.

54. Terzic O, Swahn I, Cretu G, Palit M, Mallard G. Gas chromatography–full scan mass spectrometry determination of traces of chemical warfare agents and their impurities in air samples by inlet based thermal desorption of sorbent tubes. Journal of Chromatography A. 2012 2012/02/17/;1225:182-92.

55. Ras MR, Borrull F, Marcé RM. Sampling and preconcentration techniques for determination of volatile organic compounds in air samples. TrAC Trends in Analytical Chemistry. 2009 2009/03/01/;28(3):347-61.

56. Allen NDC, Brewer PJ, Brown RJC, Lipscombe RP, Woods PT. International comparison of key volatile organic components in indoor air. Measurement. 2016 2016/03/01/;82:476-81.

57. Xu J, Chen G, Huang S, Qiu J, Jiang R, Zhu F, et al. Application of in vivo solid-phase microextraction in environmental analysis. TrAC Trends in Analytical Chemistry. 2016 2016/12/01/;85:26-35.

58. Dekeirsschieter J, Stefanuto P-H, Brasseur C, Haubruge E, Focant J-F. Enhanced Characterization of the Smell of Death by Comprehensive Two-Dimensional Gas Chromatography-Time-of-Flight Mass Spectrometry (GCxGC-TOFMS). PLOS ONE. 2012;7(6):e39005.

59. Liberto E, Bicchi C, Cagliero C, Cordero C, Rubiolo P, Sgorbini B. Chapter 1 Headspace Sampling: An “Evergreen” Method in Constant Evolution to Characterize Food Flavors through their Volatile Fraction. Advanced Gas Chromatography in Food Analysis: The Royal Society of Chemistry; 2020;1-37.

60. Wenzl T, Lankmayr E. Comparative studies of the static and dynamic headspace extraction of saturated short chain aldehydes from cellulose-based packaging materials. Analytical and Bioanalytical Chemistry. 2002 2002/03/01;372(5):649-53.

61. Curvers J, Noy T, Cramers C, Rijks J. Possibilities and limitations of dynamic headspace sampling as a pre-concentration technique for trace analysis of organics by capillary gas chromatography. Journal of Chromatography A. 1984 1984/04/27/;289:171-82.

62. Stadler S, Stefanuto P-H, Byer JD, Brokl M, Forbes S, Focant J-F. Analysis of synthetic canine training aids by comprehensive two-dimensional gas chromatography–time of flight mass spectrometry. Journal of Chromatography A. 2012;1255:202-6.

63. Stefanuto P-H, Perrault KA, Stadler S, Pesesse R, LeBlanc HN, Forbes SL, et al. GC × GC–TOFMS and supervised multivariate approaches to study human cadaveric decomposition olfactive signatures. Analytical and Bioanalytical Chemistry. 2015 2015/06/01;407(16):4767-78.

64. Armstrong P, Nizio KD, Perrault KA, Forbes SL. Establishing the volatile profile of pig carcasses as analogues for human decomposition during the early postmortem period. Heliyon. 2016 2016/02/01/;2(2):e00070.

65. Stefanuto PH, Rosier E, Tytgat J, Focant JF, Cuypers E. Profiling Volatile Organic Compounds of Decomposition. Taphonomy of Human Remains: Forensic Analysis of the Dead and the Depositional Environment: Forensic Analysis of the Dead and the Depositional Environment. 2017:39-52.

66. James AT, Martin AJP. Gas-liquid partition chromatography; the separation and micro-estimation of volatile fatty acids from formic acid to dodecanoic acid. Biochem J. 1952;50(5):679-90.

67. Black RM, Clarke RJ, Read RW, Reid MTJ. Application of gas chromatography-mass spectrometry and gas chromatography-tandem mass spectrometry to the analysis of chemical warfare samples, found to contain residues of the nerve agent sarin, sulphur mustard and their degradation products. Journal of Chromatography A. 1994 1994/02/25/;662(2):301-21.

68. Rodríguez-Navas C, Forteza R, Cerdà V. Use of thermal desorption–gas chromatography–mass spectrometry (TD–GC–MS) on identification of odorant emission focus by volatile organic compounds characterisation. Chemosphere. 2012 2012/11/01/;89(11):1426-36.

69. Poma G, Malarvannan G, Voorspoels S, Symons N, Malysheva SV, Van Loco J, et al. Determination of halogenated flame retardants in food: Optimization and validation of a method based on a two-step clean-up and gas chromatography–mass spectrometry. Food Control. 2016 2016/07/01/;65:168-76.

70. Hernández F, Cervera MI, Portolés T, Beltrán J, Pitarch E. The role of GC-MS/MS with triple quadrupole in pesticide residue analysis in food and the environment. Analytical Methods. [10.1039/C3AY41104D]. 2013;5(21):5875-94.

71. Nizio KD. Profiling Alkyl Phosphates in Petroleum Samples by Comprehensive Two-dimensional Gas Chromatography with Nitrogen-phosphorus Detection (GC×GC-NPD): University of Alberta, 2014.

72. Forbes S. Gas Chromatography. Analytical Techniques in Forensic Science; 2021;327-63.

73. Karasek FW, Clement RE. Basic gas chromatography-mass spectrometry: principles and techniques. Amsterdam: Elsevier, 2003.

74. Ramos L. Comprehensive two dimensional gas chromatography: Elsevier, 2009.

75. Brais CJ, Ibañez JO, Schwartz AJ, Ray SJ. Recent advances in Instrumental Approaches to time-of-flight mass spectrometry. Mass Spectrometry Reviews. 2021;40(5):647-69.

76. Stephens W. A pulsed mass spectrometer with time disaersion. Phys Rev. 1946;69:691.

77. Casares A, Kholomeev A, Wollnik H. Multipass time-of-flight mass spectrometers with high resolving powers. International Journal of Mass Spectrometry. 2001;206(3):267-73.

78. Brasseur C, Dekeirsschieter J, Schotsmans EMJ, de Koning S, Wilson AS, Haubruge E, et al. Comprehensive two-dimensional gas chromatography–time-of-flight mass spectrometry for the forensic study of cadaveric volatile organic compounds released in soil by buried decaying pig carcasses. Journal of Chromatography A. 2012 2012/09/14/;1255:163-70.

79. Browne C, Stafford K, Fordham R. The use of scent-detection dogs. Irish Veterinary Journal. 2006;59(2):97.

80. Statheropoulos M, Sianos E, Agapiou A, Georgiadou A, Pappa A, Tzamtzis N, et al. Preliminary investigation of using volatile organic compounds from human expired air, blood and urine for locating entrapped people in earthquakes. Journal of Chromatography B. 2005 2005/08/05/;822(1):112-7.

81. Statheropoulos M, Agapiou A, Pallis G. A study of volatile organic compounds evolved in urban waste disposal bins. Atmospheric Environment. 2005 2005/08/01/;39(26):4639-45.

82. Statheropoulos M, Mikedi K, Agapiou A, Georgiadou A, Karma S. Discriminant Analysis of Volatile Organic Compounds data related to a new location method of entrapped people in collapsed buildings of an earthquake. Analytica Chimica Acta. 2006 2006/05/04/;566(2):207-16.

83. Statheropoulos M, Agapiou A, Georgiadou A. Analysis of expired air of fasting male monks at Mount Athos. Journal of Chromatography B. 2006 2006/03/07/;832(2):274-9.

84. Vass AA, Barshick S-A, Sega G, Caton J, Skeen JT, Love JC, et al. Decomposition chemistry of human remains: a new methodology for determining the postmortem interval. Journal of Forensic Science. 2002;47(3):542-53.

85. Swann LM, Forbes SL, Lewis SW. Analytical separations of mammalian decomposition products for forensic science: A review. Analytica Chimica Acta. 2010 2010/12/03/;682(1):9-22.

86. Iqbal MA, Nizio KD, Ueland M, Forbes SL. Forensic decomposition odour profiling: A review of experimental designs and analytical techniques. TrAC Trends in Analytical Chemistry. 2017 2017/06/01/;91:112-24.

87. Patel D. Volatile profiling of human remains during the early post-mortem period in an outdoor environment: University of Technology Sydney, 2016.

88. Woolfenden E, McClenny W. Compendium Method TO-17. Determination of volatile organic compounds in ambient air using active sampling onto sorbent tubes. US EPA, Cincinnati, OH. 1999.

89. McKeage K, Perry CM. Propofol. CNS Drugs. 2003 2003/04/01;17(4):235-72.

90. Lo TS, Hammer KDP, Zegarra M, Cho WCS. Methenamine: a forgotten drug for preventing recurrent urinary tract infection in a multidrug resistance era. Expert Review of Anti-infective Therapy. 2014 2014/05/01;12(5):549-54.

91. Wescott DJ. Recent Advances in Forensic Anthropology: Decomposition Research. Forensic Sciences Research. 2018;3(4):278-93.

92. Rosier E, Loix S, Develter W, Van de Voorde W, Tytgat J, Cuypers E. Time-dependent VOC-profile of decomposed human and animal remains in laboratory environment. Forensic Science International. 2016 2016/09/01/;266:164-9.

93. Rosier E, Cuypers E, Dekens M, Verplaetse R, Develter W, Van de Voorde W, et al. Development and validation of a new TD-GC/MS method and its applicability in the search for human and animal decomposition products. Analytical and Bioanalytical Chemistry. 2014 2014/06/01;406(15):3611-9.

94. Paczkowski S, Schütz S. Post-mortem volatiles of vertebrate tissue. Applied microbiology and biotechnology. 2011;91(4):917-35.

95. Mochalski P, King J, Unterkofler K, Hinterhuber H, Amann A. Emission rates of selected volatile organic compounds from skin of healthy volunteers. J Chromatogr B Analyt Technol Biomed Life Sci. 2014 May 15;959(100):62-70.

96. Jiang R, Cudjoe E, Bojko B, Abaffy T, Pawliszyn J. A non-invasive method for in vivo skin volatile compounds sampling. Analytica Chimica Acta. 2013 2013/12/04/;804:111-9.

97. Vass AA, Smith RR, Thompson CV, Burnett MN, Wolf DA, Synstelien JA, et al. Decompositional odor analysis database. Journal of Forensic Sciences. 2004;49(4):760-9.

98. Dekeirsschieter J, Frederickx C, Lognay G, Brostaux Y, Verheggen FJ, Haubruge E. Electrophysiological and behavioral responses of thanatophilus sinuatus fabricius (coleoptera: silphidae) to selected cadaveric volatile organic compounds. Journal of Forensic Sciences. 2013;58(4):917-23.

99. Gallagher M, Wysocki CJ, Leyden JJ, Spielman AI, Sun X, Preti G. Analyses of volatile organic compounds from human skin. British Journal of Dermatology. 2008;159(4):780-91.

100. Dormont L, Bessière J-M, McKey D, Cohuet A. New methods for field collection of human skin volatiles and perspectives for their application in the chemical ecology of human–pathogen–vector interactions. Journal of Experimental Biology. 2013;216(15):2783-8.

101. Penn DJ, Oberzaucher E, Grammer K, Fischer G, Soini HA, Wiesler D, et al. Individual and gender fingerprints in human body odour. Journal of The Royal Society Interface. 2007;4(13):331-40.

102. Shirasu M, Touhara K. The scent of disease: volatile organic compounds of the human body related to disease and disorder. The Journal of Biochemistry. 2011;150(3):257-66.

103. Rosier E, Loix S, Develter W, Van de Voorde W, Tytgat J, Cuypers E. The search for a volatile human specific marker in the decomposition process. PLOS ONE. 2015;10(9):e0137341.

104. Vass AA. Odor mortis. Forensic Science International. 2012;222(1-3):234-41.

105. Trumbo ST, Steiger S. Finding a fresh carcass: bacterially derived volatiles and burying beetle search success. Chemoecology. 2020 2020/12/01;30(6):287-96.

106. Martin C, Verheggen F. Odour profile of human corpses: A review. Forensic Chemistry. 2018 2018/08/01/;10:27-36.

107. Dargan R, Samson C, Burr WS, Daoust B, Forbes SL. Validating the Use of Amputated Limbs Used as Cadaver Detection Dog Training Aids. Frontiers in Analytical Science. [Original Research]. 2022 2022-July-13;2.

108. Williams JJ, Rodman JS, Peterson CM. A Randomized Double-Blind Study of Acetohydroxamic Acid in Struvite Nephrolithiasis. New England Journal of Medicine. 1984;311(12):760-4.

109. Forbes SL, Perrault KA. Decomposition odour profiling in the air and soil surrounding vertebrate carrion. PLOS ONE. 2014;9(4):e95107.

110. Paczkowski S, Weißbecker B, Schöning MJ, Schütz S. Biosensors on the basis of insect olfaction. In: Vilcinskas A, editor. Insect Biotechnology. Dordrecht: Springer Netherlands; 2011;225-40.

111. Alfsdotter C, Petaros A. Outdoor human decomposition in Sweden: A retrospective quantitative study of forensic-taphonomic changes and postmortem interval in terrestrial and aquatic settings. Journal of forensic sciences. 2021;66(4):1348-63.

112. Anderson GS, Hobischak NR. Decomposition of carrion in the marine environment in British Columbia, Canada. International Journal of Legal Medicine. 2004 2004/08/01;118(4):206-9.

113. O'Brien RC, Appleton AJ, Forbes SL. Comparison of taphonomic progression due to the necrophagic activity of geographically disparate scavenging guilds. Canadian Society of Forensic Science Journal. 2017 2017/01/02;50(1):42-53.

114. Séguin K, Durand-Guévin A, Lavallée C, Ouimet F, Maisonhaute JÉ, Watson CJ, et al. The taphonomic impact of scavenger guilds in southern Quebec during summer and fall in two distinct habitats. Journal of forensic sciences. 2021.

115. Stadler S, Desaulniers J-P, Forbes SL. Inter-year repeatability study of volatile organic compounds from surface decomposition of human analogues. International Journal of Legal Medicine. 2015 2015/05/01;129(3):641-50.

116. Stadler S, Stefanuto P-H, Brokl M, Forbes SL, Focant J-F. Characterization of volatile organic compounds from human analogue decomposition using thermal desorption coupled to comprehensive two-dimensional gas chromatography–time-of-flight mass spectrometry. Analytical Chemistry. 2013 2013/01/15;85(2):998-1005.

117. Petrik MS, Hobischak NR, Anderson GS. Examination of factors surrounding human decomposition in freshwater: A review of body recoveries and coroner cases in British Columbia. Canadian Society of Forensic Science Journal. 2004 2004/01/01;37(1):9-17.

118. Hobischak NR, Anderson GS. Freshwater-related death investigations in British Columbia in 1995–1996. A review of coroners cases. Canadian Society of Forensic Science Journal. 1999 1999/01/01;32(2-3):97-106.

119. Cockle DL, Bell LS. The environmental variables that impact human decomposition in terrestrially exposed contexts within Canada. Science & Justice. 2017 2017/03/01/;57(2):107-17.

120. Suckling JK, Spradley MK, Godde K. A longitudinal study on human outdoor decomposition in Central Texas. Journal of forensic sciences. 2016;61(1):19-25.

121. Pecsi EL, Bronchti G, Crispino F, Forbes SL. Perspectives on the establishment of a canadian human taphonomic facility: The experience of REST[ES]. Forensic Science International: Synergy. 2020 2020/01/01/;2:287-92.

122. Watson CJ, Ueland M, Schotsmans EMJ, Sterenberg J, Forbes SL, Blau S. Detecting grave sites from surface anomalies: A longitudinal study in an Australian woodland. Journal of Forensic Sciences. 2021;66(2):479-90.

123. Dawson BM, Barton PS, Wallman JF. Field succession studies and casework can help to identify forensically useful Diptera. Journal of Forensic Sciences. 2021;66(6):2319-28.

124. Emmons AL, DeBruyn JM, Mundorff AZ, Cobaugh KL, Cabana GS. The persistence of human DNA in soil following surface decomposition. Science & Justice. 2017 2017/09/01/;57(5):341-8.

125. Finley SJ, Pechal JL, Benbow ME, Robertson BK, Javan GT. Microbial signatures of cadaver gravesoil during decomposition. Microbial Ecology. 2016 2016/04/01;71(3):524-9.

126. Dautartas A, Kenyhercz MW, Vidoli GM, Meadows Jantz L, Mundorff A, Steadman DW. Differential decomposition among pig, rabbit, and human Remains. Journal of Forensic Sciences. 2018;63(6):1673-83.

127. Megyesi MS, Nawrocki SP, Haskell NH. Using accumulated degree-days to estimate the postmortem interval from decomposed human remains. Journal of Forensic Science. 2005;50(3):1-9.

128. Javan GT, Finley SJ, Tuomisto S, Hall A, Benbow ME, Mills D. An interdisciplinary review of the thanatomicrobiome in human decomposition. Forensic Science, Medicine and Pathology. 2019 2019/03/01;15(1):75-83.

129. Talon R, Chastagnac C, Vergnais L, Montel MC, Berdagué JL. Production of esters by Staphylococci. International Journal of Food Microbiology. 1998 1998/12/08/;45(2):143-50.

130. Agapiou A, Zorba E, Mikedi K, McGregor L, Spiliopoulou C, Statheropoulos M. Analysis of volatile organic compounds released from the decay of surrogate human models simulating victims of collapsed buildings by thermal desorption–comprehensive two-dimensional gas chromatography–time of flight mass spectrometry. Analytica Chimica Acta. 2015;883:99-108.

131. Statheropoulos M, Agapiou A, Zorba E, Mikedi K, Karma S, Pallis GC, et al. Combined chemical and optical methods for monitoring the early decay stages of surrogate human models. Forensic Science International. 2011;210(1-3):154-63.

132. Mochalski P, Unterkofler K, Hinterhuber H, Amann A. Monitoring of selected skin-borne volatile markers of entrapped humans by selective reagent ionization time of flight mass spectrometry in NO+ mode. Analytical Chemistry. 2014 2014/04/15;86(8):3915-23.

133. Scherz-Shouval R, Elazar Z. Regulation of autophagy by ROS: physiology and pathology. Trends in Biochemical Sciences. 2011 2011/01/01/;36(1):30-8.

134. Carlström M, Moretti CH, Weitzberg E, Lundberg JO. Microbiota, diet and the generation of reactive nitrogen compounds. Free Radical Biology and Medicine. 2020 2020/12/01/;161:321-5.

135. Cernosek T, Eckert KE, Carter DO, Perrault KA. Volatile Organic Compound Profiling from Postmortem Microbes using Gas Chromatography–Mass Spectrometry. Journal of Forensic Sciences. 2020;65(1):134-43.

136. Matsuda K, Arima K, Akiyama S, Yamada Y, Abe Y, Suenaga H, et al. A natural dihydropyridazinone scaffold generated from a unique substrate for a hydrazine-forming enzyme. Journal of the American Chemical Society. 2022 2022/07/20;144(28):12954-60.

Appendices

Appendix A: Supporting information for Phase 2

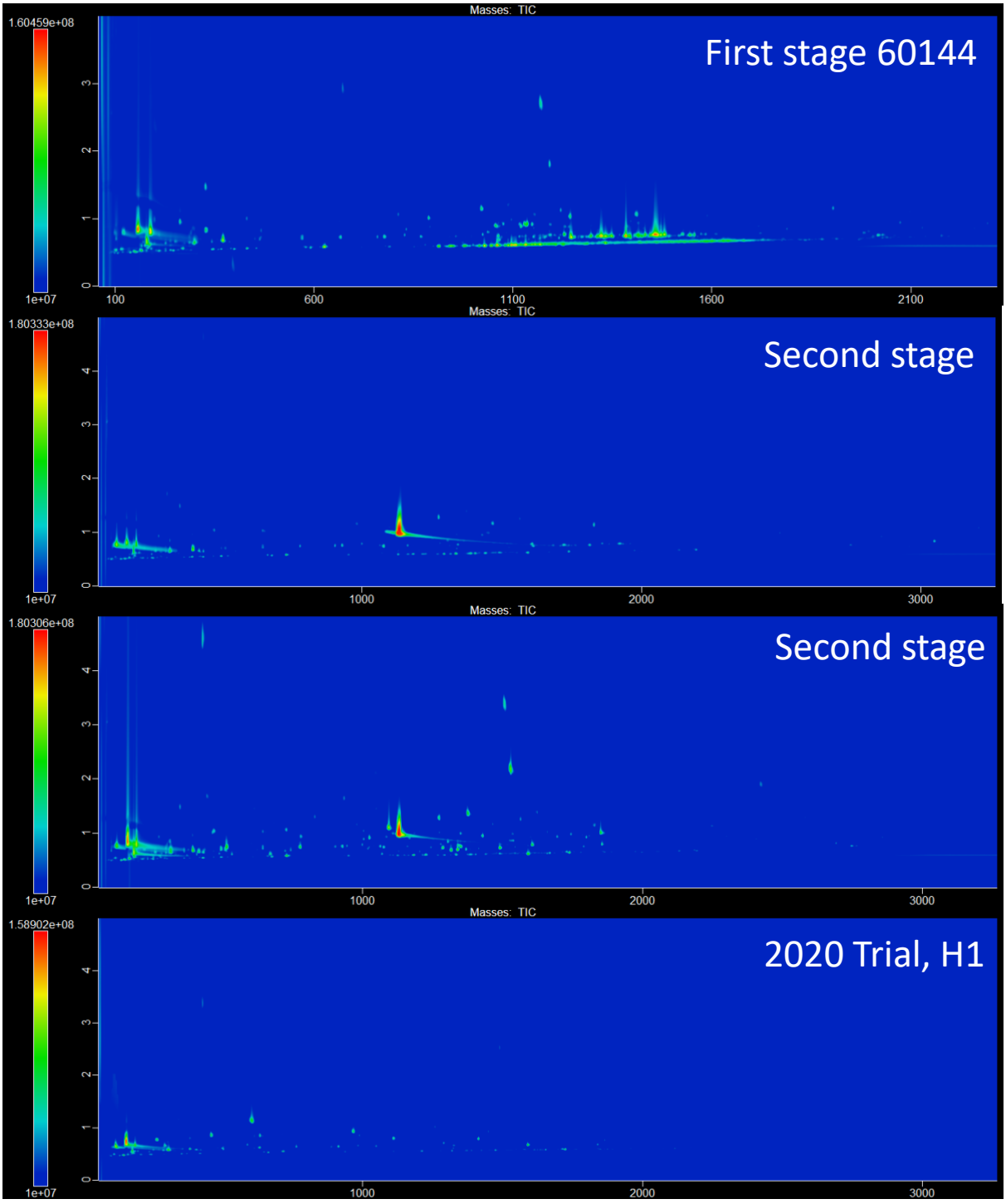

Figure A-1: *Showing comparison of GC×GC-TOFMS total ion current (TIC) contour plots of headspace VOC samples collected from the donor during first and second method optimisation stage and 2020 trial, donor H1.* ***Note:*** *(i) these are different donors (ii) the second stage and 2020 trial donor H1 have been analysed with the optimised method (iii) the minimum intensity scale has been kept the same to highlight the inter-donor variability in the chromatographs.*

Table A-1: *Decomposition standard compounds analysed and their retention times using the current optimised stage 2 method and instrumentation. Note: over the course of the study, the major peaks of all the standards appeared within ± 5 s in 1D and ± 0.1 s in 2D from the retention values listed below.*

Standard mix	**Name**	**1st Dimension retention time (s)**	**2nd Dimension retention time (s)**
Standard mix 8	Formaldehyde	89.9981	0.481
	Butanal, 3-methyl-	409.978	0.594
	Pentanal	499.972	0.622
	Hexanal	764.955	0.653
	Heptanal	1049.94	0.668
	Octanal	1329.92	0.684
	2-Octenal, (E)-	1514.91	0.763
	Nonanal	1594.9	0.699
	Decanal	1844.89	0.718
Standard mix 2	Furan, 2-methyl-	279.986	0.569
	2-Butanol	324.983	0.723
	1-Butanol	459.974	0.862
	3-Pentanol	529.97	0.743
	Disulfide, dimethyl	589.966	0.682
	1-Pentanol	714.958	0.881
	Dimethyl trisulfide	1219.93	0.817
	Furan, 2-pentyl-	1229.93	0.653
	Indole	2229.86	2.371
Standard mix 1	Acetic acid, methyl ester	199.991	0.56
	Ethyl Acetate	309.984	0.577
	2-Butanone, 3-methyl-	419.977	0.593
	2-Pentanone	484.973	0.617
	Methyl Isobutyl Ketone	609.965	0.615

	2-Heptanone	1024.94	0.664
	Butyrolactone	1254.92	1.342

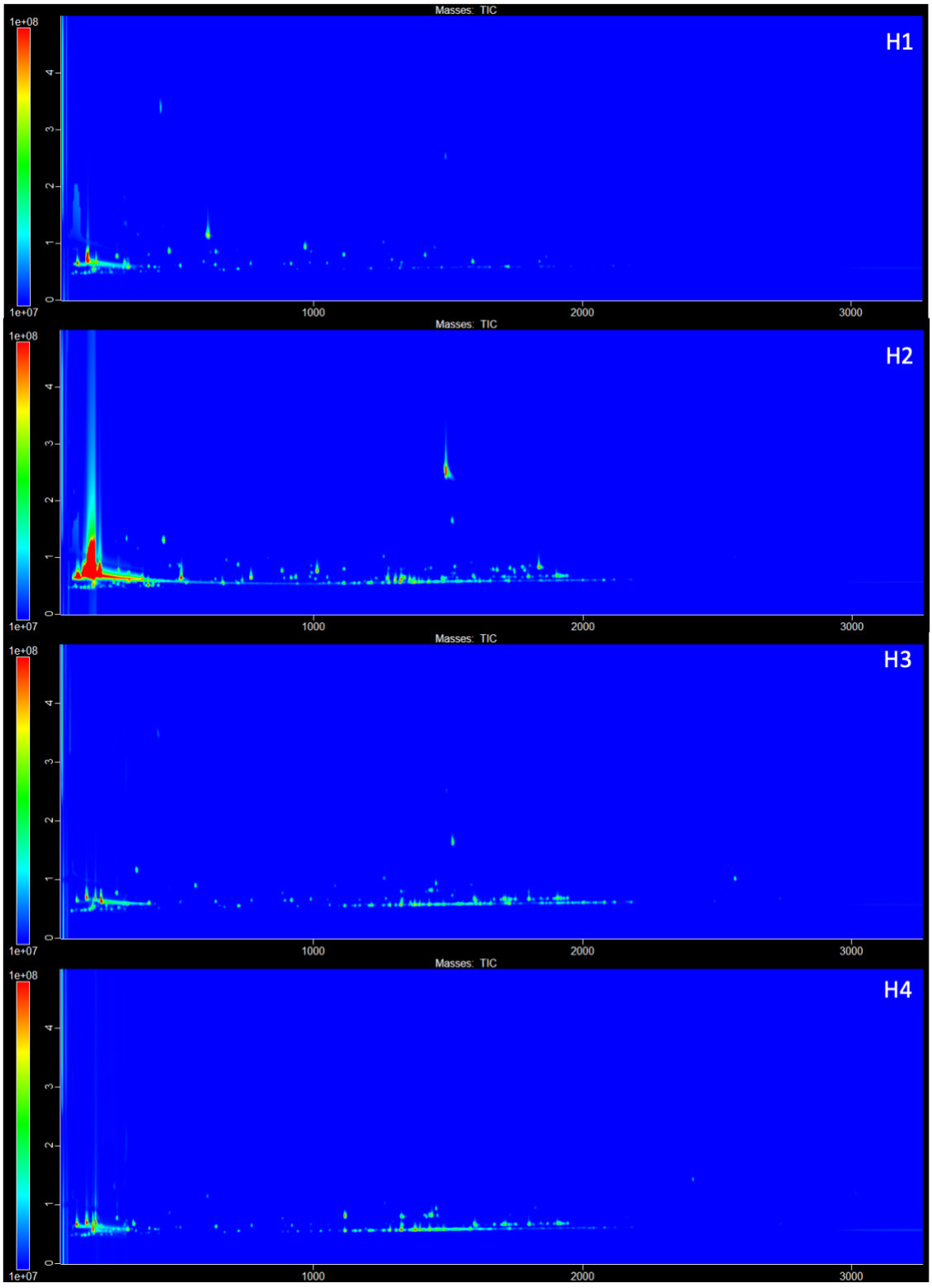

Figure A-2: *GC×GC-TOFMS total ion current (TIC) contour plots of headspace VOC samples collected from donors H1, H2, H3 and H4.*

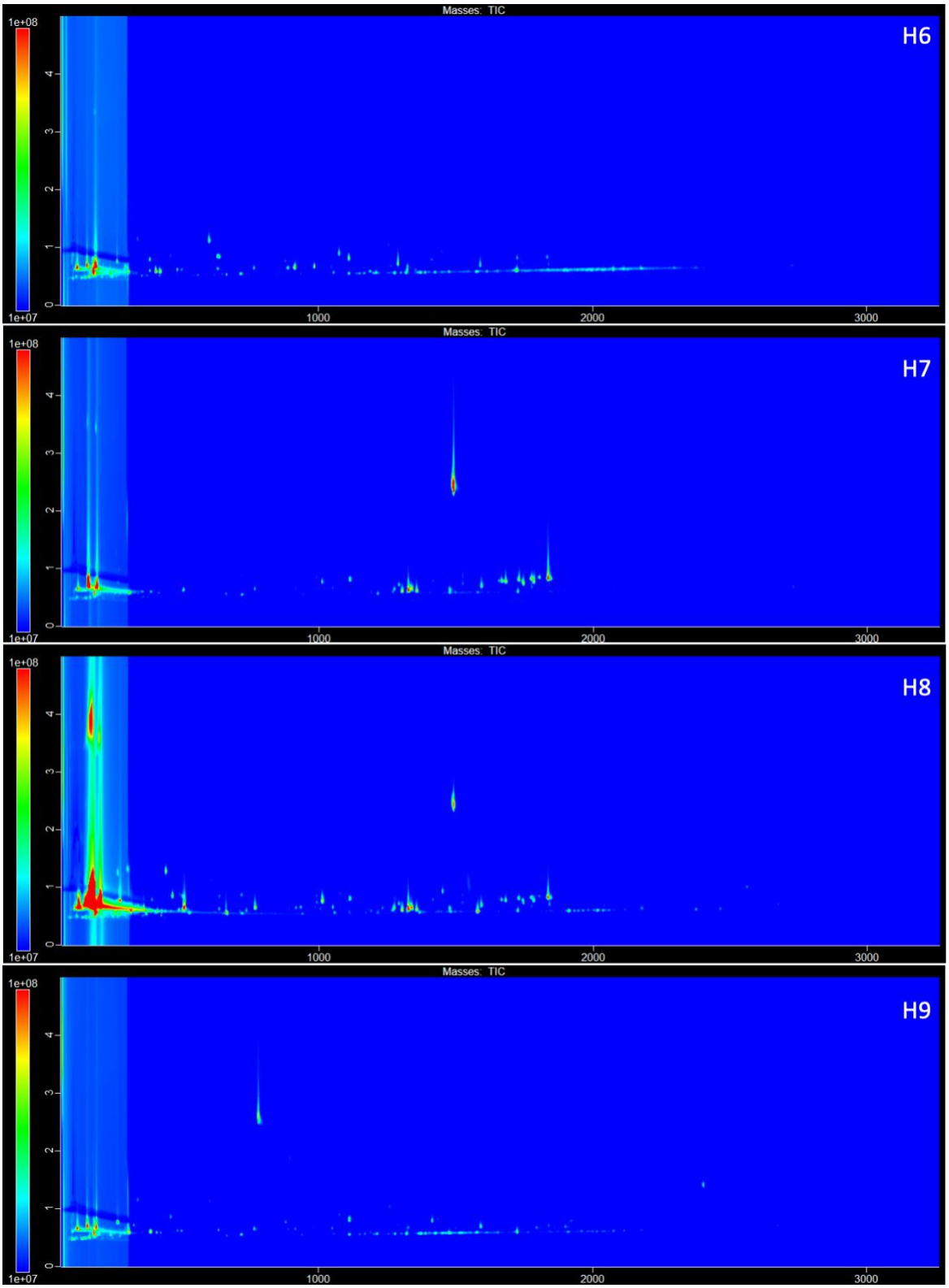

Figure A-3: *GC×GC-TOFMS total ion current (TIC) contour plots of headspace VOC samples collected from donors H6, H7, H8 and H9.*

Table A-1: *List of 104 VOCs detected in three or more donors out of eight donors in the Phase 2 (morgue study)*

Name	Compound class
Butanoic acid, 3-methyl-	Acids
Propanoic acid, 2,2-dimethyl-	Acids
1,3-Dioxan-5-ol, 4,4,5-trimethyl-	Alcohols
1-Butanol, 3-methyl-	Alcohols
1-Propanol, 2-methyl-	Alcohols
1-Penten-3-ol	Alcohols
Phenylethyl Alcohol	Alcohols
2-Pentanol	Alcohols
2-Methyl-1-hexanol	Alcohols
2-Propanol, 2-methyl-	Alcohols
3-Buten-1-ol, 3-methyl-	Alcohols
Phenol, p-tert-butyl-	Alcohols
Benzyl alcohol	Alcohols
1,4-Benzenediol, 2,6-bis(1,1-dimethylethyl)-	Alcohols
3-Octanol	Alcohols
4-Ethylcyclohexanol	Alcohols
7-Octen-2-ol, 2,6-dimethyl-	Alcohols
Œ±-Terpineol	Alcohols
Phenol, 4-(1-methylpropyl)-	Alcohols
Propylene Glycol	Alcohols
2-Ethylacrolein	Aldehydes
Butanal, 3-methyl-	Aldehydes
3-Cyclohexene-1-carboxaldehyde	Aldehydes
Hexanal, 2-ethyl-	Aldehydes
Indan, 1-methyl-	Aromatics
Benzene, 1-methyl-4-butyl	Aromatics
Benzene, 1,3-bis(1,1-dimethylethyl)-	Aromatics
Benzene, 2-propenyl-	Aromatics
Benzene, 1,2,4,5-tetramethyl-	Aromatics
1-Ethylcyclopentene	Aromatics
1H-Indene, 2,3-dihydro-4-methyl-	Aromatics
2-Ethyl-2,3-dihydro-1H-indene	Aromatics
Anisole	Aromatics
Benzaldehyde, 2-hydroxy-	Aromatics
Benzene, (2-methyl-1-propenyl)-	Aromatics
Benzene, 1-ethyl-3-methyl-	Aromatics
Benzene, 1-ethyl-4-methyl-	Aromatics
Benzene, 1-methyl-3-propyl-	Aromatics

Benzene, 1,2-diethyl-	Aromatics
Benzene, 1,4-dimethyl-2-(2-methylpropyl)-	Aromatics
Benzene, 2-methoxy-4-methyl-1-(1-methylethyl)-	Aromatics
Benzene, 4-ethenyl-1,2-dimethyl-	Aromatics
Benzene, pentyl-	Aromatics
Furan, 2-pentyl-	Aromatics
Furan, 2,5-dimethyl-	Aromatics
Indane	Aromatics
Œ≥-Terpinene	Cyclic Aliphatics
1-Nonylcycloheptane	Cyclic Aliphatics
Cyclohexane, 1,1,2,3-tetramethyl-	Cyclic Aliphatics
Cyclooctane, 1,4-dimethyl-, cis-	Cyclic Aliphatics
1,2,4,4-Tetramethylcyclopentene	Cyclic Aliphatics
7-Oxabicyclo[2.2.1]heptane, 1-methyl-4-(1-methylethyl)-	Cyclic Aliphatics
Acetic acid, butyl ester	Esters and Analogues
Octanoic acid, ethyl ester	Esters and Analogues
1,2-Ethanediol, monoformate	Esters and Analogues
Acetic acid, phenylmethyl ester	Esters and Analogues
Hexanoic acid, methyl ester	Esters and Analogues
Propanoic acid, 2-methyl-, ethyl ester	Esters and Analogues
1,2-Ethanediol, diformate	Esters and Analogues
2-Propenoic acid, butyl ester	Esters and Analogues
2-Propenoic acid, octyl ester	Esters and Analogues
4-tert-Butylcyclohexyl acetate	Esters and Analogues
Allyl acetate	Esters and Analogues
Benzenemethanol, 2-methyl-, acetate	Esters and Analogues
Benzoic acid, methyl ester	Esters and Analogues
Decanoic acid, ethyl ester	Esters and Analogues
Isopropyl acetate	Esters and Analogues
Methyl anthranilate	Esters and Analogues
Nonanoic acid, ethyl ester	Esters and Analogues
Pentanoic acid, ethyl ester	Esters and Analogues
Propanoic acid, 2-hydroxy-, ethyl ester	Esters and Analogues
Propanoic acid, butyl ester	Esters and Analogues
Thiocyanic acid, methyl ester	Esters and Analogues
1,3,5-Trioxane	Ethers
2-Propanol, 1-(2-butoxy-1-methylethoxy)-	Ethers
Diphenyl ether	Ethers
1,3-Dioxolane, 2-methyl-	Ethers

2-Propanone, 1,1-dichloro-	Halogen-containing
Acetonitrile, dichloro-	Halogen-containing
Difluorochloromethane	Halogen-containing
Phenol, 2-chloro-	Halogen-containing
5-Hepten-2-one, 6-methyl-	Ketones
2,3-Pentanedione	Ketones
1-Hydroxy-2-butanone	Ketones
1-Octen-3-one	Ketones
Ethanone, 1-(1-cyclohexen-1-yl)-	Ketones
2-Butanone, oxime	Ketones
2-Pentanone, 4-hydroxy-4-methyl-	Ketones
2-Propanone, 1-hydroxy-	Ketones
Cyclopentanone, 2-methyl-	Ketones
5-Ethyldecane	Linear Aliphatics
Heptane, 2,4-dimethyl-	Linear Aliphatics
Octane, 2,3,6,7-tetramethyl-	Linear Aliphatics
Octane, 2,5,6-trimethyl-	Linear Aliphatics
Octane, 2,6-dimethyl-	Linear Aliphatics
Octane, 4-ethyl-	Linear Aliphatics
Octane, 2,2,6-trimethyl-	Linear Aliphatics
Undecane, 2,6-dimethyl-	Linear Aliphatics
Pyridine	Nitrogen-containing
Hydrogen isocyanate	Nitrogen-containing
Butanenitrile	Nitrogen-containing
Butanenitrile, 3-methyl-	Nitrogen-containing
Disulfide, dimethyl	Sulfur-containing
Dimethylsulfide	Sulfur-containing

Table A-2: *List of compounds related to decomposition identified in lower PMI donors causing their separation and clustering in the scores plot made with seven donors. These compounds were located closest to the outer ellipses on the correlations loadings plot indicating a strong association and correlation with the donors causing variance in the VOC profiles.*

Donor	**Compound**	**Frequency of detection**	**Previously reported in decomposition literature**
H8	Heptane,2-4 dimethyl	3	(6)
H8	Thiocyanic acid, methyl ester	3	(105)
H8	1H-indene-dihydro-4-methyl	3	Not detected
H8	Butanal, 3-methyl	5	(6)
H2 and H7	Terpineol	3	(49)
H6 and H9	Acetic acid butyl ester	5	(106)
H6 and H9	2-Propenoic acid, butyl ester	3	(106)
H6 and H9	Butanenitrile	3	(63, 107)
H6 and H9	Butanenitrile 3-methyl	3	(107)
H6 and H9	2-pentanol	4	(106)

Appendix B: Supporting information for Chapter 3

WARNING: Graphic Content

The following images and/or content may be disturbing to some readers.

Reader discretion is strongly advised.

Table B-1 *Observations and photographs of donor H1 for 2020 trial.*

ED	Donor	Stage	Observations	Photograph
0	H1	Fresh stage passing	Greenish discoloration on the face, abdomen, genitals and lower limbs	REDACTED FOR PUBLICATION

Table B-2 *Observations and photographs of donor H2 for 2020 trial.*

ED	Donor	Observations	Photographs
0	H2	• Livor mortis visible in neck region • Purpura on the forearms	REDACTED FOR PUBLICATION
1	H2	• Minimal insect activity • No significant change from the previous day in terms of visual decomposition	REDACTED FOR PUBLICATION
2	H2	• Skin slippage on the lower part of the left arm • Greenish discolouration in the torso	REDACTED FOR PUBLICATION
3	H2	• Face showed signs of active decay • Greenish discoloration was seen in the torso	REDACTED FOR PUBLICATION
4	H2	• Forearms showed signs of active decay with a leathery appearance • Commencement of bloat stage in the abdomen	REDACTED FOR PUBLICATION

Table B-3 *Observations and photographs of donor H3 for 2020 trial.*

ED	Donor	Observations	Photographs
0	H3	• Upper and lower limbs were in rigor mortis • Livor mortis was seen on the side of the neck, back of the head and inner thighs	REDACTED FOR PUBLICATION
1	H3	• No significant change from the previous day in terms of visual decomposition	REDACTED FOR PUBLICATION
2	H3	• No significant change from the previous day in terms of visual decomposition	REDACTED FOR PUBLICATION
3	H3	• Greenish discolouration seen in torso, genitals and knees	REDACTED FOR PUBLICATION
4	H3	• No significant change from the previous day in terms of visual decomposition	REDACTED FOR PUBLICATION

Table B-4 *Observations and photographs of donor H4 for 2020 trials.*

ED	Donor	Observations	Photographs
0	H4	• Livor mortis was seen in the neck, shoulder, and head regions	REDACTED FOR PUBLICATION
1	H4	• No significant change from the previous day in terms of visual decomposition	REDACTED FOR PUBLICATION
2	H4	• No significant change from the previous day in terms of visual decomposition	REDACTED FOR PUBLICATION
3	H4	• Greenish discolouration seen in torso, genitals and knees	REDACTED FOR PUBLICATION
4	H4	• No significant change from the previous day in terms of visual decomposition	REDACTED FOR PUBLICATION

Table B-5 *Observations and photographs of donor H6 for 2021 trial.*

ED	Donor	Observations	Photographs
0	H6	• Livor mortis was seen on the back, and the upper and lower limbs • Rigor mortis in upper and lower limbs	REDACTED FOR PUBLICATION
1	H6	• No significant change from the previous day in terms of visual decomposition	REDACTED FOR PUBLICATION
2	H6	• No significant change from the previous day in terms of visual decomposition	REDACTED FOR PUBLICATION
3	H6	• Rigor mortis was passing from the upper and lower limbs • Initial deposits of egg masses were seen in the nose and palate	REDACTED FOR PUBLICATION
4	H6	• Greenish discolouration progressed to regions of the lower limbs such as thighs, calf, and ankle	REDACTED FOR PUBLICATION
5	H6	• Rigor mortis had completely passed	REDACTED FOR PUBLICATION

Table B-6 *Observations and photographs of donor H7 for 2021 trial.*

ED	Donor	Observations	Photographs
0	H7	• Livor mortis was observed on the back	REDACTED FOR PUBLICATION
1	H7	• No significant change from the previous day in terms of visual decomposition	REDACTED FOR PUBLICATION
2	H7	• No significant change from the previous day in terms of visual decomposition	REDACTED FOR PUBLICATION
3	H7	• Soles of the feet showed a wrinkling appearance • High insect activity was recorded along with egg masses in the mouth, eyes, and genitalia	REDACTED FOR PUBLICATION
4	H7	• Greenish discolouration progressed to regions of the lower limbs such as thighs, calf, and ankle	REDACTED FOR PUBLICATION
5	H7	• Skin slippage was observed in the face	REDACTED FOR PUBLICATION

Table B-7 *Observations and photographs of donor H8 for 2021 trial*

ED	Donor	Observations	Photographs
0	H8	• Blister was seen on the left leg which could have developed in the ante-mortem period	REDACTED FOR PUBLICATION
1	H8	• Insect activity was observed on the blister and egg masses were seen in the eyes and nose	REDACTED FOR PUBLICATION
2	H8	• Increase in the egg masses in the eyes, nose, and palate were noticed. • Skin slippage was seen around the blister	REDACTED FOR PUBLICATION
3	H8	• High insect activity was seen over the head, neck, and genital regions • Venous marbling was noted over a small region in the upper limbs and lower limbs	REDACTED FOR PUBLICATION
4	H8	• Beginning of bloat was seen in the abdomen with spreading of venous marbling occurring in the upper and lower limbs	REDACTED FOR PUBLICATION
5	H8	• Purging of decomposition fluid was seen from the head and neck region.	REDACTED FOR PUBLICATION

Table B-8 *Observations and photographs of donor H9 for 2021 trial*

ED	Donor	Observations	Photographs
0	H9	• Livor mortis was noted on the back • Patches of pink and red discolouration were seen on the forehead and small regions of the lower limb	REDACTED FOR PUBLICATION
1	H9	• A small amount of insect activity • No significant changes in terms of visual decomposition	REDACTED FOR PUBLICATION
2	H9	• No significant changes in terms of visual decomposition	REDACTED FOR PUBLICATION
3	H9	• Slight bloating of the neck region	REDACTED FOR PUBLICATION
4	H9	• Greenish discolouration was seen on the chin, upper lip, and eyelids	REDACTED FOR PUBLICATION
5	H9	• An increase in bloating across the head and neck	REDACTED FOR PUBLICATION

Appendix C: Supporting information for Chapter 4

Table C-1 *List of 27 ante-mortem VOCs detected in the dataset and also reported in the literature*

Name
1-Heptene
1-Nonene
1-Octene
1,3-Dioxolane, 2-methyl-
2-Butanone
2-Butenal, 3-methyl-
2-Butene, 2,3-dimethyl-
2-Heptanone
2-Pentanone
2-Propenal
5-Hepten-2-one, 6-methyl-
Acetaldehyde
Acetonitrile
Benzaldehyde
Butanal, 2-methyl-
Butanal, 3-methyl-
Ethanol
Ethyl Acetate
Eucalyptol
Furan, 2-methyl-
Furan, 2-pentyl-
Furan, 2,5-dimethyl-
Furan, 3-methyl-
Isopropyl acetate
p-Cymene
Propanal, 2-methyl-
Propene

Table C-2 *List of 54 decomposition VOCs detected in the dataset and also reported in the literature*

Name
1-Decene
1-Ethyl-4-methylcyclohexane
1-Heptene
1-Hexanol, 2-ethyl-
1-Hexene
1-Octen-3-ol
1-Propanol
1,1-Dichloro-1-fluoroethane
2-Butanol
2-Butanone
2-Decanone
2-Heptanone
2-Hexenal
2-Hexyl-1-octanol
2-Nonanone
2-Octanone
2-Octene
2-Pentanol
2-Pentanone
Acetaldehyde
Benzaldehyde
Benzonitrile
Benzyl alcohol
Butanoic acid
Butanoic acid, ethyl ester
Butanoic acid, methyl ester
Cyclohexanone
D-Limonene
Decanal
Dimethyl trisulfide
dimethyl disulfide
Ethanol
Ethylbenzene
Heptanal
Hexanoic acid, ethyl ester
Indole

Methanethiol
Methenamine
Nonanal
Nonane
o-xylene
Octanal
Octanoic acid
Pentadecane
Pentanal
Pentane
Pentanoic acid
Phenol
Propanal
Propanoic acid, ethyl ester
Pyridine
Styrene
Tetradecane
Toluene

Table C-3 *List of ante-mortem and decomposition VOCs detected in donor H1 and also reported in the literature.*

Name	**H1_M**	**H1 ED 0**
	Ante-mortem VOCs detected in donor H1 and also reported in the literature	
p-Cymene	✓	✓
1-Octene		✓
5-Hepten-2-one, 6-methyl-	✓	
Butanal, 3-methyl-	✓	
Ethanol		✓
Ethyl Acetate		✓
Eucalyptol		✓
Furan, 2-pentyl-		✓
Isopropyl acetate		✓
	Decomposition VOCs detected in donor H1 and also reported in the literature	
Dimethyl trisulfide	✓	✓
1-Hexene		✓
1-Octen-3-ol	✓	
2-Butanol	✓	
2-Nonanone	✓	
Decanal	✓	
Ethanol		✓
Hexanoic acid, ethyl ester		✓
Phenol		✓
Dimethyl disulfide	✓	✓

Table C-4 *List of ante-mortem and decomposition VOCs detected in donor H2 and also reported in the literature.*

Name	H2_M	H2 ED 0	H2 ED 1	H2 ED 2	H2 ED 3	H2 ED 4
	Ante-mortem VOCs detected in donor H2 and also reported in literature					
2-Butanone	✓		✓	✓		✓
5-Hepten-2-one, 6-methyl-	✓		✓			✓
Butanal, 3-methyl-			✓	✓	✓	
Ethanol		✓		✓		
Furan, 2-methyl-			✓			✓
Isopropyl acetate	✓					✓
1-Octene		✓				
2-Butenal, 3-methyl-	✓					
Acetaldehyde			✓			
Dimethyl sulfide						✓
Ethyl Acetate	✓					
Furan, 2-pentyl-	✓					
	Decomposition VOCs detected in donor H2 and also reported in the literature					
2-Butanone	✓		✓	✓		✓
Phenol		✓	✓			✓
Pyridine	✓				✓	✓
1-Propanol				✓		✓
2-Nonanone	✓					✓
Benzyl alcohol	✓					✓
Butanoic acid, ethyl ester	✓					✓
Dimethyl trisulfide					✓	✓
Ethanol		✓		✓		
Methenamine			✓		✓	
Octanoic acid			✓			✓
Propanoic acid, ethyl ester	✓					✓
1-Octen-3-ol	✓					
1,1-Dichloro-1-fluoroethane						✓
2-Decanone	✓					
2-Hexenal	✓					
2-Octanone						✓
2-Octene						✓
Acetaldehyde			✓			
Butanoic acid						✓

Butanoic acid, methyl ester				✓		
Cyclohexanone					✓	
D-Limonene	✓					
Decanal						✓
Indole						✓
Methanethiol						✓
Nonanal						✓
Pentadecane	✓					
Pentanal			✓			
Pentane		✓				
Pentanoic acid						✓
Styrene	✓					
Dimethyl disulfide			✓		✓	✓

Table C-5 *List of ante-mortem and decomposition VOCs detected in donor H3 and also reported in the literature.*

Name	H3_M	H3 ED 0	H3 ED 2	H3 ED 3	H3 ED 4
	Ante-mortem VOCs detected in donor H3 and also reported in the literature				
5-Hepten-2-one, 6-methyl-	✓	✓		✓	
Acetaldehyde		✓	✓		
Acetonitrile	✓	✓			
1,3-Dioxolane, 2-methyl-	✓				
2-Propenal					✓
Butanal, 3-methyl-			✓		
Ethyl Acetate					
Furan, 2-pentyl-	✓				
Isopropyl acetate	✓				
	Decomposition VOCs detected in donor H3 and also reported in the literature				
Acetaldehyde		✓	✓		
Butanoic acid, methyl ester	✓	✓			
Dimethyl trisulfide	✓	✓			
Methenamine			✓		✓
1-Octen-3-ol		✓			
2-Decanone	✓				
2-Hexenal	✓				
2-Nonanone			✓		
Butanoic acid, ethyl ester		✓			
Nonanal				✓	
Nonane	✓				
Octanal			✓		
Propanal					✓
Tetradecane				✓	

Table C-6 *List of ante-mortem and decomposition VOCs detected in donor H4 and also reported in the literature.*

Name	H4_M	H ED 0	H4 ED 1	H4 ED 3
	Ante-mortem VOCs detected in donor H4 and also reported in the literature			
5-Hepten-2-one, 6-methyl-	✓	✓		
1,3-Dioxolane, 2-methyl-	✓			
Butanal, 2-methyl-			✓	
Butanal, 3-methyl-			✓	
Ethyl Acetate		✓		
Eucalyptol		✓		
Furan, 2,5-dimethyl-	✓			
Isopropyl acetate		✓		
Propanal, 2-methyl-			✓	
	Decomposition VOCs detected in donor H4 and also reported in the literature			
Methenamine	✓			✓
2-Hexyl-1-octanol			✓	
2-Pentanol	✓			
Benzyl alcohol	✓			
Butanoic acid	✓			
Decanal		✓		
Nonanal	✓			
Octanal	✓			
Octanoic acid	✓			
Pentanal	✓			
Pentane	✓			
Propanal			✓	
Propanoic acid, ethyl ester	✓			
Pyridine	✓			
Tetradecane		✓		

Table C-7 *List of ante-mortem and post-mortem VOCs detected in donor H6 and also reported in the literature.*

Name	H6_M	H6 ED 0	H6 ED 1	H6 ED 2	H6 ED 3	H6 ED 4	H6 ED 5
	Ante-mortem VOCs detected in donor H6 and also reported in the literature						
Furan, 2-pentyl-	✓					✓	✓
1-Octene	✓						✓
Ethanol		✓	✓				
Furan, 2,5-dimethyl-	✓					✓	
1-Nonene						✓	
2-Butanone						✓	
2-Heptanone			✓				
5-Hepten-2-one, 6-methyl-							✓
Butanal, 2-methyl-						✓	
Butanal, 3-methyl-			✓				
Furan, 2-methyl-						✓	
	Decomposition VOCs detected in donor H6 and also reported in the literature						
Ethanol		✓	✓				
1-Hexanol, 2-ethyl-					✓		
2-Butanone						✓	
2-Heptanone			✓				
2-Nonanone					✓		
2-Pentanol	✓						
Benzyl alcohol	✓						
Butanoic acid, methyl ester	✓						
D-Limonene					✓		
Decanal						✓	
Ethylbenzene						✓	
Heptanal				✓			
Nonanal					✓		
Pentane		✓					
Phenol	✓						
Pyridine	✓						

Table C-8 *List of ante-mortem and decomposition VOCs detected in donor H7 and also reported in the literature.*

Name	H7_M	H7 ED 0	H7 ED 1	H7 ED 2	H7 ED 4	H7 ED 5
	Ante-mortem VOCs detected in donor H7 and also reported in the literature					
5-Hepten-2-one, 6-methyl-	✓	✓	✓	✓	✓	✓
2-Butanone		✓	✓	✓	✓	
Butanal, 3-methyl-	✓		✓			✓
1-Octene	✓					
2-Heptanone					✓	
2-Pentanone						✓
Acetaldehyde		✓				
Ethanol				✓		
Furan, 3-methyl-						✓
	Decomposition VOCs detected in donor H7 and also reported in the literature					
2-Butanone		✓	✓	✓	✓	
Benzonitrile		✓	✓		✓	
D-Limonene		✓	✓			
Propanal		✓	✓			
Styrene		✓				✓
1-Propanol	✓					
2-Heptanone					✓	
2-Nonanone				✓		
2-Pentanol						✓
2-Pentanone						✓
Acetaldehyde		✓				
Butanoic acid				✓		
Decanal						✓
Dimethyl trisulfide						✓
Ethanol				✓		
Hexanoic acid, ethyl ester	✓					
Methenamine						✓
Nonanal				✓		
Octanal	✓					
Pyridine						✓
Toluene		✓				
Dimethyl disulfide				✓		✓

Table C-9 *List of ante-mortem and decomposition VOCs detected in donor H8 and also reported in the literature.*

Name	H8_M	H8 ED 0	H8 ED 1	H8 ED 2	H8 ED 3	H8 ED 4	H8 ED 5
	Ante-mortem VOCs detected in donor H8 and also reported in the literature						
5-Hepten-2-one, 6-methyl-	✓	✓	✓	✓	✓		✓
1,3-Dioxolane, 2-methyl-	✓			✓		✓	✓
Butanal, 3-methyl-	✓				✓	✓	✓
Ethanol	✓			✓		✓	✓
Acetaldehyde			✓			✓	✓
Furan, 2-pentyl-					✓	✓	✓
1-Heptene			✓		✓		
2-Butenal, 3-methyl-						✓	✓
2-Heptanone			✓				✓
2-Propenal						✓	✓
Ethyl Acetate	✓	✓					
Furan, 3-methyl-					✓	✓	
Isopropyl acetate	✓						✓
1-Nonene			✓				
2-Butanone				✓			
2-Butene, 2,3-dimethyl-							✓
2-Pentanone							✓
Benzaldehyde						✓	
Butanal, 2-methyl-				✓			
Eucalyptol							✓
Furan, 2,5-dimethyl-						✓	
Propanal, 2-methyl-	✓						
	Decomposition VOCs detected in donor H8 and also reported in the literature						
Ethanol	✓			✓		✓	✓
1-Propanol					✓	✓	✓
2-Pentanol	✓					✓	✓
Acetaldehyde			✓			✓	✓
Benzonitrile					✓	✓	✓
Nonanal					✓	✓	✓
Nonane			✓		✓		✓
Pyridine	✓					✓	✓
1-Heptene			✓		✓		
2-Decanone			✓			✓	
2-Heptanone			✓				✓

2-Octene			✓			✓	
Dimethyl trisulfide						✓	✓
Methenamine						✓	✓
Pentane	✓					✓	
Propanal			✓			✓	
Styrene	✓	✓					
1-Decene			✓				
1-Octen-3-ol						✓	
1,1-Dichloro-1-fluoroethane						✓	
2-Butanol						✓	
2-Butanone				✓			
2-Nonanone						✓	
2-Pentanone							✓
Benzaldehyde						✓	
Butanoic acid, ethyl ester							✓
Decanal						✓	
Hexanoic acid, ethyl ester	✓						
Octanal						✓	
Phenol							✓
Tetradecane			✓				
Dimethyl disulfide	✓			✓		✓	✓

Table C-10 *List of ante-mortem and post-mortem VOCs detected in donor H9 and also reported in the literature.*

Name	H9_M	H9 ED 0	H9 ED 1	H9 ED 2	H9 ED 3	H9 ED 4	H9 ED 5
	Ante-mortem VOCs detected in donor H9 and also reported in the literature						
5-Hepten-2-one, 6-methyl-	✓		✓	✓	✓	✓	✓
Butanal, 3-methyl-	✓			✓		✓	✓
1-Heptene	✓				✓	✓	
1,3-Dioxolane, 2-methyl-		✓				✓	✓
2-Heptanone	✓		✓				
Acetonitrile						✓	✓
Benzaldehyde				✓			✓
Furan, 2,5-dimethyl-	✓					✓	
Isopropyl acetate						✓	✓
Propanal, 2-methyl-	✓		✓				
1-Octene							✓
2-Butanone					✓		
2-Butenal, 3-methyl-						✓	
2-Butene, 2,3-dimethyl-	✓						
2-Propenal	✓						
Acetaldehyde							✓
Butanal, 2-methyl-							✓
Ethanol							✓
	Decomposition VOCs detected in donor H9 and also reported in the literature						
Benzonitrile	✓			✓	✓		✓
1-Heptene	✓				✓	✓	
2-Heptanone	✓		✓				
2-Pentanol	✓						✓
Benzaldehyde				✓			✓
Dimethyl trisulfide						✓	✓
Octanoic acid				✓		✓	
Phenol				✓			✓
1-Decene		✓					
1-Ethyl-4-methylcyclohexane							✓
1-Propanol							✓
1,1-Dichloro-1-fluoroethane	✓						
2-Butanone					✓		
2-Hexyl-1-octanol						✓	

2-Nonanone							✓
Acetaldehyde							✓
Butanoic acid, methyl ester				✓			
Ethanol							✓
Ethylbenzene	✓						
Heptanal							✓
Nonanal			✓				
Nonane	✓						
o-xylene	✓						
Pentane							✓
Pentanoic acid						✓	
Pyridine							✓
Styrene	✓						
Toluene	✓						
Dimethyl disulfide	✓	✓			✓		✓